EXPLORING DOPAMINE FUNCTION IN THE RAT VENTRAL TEGMENTAL AREA: THE INFLUENCE OF PERSISTENT PAIN

Lauren Friend

A thesis submitted to University College London for the degree of Doctor of Philosophy

Department of Neuroscience, Physiology and Pharmacology

Gower Street, London, WC1E 6BT

This work was supported by the Medical Research Council, as part of the 4-year MRC-funded PhD programme in Biomedical and Life Sciences

Declaration

I, Lauren Friend, confirm that the work presented in this thesis is my own. Where information has been derived from other sources, I confirm this has been indicated in the thesis.

Abstract

This thesis describes an investigation into the pharmacological and neurobiological nature of one of the key neural populations in the interactions between pain- and reward-related information - the dopaminergic (DA) neurones of the ventral tegmental area (VTA). The aim of these experiments collectively was to increase understanding of the functioning of the VTA neurones in various pain-related contexts, in the hope that this information will act as a foundation upon which further developments in knowledge occur. Ultimately, it is hoped that such advances in understanding could lead to the development of effective therapeutics down the line. Through a series of five projects employing intra-VTA *in vivo* electrophysiology in the anaesthetised rat in combination with a variety of pharmacological and nociceptive manipulations, the work described in this thesis explored the activity of spontaneously firing VTA neurones. Initial experiments attempted to both electrophysiologically and pharmacologically identify the DA neurones amongst interspersed non-DA populations *in vivo.* From a series of results, it was concluded that there was likely significant heterogeneity amongst VTA DA and non-DA groups, resulting in a confusing picture of cell identity. Through adopting the pharmacological measure of response to systemic L-DOPA injection, recorded neurone populations were reliably split into two sub-populations with a size, response direction and dose dependency in line with DA and GABAergic identities, respectively. However, neurochemical identity was not confirmed, and the possibility of alternatives was considered throughout the thesis. Subsequent investigations moved on to test how the induction of persistent pain altered the activity of VTA neurones: first in a carrageenan-induced tonic inflammatory pain model, and secondly, in a spinal nerve ligation-induced chronic neuropathic pain model. Concurrently, the role of endogenous μ-opioid receptor (MOR) agonists in regulation of VTA neurone activity was unmasked though administration of the MOR antagonist, naloxone. It was found that the induction of a tonic inflammatory pain state caused changes in the firing rate and pattern of VTA neurones subpopulations. An effect of naloxone on neuronal firing rate was no longer apparent in the tonic inflammatory pain state, suggesting a down-regulation of tonic μ-opioid control. Unexpectedly, neurones recorded in naïve and neuropathic pain states showed very similar characteristics. It was suggested that this result may be underlined by longer-term reactions to the sustained increased nociceptive input. Several possible explanations for the above results are discussed, along with the functional implications in terms of a wider role for VTA dopamine neurones in the pain-processing system. Finally, it was noted that the current methodology possessed a few inherent limitations when it comes to translating these findings to an awake, freely moving state, and that that future efforts should attempt to address these.

Abbreviations

6-OHDA	6-Hydroxydopamine
ACC	Anterior cingulate cortex
AP	Action potential
cAMP	Cyclic adenosine monophosphate
CCK	Cholecystokinin
CLi	Caudal linear nucleus
CNS	Central nervous system
DA	Dopamine
DAMGO	[D-Ala^2, N-MePhe^4, Gly-ol]-enkephalin
DAT	Dopamine transporter
DOR	Delta-opioid receptor
fMRI	Functional magnetic resonance imaging
GABA	Gamma-aminobutyric acid
HCL	Hydrochloric acid
IF	Interfascicular nuleus
KOR	Kappa-opioid receptor
L-DOPA	L-3,4-dihydroxyphenylalanine
LDE	L-DOPA-excited
LDI	L-DOPA-inhibited
MOR	μ-opioid receptor
mPFC	Medial prefrontal cortex
NAcc	Nucleus accumbens
$NaHCO_3$	Sodium bicarbonate
OCT	Optimal cutting temperature fluid
ORL-1	Opioid receptor like-1
PAG	Periaqueductal grey
PBP	Parabrachial pigmented nucleus

PDYN	Prodynorphin
PENK	Proenkephalin
PET	Positron emission tomography
PFC	Prefrontal cortex
PIF	Parainterfascicular nucleus
PN	Paranigral nucleus
POMC	Proopiomelanocortin
RAIC	Rostral agranular portion of the insula cortex
RLi	Rostral linear nucleus of the raphe
RMTg	Rostromedial mesopontine tegmental nucleus
RPC	Red nucleus, parvicellular part
RVM	Rostroventral medulla
SFR	Spontaneous firing rate
SNc	Substantia nigra pars compacta
TH	Tyrosine hydroxylase
VMAT2	Vesicular monoamine transporter-2
VTA	Ventral tegmental area

List of Figures

Table of Contents

I. Introduction

I.I Pain: a blessing and a curse

It is down to the sensory aspects of our nervous system that we are able to behave in a circumstantially appropriate nature, allowing us not only to survive but also to thrive in the complex and unpredictable world we live in. One of the most crucial senses in this respect is nociception, alerting us to damaging or potentially harmful events through the encoding and transduction of noxious stimuli. The nociceptive signals are then further integrated with a variety of complex emotional and cognitive factors by a vast array of central nervous system structures, ultimately resulting in the emotional, sensory and behavioural experience that we call pain (Melzack and Casey, 1968).

Pain as a concept has been hard to define, with the past two centuries seeing major alterations in thinking. The study of different aspects of pain has led to previous theories ranging from it being a specific sense to simply an emotion. Fortunately, these differing concepts have since been amalgamated, leading to the currently accepted definition given by IASP describing pain as "*an unpleasant sensory and emotional experience associated with actual or potential tissue damage, or described in terms of such damage*" (Merskey and Bogduk, 1994). Although it clearly shares fundamental elements with the other individual senses, pain is undoubtedly unique, and it is only through advancements in research in this field that we will be able to understand how and why.

Crucially, there is an enormous drive to do so. The survival advantage of possessing the ability to experience pain is obvious, particularly when we consider the rare cases in which this is missing: congenital insensitivity to pain is a syndrome shared by only a very few individuals, and invariably leads to excessive damage including loss of limbs, multiple burns and even death (Cox et al., 2006). However, the catch of possessing this critical function is that the pathological dysfunction of the pain system has an immense negative impact on quality of life. When pain outlasts the initiating stimulus for at least 3 to 6 months, such that it no longer serves the individual a useful purpose, it is classified as a chronic condition (McMahon et al., 2013). Co-morbidities such as depression, anxiety,

insomnia and restricted mobility are commonplace amongst patients, rendering chronic pain severely debilitating (Nicholson and Verma, 2004). What's more, with around 19% of the European adult population suffering from chronic pain at one point in their lives, and 59% of these individuals being affected for up to 2 to 15 years, frequencies of these conditions are worryingly high (Breivik et al., 2006).

Many treatments have made it through extensive clinical trials to patient treatment, including tricyclic antidepressants, serotonin and noradrenaline reuptake inhibitors, the anticonvulsants gabapentin and pregabalin, and opioids. However, even with the combined employment of a variety of these agents, efficacy is modest, with up to 40% of patients failing to enjoy significant alleviation of their symptoms (Breivik et al., 2006; Finnerup et al., 2007; Gilron et al., 2015). Hence, it appears there is a huge scope and demand for both a better utilisation of currently available treatments and the development of new and improved therapies for these debilitating conditions.

I.2 An overview of the pain system

For typical, every-day adaptive pain experienced by healthy individuals, the nociception begins in the periphery. At a very simplistic level, highly specialized 'nociceptors', so-called because they respond preferentially to noxious stimuli, detect thermal, chemical and mechanical damaging events in virtually all tissues of the body (Sherrington, 1900). These peripheral afferent fibres, including myelinated A-δ and unmyelinated C fibre subtypes (Bessou and Perl, 1969; Burgess and Perl, 1973), synapse onto second-order projection neurones in the superficial dorsal horn of the spinal cord, which in turn relay nociceptive information up to intercepting supra-spinal sites such as the brainstem, medulla and thalamus (Willis and Coggeshall, 1991).

The relationship between nociception and pain can vary widely in terms of complexity. At the most basic and primitive end of the scale are nociceptive reflexes involving as little as three neurones from initial stimulus-detection to withdrawal action. This serves as an excellent rapid protection mechanism for relatively simple noxious events, such as contact with a burning hot object. However, this quick-fire response doesn't often represent the optimal behavioural outcome in our multifaceted encounters with potentially damaging stimuli. Fortunately, through integration with memory, and emotional and cognitive factors by a whole matrix of supra-

spinal structures, we have evolved the ability to modify the pain experience and therefore response, such that it is appropriate in any possible situation.

I.3 The pain "matrix"

Despite extensive investigation, the role of the brain in pain processing remains relatively ambiguous. Initial early observations on lesioned patients and epileptic individuals, as well as animal model-based experiments, provided evidence, albeit limited, for a cortical involvement in pain (Young and Blume, 1983; Young et al., 1986; White and Sweet, 1969; Robinson and Burton, 1980; Kenshalo et al., 1988; Mantz et al., 1988, 1990). However, it wasn't until the advent of modern brain imaging techniques, and the first of these experiments on the human brain in pain were published by Talbot and colleagues (1991), Jones and co-workers (1991) and Apkarian and associates (1992), that we first appreciated the extent of the multifaceted cortical and sub-cortical activation.

As technology has evolved, imaging studies have been able to elucidate the neural correlates of the subjective experience of pain with progressively greater detail and understanding. Nociceptive representation has been observed within many regions, including several divisions of the brainstem and thalamus, limbic areas such as the amygdala, the cerebellum, ventral tegmental area (VTA), nucleus accumbens (NAcc) and other nuclei of the basal ganglia, as well as anterior cingulate, somatosensory, insular and prefrontal cortices (Apkarian et al., 2005; Leknes and Tracey, 2008; Rainville, 2002). All of these brain areas have the power to contribute either directly or indirectly to the pain experience, conveying and transforming the original nociceptive signal and mediating effects on behaviour according to circumstance.

Crucially, distinctive components of the pain system within the brain are thought to be involved preferentially in different aspects of our experience. For example, characteristics of the nociceptive stimulus such as quality, intensity and location are represented in the somatosensory and insular cortices, whilst the anterior cingulate cortex covers the implementation of pain as a learning signal and the direction of behaviour accordingly. Further, ascending pathways to forebrain structures including the PFC are suggested to mediate the interactions between pain and cognitive processes (Rainville, 2002; Tracey, 2010). In the midbrain, regions of the limbic system such as the amygdala contribute to emotional aspects of pain, while the mesolimbic dopamine system projecting from the VTA to the NAcc covers the motivational qualities of nociceptive events. Finally, the brainstem acts as a relay

between supraspinal and spinal sites, processing both ascending and descending information. A key component of this is the rostroventral medullar (RVM), which has been found to mediate the descending modulation of spinal activity that acts to control nociception at the first synapse (Fields, 2000).

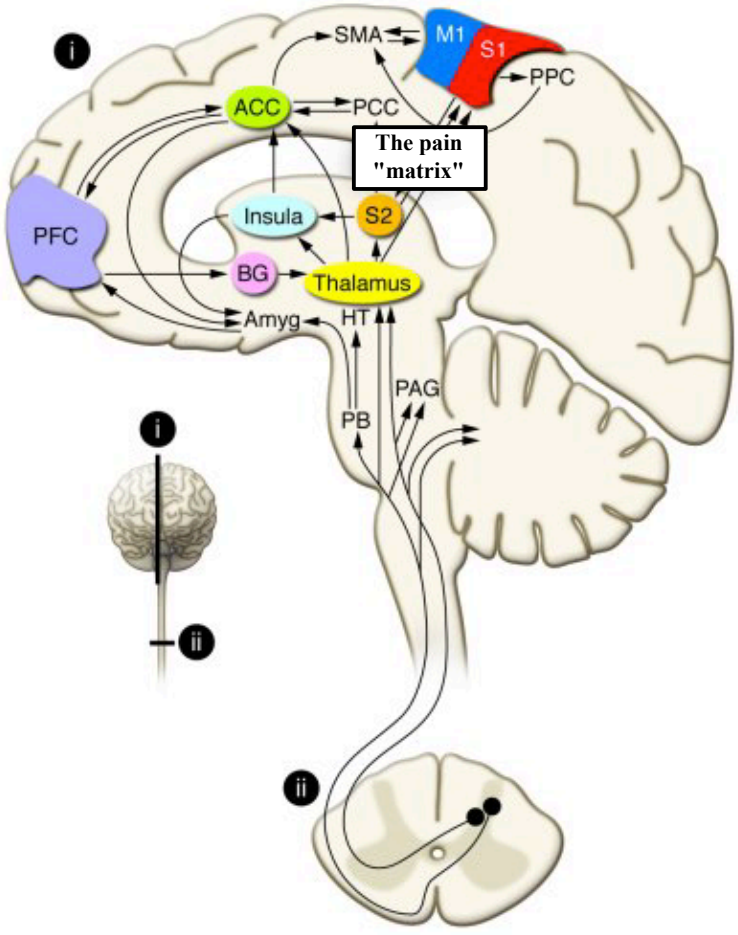

Figure I.I Schematic representation of ascending pain pathways and brain regions involved in pain processing. ACC, anterior cingulate cortex; amyg, amygdala; BG, basal ganglia; HT, hypothalamus; M1, primary motor cortex; PAG, periaqueductal grey; PB, parabrachial nucleus of the dorsolateral pons; PCC, posterior cingulate cortex; PFC, prefrontal cortex; PPC, posterior parietal complex; S1, primary somatosensory cortex; S2, secondary somatosensory cortex; SMA, supplementary motor area. *Adapted from Apkarian et al., 2005.*

I.4 Modulatory mechanisms

Our ability to modify the pain experience when it is advantageous to do so is down to more than just the involvement of multiple brain areas. There are distinct neurochemical systems existing throughout the pain system instigating state-dependent biases on processing neurones. Alongside serotonin and noradrenaline, endogenous opioids play a major role in pain modulation with significant effects occurring throughout the pain pathway.

I.4.1 Endogenous opioids

Three main groups of endogenous opioids exist: the enkephalins, dynorphins and β-endorphins, derived from proenkephalin (PENK), prodynorphin (PDYN), and proopiomelanocortin (POMC), respectively. Expression pattern analysis of these peptides shows a heavy representation in neurones within regions associated with nociceptive processing, such as the thalamus, periaqueductal grey, limbic system, pre-frontal, insular and anterior cingulate cortices and the spinal cord (Bronstein et al., 1992; Höllt, 1990; Khachaturian et al., 1985; Maley, 1996; Viveros et al., 1979; Watson et al., 1981; Navratilova et al., 2015). The most recently discovered group of peptides, the endomorphins, also appear to be localized within central components of the pain system, from primary sensory afferents to neurones of the supraspinal structures (Zadina et al., 1999). This anatomical distribution suggests the opioid peptides are potentially extremely influential in terms of pain perception. In the early 1990s, three subtypes of opioid receptor were cloned: first the δ-opioid receptor (DOR) (Evans et al., 1992; Kieffer et al., 1992), and then the μ- and κ-opioid receptors a year later (MORs: Chen, Mestek, Liu, Hurley, & Yu, 1993; Fukuda, Kato, Mori, Nishi, & Takeshima, 1993; KORs: Li et al., 1993; Meng et al., 1993; Thompson, Mansour, Akil, & Watson, 1993). A fourth subtype, called opioid receptor-like 1 (ORL-1) has more recently been characterised. There is significant structural homology existing within the family, with all receptor subtypes possessing 7-transmembrane spanning domains that couple to inhibitory G-proteins. Consequently, agonist binding leads to a reduction in neuronal cAMP production and hyperpolarisation, ultimately resulting in a suppression of activity (Al-Hasani and Bruchas, 2011). Despite the structural similarities, all three receptor subtypes have distinct affinities for different endogenous peptides, with the β-endorphins and endomorphins preferentially binding MORs, enkephalins DORs, and dynorphins, KORs.

The expression patterns of these opioid receptors are also compatible with theories of their significant role in nociceptive modulation. μ-, κ- and δ-opioid receptors are expressed in neurones of regions involved in pain

processing, such as the periaqueductal grey, rostral ventromedial medulla, locus coeruleus, substantia nigra, VTA, raphe nuclei, nucleus tractus solitarii and substantia nigra (Przewłocki and Przewłocka, 2001). There is also significant expression within components of the limbic system, cortex and spinal cord, suggesting roles in the modulation of emotional, cognitive and transmission aspects of pain, respectively (Navratilova et al., 2015).

The adoption of pharmacological techniques when investigating pain mechanisms has provided evidence suggesting that indeed opioidergic action induces an endogenous analgesic effect. Specifically, the μ-opioid receptors appear to play the largest role in this aspect of opioid action; lesions of the arcuate nucleus of the hypothalamus, the main area of POMC and therefore endogenous MOR agonist production, reduce stress-induced analgesia. Further, administration of beta-endorphins into the ventricles results in significant antinociception (Przewłocki and Przewłocka, 2001). Importantly, synthetic and plant-derived MOR agonists such as morphine are effective analgesics, resulting in wide clinical employment in the alleviation of severe and chronic pain despite often-serious side effects.

When investigating the analgesic mechanisms of systemic opioids, it has become apparent that they act in a distributed and simultaneous manner at multiple spinal and supra-spinal sites (Fields, 2007). Crucially, it appears that opioids have the capacity to influence transmission at all levels of a modulatory "top-down" pathway, incorporating projections from cortical and limbic structures down to neurones of the rostroventral medulla (RVM), which then go onto directly inhibit or facilitate neurones of the spinal cord dorsal horn (Fields et al., 2005). The current theory surrounding this pathway suggests that it implements a "do not respond to pain" behavioural decision when a situation calls for it (Fields, 2007): in short, endogenous opioids, released under certain circumstances, activate a pain-inhibiting descending pathway originating with the "OFF" cells of the RVM, over-riding parallel pain-facilitatory signals of the neighbouring "ON" cells to inhibit an avoidance response to the noxious stimulus. The neural correlate of the behavioural decision process itself has not been easy to clarify, but evidence suggests, when it comes to a conflicting motivation of reward specifically, the dopamine neurones of the ventral tegmental area play the key role. Alongside behavioural aspects of opioid-induced antinociception, a reduction in the subjective aversiveness of pain has also been shown to occur upon the injection of an exogenous MOR agonist. This mechanism is thought to be mediated by direct μ-opioid action within the anterior cingulate cortex, which leads to altered dopamine release in the NAcc (Navratilova et al., 2015).

I.5 When pain becomes pathological

The fine details of nociceptive processing, such as the balance of modulatory influence and contributions of signal transduction components, are by no means set in stone. The pain system is highly dynamic, and no situation shows this more than the case of when pain becomes pathological.

Pathological pain states can vary dramatically in time-scale, ranging from tonic pain that lasts for a few hours to days, to chronic pain that can persist for a lifetime. Further, there are a variety of possible causes of pain conditions, including prolonged inflammation (inflammatory pain), actual tissue damage (nociceptive pain), nerve damage (neuropathic pain), or conversely, there may even be no apparent cause (idiopathic pain). These factors introduce significant variability in pathological mechanisms underlying pain states; however, what these pain states do all have in common is that the pain experience no longer serves to direct behaviour in the most evolutionarily advantageous way. Typical aspects of pathological pain include "allodynia", or the triggering of a pain response by normally innocuous stimuli, and "hyperalgesia", meaning the increased intensity of pain sensation to a given noxious stimulus, and both phenomena have separable modality-specific mechanisms; the development of mechanical hyperalgesia doesn't necessarily come hand in hand with the simultaneous development of thermal hyperalgesia, for example.

In order to progress in the development of preventative or reversing therapies for persistent pain, much research has gone into the understanding of the pathological mechanisms. In general, it appears that processes responsible for the enhanced pain sensitivity can include any combination of 'peripheral sensitization' and 'central sensitization' events.

Peripheral sensitization incorporates any mechanism that acts to enhance the excitability of peripheral sensory afferents to a given stimulus intensity (Basbaum et al., 2009; Gold and Gebhart, 2010). It is caused by the release of a concoction of inflammatory mediators, the so-called "inflammatory soup", containing adenosine triphosphate, nerve growth factor, prostaglandins, bradykinin, and pro-inflammatory cytokines, among others (Sikandar et al., 2013; Zhang et al., 2005), and typically involves many surrounding non-neural cells as well as the nerve terminals themselves (Basbaum et al., 2009; Gold and Gebhart, 2010; Sikandar et al., 2013). This reaction can be triggered by either tissue damage or an immune response, and ultimately leads to decreased activation thresholds of the nociceptor afferents and an increased frequency of action potential discharge to suprathreshold stimuli: potential

neural correlates of allodynia and hyperalgesia, respectively. Crucially, this phenomenon is relatively localised to the site of injury.

In contrast, central sensitization describes transformations occurring within the central nervous system (CNS), such that the incoming sensory information from the periphery is amplified to produce a much more widespread hypersensitive state. Plastic changes classified as central sensitization often occur in parallel with those acting in the periphery and include modifications in the spinal cord, supraspinal descending controls, and many cortical and sub-cortical aspects of pain processing.

The best way to highlight how these mechanisms can combine to produce a persistent pain state is to consider the examples of different conditions with specific etiological and timescale characteristics. The development of customised animal models representing individual human pain disorders has allowed researchers to elucidate many of the mechanisms involved in each case, concurrently emphasising the fundamental differences between different pain conditions and the respective challenges in the development of targeted treatment.

One of the most frequently adopted models is the carrageenan-induced rodent model of tonic inflammatory pain. A polysaccharide derived from red alga, carrageenan leads to an inflammatory reaction with all the cardinal signs of edema, hyperalgesia and erythema developing immediately following subcutaneous injection (Winter et al., 1962; Winyard and Willoughby, 2003). The resultant local hyperalgesia and allodynia are predominantly caused by peripheral sensitization, attributable to the actions of the inflammatory soup; however, there is a large body of evidence implicating the involvement of central sensitization processes in the model. For example, the finding that intrathecal morphine is 30 times more potently analgesic 3 hours post-carrageenan injection suggests that the influence of endogenous opioids at the level of the spinal cord dorsal horn neurones is enhanced, presumably down to plasticity in opioid receptor expression and/or function (Hylden et al., 1991; Stanfa et al., 1992). Similarly, mu and delta opioid agonists administered directly into the RVM of the brainstem have a greater antinociceptive effect in a state of tonic inflammatory pain, with respect to noxious stimuli applied to both the inflamed ipsilateral but also non-inflamed contralateral paws (Hurley and Hammond, 2000). Further, the evoked response of these neurones from a given C- or A-delta fibre input was significantly altered following the induction of inflammation, allowing us to conclude that modifications occur both in spinal transmission and modulatory components (Stanfa et al., 1992).

Another common and well-established model of persistent pain presents a very different picture than that of carrageenan inflammation. In contrast to carrageenan-induced tonic sensitization lasting only up to 72 hours, the spinal nerve ligation (SNL) model of chronic neuropathic pain induces a pain state with complex symptoms lasting for up to 5 to 10 weeks (Kim and Chung, 1992). This model is generated by the ligation of spinal nerves L5 and L6 that innervate the left hindpaw, followed by a latent period of two weeks to allow the surgical injuries to heal and the neuropathy to develop. While peripheral sensitization mechanisms, including those evoked by inflammatory mediators, are thought to contribute to the initiation of chronic pain of this calibre (West et al., 2015), the majority of the long-term symptoms, including mechanical and thermal hyperalgesia and allodynia, are sustained by central pathologies (Dubner and Ruda, 1992; Ji et al., 2003; Woolf and Salter, 2000). Hence, the main focus of research into the chronic neuropathic condition surrounds the changes occurring much further down the cascade of events from the initiating neural damage.

Extensive research has revealed a large selection of potentially causative mechanisms that take place post-surgery. In the spinal cord dorsal horn a reduction in GABAergic tone has been shown (Lever et al., 2003; Moore et al., 2002), along with dendritic spine remodelling of the projection neurones (Tan et al., 2011) and the formation of new connections between these cells and non-nociceptive afferent fibres (Lu et al., 2013). Ultimately these changes summate to result in enhanced nociceptive signalling up to supraspinal sites. In addition, the balance of pro-nociceptive serotonergic and anti-nociceptive noradrenergic descending controls from the brainstem to the spinal cord is altered, such that the bias leans towards further promotion of transmission at the first synapse (Millan, 2002; Suzuki et al., 2004). Significant changes in the relative contributions of different brain regions are also thought to occur (Seminowicz et al., 2009). Brain imaging studies of rats with neuropathy induced by the spared nerve injury model showed that several months after surgery, frontal, retrosplenial and entorhinal cortical volumes were decreased relative to that of sham control animals (Seminowicz et al., 2009). Further, the degree of mechanical hyperalgesia associated with this condition was correlated with decreases in the volume of the insula and anterior cingulate cortices, as well as the hindlimb area of the primary somatosensory cortex. Unfortunately, however, although there is a clear association between the pain traits and cortical alterations, one cannot assume a causative link from these results. Finally, supraspinal molecular changes, from the level of individual neurones to whole transmitter systems, have been shown to occur upon the induction of neuropathic pain. For example,

studies hint at a general decrease in density (Maarrawi et al., 2007) and a VTA dopamine neurone-specific desensitization of the μ-opioid receptors in this chronic pain state (Ozaki et al., 2003).

Overall, it appears that both tonic inflammatory and long-term neuropathic pain have widespread yet somewhat differing effects on peripheral and central pain-processing regions, ultimately resulting in the specific pathology of the respective conditions. There are many more subtle and significant changes taking place on top of those discussed, making the unpicking of the underlying cause a monumental task. What we can do, however, is narrow our focus on a single mechanism or area to increase understanding of the relative impact this component has: an absolute necessity for the eventual piecing-together of the pathology in its entirety.

I.6 The ventral tegmental area

The VTA, located on the floor of the midbrain, has long been considered an influential component of the pain-processing system. Previously named the 'ventral tegmental *nucleus*' (Tsai, 1925), it is now defined as the 'ventral tegmental *area*' due to its cytoarchitectural heterogeneity (Nauta, 1958), accountable to the presence of several separate nuclei that it encompasses (figure I.2). The precise collection of nuclei that make up the ventral tegmental area remains controversial, but in general they are thought to include the parabrachial pigmented nucleus (PBP), paranigral nucleus (PN), caudal linear nucleus (Cli), interfascicular nucleus (IF), parainterfascicular nucleus (PIF), and the rostral linear nucleus of the raphe (RLi). Importantly, striking similarity amongst mammals enables the use of well-established rodent models for further investigation towards an understanding of VTA structure and function.

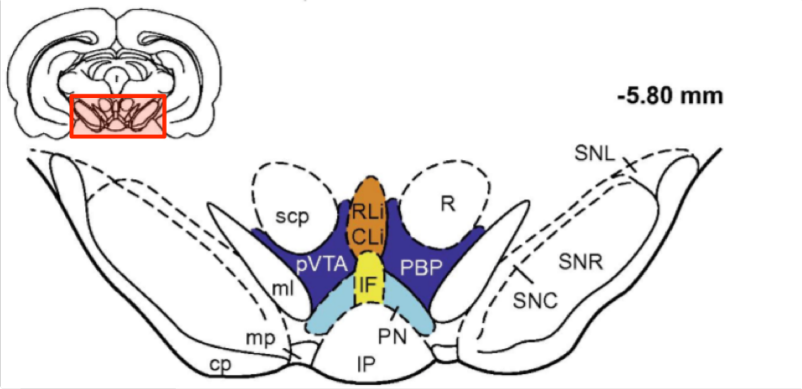

Figure I.2 Schematic of the organisation of the rat VTA. The nuclei of the VTA are shown in a coronal section adapted from a rat brain atlas. The anteroposterior distance from Bregma of this representative section is shown (-5.80mm). *VTA nuclei abbreviations:* CLi, caudal linear nucleus; IF, interfascicular nucleus; pVTA, posterior VTA; PBP, parabrachial pigmented nucleus; PN, paranigral nucleus; RLi, rostral linear nucleus. *Non-VTA nuclei abbreviations:* cp: cerebral peduncle; IP, interpeduncular nucleus; ml, medial lemniscus; mp, mammillary peduncle; R, red nucleus; scp, superior cerebellar peduncle; SNC, substantia nigra, compact part; SNL, substantia nigra, lateral part; SNR, substantia nigra, reticular part. *Adapted from Sanchez-Catalan et al., 2014.*

The neural cellular composition of the VTA was first suggested by Johnson and North (1992) when they described two major types of neurone – primary and secondary – on the basis of electrophysiological and pharmacological differences. Characterisation of these neurones is detailed in section 3., but in brief, a putative dopaminergic identity was attributed to a spontaneously firing population displaying relatively long-duration action potentials (APs), whilst those neurones with shorter APs and exogenous opioid sensitivity were presumed to be GABAergic. Subsequent investigations clarified some controversial findings of heterogeneity within these characteristics by identifying a tertiary population, which are now known to represent the glutamatergic contingent (Hur and Zaborszky, 2005). Although many aspects of these early findings have since been found to underestimate the complexity within VTA neurone populations, the neurochemical composition remain accurate, with current predictions of relative proportions being that of ~60% dopaminergic, ~25% GABAergic, and only a very small number of glutamatergic neurones (2-15%; Margolis et al., 2012, 2006; Nair-Roberts et al., 2008a; Swanson, 1982; Ungless and Grace, 2012; Yamaguchi et al., 2011). Despite the different neuronal populations being more or less intermixed through the VTA, there are suggestions of regional differences in cellular composition, particularly between the lateral (PN and PBP) and midline (RLi, Cli and IF) nuclei. For example, a lateromedially-increasing gradient of glutamate neurone distribution has been observed (Yamaguchi et al., 2007a), whilst the more lateral PBP and PN were found to have the highest concentrations of DA neurones (Nair-Roberts et al., 2008b).

I.7 A focus on dopamine

For reasons that will be discussed, it is the DA neurones that have been of primary focus for researches investigating the ventral tegmental area.

Action of the neurotransmitter dopamine (DA) within the central nervous system has been implicated in many functions including arousal, reward, memory, motor control and pain. There are several relatively small DA neurone loci within the brain, denominated A8 through to A14: A8 and A9 represent the substantial nigra populations, whilst A10, A11, A12, A13 and A14 represent that of the VTA, posterior hypothalamus, arcuate nucleus, zona incerta and periventricular nucleus, respectively (Dahlstroem & Fuxe, 1964). Outside the CNS, DA also acts to modulate several functions as a chemical messenger, including those affecting the blood flow and kidney function (Carey, 2001; Missale et al., 1998).

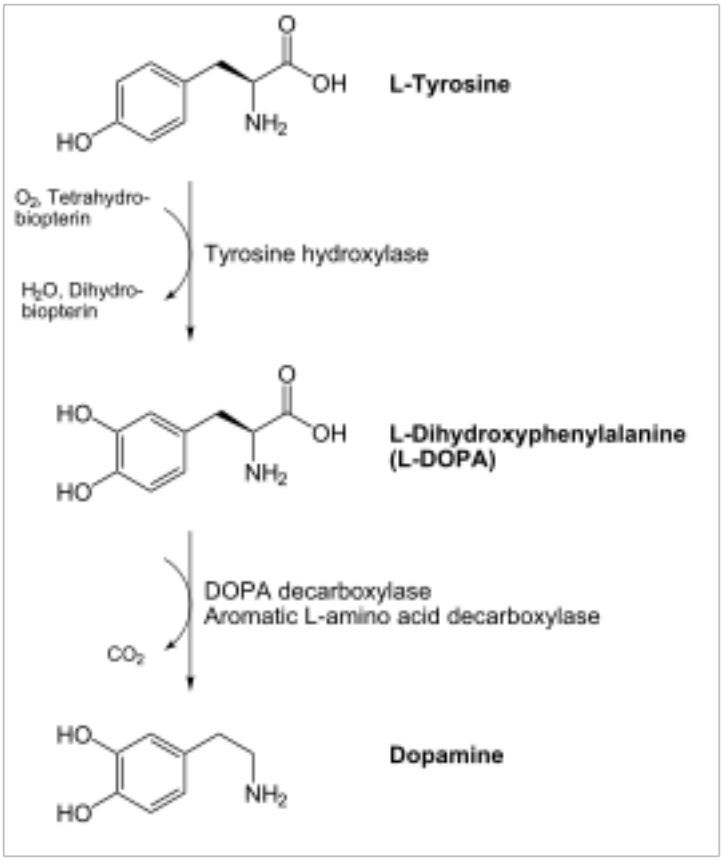

Figure I.3 Structural formula for dopamine synthesis. L-Tyrosine, derived from the essential amino acid phenylalanine, is converted to L-DOPA by the enzyme tyrosine hydroxylase, using molecular oxygen and tetrahydrobiopterin as cofactors. This represents the rate-limiting step in the dopamine synthesis pathway. Finally, the enzyme aromatic L-amino acid decarboxylase (DOPA decarboxylase) converts L-DOPA into dopamine, using pyridoxal phosphate as the cofactor. *Adapted from Proteopedia page "dopa decarboxylase".*

Figure I.3 depicts the pathway of dopamine synthesis, including crucial enzymes and cofactors involved. Following synthesis, dopamine is packaged into synaptic vesicles by the vesicular monoamine transporter-2, VMAT2 (Eiden et al., 2004), for storage at the axon terminals in preparation for exocytotic release into the synaptic cleft. Interestingly, however, dopamine release isn't exclusive to the neuronal terminal fields; there is now strong evidence for significant somatodendritic release of dopamine in and around the cell body of the neurone in question (Adell and Artigas, 2004). Following the initial discovery of this phenomenon in the substantia nigra (Geffen et al., 1976), it has since been established that DA release within the VTA is both prominent and dynamic under different behavioural and pharmacological conditions (Beart and McDonald, 1982; Bernardini et al., 1991; Bradberry and Roth, 1989; Zhang et al., 1994). This somatodendritic release represents a crucial part of an important autoinhibitory mechanism for the dopaminergic neurones, regulating cells' firing through high-affinity D2 receptors present on their soma and dendrites (Bernardini et al., 1991; White and Wang, 1984). The implications of this self-modulatory mechanism in the functioning of the DA neurones in the VTA are considered in sections 4 and 5.

Neurotransmitter uptake is the major mechanism adopted to inactivate released monoamines (Adell and Artigas, 2004). For dopamine, this is carried out by the dopamine transporter (DAT), after which it is either repackaged into presynaptic vesicles or broken down enzymatically by monoamine oxidase (Wood, 2008). The impact of the reuptake mechanism on dopamine signalling is made apparent with the huge reinforcing potential of drugs that directly inhibit the DAT, including cocaine and amphetamines, leaving projection targets with sustained increases in extracellular dopamine concentration (Bernardini et al., 1991; Bradberry and Roth, 1989; Chen and Reith, 2002; Kalivas, 1993). Interestingly, the number of DAT molecules in somatodendritic regions of the VTA is significantly lower than that in axon terminals (Reith et al., 1997), making dopamine reuptake in the former much less efficient (Cragg et al., 1997). Conversely, in areas such as the prefrontal cortex in which DAT expression is similarly low, it is thought that converging noradrenergic terminals takeover the task of DA reuptake (Gresch et al., 1995).

There are five types of dopamine receptor through which the released neurotransmitter can exert an effect, D1 to D5, all of which are metabotropic G protein-coupled receptors (Sibley et al., 1993). These can be grouped into the D1 subtype (D1 and D5), which typically exert excitatory actions on the host neurone through coupling with the stimulatory G_s protein, and the D2 subtype (D2, D3 and D4), which conversely inhibit neurones through the

G_i protein (Wood, 2008). Each of the receptor classes has a unique expression pattern throughout the brain and spinal cord: for example, whilst D2 receptors are present in abundance within the VTA, D3 receptors are not significantly expressed within this region (Wood, 2008). The diversity in receptor properties and expression patterns puts this single chemical that is dopamine in a position to mediate many discrete functions with a great deal of flexibility.

I.8 VTA neurone connectivity

Through a combination of both light microscopy and electron microscopy techniques, we have been able to not only elucidate connectivity between different brain structures but also reveal precise synaptic networks through detailed ultrastructural analysis. These approaches have been adopted in a number of studies on the VTA, leaving us with a relatively comprehensive picture of where this region "fits in" to the brain-wide circuitry.

I.8.I Inputs

VTA DA neurones *in vivo* exhibit spontaneous activity that has been shown to arise from self-generated depolarisation. This finding has led to suggestions that DA neurone activity is self-driven; however, stark differences between DA neurone recordings in *in vitro* slice and *in vivo* intact preparations indicate that both inhibitory and excitatory synaptic inputs exert significant tonic control over the ultimate output (S. W. Johnson and North, 1992; Marinelli and McCutcheon, 2014).

The major extrinsic inputs to the VTA neurones are from glutamatergic and GABAergic neurones. Glutamatergic inputs from the PFC (Kornhuber et al., 1984; Sesack and Pickel, 1992), subthalamic nucleus (Kita and Kitai, 1987; Rinvik and Ottersen), mesopontine tegmentum nucleus (Clements and Grant, 1990), lateral habenula (Omelchenko et al., 2009), and periaqueductal grey (Omelchenko and Sesack, 2010) have been found to synapse onto VTA DA neurones. These influences are thought to play a role in DA neurone burst firing instigation (detailed later in section I.9.4), following findings that neurones fail to display this high-frequency pattern of activity *in vivo* when the corresponding connections are severed, or in the *in vitro* preparation (Johnson and North, 1992b; Marinelli and McCutcheon, 2014a). Further, there are significant glutamatergic inputs to non-DA VTA neurones (Sesack and Pickel, 1992), most notably from the lateral habenula, periaqueductal grey and the PFC (Carr and Sesack, 2000; Omelchenko and Sesack, 2010; Omelchenko et al., 2009). Interestingly, there appears to

be a degree of VTA neurone segregation when it comes to glutamatergic inputs; glutamatergic inputs from the medial prefrontal cortex (mPFC) synapse onto VTA DA neurons that project back to the mPFC, but not DA neurons that project to the NAcc (Carr and Sesack, 2000).

GABA inputs to VTA neurones are extensive, with GABAergic neurones from a region called the rostromedial mesopontine tegmental nucleus (RMTg), often referred to as the tail of the VTA due to anatomical location, forming synapses on ~80% of VTA DA neurones (Balcita-Pedicino et al., 2011). To date, the RMTg represents the largest source of GABAergic input to the VTA; however, there are also indications of GABAergic projections from nucleus accumbal medium spiny neurones onto non-DA VTA cells (Xia et al., 2011). These synapses are inhibitory in nature, and therefore represent a powerful breaking influence on the VTA neurone activity. There is evidence to suggest that GABAergic afferent inputs selectively synapse onto specific subpopulations of VTA neurones; functional GABAergic inputs to the VTA from the NAcc synapse specifically on non-DA neurones, whereas GABAergic inputs arising from the ventral pallidum synapse onto both DA and non-DA neurones (Hjelmstad et al., 2013; Xia et al., 2011). These findings, together with the specificity of region-specific glutamatergic inputs, hint at the existence of differential activity within parallel and potentially independent circuits involving the VTA neurones, adding an additional layer of complexity to the functioning of this brain region.

Alongside these GABAergic and glutamatergic drives, it has been found that both DA and non-DA neurones of the VTA receive significant input from serotonergic and noradrenergic neurones (Hervé et al., 1987; Phillipson, 1979). Dense serotonergic projections from the dorsal raphe nucleus and the medial raphe nucleus have been found to synapse onto VTA neurones (Adell and Artigas, 2004), and the regulatory influence of this neurotransmitter is thought to be complex, depending on the type of 5-HT receptor expressed and the physiology of the neurone expressing it.

I.8.2 Intrinsic connections

On top of these external influences, there are many intrinsic connections within the VTA itself: ultrastructural findings reveal inhibitory GABAergic interneurones synapse onto local DA neurone dendrites (Omelchenko et al., 2009), and there are suggestions of similar local excitatory regulation from glutamatergic neurones (Dobi et

al., 2010; Yamaguchi et al., 2007b, 2011). These connections are significant, as ultimately they modulate the output of the DA projection neurones, adding another dimension of flexibility to their signalling.

I.8.3 Outputs

The definitive outcome from the integration of the plethora of extrinsic and intrinsic synaptic influences with the self-driven activity of the DA neurones is the release of this neurotransmitter at axon terminals. An additional layer of complexity is added to the picture of DA neurone function when we consider the location and nature of axon projection targets, of which there are many. Interestingly, evidence suggests that, whereas substantia nigra pars compacta DA neurones send axon collaterals to multiple brain regions, individual VTA neurones project to single target brain regions (Margolis et al.; Matsuda et al., 2009; Swanson, 1982).

One of the major targets of projecting VTA neurones is the PFC. This 'mesocortical' projection system is thought to consist mainly of GABAergic neurones (~60% according to Carr and Sesack, 2000), but also contains a significant proportion of dopaminergic connections (~25% according to Yamaguchi et al., 2011). It is possible that through this pathway, the motivational aspects of the nociceptive stimulus are integrated with cognitive contextual information, which is subsequently relayed back to the behavioural decision-making regions such as the NAcc.

The other significant pathway to take into consideration is the mesolimbic system, describing the DA and non-DA projections from the VTA to areas comprising the limbic system through the medial forebrain bundle. These regions are inherent to the pain system, processing the emotional and motivational aspects of nociceptive information, and include the amygdala, the entorhinal area, parts of the hypothalamus, and the NAcc of the ventral striatum (Swanson, 1982). The focus of a large proportion of the research on VTA DA neurones relates to their projections to the NAcc, due to both the importance and complexity of the role the separable 'core' and 'shell' accumbal regions play in pain and reward (Altier and Stewart, 1999). This interesting structural and functional heterogeneity is touched on later (section I.9.3).

In summary, the dopaminergic, GABAergic and glutamatergic neurones of the VTA are under control from an extensive array of extrinsic and intrinsic synaptic inputs, resulting in a large capacity for subtle modulations of

activity. The combination of this flexibility together with the diversity in projection targets puts the VTA in a good position for integration of sensory information for circumstantial direction of behaviour. Indeed, there is vast evidence suggesting that the VTA neurones, most notably the dopaminergic contingent, are pivotal in the processing of the competing motivations of pain and reward towards optimal behavioural decisions.

I.9 Functional role of mesolimbic dopamine

I.9.I Mesolimbic dopamine plays a crucial role in reward

The mesolimbic DA neurones have a well-established role in reward processing. It has been shown that they receive reward-related inputs and consequently display phasic excitation responses to natural and conditioned rewards (Berridge and Robinson, 1998; Grace and Bunney, 1983; Schultz, 1998), possibly signalling reward prediction-error (Schultz, 1997). There is evidence to suggest that DA signalling in the mesolimbic system contributes specifically to motivational control aspects of reward, including reinforcement learning and incentive to seek reward (Berridge, 2007). For example, animals will learn quickly to self-stimulate electrodes placed in their ventral tegmental area through lever pressing, indicating the reinforcing nature of activation here. Crucially, microinjection of the DA receptor antagonist spiroperidol into the NAcc (Mogenson et al., 1979), or 6-hydroxydopamine (6-OHDA) neurotoxin destruction of DA neurones in the VTA (Fibiger et al., 1987), significantly reduces the frequency at which they are driven to self-stimulate, suggesting that DA release in the NAcc is necessary for motivating actions to achieve reward. Even more dramatically, 6-OHDA VTA lesions render rats completely indifferent to food and other rewards, to the extent that they neglect to eat and drink to the point of starvation when left to their own devices (Marshall et al., 1974; Teitelbaum and Wolgin, 1975; Zigmond and Stricker, 1972). In support of a role in reinforcement learning, the pairing of location with optogenetically-targeted activation of VTA DA neurones in mice is sufficient to produce conditioned place preference (Tsai et al., 2009). Similarly, in humans, presentation of rewards such as cocaine, drug-associated stimuli or even video games has been shown to modulate the activity of DA neurone projection sites such as the NAcc and PFC through fMRI and PET studies (Breiter et al., 1997; Firestone et al., 1996; Koepp et al., 1998; Volkow et al., 1997).

How could DA signalling support reinforcement learning? One theory is that phasic DA release onto cells in the NAcc and PFC target neurones, among others, leads to a strengthening of any concurrently active synaptic connections onto the same target neuron, according to the rules of Hebbian plasticity (Montague, 1996). Thus, synapses active during behaviours that result in reward, and therefore DA release, are strengthened, resulting in these behaviours being reinforced and the animal learning the optimal choice of action to gain reward. In support of this theory, there is evidence for Hebbian plasticity underlying reinforcement learning of intracranial self-stimulation of the neighbouring substantia nigra DA neurone population (Reynolds et al., 2001).

I.9.2 … And in pain

Although less extensively studied, the role of VTA DA neurones in the processing of nociception towards a sensation of pain is no less significant than that in reward. DA neurones of the VTA have been shown to display phasic responses to acute noxious stimulation (Brischoux et al., 2009; Cohen et al., 2012; Ungless et al., 2004), and studies using fast scan cyclic voltammetry (FSCV) and microdialysis have shown elevated dopamine levels in the NAcc and medial prefrontal cortex in response to aversive stimuli (Bassareo et al., 2002; Budygin et al., 2012). Further, direct electrical stimulation of the DA neurones in the VTA (Sotres-Bayón et al., 2001), and activation of the dopamine D2 receptors in the NAcc with local application of the selective agonist quinpirole (Taylor et al., 2003) both have antinociceptive effects in rodent models of tonic pain. Conversely, administration of D2 receptor antagonists in the NAcc (Taylor et al., 2003) as well as targeted 6-OHDA lesions of the VTA (Saadé et al., 1997; Sotres-Bayón et al., 2001; Takeda et al., 2005) result in increased pain sensitivity, further suggesting a tonic pain-dampening role of DA signalling (Altier and Stewart, 1993, 1999; Wood, 2008). In humans, levels of D2 receptor binding (an indirect measure of DA levels) are associated with an individual's response to painful stimulation (Hagelberg et al., 2002), and patients with Parkinson's disease resulting from the death of dopaminergic neurones often develop chronic pain (Silva et al., 2008).

Hence, there is significant evidence that activation of these DA neurones and their subsequent DA release occurs during nociception, and that enhancement of activity likely exerts an inhibitory influence on the level of pain perceived, acting as an endogenous analgesic mechanism. How exactly do actions at VTA DA neurone projection targets contribute to pain processing? The above evidence showing that dopamine receptor blockade in the NAcc causes increased pain sensitivity, together with findings of this intervention blocking analgesic effects of

amphetamines (Altier and Stewart, 1993, 1999; Clarke and Franklin, 1992; Gear et al., 1999; Taylor et al., 2003), strongly implicate the VTA-NAcc pathway in DA-related analgesia. As discussed below, however, the precise nature and function of this output is far from straightforward (sections I.9.3, I.9.4). Further, there is significant support for additional contributions from cortical connections. For example, the rostral agranular portion of the insula cortex (RAIC) receives substantial dopaminergic input from the VTA, and inhibition of DA uptake in the RAIC, specifically, (thereby potentiating local DA function) results in analgesia (Burkey et al., 1999). This antinociceptive system has been shown to be tonically active through findings that D1 receptor antagonist application enhances pain sensitivity (Burkey et al., 1999). It is thought that descending projections from the RAIC act to connect this processing component to the descending pain modulatory pathways originating in the brainstem.

I.9.3 Compartmentalization of the nucleus accumbens: shell versus core subregions

When we consider the VTA outputs to the NAcc it is important to take into account the building body of evidence for functional compartmentalization. Unique to the rest of the striatum, the accumbens can be divided into a central core surrounded medially, ventrally, and laterally by a shell region (Záborszky et al., 1985).

Interestingly, the shell portion of the NAcc appears to be more important than the core for drug reward (Ikemoto, 2007). While presentation of rewarding stimulus leads to dopamine release in both the NAcc shell and core (Roitman et al., 2008), rats learn to self-administer psychomotor stimulants such as amphetamine, cocaine or dopamine receptor agonists into the accumbens shell region only (Carlezon et al., 1995; Ikemoto, 2003; Ikemoto et al., 1997; Rodd-Henricks et al., 2002). In addition, microinjections of dopaminergic antagonists into the shell, but not the core, disrupt conditioned place preference induced by systemic nicotine or morphine (Fenu et al., 2006; Spina et al., 2006). In particular, the rostrodorsal proportion of the medial shell has been referred to as a "hedonic hotspot" (Peciña et al., 2006).

A similar functional division of the dopamine projections to the NAcc has been found for nociceptive processing (Wenzel et al., 2015). Studies using fast-scan cyclic voltammetry (FSCV) have shown that the presentation of a negative stimulus inhibits dopamine release in the shell, in contrast to the increase seen with appetitive stimuli (Navratilova et al., 2016; Park et al., 2015; Roitman et al., 2008). Conversely, aversive stimuli simultaneously

enhance dopamine release in the neighbouring core subregion, suggesting that the NAcc core neurones play an entirely different role in motivational control of behaviour (Budygin et al., 2012; Wilkinson et al., 1998; Young et al., 1993).

There is evidence to suggest that the location of neurones within the VTA predicts their NAcc projection target; Lammel and colleagues (2008) showed that DA neurones projecting to the medial PFC, NAcc core, and medial shell tend to cluster in the medial posterior VTA (PN and medioventral PBP), whereas DA neurones projecting to the NAcc lateral shell are more scattered throughout the PB nucleus and absent from the PN. These findings together with the aforementioned functional division of the NAcc suggests that parallel, functionally distinct independent VTA-NAcc circuits exist (Marinelli and McCutcheon, 2014a).

I.9.4 Tonic versus phasic DA neurone activity

When referring to DA neurones' roles in pain control and reward representation, it is important to note that there are generally considered to be two temporarily dissociable modes of activity labelled 'tonic' and 'phasic' (Floresco et al., 2003; Grace, 1991; Wood, 2006). Phasic activity refers to stimulus-induced rapid burst firing (>20Hz, Grace, 1988) that is typically associated with the presentation of a salient rewarding stimulus (Grace, 1991). It is important to note, however, that this burst-firing pattern of activity has also been demonstrated in response to non-affective salient stimuli, as well as spontaneously (Freeman et al., 1985; Horvitz, 2000; Rebec et al., 1997; Wightman et al., 2007). A burst consists of a cluster of action potentials emitted at high frequencies (typically ~2-5 spikes at approximately 10-20 Hz; Grace and Bunney, 1984b). This firing pattern leads to a rapid increase in synaptic dopamine levels sufficient to overwhelm dopamine reuptake mechanisms, thereby facilitating activation of low-affinity post-synaptic D1 receptors at projection targets such as the NAcc (Dreyer et al., 2010). Consequently, burst firing has important functional consequences over and above that of a simple increase in firing rate and has therefore been extensively investigated. Several attempts at defining what constitutes a DA neurone burst of action potentials have been made by various different researchers, but the method of burst identification described by Grace and Bunney (1984b) has been most universally accepted and therefore adopted; according to their investigations, bursts are most appropriately defined as clusters of spikes in which the first interspike interval (ISI; the time between the start of two consecutive spikes) is less than 80msec and the interval following the cluster is greater than 160msec.

Given that spontaneous burst firing of VTA DA neurone burst firing is not witnessed during recordings in tissue slices *in vitro*, it is thought that this form of activity is primarily derived from synaptic input (Grace and Onn, 1989; Kalivas, 1993; Sanghera et al., 1984). PFC-derived glutamate represents one such input; increased activation of PFC glutamatergic projection neurones acts to increase the amount of burst firing of VTA DA neurones independently of mean firing rate (Carr and Sesack, 2000; Charlety et al., 1991; Overton and Clark, 1992; Sesack and Pickel, 1992; Tong et al., 1996). Selective knockout of NMDA receptors in DA neurones induces a specific disruption of burst firing without affecting background firing rate, implying that the NMDA receptors are key in mediating the glutamate effect on DA neurone firing pattern (Paladini and Roeper, 2014; Zweifel et al., 2009).

Tonic activity, in contrast, describes the spontaneous firing of DA neurones at frequencies of around 1-5Hz. The spontaneous depolarisation mediating this so-called "pacemaker" activity can be triggered by administering a depolarizing pulse during intracellular *ex vivo* recordings, or by rebound from a hyperpolarising pulse (Grace and Bunney, 1984a; Kita et al., 1986), and is therefore thought to arise from mechanisms intrinsic to dopamine cells. There is evidence to suggest that this pacemaker activity is caused by a feedback loop involving a TTX-insensitive and non-voltage-dependent Na^+ current to begin depolarisation in between spikes, followed later by a low-threshold TTX-sensitive depolarising Na^+ current bringing the membrane to spike threshold (Khaliq and Bean, 2010; Morikawa and Paladini, 2011). This process is then thought to be followed by a Ca^{2+}-dependent depolarisation, and finally, a Ca^{2+}-activated K^+ conductance which acts to reset the membrane potential (Fujimura and Matsuda, 1989; Grace, 1991; Harris et al., 1989). The result of the tonic spontaneous activity is a steady and low-level release of dopamine that, whilst failing to raise extracellular DA levels sufficiently to activate the postsynaptic D1 receptors, does have a tonic influence on the higher-affinity inhibitory D2 receptors. These D2 receptors are found on some neurones of the NAcc, mediating a tonic dopaminergic tone, as well as on the cell bodies and dendrites of the DA neurones themselves, where they function as inhibitory auto-receptors (Cooper, 2002; Dreyer et al., 2010; Grace, 1991). Through this latter mechanism, tonic activity acts to put a brake on DA neurone activity, generating an inverse relationship between tonic and phasic DA neurone activity (Wood, 2006).

I.I0 A note on GABA neurones

It is important to note that the connectivity of the GABAergic VTA neurones puts them in a position of potentially large influence, both in the regulation of dopamine neuron activity through their local axon collaterals, and in the regulation of the activity of striatal and cortical neurons through their projecting axons (Bayer and Pickel, 1991; Van Bockstaele and Pickel, 1995; Carr and Sesack, 2000; Korotkova et al., 2004; Melis et al., 2002; Szabo et al., 2002). Hence, investigations into the functioning of the VTA mesolimbic and mesocortical pathways need to also consider the activity of this cohort alongside the more extensively studied DA neurones.

I.II The role of the VTA in the pain-reward interaction

The fact that DA signalling, particularly in the VTA-NAcc pathway, clearly contributes to the processing of both noxious and rewarding stimuli is significant, as it places the VTA in prime position to mediate the pain-reward interaction when a situation involving these competing motivations calls for it.

Such motivational conflict arises more often than we might imagine; in the real world, at any one time, there can be several motivations. These, by definition, each has the potential to direct behaviour, whether it be to seek rewarding and appetitive events like palatable food consumption or to avoid aversive events, of which pain is arguably the most unpleasant. In the face of all of this, the animal has to decide on an action that is most beneficial to its survival. According to Howard Fields' Motivation-Decision model, this decision is driven by the motivation of the highest priority. Ultimately, the selection of action must involve inhibition of competing behavioural programs driven by the conflicting motivations. For example, if the benefit to survival of obtaining a reward is large enough, it can make sense to inhibit the 'escape' response to a noxious stimulus, either through subconscious (reduction of the pain experienced) or conscious (endurance of perceived pain) intervention.

This has been illustrated in animals by the study of Dum and Herz, which importantly showed that rats expecting rewarding food remained on a hot plate for twice as long as those expecting a less palatable variety, enduring higher, more noxious temperatures (Dum and Herz, 1984).

Conversely, it can also be beneficial for the animal to ignore a reward in order to appropriately respond to a noxious stimulus. Successful direction of behaviour in this way naturally requires the competing drives of noxious

input and reward to be able to modulate each other's effects on the brain, demanding a mutually inhibitory interaction between the pain and reward systems.

I.II.I Evidence for the existence of a pain-reward interaction

Exploration of the literature quickly confirms that such an interaction likely exists. In animals, noxious stimuli will interrupt feeding behaviour (Stevenson et al., 2006), whereas food consumption raises escape thresholds for noxious stimuli (Casey and Morrow, 1983; Dum and Herz, 1984). In humans, a similar relationship is shown by findings that perceived pain is reduced by pleasant stimuli, such as odours (Villemure et al., 2003), images (Kenntner-Mabiala and Pauli, 2005) and music (Roy et al., 2008). On a more serious note, patients with chronic pain typically have a reduced ability to gain pleasure from everyday rewards, leading to the higher prevalence of depression among these populations (Marbach and Lund, 1981). Presumably, this results from dysfunction of the reward system, perhaps as a result of the long-term, inescapable pain experienced by these patients. The case for an interaction between pain and reward-processing systems is further strengthened by the neuroanatomical overlap in the regions involved in each case (Leknes and Tracey, 2008). In fact, the pattern of brain activation seen during reward is so similar to that seen during pain that it has led some researchers to question if there is actually only one neural system underpinning both appetitive and aversive processing (Seymour et al., 2007). Finally, certain drugs of abuse including opioids and psychostimulants, addictive partly due to actions on the reward system, also have analgesic effects (Franklin, 1998, 1989), again suggesting an overlap of reward- and pain-related information processing. As discussed above, the VTA represents one possible key location of overlap and therefore integration of this information.

I.II.2 The role of opioids: instigating a hedonic bias

The question of how, in a conflict situation, the competing motivational reward and pain-related signals might interact within the VTA brings us back to the endogenous opioidergic modulatory system introduced in section I.4.I. Crucially, experiments with exogenous agonists show that these compounds simultaneously suppress nociception and directly activate the reward system. The latter action renders MOR agonists such as heroin highly addictive, leading to widespread recreational abuse.

The dual rewarding and analgesic properties of the μ-opioid system make it a focus of research in both the fields

of addiction and pain. Significantly, in the rat hot-plate experiments of Dum and Herz (1984), the suppression of pain responses by predicted food reward was prevented by administration of the μ-opioid receptor antagonist, naloxone. This provides strong evidence supporting the idea that, in circumstances in which a compelling reason not to respond to a noxious stimulus exists, endogenous opioids are released and act to mediate the inhibition of escape behaviours (Fields, 2007). In fact, opioids are thought to produce a shift in the 'hedonic spectrum' away from noxious avoidance behaviours and towards a reward-seeking bias. This is supported by observations that μ-opioid receptor (MOR) agonists enhance the subjective pleasantness and consumption of palatable foods and decrease the aversiveness of bitter foods as well as responses to noxious stimuli (Berridge, 2003; Kelley and Berridge, 2002), whereas, MOR antagonists decrease pleasantness of foods for rats (Hill and Kiefer, 1997; Parker and Rennie, 1992) and humans (Drewnowski et al., 1995; Yeomans and Gray, 1996). Thus, it appears that the opioid system, and μ-opioid receptors, in particular, are involved in reward-dependent inhibition of nociception.

Interestingly, studies bridging the gap between these two areas of research have revealed that the reward value and therefore addictive potential of exogenous MOR agonists is reduced when a patient or animal is in chronic pain (Ewan and Martin, 2011; Taylor et al., 2016). These results implicate opioidergic mechanisms in pain-induced inhibition of reward.

I.II.3 μ-opioid receptor action in the VTA: the disinhibition theory

Direct action of MOR agonists within the VTA has been of key interest to investigations into pain-reward interactions. The ventral tegmental area possesses high densities of μ-opioid receptors (Garzón and Pickel, 2001), and microinjection of MOR agonists directly into the VTA produces conditioned place preference, while at the same time increasing DA turn over in the NAcc (Funada et al., 1993). This suggests that the mesolimbic DA system mediates the reinforcing effects of morphine, and is supported by findings that morphine and heroin-induced conditioned place preference can be blocked by 6-OHDA destruction of the VTA DA neurones or DA antagonists in the NAcc (Phillips and LePiane, 1980; Shippenberg et al., 1993; Spyraki et al., 1983).

A widely accepted mechanism behind the activation of the mesolimbic DA system by opioids is indirect disinhibition via actions on the VTA GABAergic interneurones (figure I.4, Johnson & North, 1992). This mechanism was proposed on the grounds that systemic opioids increase VTA DA neuron firing (Gysling and Wang, 1983; Matthews and German, 1984), but decrease the activity of non-DA VTA neurones *in vivo* (Gysling and Wang, 1983). Furthermore, direct action of MOR agonists on neurones elsewhere in the nervous system tends

to be inhibitory (reviewed in North, 1992), making a chain of events involving MOR inhibition of non-DA neurones preceding DA neuron activation likely (Johnson and North, 1992). Studies have since shown that VTA microinjection of the selective MOR agonist DAMGO reduces GABA release in the VTA (Narita et al., 2001), further supporting the disinhibition theory.

Hence, a seemingly likely theory of the mechanism behind the pain-reward interaction during conflict situations implicates the dopaminergic neurones of the VTA in the decision-making process. It is suggested from the literature that the indirect opioidergic activation of these neurones, causing a rise in accumbal DA release, promotes a hedonic bias towards reward responsivity and a suppression of pain sensitivity and related behaviours. This is evidently an over-simplified vision of the interaction mechanism, which will inevitably need to possess a subtle flexibility if the outcome is to be optimal in our complex environments. Indeed, the original two-neurone model of Johnson and North has since been complicated by findings of opioid-inhibited dopamine neurones (Margolis et al., 2012) and opioid-unresponsive GABA neurones, implying that the model of Johnson and North is by no means the only mechanism of opioid action within the VTA (Margolis et al., 2012). Nevertheless, this theory at the very least represents a handy framework from which to expand or contradict.

As an aside, it is important to note that there is likely a significant influence of the anterior cingulate cortex (ACC) in the opioidergic control of DA release in the NAcc (Navratilova et al., 2015). Studies showed that relief of pain aversiveness was, at least in part, mediated by opioid action within the ACC, which in turn resulted in increased accumbal dopamine levels (LaGraize et al., 2006; Navratilova et al., 2015). The connection between neuronal activity in the ACC and that of the VTA remains ambiguous, but what is clear is that this mechanism specifically concerns suppression of affective components of pain, having no effect on sensory-discriminative aspects of perception (LaGraize et al., 2006). This is just one example of the complexity confronted when it comes to understanding pain processing in the brain, reinforcing the need to elucidate the functioning of this system through thorough investigation.

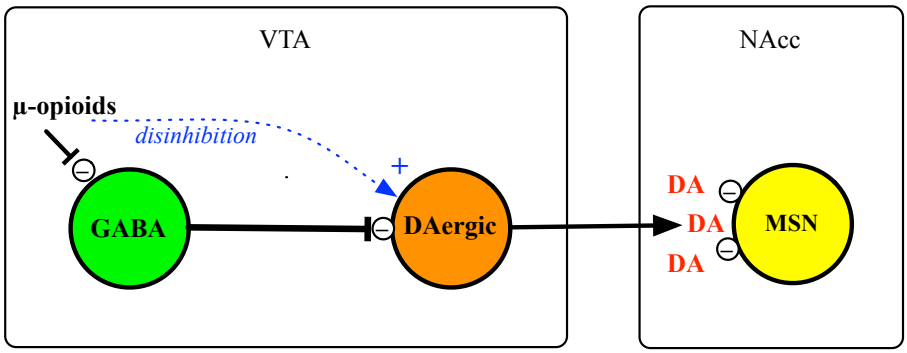

Figure I.4 Schematic diagram of opioid action in the VTA: the disinhibition mechanism. Diagram depicts the mechanism proposed by Johnson and North (1992). M-opioids inhibit GABA neurones (here shown to be located in the anterior tail of the VTA) via inhibitory μ-opioid receptors. The GABA neurones tonically inhibit VTA DA neurones via GABA(A) receptors, thus the action of μ-opioid receptor agonists within this region indirectly causes an increase in DA neurone activity (labelled disinhibition). This action in turn causes an increase in DA release in the NAcc (as well as other projection targets: not shown), and increased activation of inhibitory D2 receptors on medium spiny neurones of this area (MSN).

I.I2 The dopamine system in persistent pain

Despite extensive research, little is known about how persistent pain actually alters behaviour at the molecular and circuit level (Fields, 2007). What is becoming apparent, however, is that there are key differences in the way in which incoming nociceptive information is processed by higher centres during tonic versus phasic stimulation. Crucially for this investigation, evidence suggests that the functioning of the mesolimbic dopaminergic system is significantly altered in long-term pain (Altier and Stewart, 1999; Zhang et al., 2017). For example, DA agonists have been shown to induce analgesia in tonic but not phasic pain tests (Altier and Stewart, 1999), supporting theories of an enhanced role for mesolimbic DA signalling in pain relief in the former state. Further, NAcc-projecting VTA DA neurones display elevated firing rates in mice following chronic constriction injury (Zhang et al., 2017), and enhanced burst firing activity and concomitant NAcc dopamine release have been found in rats following peripheral nerve injury (Sagheddu et al., 2015). In contrast - or perhaps in response - to these hints of an upregulation of the dopamine system, there is evidence suggesting that the chronic pain condition ultimately results in a hypodopaminergic tone (Taylor et al., 2016); human imaging studies have found lowered responsiveness within the mesolimbic dopamine system in response to salient stimuli in patients with chronic pain (Loggia et al., 2014; Martikainen et al., 2015), and, in animal studies, chronic pain is associated with decreased c-Fos activation in the VTA (Narita et al., 2003) and decreased overall expression of striatal D2 receptors (Chang et al., 2014; Taylor et al., 2014; Wu et al., 2014). Interpreting these results in light of evidence supporting a

motivational salience encoding role of mesolimbic dopamine in Howard Fields' "Motivation-Decision Model" of pain (Fields, 2007) explains the witnessed disruption of motivated behaviour in the chronic pain state (Taylor et al., 2016). Hence, current evidence pains a confusing picture of the VTA's role in persistent pain, with hints of both up- and down-regulation of the functional role of the dopamine neurones. This is perhaps unsurprising given the suggested heterogeneity amongst this neuronal population in terms of reward and pain-related function in the naïve state (see section I.9).

One mechanism that may go some way towards explaining VTA neurone changes associated with persistent pain is endogenous opioid modulation. Given that endogenous opioid action and DA neurone activity are inextricably linked, it isn't unexpected that alterations in DA system function during persistent pain occur alongside changes in opioid control. In animal models of tonic inflammatory pain, such as carrageenan or formalin injection, an increase in the release of beta-endorphins is witnessed, and the analgesic efficacy of MOR agonists is enhanced (Hylden et al., 1991; Kayser and Guilbaud, 1981; Porro et al., 1991). VTA 6-OHDA lesions have been found to occlude the analgesic effects of systemic morphine in these tonic pain models, but not in the tail flick phasic pain test (Morgan and Franklin, 1990), implicating a DA-dependent mechanism of MOR agonist analgesia in tonic but not phasic pain. Together this evidence suggests an up-regulation of the μ-opioid modulatory influence, including that on VTA DA neurones, in inflammatory tonic pain states. In contrast, opioid action on the dopamine system appears to be reduced when a pain condition is chronic in nature; morphine-stimulated GTPyS (a measure of μ-opioid receptor activation) is reduced in the VTA, and systemic opioids fail to stimulate extracellular dopamine in the striatum in animals with chronic pain (Hipólito et al., 2015; Narita et al., 2004; Ozaki et al., 2002; Taylor et al., 2015, 2016). This manifests as a reduced effect of exogenous opioid administration in a chronic pain state, both in terms of rewarding effects (a higher dose was required to maintain self-administration; Ewan and Martin, 2011), and analgesic effects (clinical evidence suggests the analgesic properties of exogenous MOR agonists such as morphine are significantly reduced in patients with persistent pain conditions; Arnér and Meyerson, 1988).

In summary, evidence suggests that significant but divergent modifications occur in pathological pain states of differing nature: whist localised tonic pain is associated with a gain in DA and MOR-mediated analgesic influence, chronic neuropathic pain results in a contrasting reduction in the efficacy of these endogenous mechanisms. Despite substantial progress, there remain large gaps and substantial controversies in existing knowledge surrounding these neurotransmitter systems in pain, leaving confusion in the field.

One significant ambiguity that needs to be clarified is exactly where DA and opioid changes fit into the pathology of chronic pain. When the incoming nociceptive information to the VTA neurones persists over a long period of time, the evolutionary challenge changes; ignoring other motivations for the duration is potentially a very bad idea. Consequently, one might expect the role of DA in behavioural decision-making to be altered in persistent pain to maintain the optimal outcome. Following another logic, given the proposed analgesic role of a large subset of these neurones, dysfunction of the dopaminergic system could feasibly lead to the maladaptive pain sensitivity that characterises a chronic pain condition. Hence, when investigating pain system modifications in tonic or chronic conditions, we need to attempt to distinguish between adaptive counteractive measures that act to suppress any on-going pain, and causative pathological changes that contribute negatively to symptoms.

I.I3 Conclusions

In summary, it is well established that pain is unique as a sense, not only through possessing a powerful emotional component but also in relation to the complex and non-linear relationship between stimulus and the pain experience. This is heavily influenced by the extensive modulatory potential of the widespread supraspinal pain-processing regions, in concert with circumstantial neurochemical bias. The ventral tegmental area is one such region, balancing the potentially powerful motivational drive of reward with that of pain when these events are in competition. The inputs and outputs of the VTA cells are extensive, adding a layer of complexity to investigations into function; however, there is significant evidence to suggest that it is the DA neurones, under the biasing influence of opioids, that act to mediate the all-important pain-reward interaction. Aside from hints that this role is significantly up-regulated in persistent pain, there is a lot that remains unclear when it comes to the nature of these neurones' involvement in pain processing, suggesting further investigation will be both necessary and interesting.

Of key importance in the field of pain is the progression from acute nociceptive pain to a debilitating chronic pain condition. It is likely that many factors influence the precise mechanisms of persistent pain pathology, including the nature of the nociception such as inflammatory versus nociceptive, the duration of tonic versus chronic pain, and individual genetic differences. The variability of individual cases ultimately dictates that targeted treatments

need to be carefully designed and designated, and it is for this reason that we must invest significant efforts into understanding as much as we can on how factors such as these affect pain processing.

I.I4 Thesis aims

This thesis describes an investigation into the pharmacological and neurobiological nature of the role of the dopamine-releasing neurons of the ventral tegmental area in the interactions between pain and reward processing. The ultimate aim of these experiments collectively is to increase understanding of pain, in the hope that this information will act as a foundation upon which further developments in knowledge and ultimately the development of effective pain therapies can be developed.

Through a series of five projects employing intra-VTA *in vivo* electrophysiology in combination with a variety of pharmacological and nociceptive manipulations, this thesis explores this role of VTA neurones in the rat.

The individual experimental projects had the following aims:

1. To investigate further the electrophysiological markers of dopaminergic neurones in order to reliably identify these amongst the interspersed GABAergic and glutamatergic contingents. In these experiments, all neurones found in the VTA with a steady spontaneous firing rate will be characterised electrophysiologically, in terms of their action potential profile and spontaneous firing properties, functionally, in terms of responses to acute noxious stimuli, and pharmacologically, using morphine and naloxone to explore MOR functionality.

2. To assess the validity and reliability of using L-DOPA injection as a method of pharmacologically identifying VTA DA neurones: in short, to establish whether changes in SFR of VTA neurones in response to L-DOPA injection leads to the formation of putative neurochemically-distinct groups, and subsequently, whether confidence can be maintained in these groupings through further testing.

3. To move towards confirmation of the predicted L-DOPA mechanistic model of action on VTA neurones. Specifically, to establish the involvement of intra-VTA D2 activation in the mechanisms of L-DOPA action on VTA neurones.

4. To explore alterations in VTA neurone functioning in the more clinically-relevant state of tonic inflammatory pain. There is much evidence suggesting that activity of the DA neurones specifically will be modified upon induction of this carrageenan-induced condition. The potential role of endogenous mu-opioids in mediating these activity changes will subsequently be investigated with the systemic application of the MOR antagonist, naloxone.

5. Finally, to consider the case of chronic neuropathic pain. VTA neurones will be studied in the spinal nerve ligation rat model of this condition, and, as before, the influence of endogenous opioids will be assessed in order to probe the underlying mechanisms of enhanced pain sensitivity. Ultimately, it is hoped this will allow presumptions to be made on the role of the VTA neurones in the pathological state of chronic pain.

2. Materials and Methods

2.I *In vivo* electrophysiological recordings from ventral tegmental area neurones

2.I.I Animals

Male Sprague Dawley rats (250-350g) bred by the Biological Service Unit (University College London, UK) were used for electrophysiological experiments. Rats were group housed on a 12 h: 12 h light-dark cycle; food and water were available *ad libitum*. Temperature (20-22°C) and humidity (65-75%) of holding and procedure rooms were closely regulated. All procedures described were approved by the UK Home Office and in accordance with the Animals (Scientific Procedures) Act 1986 and IASP ethics guidelines (Zimmermann, 1983).

2.I.2 Set-up

2.I.2.I Anaesthesia, tracheotomy and positioning of animals

Awake rats were initially anaesthetised in a sealed induction box with an air inflow consisting of 5% v/v isoflurane delivered in a 3:2 ratio of nitrous oxide and oxygen. Once unconscious, rats were transferred to a nose cone delivering 3.5% v/v isoflurane and tested by pinching a hind paw with forceps to ensure they were areflexic; if anaesthesia was too light, a pinch of the hind paw caused the reflexive withdrawal of the corresponding leg. Once it was confirmed that the rat was in a state of sufficient anaesthetic depth, an incision was made in the skin above the throat, and the trachea exposed through blunt dissection of the surrounding muscle. A transverse incision was then made into the trachea and a polyethylene cannula was inserted and tied in place with sutures. The anaesthetic delivery tube, previously attached to the nose cone, was immediately attached to the tracheal tube, and rate of delivery was turned down to 1.5% v/v isoflurane to account for the more direct delivery via this route. Rats were then placed in a stereotaxic frame with the head firmly secured by ear bars and upper-jaw clamp. A rectal probe was inserted to monitor body temperature, which was maintained at 37°C through automatic feedback to a heat blanket.

2.I.2.2 Locating the ventral tegmental area

Immediately following the tracheotomy and stereotaxic positioning, a skin incision was made to expose the skull between and inclusive of bregma and lambda anatomical reference points (see figure 2.1). Desirable coordinates for electrode implantation into the VTA were determined as follows: 0.1-1.0 mm lateral, 5.6-6.9 mm caudal, and 8.9-9.0mm ventral to bregma (Paxinos & Watson, 1998), and a small hole for electrode insertion was drilled in the corresponding skull location. The dura was subsequently carefully removed with fine-tipped forceps such that the electrode could be inserted into the brain with minimal resistance.

Throughout the duration of each experiment, breathing rate, breathing pattern and skin colour were monitored and kept at one breath per second, in a regular pattern, and of a light pink hue, respectively. These measures were used to guide depth of anaesthesia and identify possible trachea cannula fluid blockages. If measures varied from these optimal states the level of anaesthesia was adjusted accordingly.

Schedule 1 was performed at the end of each experiment through isoflurane overdose (5% v/v) and cervical dislocation.

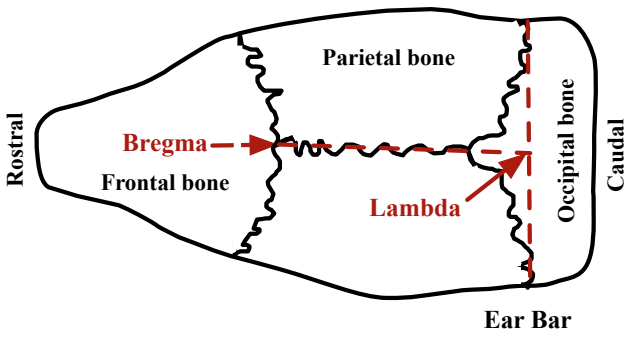

Figure 2.1 Diagram of the exposed rat skull. The diagram depicts the exposed rat skull as seen from above, with the rostrocaudal axis running from left to right. Black lines separating the skull bones depict cranial sutures. Reference points bregma and lambda are shown by the respective arrow tips, and red dashed lines show how lambda is found.

2.I.2.3 Recording location: electrolytic lesion confirmation

At the end of the first 19 successful experiments, an electrolytic lesion was made around the electrode tip to verify the position of the recording site in the brain. These lesions were achieved by switching the headstage (NL100RK Stimulus Control Headstage, Neurolog by Digitimer Ltd.) from recording to stimulating mode, allowing a stimulus of up to 100V to be applied through the recording electrode. An NL800 current stimulus isolator was connected to the NL100RK to deliver 10mA constant current output for 3 seconds through the electrode tip into the immediately surrounding region of the brain. This procedure creates a scar at the location of the recording electrode tip. The electrode was then removed, and the brains extracted carefully from the skull and placed in PFA for preservation. When it was time to determine the location of the electrolysis scar and therefore the recording location within each brain, the extracted brains were removed from the PFA solution, embedded in moulds with Optimal Cutting Temperature fluid (OCT), and flash frozen in a -80ºC freezer. The samples were then transferred to the cryostat chamber maintained at -16ºC to keep them frozen. One-by-one, the OCT-embedded brains were then mounted onto the cryostat platform and dissected into 30µm sagittal sections using a microtome until the electrolytic scar was visible. Slices were collected on glass slides and, once the OCT had melted and set, were placed in a freezer at ~-18ºC. The slides were viewed under a light microscope with 25x magnification, and photomicrographs were then taken of the coronal slices containing visible evidence of the electrolytic lesions by placing a smart phone camera lens on the microscope eye-piece. Photomicrograph images of the coronal sections were subsequently compared to those pictured in the rat brain atlas of Paxinos and Watson (1998) in order to establish the rostrocaudal location relative to bregma of each lesion-containing coronal slice, as well as the estimated dorsoventral and mediolateral coordinates of the lesion itself. The VTA was considered to include the parabrachial pigmented nucleus (PBP), paranigral nucleus (PN), caudal linear nucleus (Cli), interfascicular nucleus (IF), parainterfascicular nucleus (PIF) and the rostral linear nucleus of raphe (RLi). The recording locations (either within or surrounding the VTA) for all experiments during which electrolytic lesioning was performed were plotted on the Paxinos and Watson (1998) coronal slice map corresponding to the estimated rostrocaudal distance from bregma. An example photomicrograph with the corresponding atlas image revealing the location of different VTA nuclei is shown in figure 2.2.

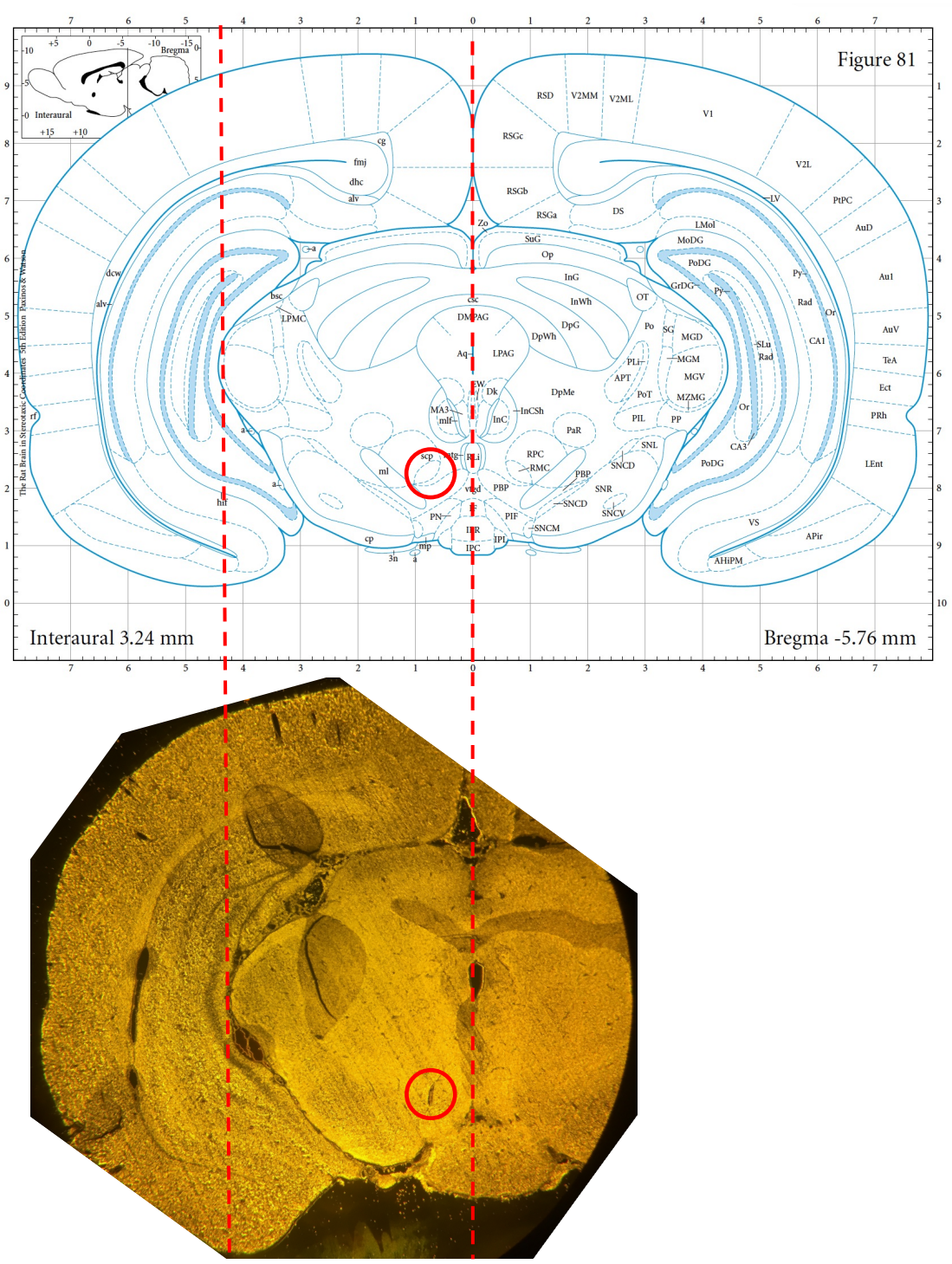

Figure 2.2 Example photomicrograph taken at 25x magnification under a light microscope of coronal brain sections containing electrolytic lesions. The bottom photomicrograph shows a representative 30µm coronal section cut from an OCT-embedded frozen rat brain specimen using a microtome. The diagram above is an extract from the Paxinos and Watson (1998) Rat Brain Atlas believed to most-accurately correspond to this coronal slice (rostrocaudal coordinates = bregma -5.72mm). The vertical dashed red lines indicate how the diagram and photomicrograph have been lined up. The diagram has been used to suggest a VTA sub-nucleus location of the lesion seen in the photomicrograph (red circles).

2.I.3 Electrophysiological recording procedure

See figure 2.3 for a schematic diagram of the recording system. Recordings were made using a parylene-C coated tungsten electrode with a shaft diameter of 127µm and a 12º tapering of the tip. For a 1kHz sine input, these microelectrodes have an impedance of 2MOhms (A-M Systems Ltd.). Electrodes were replaced every five experiments to avoid large deteriorations in recording quality due to the accumulation of tissue residue from repeated insertions into the brain. The recording system was grounded via a lead attached to the stereotaxic frame. A second lead ("B") was attached to the rat. The signal from the rat ("B") was subtracted from the signal from the electrode ("A") by the NeuroLog differential recording mode to reduce interference. Neuronal activity was amplified x10,000 by an AC pre-amp, filtered and then displayed on an oscilloscope as well as being made audible via a speaker system (figure 2.3). An amplification of 10,000x was chosen such that action potentials with amplitudes of around 100 microvolts would be optimally represented within the ±5V range of the 1401 and Spike2 waveform visualisation ($0.0001V \times 10^4 = 1V$). For all recordings, high pass (low cut) and low pass (high cut) filters were fixed at 500Hz and 1300Hz, respectively. These filtering parameters were deemed the most appropriate for the current experimental set-up for a number of reasons:

1) Recording within this range of frequencies allows capture of biphasic action potential waveforms of between 0.769 – 2.000msec in duration, thus ensuring minimal distortion of waveforms within the range of wavelength values implied from the various action potential duration measures quoted for dopaminergic and GABAergic VTA neurons in the literature (Li et al., 2012; Margolis et al., 2012; Ungless et al., 2004).
2) These frequency cut off values are similar to those used in previous *in vivo* extracellular electrophysiological characterisation studies of the VTA neurones (Brischoux et al, 2009: 300-5000Hz; Steffensen, 2008: 300-10,000Hz; Ungless and Grace, 2012, Ungless et al., 2004: 300-5000Hz; Panin et al., 2012: 400-1000Hz; Li et al., 2012: 600-5000Hz).
3) It was found by initial trial and error that lowering the high pass filter cut off below 500Hz, or raising the low pass filter cut off above 1300Hz caused significant reductions in signal quality and clarity. Hence, for the experimental set-up described, filtering out signals beyond these cut off frequencies was considered to be optimal.

Analogue signals were digitalised by a CED Micro 1401 mark II interface coupled to Spike2 software (version 6; Cambridge Electronic Design, UK). The Micro 1401 recorded waveform data, digital and marker information and simultaneously generated waveform and digital outputs in real-time with 16-bit resolution. A sampling rate of 20kHz was chosen for all recordings, as this rate allows sufficient resolution of extracellular action potential waveforms of the duration of around 1msec (Harris et al., 2016), whilst maintaining a manageable file size for recordings up to ~5 hours.

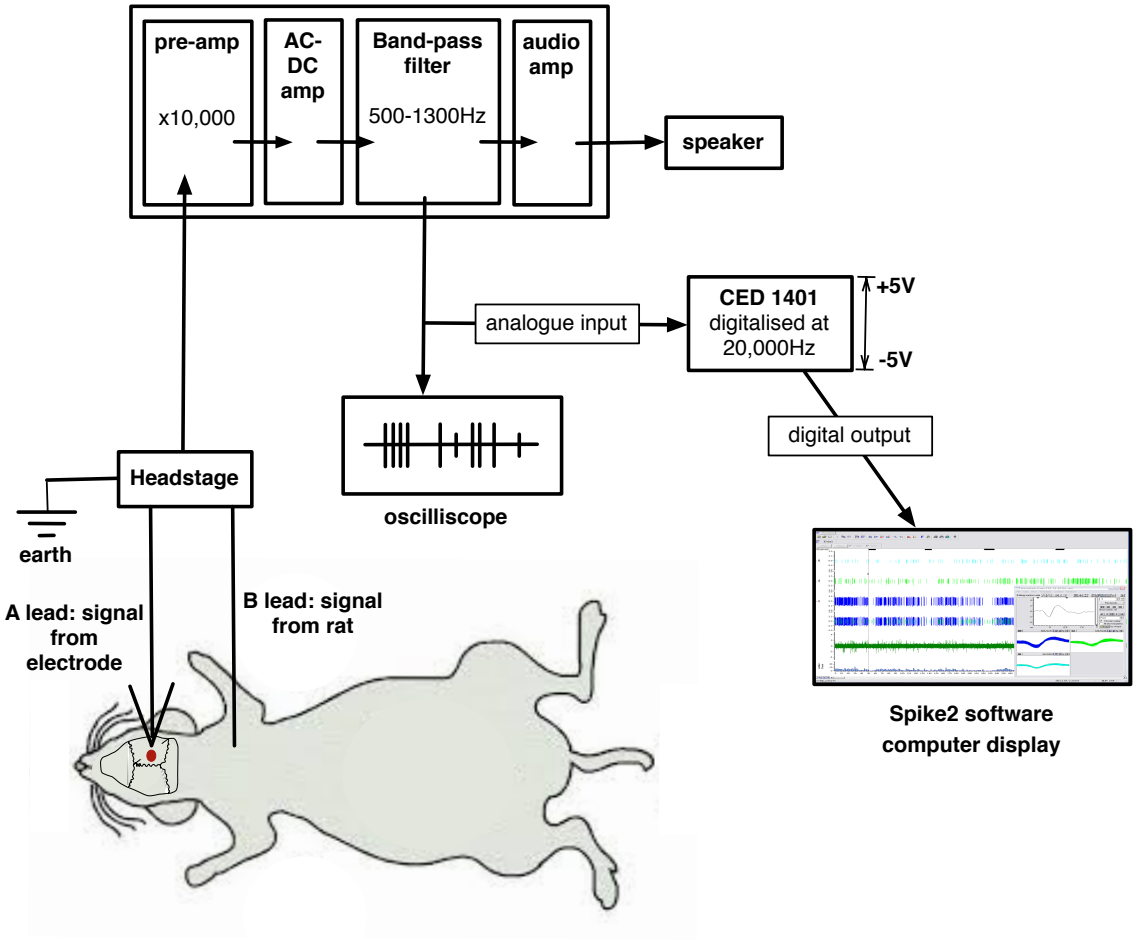

Figure 2.3 Overview of CED NeuroLog recording system. Input from the electrode inserted in the VTA (A), reference lead attached to the rat (B), and ground lead (earth), are fed into the headstage. Following subtraction of the B lead and ground inputs, the electrode signal is amplified by the pre-amp and AC/DC differential amplifier, passed through a high-pass and low-pass filter and then displayed on an oscilloscope. At the same time, the CED Micro 1401 mark II coupled to the computer Spike2 software digitalises and captures the resulting amplified and filtered signal throughout the experiment. To aid initial neurone detection a speaker is incorporated, making the resulting signal audible.

2.I.4 Searching for neurones

Once the desirable range of coordinates for the electrode tip had been calculated and an appropriate skull hole drilled (see section 2.1.2.2), the electrode tip was slowly lowered into the hole using the headstage micromanipulator. The insertion of the electrode continued until the tip rested in a position corresponding to the ventral boundary of the ventral tegmental area according to the reading of the dorsoventral coordinates. Typically, several spontaneous firing neurones were observable at this stage. The electrode was left in this position for 10 minutes to allow reactive distribution of the neural tissue to occur and deformation-related neural activity to subside. Following this, the electrode tip was slowly descended into the VTA until clear action potential signals were witnessed. The reliability of this activity was tested by again waiting for ~10 minutes to allow for subsiding/ relaxing of the neural tissue following distortion by the electrode to take place and to make sure that the activity was indeed spontaneous rather than evoked by electrode-related tissue distortion. If a clear signal (good signal to noise ratio) of action potentials of one or more amplitudes was observed on the oscilloscope and heard through the speakers, this location was selected for recording. If this was not found to be the case, the search for neurones continued by either descending the electrode more dorsally into the VTA (if not already near the dorsal boundary of the range of coordinates corresponding to the VTA location), or by raising the electrode out of the brain and selecting a new set of mediolateral and rostrocaudal coordinates within the range determined for the VTA and performing a subsequent descent.

2.2 Analysis

2.2.I "Spike sorting"

A single electrode will typically detect neurones over an area of 150-200μm from the tip (Harris, 2016). The majority of the incoming neuronal electrical signals will be indiscernible from the rest of the background noise – itself generated by a combination of multiunit activity and other electrical interference sources; however, neurones located within a ~50μm radius from the tip are likely to produce signals that are large enough to be detected reliably and distinguished from the background noise. Consequently, it is assumed that all neurones selected to be recorded in the current experiments lie within a ~50μm range from the electrode tip; however, it is important to note that the area over which neurones can be recorded will decrease as electrode impedance increases, which is both a factor of the electrode composition and tip diameter (Harris et al., 2016). The precise range of the 2MΩ

tungsten electrode with 12º tapering at the tip used in the current experiments was not found in the literature, but it is thought to be reasonably safe to assume that it is not far off the above-quoted range of 50µm. If the density of neurones within the ventral tegmental area is similar to that of the cortex, the estimated distance between neurone cell bodies would be around 40µm. This would mean that a single extracellular electrode would typically pick up more than one spontaneously active neurone at a time. It is possible to take advantage of the simultaneous recording of several surrounding neurones by separating out their electrical signals emerging using dimensions other than waveform amplitude. This was done in this instance through the analysis of action potential ('spike') waveform shape using Spike2 template-sorting software (Cambridge Electronic Design, version 6) both before and after each recording was undertaken. The shape of an action potential recorded through an extracellular microelectrode is determined by the morphology of the dendritic tree, as well as the distance and orientation relative to the electrode itself (Gold et al., 2006). Consequently, differences in waveform were assumed to represent different neuronal sources, and all spikes that fit into one waveform template were assumed to come from an individual neurone, provided template selection was performed to an optimal standard.

2.2.I.I Online template selection

Once a recording location had been selected, a new Spike2 data file was created. This caused the template setup window to open. This window displayed the real-time waveform on voltage and time axes and allowed the adjustment of upper (positive) and lower (negative) amplitude thresholds (referred to as "trigger levels") in order to optimize the trade-off between filtering out the background noise and capturing discernible neuronal activity. Waveform "templates" were then generated via an automated Spike2 process until each waveform reappearing at least 8 times, at a frequency of at least one per 50 spikes, was found to already be represented in the existing selection of templates. If templates appeared to be too selective, resulting in multiple templates with visibly similar shapes produced, or too unselective (waveforms falling into any one template were visibly too variable), selectivity could be adjusted by either manually widening or narrowing the template boundaries (the boundaries within which a waveform had to fall in order to be classified under that template identity), or adjusting the percentage of points along a waveform that had to fall within the template boundaries in order to be classified under that template identity (this value was always initially set at 60%). Visually similar templates could be manually merged if it was deemed necessary. Once confident in the selection of templates that resulted, the recording of spikes in the respective template channels begun. To enable the visualisation of neuronal activity during the experiment, spikes belonging to the different templates were shown in different "wavemark channels"

in the trace window (figure 2.5). Wavemark channels only contain selected sections of the raw waveform trace – specifically, the sections of the waveform classified as an action potential according to the Spike2 algorithm for spike detection. Steps involved in this are as follows (figure 2.4):

1. Wait for the signal to lie within half the trigger levels (upper and lower amplitude thresholds, see above). When it does, go to step 2
2. Wait for the signal to cross either trigger level. If it crosses the upper trigger level go to step 3. If it crosses the lower level, go to step 4
3. Track the positive peak signal value. If the signal falls below the peak and there are sufficient post-peak points to define a spike, go to 5. If the signal falls below half the upper trigger level, we ignore further peaks
4. Track the negative peak signal value. If the signal rises above the peak, see if we have sufficient post-peak points to define the spike. If so, go to 5. If the signal rises above half the lower trigger level, we ignore further peaks.
5. Save the waveform and first data point time and go to step 1 for the next spike.

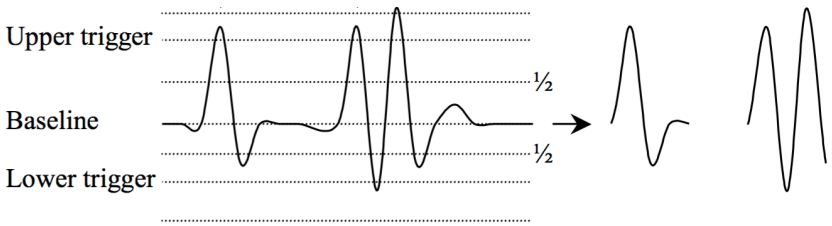

Figure 2.4 Diagram of the spike detection algorithm from Spike2 software. The diagram shows upper and lower triggers, which represent the amplitude thresholds set to capture spike signals and filter out the majority of the noise, and two example waveforms representing biphasic (left) and triphasic (right) action potentials. The two waveforms on the right-hand side of the horizontal arrow show the traces that would result from the signal shown on the left-hand side after the Spike2 spike detection algorithm is run. *Adapted from the Spike2 for Windows version 6 manual.*

The waveforms within the wavemark channels are colour-coded according to template identity, and "action potentials" not falling into any of the generated templates are presented in black. For the sake of clarity, a separate wavemark channel was created for every one of the spike templates such that activity thought to originate from different neurones could be monitored separately. Examples of individual action potential waveforms as recorded on the Spike2 software are shown in Appendix A.

2.2.I.2 Post-hoc offline template selection

Once the experiment had been completed and the recording terminated, it was possible to re-define waveform templates according to the various action potential shapes featuring in the electrode input throughout the entire experiment (figure 2.5: waveform templates). The purpose of this re-defining stage was to further optimize the template parameters, such as to maximise the chance that action potentials belonging to the different waveform templates originated from different neurones. Re-defining was done using the offline "Edit Wavemark" window in Spike2 (figure 2.5). The selection of optimal templates was guided by three main principles:

1) Principle component-related cluster analysis was performed in Spike2. This process selects three action potential waveform elements (e.g. slope of the upwards inflexion or duration of the trough) that best differentiate all spikes within the sample which consisted of the entire recording period. The measurements of these elements for all spikes are then represented on a 3D interactive graph (figure 2.5), enabling visualisation of any clustering within the population. Action potentials positioned closer together within the 3D space are deemed more likely to have been generated by the same neurone.
2) The firing rate histogram for the entire duration of the experiment was visualised for each template's wavemark channel. If two channels appear to be showing a strong degree of mirroring in the minute-to-minute changes in firing rate, the corresponding templates were combined.
3) Amplitude differences were largely ignored if criterion 2) was met, and all other shape properties of the spike templates lined up. Action potentials emanating from any one neurone are known to change for a number of reasons, including a diminishing of amplitude during burst firing, and a slow reduction or increase as neural tissue gradually relaxes away from or towards the recording electrode.

Following this template selection process, every action potential occurring throughout the entire experiment was sorted into the template of best fit. If a waveform fell outside the criteria for all selected templates, it was filtered out as noise. All action potentials for any given template were subsequently represented in a corresponding a wavemark channel (figure 2.5). Traces showing the firing rate histogram (i.e. how many action potentials fitting into a given template are detected every 1 second) or individual action potentials of a given wavemark channel are shown on different time scales in Appendix A.

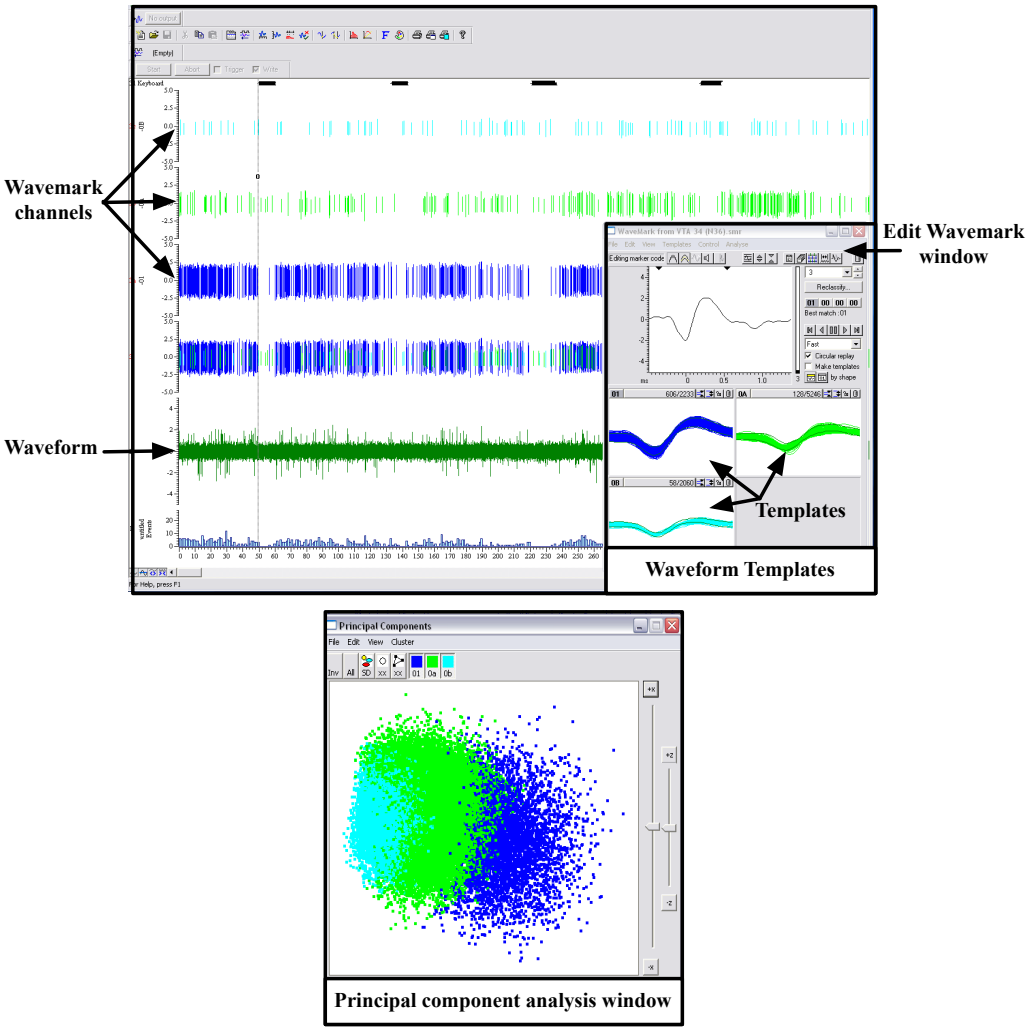

Figure 2.5 Template generation and spike sorting using Spike2 software. *Edit Wavemark window*: enables post-hoc offline template generation and optimisation. *Waveform Templates*: templates are formed from the incoming signal from the electrode (visible in the Edit Wavemark window), with a different template for each differing waveform shape consistently present in the input (three different templates- blue, green and turquoise- are shown here). *Principal components analysis window*: the template array is optimised using principal components analysis, such that different templates most likely represent action potentials derived from different surrounding neurones. *Wavemark Channels:* when optimal templates are decided upon, the action potentials occurring throughout the duration of the experiment are represented as individual waveform traces in a wavemark channel. Separate colour- and number-coded wavemark channels exist for each template, such that only action potentials fitting into a given template are shown in that template's corresponding wavemark channel. Small black dashes positioned above the wavemark channels represent keyboard input and indicate where a stimulus, noxious or innocuous, was applied.

2.2.2 Noxious and innocuous stimulation

Two noxious and two innocuous control stimuli were repeated as a set of four at chosen time points throughout the experiment; presentation of the four stimuli for 5 seconds each, separated by 20s, formed one 'stimulation

round'. A minimum of four stimulation rounds were performed before any pharmacological procedure was undertaken to ensure each neurone displayed visibly stable spontaneous and stimulus-evoked firing rates.

The stimuli, presented in innocuous-noxious pairs, were as follows:

- **4g von Frey filament, 60g von Frey filament** – applied to the left hind paw with sufficient force to bend the filament repeatedly at a rate of 1 application per second throughout the 5-second stimulation time window. The von Frey stimulation was limited to the glabrous skin on the base of the paw, and the precise location at which the von Frey made contact with the skin was varied during each 5-second stimulation in order to not over-stimulate and sensitize a particular section of the paw.
- **Paw immersion in 35°C water; paw immersion in 50°C water** – the left hind paw was placed in a small vessel such that the joint between the top of the paw and the leg rested on the near edge, and the paw was angled downwards into the vessel. Water of the respective temperatures was poured into the vessel until it reached the top and the majority of the paw was submerged (with the exception of the heel that was raised above the vessel rim). The paw remained submerged in the water for 5 seconds, and then the vessel was removed from underneath the paw, terminating contact with the water. After removing the water from the vessel, it was again placed underneath the paw in the same position, such that the paw was rested at the same angle for all measurements of spontaneous and evoked firing rate.

2.2.3 Quantifying VTA neurone activity:

2.2.3.I Spontaneous activity

Many neurones of the VTA display spontaneous activity in the anaesthetised condition. As noted above, only neurones maintaining a relatively stable spontaneous firing rate for the duration of the four pre-drug stimulation rounds were used for further experimental protocols. Neurones failing to show this stability were rejected and a new search in the anaesthetised animal was conducted. Values of spontaneous firing rate were calculated as the mean of the mean spontaneous firing rate (SFR; action potentials per second) in each 10-second time bin before application of each of the 4 x 4 stimuli (i.e. the mean of all 16 readings of mean SFR). This pre-pharmacological manipulation condition is referred to as the "baseline condition", and SFR during this time is referred to as baseline SFR (BL SFR). On average, the baseline period lasted for ~40 minutes, with exact durations depending on how

long it took for a neurone or set of neurones to "settle" into a more stable firing behaviour following the distortion of the tissue by the electrode insertion.

2.2.3.2 Stimulus-evoked activity

A neurone was classified as responsive to a noxious stimulus if the mean of the mean SFR during each 5s stimulation of that kind during the baseline recording period was greater or less than the mean baseline SFR ± 1.96 times the standard deviation of the mean baseline SFR. I.e. for any given stimulus, a neurone is classified as responsive if:

$$\sum(mean\ SFR\ during\ 5s\ stimulation) \gtrless mean\ baseline\ SFR \mp 1.96 \times SD\ mean\ baseline\ SFR$$

2.2.3.3 Pharmacological effect

Several different pharmacological agents were administered throughout the described sets of experiments. The main effect of interest in these experiments is an alteration in the spontaneous firing rate of the recorded neurones (other effects were also explored in a few instances – see individual chapter materials and methods). At each time point of interest post-agent injection there were 4x measurements of mean SFR, each taken across 10-second time bins (Hz). The mean SFR for any particular time point was taken as the mean of these 4 values. The time points recorded varied for the different pharmacological agents (see chapter 3,4,5,6 & 7 materials and methods sections), with a frequency depending on the predicted speed of action. Cluster analysis was performed using SPSS software to establish the existence of any response-based groups within the recorded populations; for each pharmacological test, two-step cluster analysis with an Euclidean distance measure on mean SFR values of all experimental neurones at all time points (unless otherwise specified) post-injection was conducted to reveal the number of natural clusters within the dataset (see section 2.2.4). Subsequently, an iterative K-means cluster analysis (Euclidean distance measure) was conducted to identify the optimal cluster centres within the population and to assign cluster membership to each neurone. All clusters established were given a name that reflected both the analysis resulting in the cluster assignment and the state in which the neurone was recorded – see appendix C for a list of all clusters established throughout this thesis.

If the baseline SFR within a given recorded population was too variable to visualise group patterns in response to a pharmacological agent using the untransformed dataset, neuronal responses were normalized by converting

mean SFR at each time point post-injection into a percentage of the mean pre-injection SFR of that neurone. Subsequent analyses were then performed using mean normalized SFR values, including cluster analysis as described above.

2.2.4 Statistical analysis

All statistical analyses were performed using SPSS v22 (IBM, NY, USA). Specific details of tests used are described in individual sections. Bonferroni-adjusted alpha values were used when repeated tests were conducted on any one data set. Equivalent non-parametric tests were performed if data were not normally distributed, or violated any other assumptions of a given parametric test. Cluster analyses were used to establish natural groupings within a population of recorded neurones according to any one or a range of characteristics. Two-step cluster analysis works by comparing the values of a model-choice criterion across different clustering solutions to automatically determine the optimal number of clusters (IBM support). Hence, before any subsequent cluster analysis was conducted, the two-step process was adopted to first establish the number of clusters the data should be sorted into.

2.2.5 Reasons for data omission

Data collected from recorded neurones was occasionally omitted from further analysis to increase the validity of population results. The criteria for rejection included:

1) BL SFR <0.1 Hz
2) Post-injection drop-off of SFR to values ~<0.1 Hz, unless SFR recovered as the pharmacological agent effects reduced, or upon antagonist injection/ injection of another agent
3) Premature termination of the experiment (due to unexpected death of the animal, for example) such that relevant time points were not reached
4) Non-representative increases of SFR post injection of a pharmacological agent, such that normalized values at any time point post-injection were greater than 1000%
5) A highly variable SFR within the baseline condition (not recorded for the duration of the experiment unless a stable neurone was simultaneously recorded from that location)

The numbers of neurones recorded for the duration of the experiment in each of the experimental investigations that were omitted from analyses are detailed in Appendix B.

3. Electrophysiological Characterisation

3.I Introduction

3.I.I Cell characterisation in the VTA

In order to fully understand dopaminergic participation in pain and reward processing, one needs to study the system *in vivo* with both local and brain-wide connections, such as the mesolimbic pathway, intact. Unfortunately, however, a consequence of an *in vivo* approach is that experimental procedures typically involve going in 'blind' in the traditional sense: unable to actually visualise the centre of interest before or during the investigation. As a result, reliable neurochemical identification of a neurone, essential if results are to be integrated into the wider literature, can prove difficult.

In attempts to dismiss lack of visual access as a limitation, several researchers have set out to characterise, thereby creating a marker for, DA neurones in the VTA both pharmacologically and electrophysiologically. Due to proximity and roughly similar electrophysiological properties to the VTA, the relatively straightforward electrophysiological classification of substantia nigra (SNc) DA neurones, defined as having relatively long-duration action potentials, low firing rates (<10Hz), irregular or burst firing, relatively broad duration action potentials (>1.1msec) and DA agonist-induced inhibitions, served as a model for the initial studies of those in the VTA (Grace and Bunney, 1983; Grace and Onn, 1989). Predictions of simplistic cytoarchitecture were reinforced by the pharmacological investigations of Johnson and North. They proposed a model circuit of the VTA consisting of two neuronal types: the 'principal' neurones, presumed to be dopaminergic based on their inhibition by DA agonists and lack of response to MOR agonists, were more numerous and displayed lower spontaneous firing rates as well as longer action potentials than the other 'secondary' neurones (Johnson and North, 1992b). Immunohistochemistry using tyrosine hydroxylase (TH), the rate-limiting enzyme involved in the production of DA, further supported the dopaminergic identity of the principal neurons. The secondary neurones, characterised

by short-duration action potentials (0.5ms), rapid firing rates and MOR agonist-inhibition, have been identified as GABAergic in intracellular single-cell labelling studies *in vivo* (Steffensen et al., 1998).

Despite wide acceptance, however, this model was eventually found to be too simplistic. Discovery of a third type of VTA neurone now known to be glutamatergic, lacking TH immunoreactivity, but displaying the characteristics previously thought to be exclusive to dopaminergic neurones, soon added complexity to the picture (Cameron et al., 1997). Proportions of these three types are now thought to be around 60-70% dopaminergic ('principal'), up to 30% GABAergic ('secondary') and perhaps 2-3% glutamatergic ('tertiary', Ford et al., 1995; Kalivas, 1993; Nair-Roberts et al., 2008b; Tsuyoshi et al., 2007b). Over time, more of the common putative DA-specific criteria taken from the SNc were found to be inconsistent in differentiating DA neurones from non-DA neurones in the VTA (Margolis et al., 2006), resulting in a confusing and ambiguous picture. What is becoming indisputable, however, is that the VTA is a region with high heterogeneity within neurochemical populations. For example, a subset of cortically projecting DA neurones have been shown to display high firing rates (a trait previously attributed to only GABAergic neurones) and a greater degree of burst firing than the rest of the population (Chiodo et al., 1984). Further, significant overlap in the AP durations reported for GABA and DA neurones has been reported (Hyland et al., 2002; Kiyatkin and Rebec, 2001; Li et al.; Margolis et al., 2012; Pan et al., 2008), and heterogeneity in response to MOR activation has been shown in both confirmed GABA and DA neurones (Cameron et al., 1997; Ford et al., 2006; Gysling and Wang, 1983; Margolis et al., 2012, 2003; Matthews and German, 1984). The number and structure of functional subgroups within VTA DA and GABA neurone populations are yet to be determined, necessitating the further exploration of this crucial part of the pain-processing pathway.

3.2 Aims and predictions

This set of experiments attempts to generate a robust electrophysiological marker of dopaminergic neurones in order to reliably identify these amongst the interspersed GABAergic and glutamatergic contingents. Given that current literature suggests dopaminergic neurones largely display slow irregular or burst firing, it is predicted that a subset of the recorded population will possess these baseline firing characteristics. Furthermore, given the dopaminergic contingent is estimated to make up around 60-70% of the VTA neurones, it is predicted that these characteristics will be more prevalent in the population than those thought to be characteristic of the GABAergic contingent (fast, regular firing). This hypothesis will be tested by establishing overlap between measures of the continuous and discretely defined characteristics. Further, despite established heterogeneity within neurochemical groups, response to MOR activation and noxious stimulation will be investigated in order to further characterise the VTA neural population and to allow comparison with findings in the previous literature.

All neurones found in the VTA with a relatively stable spontaneous firing rate will be characterised electrophysiologically, in terms of their spontaneous firing rate and degree of burst firing, functionally, in terms of responses to acute noxious stimuli, and pharmacologically, using morphine to explore MOR functionality.

3.3 Materials and methods

3.3.I Animals

Male Sprague Dawley rats (250-350g), bred by the Biological Services Unit (UCL, London, UK) were used for electrophysiological experiments.

3.3.2 Experimental protocol

In vivo electrophysiology was performed as described in section 2. See figure 3.I for the experimental timeline. One stimulation round in this study consisted of two 5-second paw von Frey stimuli (4g followed by 60g), followed 10 seconds later by a 5-second innocuous (35ºC water) and then noxious thermal stimulus (50°C water). At least four stimulation rounds covering at least 30 minutes of recording time were undertaken in the baseline condition to ensure a stable spontaneous firing rate, after which rats were dosed subcutaneously with $2mgkg^{-1}$ morphine sulphate (MOR agonist, Thornton and Ross Ltd., UK), or with an equivalent volume of the saline injection vehicle only ("vehicle control experiments"). Spontaneous firing rates were monitored for the next hour post-injection through repetition of stimulation rounds at every 10 minutes up to 60 minutes post-injection. Separate "time-control" experiments were performed in five rats to check for any significant set-up influences on neuronal firing rates throughout a two-hour recording period. In these experiments, neuronal recordings were undertaken for a duration of two hours with no pharmacological intervention taking place, and measurements of mean spontaneous firing rate (calculated from measurements across 4 x 10-second time bins) taken every 10 minutes.

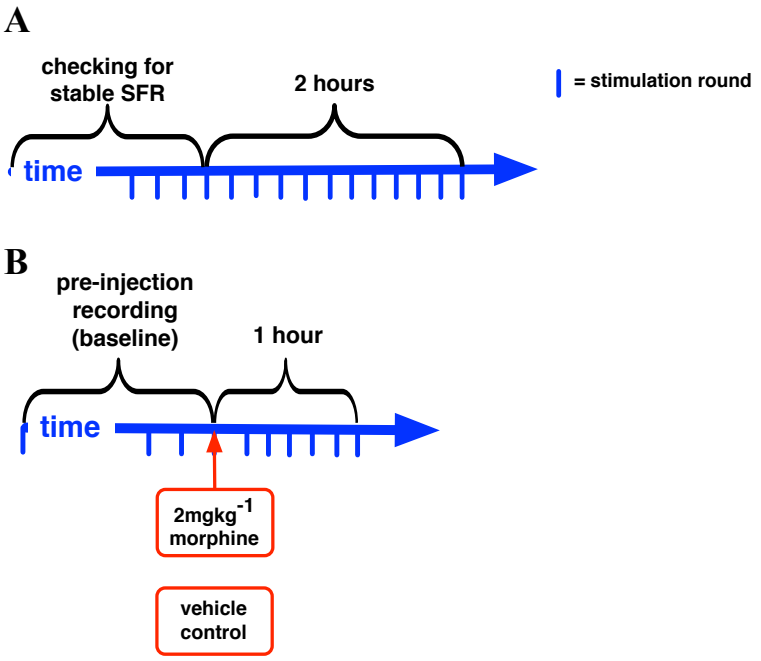

Figure 3.1 Experimental timeline of characterisation experiments. The thick blue horizontal arrow represents the progression of time during the experiment, while vertical blue dashes indicate the times at which stimulation rounds were performed (stimulation round = presentation of 2 noxious and 2 innocuous stimuli). In all experiments, at least 4 stimulation rounds were performed in the baseline condition in order to check that the neurones had a relatively stable spontaneous firing rate (not all rounds are depicted). A) *Time controls:* stimulation rounds were performed every 10 minutes up until the 120-minute time point, as measured from the point at which it was decided that the neurones were stable enough for a recording. B) *Morphine or vehicle control injection*: stimulation rounds were performed every 10 minutes up to an hour post morphine or vehicle control injection.

3.3.3 Analysis

Following template-based data extraction methods detailed in section 2.2.I, both stimulus-evoked and spontaneous SFR values at each time point were extracted from each neurone's corresponding firing rate histogram.

3.3.3.I Analysis of spontaneous firing characteristics

The spontaneous firing of all recorded neurones was characterised according to:

1) the mean spontaneous firing rate in the baseline condition (BL SFR)
2) the pattern of firing in the baseline condition

3.3.3.2 Baseline spontaneous firing rate (BL SFR)

The mean BL SFR was measured for all neurones recorded in all experiments, and all values were included in the analysis described in this chapter (excluding those recorded from neurones in animals that received pre-experimental treatment). Two-step cluster analysis followed by K-means cluster analysis was performed on values from all neurones in SPSS to establish the existence and characteristics of natural clusters within the dataset.

3.3.3.3 Burst firing

The degree of burst firing of any given neurone was measured as the percentage of spikes fired within a burst (%SIB). A burst is defined as a period of rapid firing with an onset threshold interspike time interval (ISI) of 80ms, and an offset defined as an ISI of ≥160ms (Brischoux et al., 2009; Grace and Bunney, 1984b). The mean number of spikes in each burst and the burst frequency (1/mean inter-burst interval) was also extracted for each neurone. The extraction of these values was done using the Bursts2 script downloaded from the Cambridge Electronics Design Ltd. website with the following parameters manually defined: minimum number of spikes in a burst = 2, max interval for burst onset = 80ms, and max interval within a burst =160ms, respectively. Two-step and K-means cluster analysis was performed in SPSS to establish the existence and characteristics of natural clusters within the dataset. Finally, ISI frequency histograms for individual neurones (assuming that a given waveform template represents activity from a single neurone) with low, medium and high %SIB and low and high BL SFR (as sub-divided cluster analysis) by were constructed as representative examples for visualisation.

3.3.3.4 Noxious responsivity of neurones

The responsivity of neurones to both paw von Frey and paw heat stimuli was assessed using criteria detailed in section 2.2.3.2 during the baseline condition.

3.3.3.5 Morphine effects on firing rate

Morphine effects on spontaneous firing rate were quantified as described in section 2.2.3.3. The time points analysed were 10, 20, 30, 40, 50 and 60 minutes post-injection of morphine. These effects were compared to those seen amongst the neurones recorded in the vehicle control injections in order to separate pharmacological effects from other injection-related effects.

3.3.3.6 Neurone location: histological confirmation

Recording electrode locations were established through electrolytic lesioning and subsequent slicing of the brains of 19 animals used for experiments, as described in section 2.1.2.3. These locations in terms of dorsoventral and mediolateral coordinates were plotted on a coronal section diagram taken from the rat brain atlas of Paxinos and Watson (1998), with the chosen section (i.e. rostrocaudal distance from bregma) being that judged to be the closest resembling anatomical shape to that seen in the photomicrograph of the brain slice of interest. The following data were collected:

1) Number of brain specimens sliced with no clear lesion found
2) Number of recording locations residing within designated VTA sub-nuclei (see section 2.I.2.3)
3) Number and identity of recording locations residing outside the designated VTA sub-nuclei (i.e. extra-VTA recordings)

3.3.3.7 Neurone location: graphical representation

Electrode tip position in terms of dorsoventral (y-axis) and mediolateral (x-axis) stereotaxic coordinate measurements was plotted on an x-y scatter graph superimposed on an atlas image (Paxinos and Watson, 1998) corresponding to the coronal plane given by the rostrocaudal stereotaxic coordinates. The rostrocaudal and dorsoventral coordinates were also plotted on the sagittal plane corresponding to the mediolateral coordinates of a given recording. Neurones excited or inhibited by noxious stimuli, or displaying a response to morphine injection, were mapped in this way to establish location differences of neurones with given characteristics.

3.4 Results

3.4.I Time control experiments

Five "time control" experiments were conducted, from which seven neurones were recorded for the duration of the two-hour period. Two neurones were discarded because firing rates were deemed too variable within each time point to compare across the time points. It was decided that neurones displaying similar variability in BL SFR across short timescales would be rejected in the remainder of the investigations described in this thesis. The remaining neurones (figure 3.2A) showed a varying degree of fluctuation in SFR throughout the 2-hour recording period, typically involving ~20-minute deviations from the SFR values of the previous few time points (e.g. neurone N1 30-50 minutes, N4 40-60 minutes). For 3/5 of the recorded neurones, there was no significant difference between the mean spontaneous firing rate at t = 0 minutes and t = 120 minutes (N5, N4 and N1; Figure 3.2B). The remaining two neurones showed a significant decrease in spontaneous firing rate when comparing the first and last time point (paired-samples *t*-test: neurone N3 $t(4) = 4.279$, $p<0.05$; neurone N2 $t(4) = 4.484$, $p<0.05$).

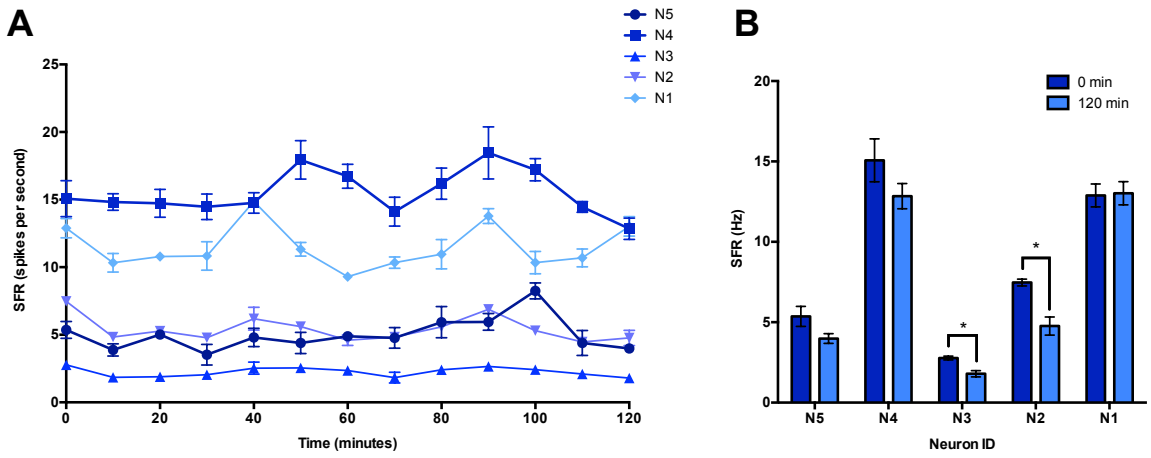

Figure 3.2 Spontaneous firing rate of neurones recorded in time-control experiments. A) Graph shows traces corresponding to the mean spontaneous firing rate value (Hz, y-axis) of a set of 5 individual neurones at 10-minute intervals (x-axis) up to the 120-minute time point. Data points and bars show mean ± SEM. B) Bars shown mean ± SEM SFR values (Hz, y-axis) of each neurone at time points of 0min (darker blue bars) and 120min (lighter blue bars). Comparisons between mean SFR values at the two time points were made for each neurone with paired-samples *t*-tests. * P<0.05.

3.4.2 Spontaneous firing rate

Mean baseline spontaneous firing rate was calculated for 222 recorded neurones. Neuronal BL SFR ranged between 0.10-14.58Hz, and the mean value for the whole population was 3.22Hz ±0.22Hz. The population SFR

values were not normally distributed (Shapiro-Wilk's test: $p<0.05$), with skewness of 1.503 (SE = 0.170) and kurtosis of 1.824 (SE = 0.339). Two-step cluster analysis on SFR values established the existence of two high-quality clusters within the population values (figure 3.3), and K-means cluster analysis deemed cluster centres to be 2.00Hz±0.11Hz (BL SFR cluster 2n, N=193) and 8.94Hz±0.38Hz (BL SFR cluster 1n, N=29). An independent-samples *t*-test was conducted to assess the statistical validity of the two cluster-based separation. Results of this analysis revealed a highly significant difference between mean BL SFR values of BL SFR cluster 1n and 2n (figure 3.3B; independent-samples *t*-test: $t(220)=21.30$, $p<0.0001$).

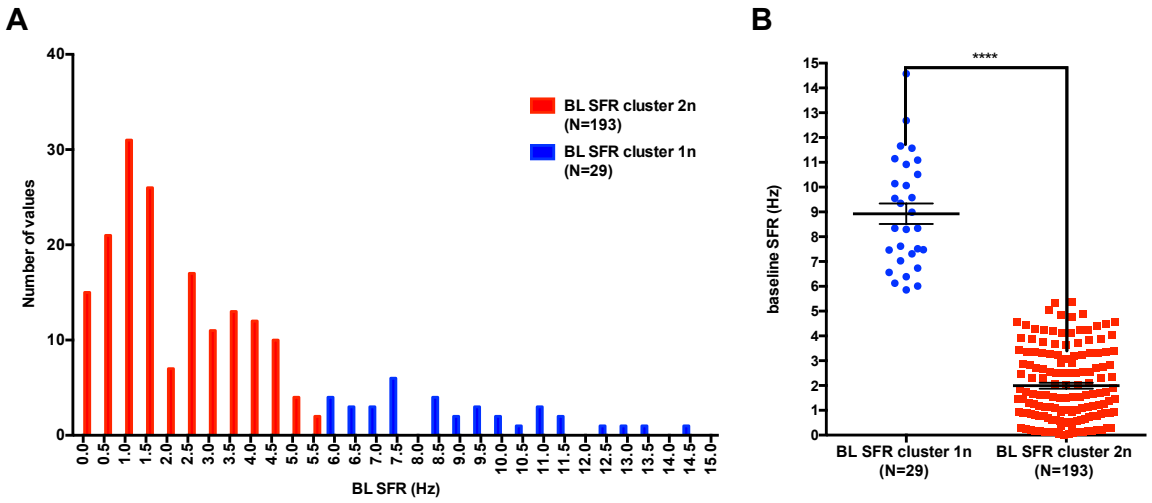

Figure 3.3 Frequency histogram of mean baseline SFR values of two naïve-state neurone clusters. A) Graph shows the count (y-axis) of neurones possessing mean baseline SFR values (Hz) falling within each 0.5 Hz time bin. Neurones are cluster-sorted into two clusters according to mean BL SFR values: BL SFR cluster 1n (N=29, blue bars) and BL SFR cluster 2n (N=193, red bars). B) Data points show the mean BL SFR values (Hz, y-axis) of neurones belonging to BL SFR cluster 1n (N=29, blue symbols) and 2n (N=193, red symbols). Bars represent mean ± SEM. Independent sample *t*-tests were conducted to test for differences between mean SFR of the two clusters, **** $P<0.0001$.

To assess alternative groupings, K-means cluster analysis was repeated with the assumption of 3 natural cluster centres within the population (figure 3.4A). Clusters emerging from this analysis were as follows: BL SFR cluster 1b (N=132) = 1.14Hz, BL SFR cluster 2b (N=26) = 4.19Hz, BL SFR cluster 3b (N=64) = 9.93Hz. To test validity of these three clusters, mean SFR values of the low (1b) and medium (2b), and high (3b) clusters were compared, and both differences were found to be highly significant (figure 3.4B; two-sample *t*-test: cluster 1 vs 2, $t(176) = 21.14$, $p<0.0001$; cluster 2 vs 3, $t(138) = 16.67$, $p<0.0001$).

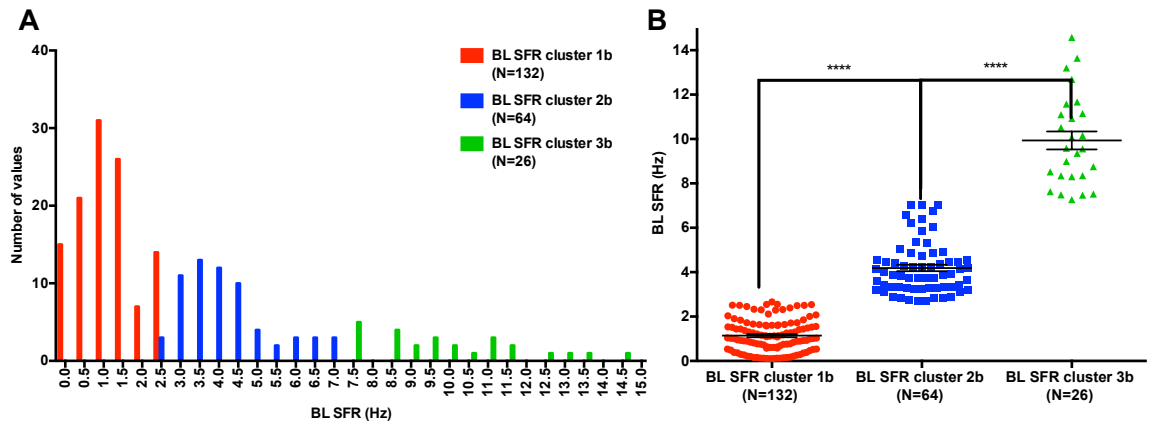

Figure 3.4 Frequency histogram of mean BL SFR values of three naïve-state neurone clusters. A) Graph shows the count (y-axis) of neurones possessing mean baseline SFR values (Hz) falling within each 0.5 Hz time bin. Neurones are cluster-sorted into three clusters: BL SFR cluster 1b (N=132, red bars), BL SFR cluster 2b (N=64, blue bars) and BL SFR cluster 3b (N=26, green bars). B) Data points show the mean BL SFR values (Hz, y-axis) of neurones belonging to BL SFR cluster 1b (N=132, red symbols), 2b (N=64, blue symbols) and 3b (N=26, green symbols). Bars represent mean ± SEM. Independent sample *t*-tests were conducted to test for differences between mean SFR of the three clusters, **** P<0.0001.

3.4.3 Firing pattern

3.4.3.I Amount of burst firing

Burst firing of all neurones (those recorded as the original spike data rather than firing rate - initial experiments were recorded using the latter) was quantified as the percentage of spikes existing within a burst (%SIB) in the baseline condition (N=111; figure 3.5). %SIB ranged from 0.43-93.97%, with a population mean of 39.28±2.56%. The population values were not normally distributed (Shapiro-Wilk's test: $p<0.05$). Two-step and K-means cluster analysis identified three clusters within the population values: SIB cluster 1 (N=25) with mean %SIB of 79.24±2.091%, SIB cluster 2 (N=39) with mean %SIB of 43.80±1.52%, SIB cluster 3 (N=47) with mean %SIB of 14.28±1.30%. SIB clusters 1 and 2 are approximately normally distributed (Shapiro-Wilk's test: $p>0.05$), but cluster 3 is not. Group mean %SIB of cluster 1 was significantly different from that of cluster 2 (two-sample *t*-test: $t(62) = 14.00$, $p< 0.0001$), which in turn was significantly different from that of cluster 3 (Mann-Whitney *U* test: $U=0.0$, $p<0.0001$).

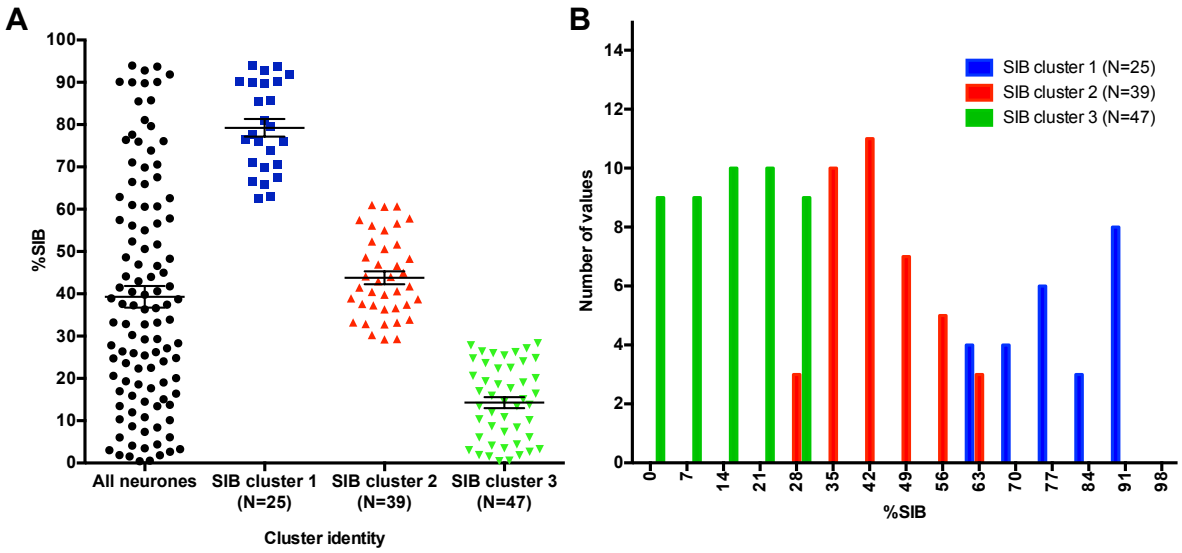

Figure 3.5 The percentage of spikes present within a burst in the baseline condition of all neurones recorded. A) Graph shows %SIB values (y-axis) of individual neurones recorded in the naïve condition (N=111; black data points), as well as the population mean ± SEM values (bars). Mean ± SEM values are also shown for SIB cluster 1 (blue symbols, N=25), SIB cluster 2 (red symbols, N=39) and SIB cluster 3 (green symbols, N=47), established by performing cluster analysis on %SIB values for all 111 neurones. B) Frequency histogram of neurones belonging to SIB clusters 1 (blue bars), 2 (red bars) and 3 (green bars), using a %SIB bin width of 7% (x-axis).

3.4.3.2 Interspike interval histograms

Interspike interval histograms were constructed from example neurones (assuming that a given waveform template represents an individual neurone) differing in spontaneous firing rate and burst firing characteristics (figure 3.6).

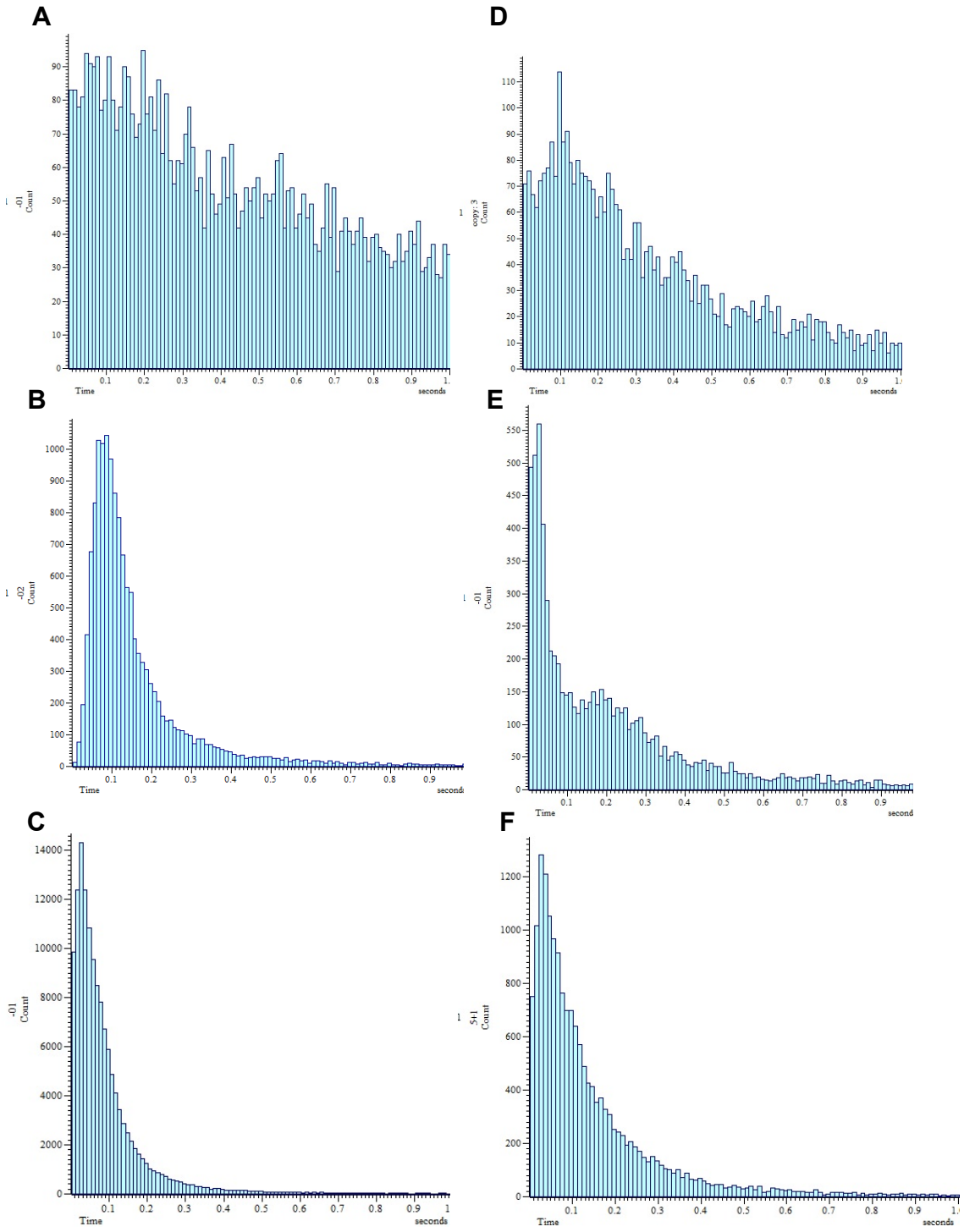

Figure 3.6 ISI histograms of neurones representing different combinations of mean BL SFR and percentage of spikes within a burst. Graphs show frequency histograms of all of the time intervals between all action potentials (interspike interval in seconds, ISI) of a given waveform template (considered to be a single neurone) occurring throughout recording during the baseline condition. Y-axis shows the number of counts in each 0.01-second ISI time bin (x-axis). ISI histograms are of "neurones" (a given waveform template) with the following BL SFR and %SIB cluster memberships: A) BL SFR cluster 1n (high) and SIB cluster 3 (low), B) BL SFR cluster 1n (high) and SIB cluster 2 (medium), C) BL SFR cluster 1n (high) and SIB cluster 1 (high), D) BL SFR cluster 2n (low) and SIB cluster 3 (low), E) BL SFR cluster 2n (low) and SIB cluster 2 (medium), F) BL SFR cluster 2n (low) and SIB cluster 3 (high).

3.4.3.3 %SIB versus firing rate

The %SIB was plotted against baseline spontaneous firing rate for all neurones with a baseline measure of the former (figure 3.7A, N=111). %SIB was strongly positively correlated with BL SFR (Spearman's rank correlation coefficient, r = 0.731, p<0.0001). The correlation between BL SFR and %SIB for neurones with BL SFR <6Hz was also calculated to account for the effects of direct influences of SFR on amount of burst firing on the relationship between these two variables. BL SFR and %SIB values were found to be significantly positively correlated at BL SFR values below 6Hz alone (r = 0.917, p<0.0001). Cluster membership for the %SIB variable (either SIB cluster 1, 2 or 3) was dependent on the cluster membership for BL SFR (either BL SFR cluster 1n or 2n; Pearson Chi-Square test: Cramer's V= 0.670, p<0.0005). A frequency histogram plot of BL SFR values of SIB clusters 1, 2 and 3 depicted the spread of BL SFR values of these three groups (figure 3.7B; mean BL SFR values: %SIB cluster 1 = 7.22±0.73Hz, %SIB cluster 2 = 2.72±0.23Hz, %SIB cluster 3 = 1.39±0.23Hz). Mean BL SFR of SIB cluster 1 significantly differed from that of SIB cluster 2 (two-sample t-test: t(62)=6.98, p<0.0001), and SIB cluster 2 significantly different from SIB cluster 3 (Mann-Whitney *U* test: U=363.0, p<0.0001).

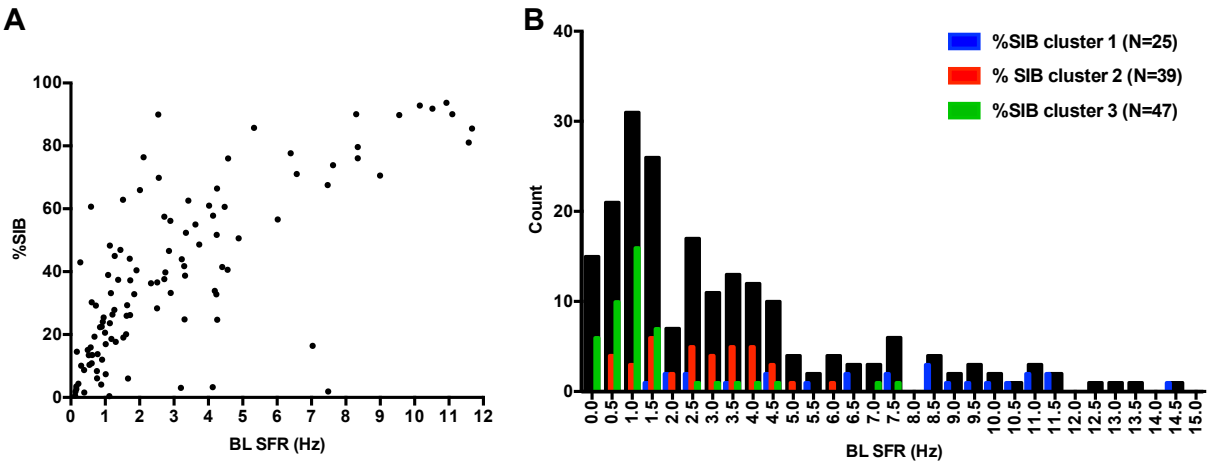

Figure 3.7 Investigating the relationship between BL SFR and %SIB characteristics. A) Scatter plot showing the BL SFR (Hz, x-axis) versus %SIB (%, y-axis) of each neurone recorded in the baseline condition. B) Frequency histogram showing the count of neurones (y-axis) possessing a given BL SFR value (bin width = 0.5Hz). Black histogram bars represent the count within the total recorded population; blue, red and green histogram bars represent the count of neurones classified as SIB cluster 1 (N=25), SIB cluster 2 (N=39) and SIB cluster 3 (N=47), respectively.

In order to shed light on the cause of the correlation between %SIB and BL SFR, the mean number of spikes per burst (SpB) as well as the burst frequency for each neurone in the baseline condition was computed by running the Bursts2 script on Spike2 software.

3.4.3.4 Number of spikes per burst

Values of SpB ranged from 0 to 25 spikes per burst, and the population mean was 4.05±0.35 spikes per burst. The relationship between SpB values and BL SFR was assessed. SpB was positively correlated with BL SFR (figure 3.8A; Spearman's rank correlation coefficient, $r = 0.649$, $p<0.0001$).

3.4.3.5 Burst frequency versus firing rate

Mean neuronal values of burst frequency ranged from 2.159-0.001 bursts per second with a population mean of 0.45±0.05 bursts per second. Burst frequency was positively correlated with BL SFR (figure 3.8B; Spearman's rank correlation coefficient, $r = 0.831$, $p<0.0001$).

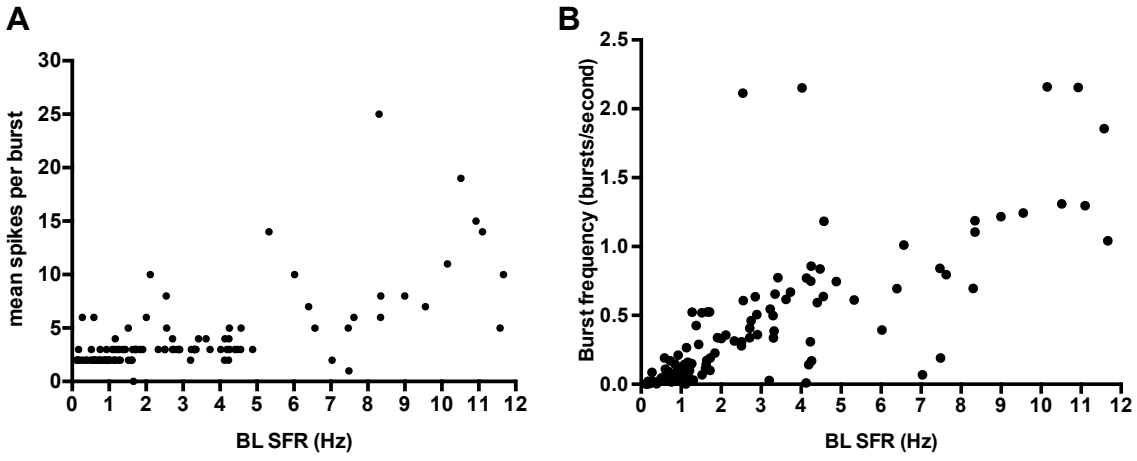

Figure 3.8 Investigating the relationship between BL SFR and other burst firing characteristics. A) Scatter plot showing the BL SFR (Hz, x-axis) versus mean number of spikes within a burst (y-axis) of each neurone recorded in the baseline condition. B) Scatter plot showing the BL SFR (Hz, x-axis) versus burst frequency (bursts per second, y-axis) of each neurone recorded in the baseline condition.

3.4.4 Location confirmation

An electrolytic lesion was created at the position of the electrode tip in 19 of the initial experiments. These brains were subsequently sliced into coronal sections in an attempt to localise the recording position for that experiment (see sections 2.I.2.3 and 3.3.3.5). Out of the 19 brain specimens, 16 were successfully sectioned. Clear and un-broken sections were not obtained from the remaining three brains, either due to significant tearing of the sections, damage to the specimen because of OCT thawing, or curling of the sections before they could be mounted on a slice (due to an inappropriate temperature within the recording chamber). Lesions were located in 11 out of the 16 successfully sectioned brains. The location of the lesions in terms of dorsoventral, mediolateral and rostrocaudal coordinates are shown in figure 3.10, and in terms of a best-estimated VTA sub-nucleus in table 3.1.

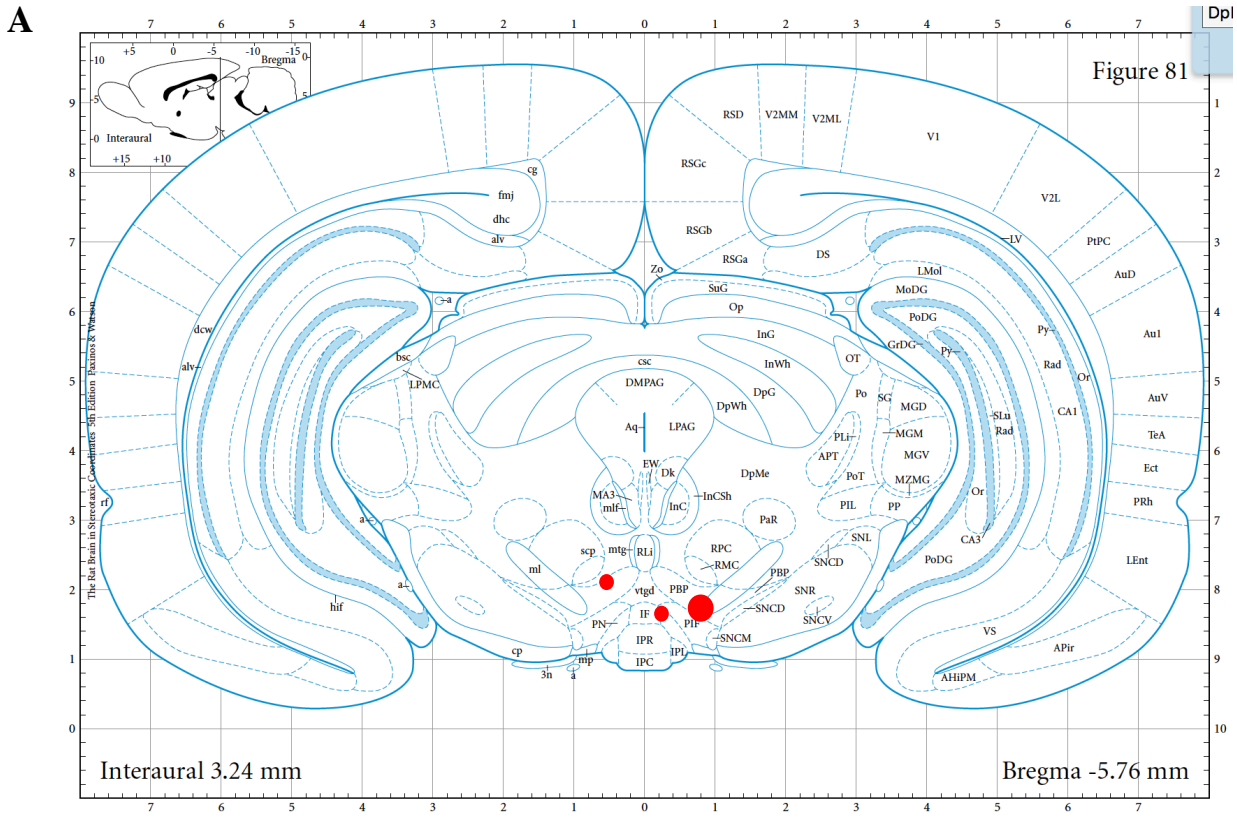
A
Figure 81
Interaural 3.24 mm
Bregma -5.76 mm
The Rat Brain in Stereotaxic Coordinates 5th Edition Paxinos & Watson

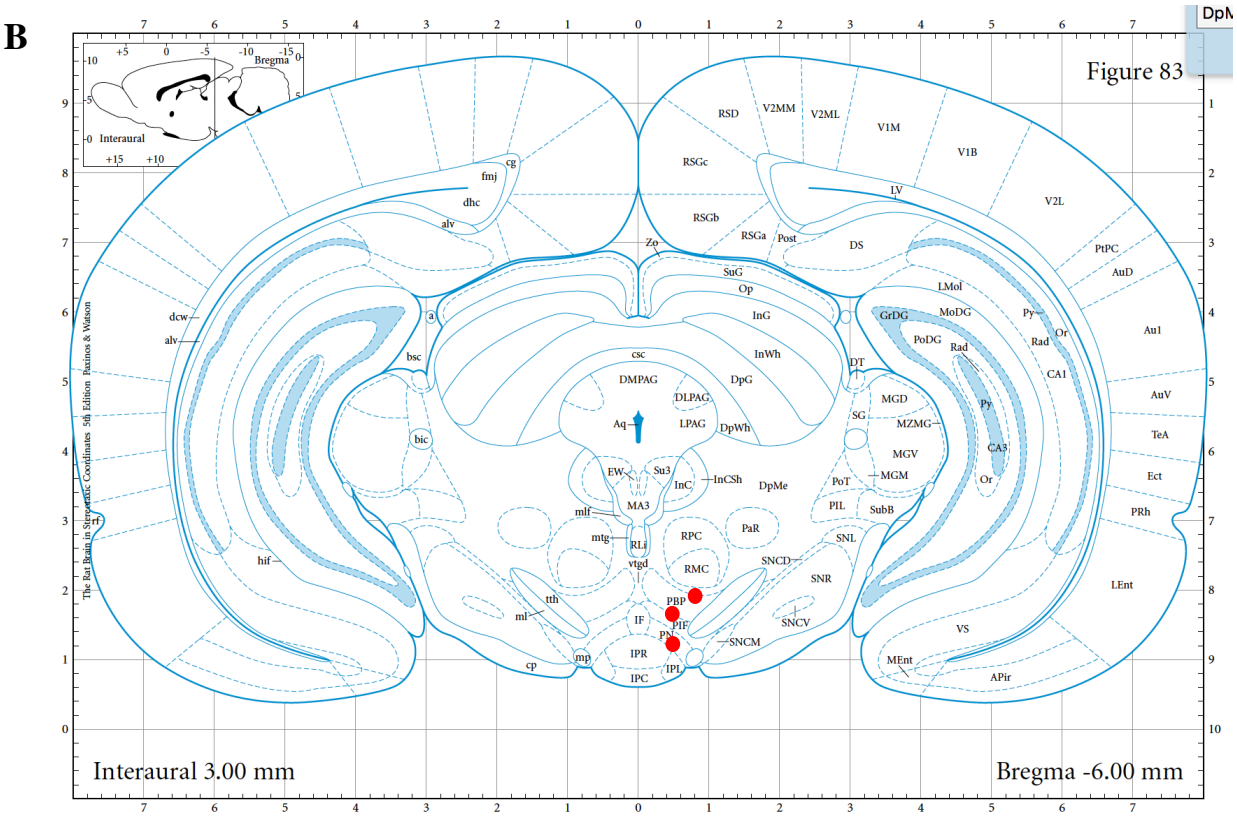
B
Figure 83
Interaural 3.00 mm
Bregma -6.00 mm
The Rat Brain in Stereotaxic Coordinates 5th Edition Paxinos & Watson

Figure 3.9

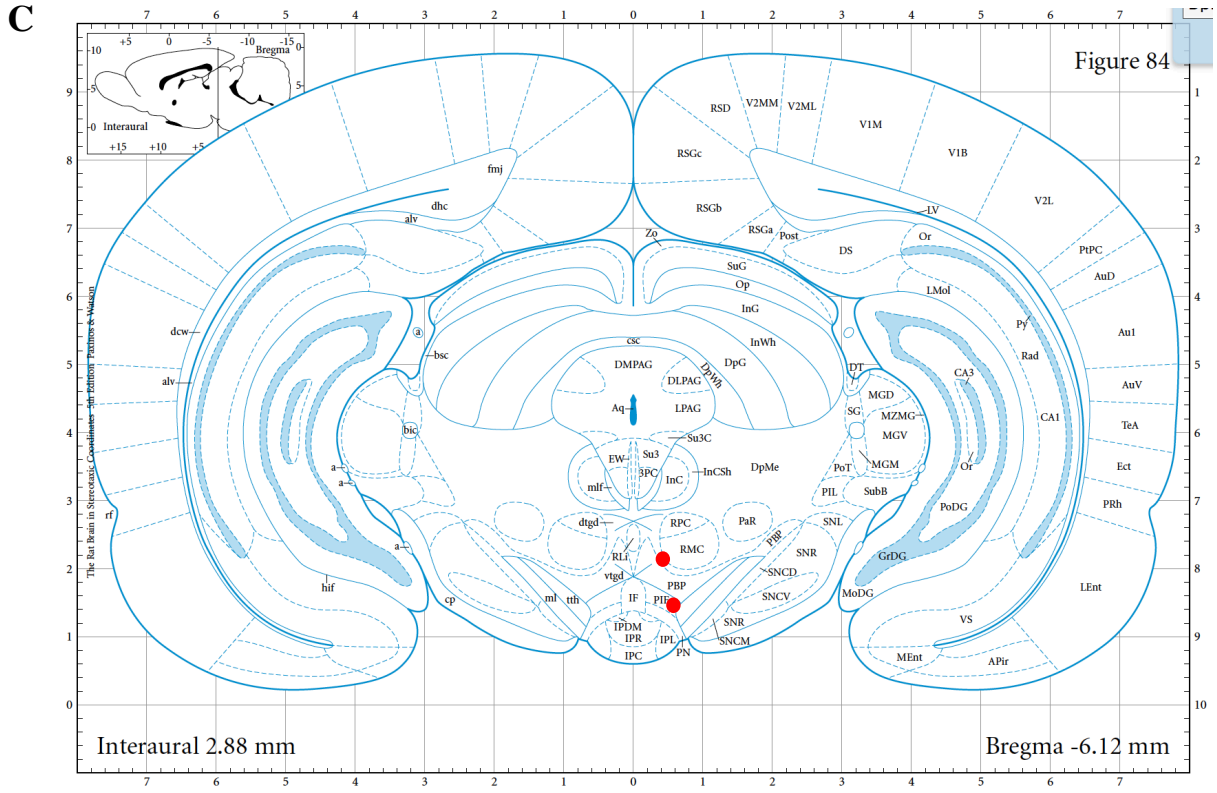
C
Figure 84
Interaural 2.88 mm
Bregma -6.12 mm
The Rat Brain in Stereotaxic Coordinates - 5th Edition Paxinos & Watson

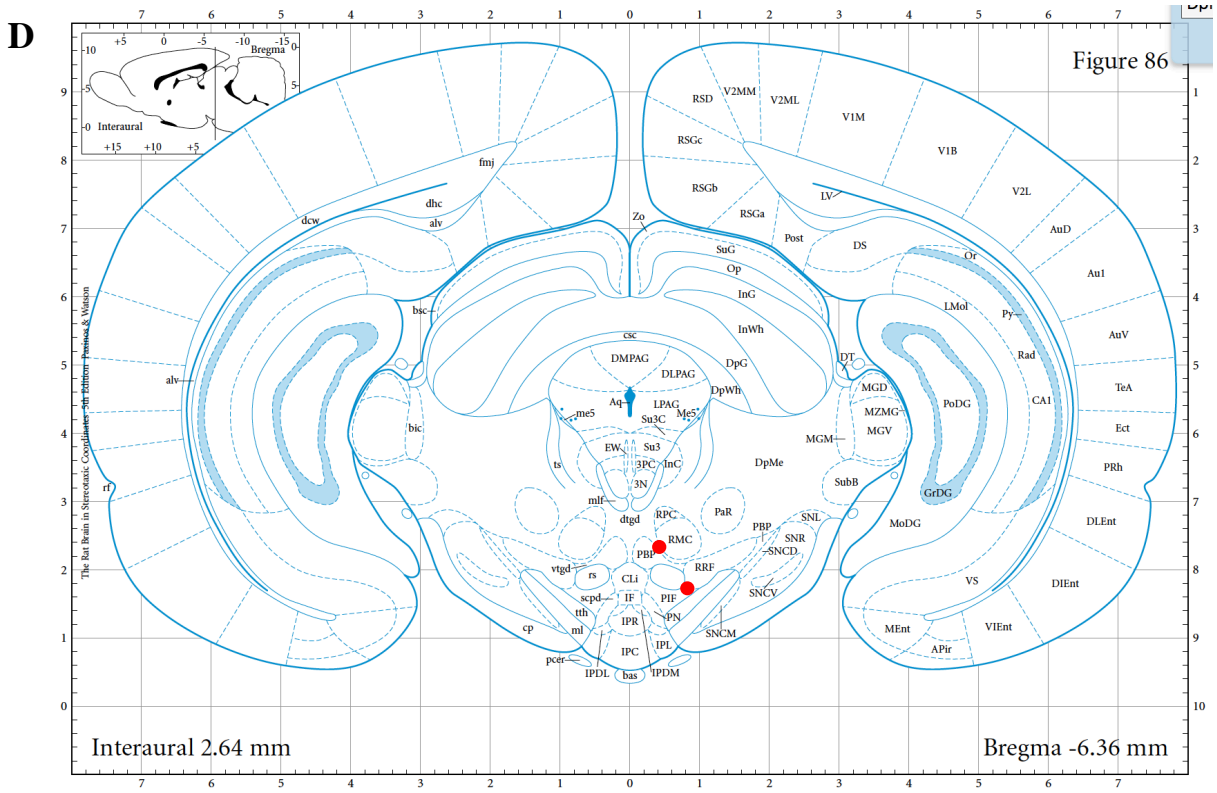
D
Figure 86
Interaural 2.64 mm
Bregma -6.36 mm
The Rat Brain in Stereotaxic Coordinates - 5th Edition Paxinos & Watson

Figure 3.9

E

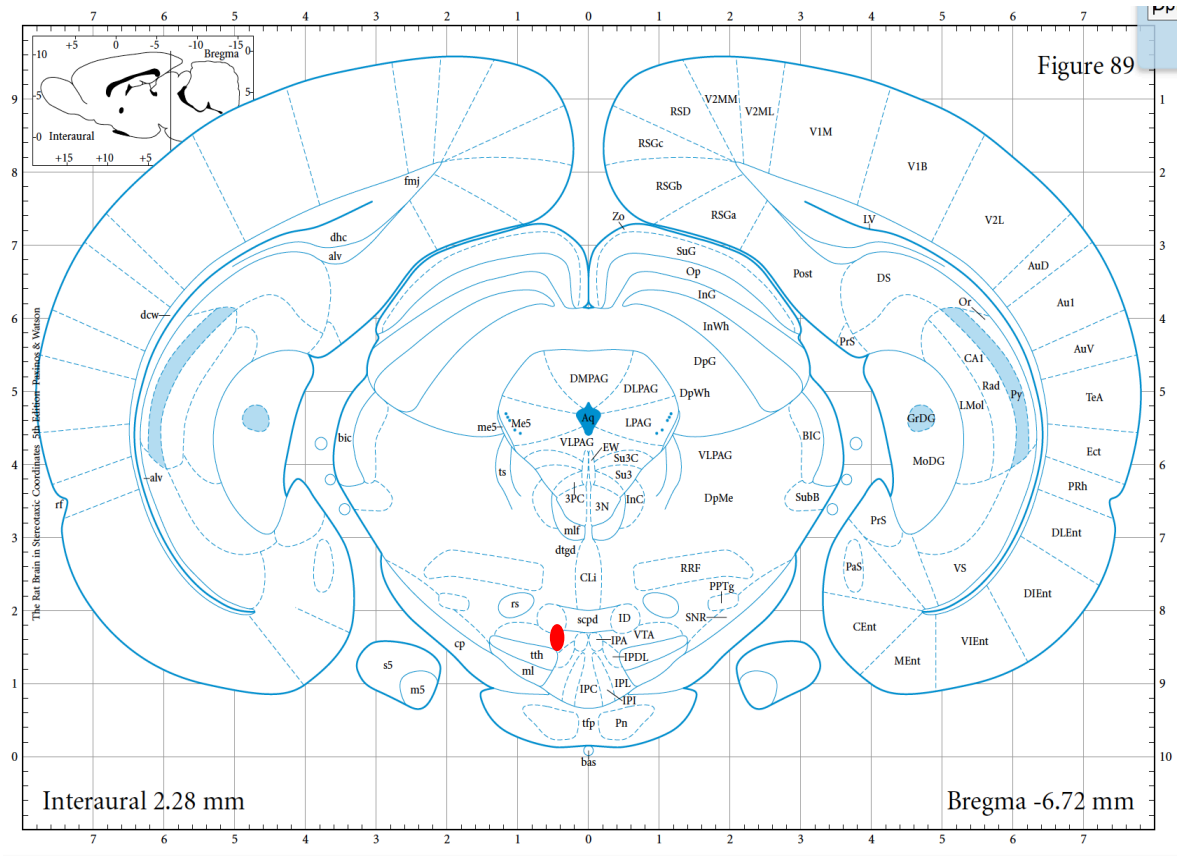

Figure 3.9 Lesion localisation mapped onto the Paxinos and Watson rat brain atlas. Images show coronal sections from the Paxinos and Watson rat brain atlas (1998) that correspond to the estimated rostrocaudal coordinates of each electrolytic lesion-containing brain slice, as determined by comparing slice photomicrographs with the rat brain atlas diagrams. The coronal sections in which lesions were found included A) Bregma -5.76mm, B) Bregma -6.00mm, C) Bregma -6.12mm, D) Bregma -6.36mm, E) Bregma -6.72mm. Red circles and ovals represent the location of individual lesion scars seen on the coronal section photomicrographs, with the shape changing according to the size and shape of the lesion hole to account for uncertainty in precise location.

Recording (animal) ID	Coronal section (mm from Bregma)	Estimated location of lesion	Within VTA?
N11	-5.76	PBP	Yes
N15	-5.76	PN	Yes
N21	-6.00	PBP/PIF	Yes
N22	-6.00	PBP	Yes
N25	-6.12	PIF	Yes
N29	-5.76	PBP	Yes
N32	-6.36	PIF	Yes
N38	-6.72	VTA	Yes
N20	-6.36	PBP	Yes
N13	-6.00	PN	Yes
N27	-6.12	RPC	No

Table 3.1 Intra- or extra-VTA location of electrolytic lesions seen in coronal brain slices. Table shows the recording ID (i.e. the ID of a particular animal/ brain specimen), the rostroventral coordinates of the coronal section (mm from Bregma), the estimated location of the lesion in terms of sub-nucleus abbreviation, and whether or not that location was within the VTA, as defined in section 2.I.2.3. PBP = parabrachial pigmented nucleus, PN = paranigral nucleus, PIF = parainterfascicular nucleus, VTA = ventral tegmental area, RPC = parvicellular part of the red nucleus.

Lesions were found to be located within VTA sub-nuclei in 10 of the 11 recordings for which brain slices with visible lesions were obtained. The remaining 1 recording was found to be located in the parvicellular part of the red nucleus (RPC). Two out of the 11 recordings were located in the paranigral nucleus (PN), four and a half out of the 11 recordings were located in the parabrachial pigmented nucleus (PBP, with the 'half' representing a lesion falling over both PBP and PIF nuclei), and two and a half out of the 11 recordings were located in the parainterfascicular nucleus (PIF).

3.4.5 Noxious response

The nociceptive responsivity to both paw von Frey and paw heat stimuli was assessed in 75 neurones in the baseline condition by comparing mean SFR during noxious stimulus presentation with values of 1.96 x standard deviation of the mean BL SFR.

3.4.5.I Paw von Frey

Out of all 75 neurones characterised, 13 neurones (17.3%) showed an excitatory response to the paw von Frey stimulus, and 2 (2.7%) showed an inhibitory response.

3.4.5.2 Paw heat

4 neurones (5.3%) showed and excitatory response to paw heat, and 1 (1.3%) showed an inhibitory response.

3.4.5.3 Location of neurones showing a noxious response

Due to the low number of noxious-responsive neurones for each stimulus modality, neurones from the separate groups were grouped and re-classified as noxious-excited or noxious-inhibited. The locations of all noxious-excited and noxious-inhibited neurones were plotted on the Paxinos and Watson (1998) rat brain atlas according to the noted coordinates of the electrode tip during the corresponding recording (figure 3.10). Noxious-inhibited neurones were recorded in the PIF (N=1), PBP (N=1) and the TTH (N=2). Noxious-excited neurones were recorded in the PBP (N=4), PIF (N=2), PN (N=5), PR (N=1) and TTH (trigeminothalamic tract; N=1). The noxious-excited neurones were present throughout the rostro-caudal range of recording locations, from bregma-5.52-6.24mm, whereas the noxious-inhibited neurones were only present in the more caudal range of recording locations (between bregma -6.0mm and bregma -6.24mm).

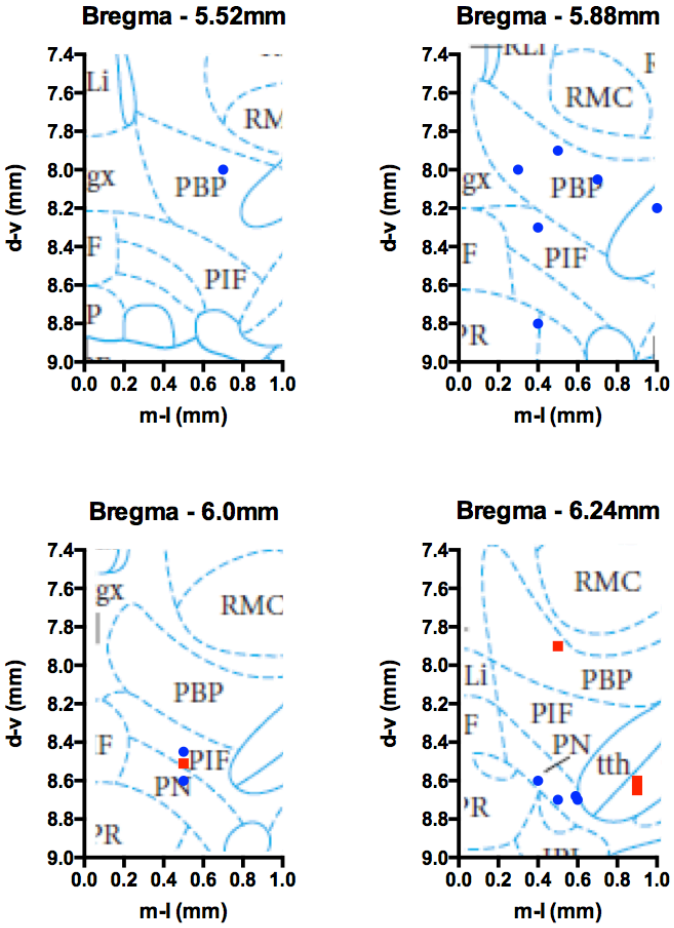

Figure 3.10 Recording location of neurones excited and inhibited by noxious stimuli. Scatter plots of neurone location are superimposed onto sections of coronal images from the Paxinos and Watson rat brain atlas (1998). Coordinates corresponding to the coordinates of the electrode tip according to readings on the stereotaxic frame are plotted in terms of distances from Bregma (mm) along the dorsovental (d-v, y-axis) and mediolateral (m-l, x-axis) axes. Separate plots are shown for different locations along the rostro-caudal axis. Noxious-excited neurones are represented by blue symbols, and noxious-inhibited neurones, by red symbols.

3.4.5.4 Firing pattern and rate of noxious-responsive neurones

To establish any differences in spontaneous firing characteristics of neurones inhibited by, excited by or non-responsive to acute nociceptive stimulation, the percentage of spikes in bursts (%SIB) and mean baseline SFR of these groups were compared (figure 3.11). For this analysis, neurones excited or inhibited by either the paw von Frey or paw heat stimuli were grouped into a general noxious-excited (N=14) or noxious-inhibited (N=2) group, respectively. There were 59 neurones in the "unresponsive" group. The low number of neurones in the noxious-inhibited group made any interpretation of firing characteristics or comparison with excited or unresponsive groups unreliable, so this group was omitted from further analysis.

The mean BL SFR of neurones in the noxious-excited (NE) and -unresponsive (NU) groups were similar (figure 3.11A; NU = 2.029Hz ± 0.350Hz; NE = 1.891Hz ±0.381Hz), and no significant difference was found between values of these two groups (two-sample *t*-test: t(71)=1.261, p=0.211).

The %SIB of neurones in the noxious-excited (NE) and unresponsive (NU) groups were also similar (figure 3.11B; NE = 44.90%±4.68%, NU = 32.05%±3.97%) and no significant difference was found between values of these two groups (two-sample *t*-test: t(36)=1.797, p=0.081).

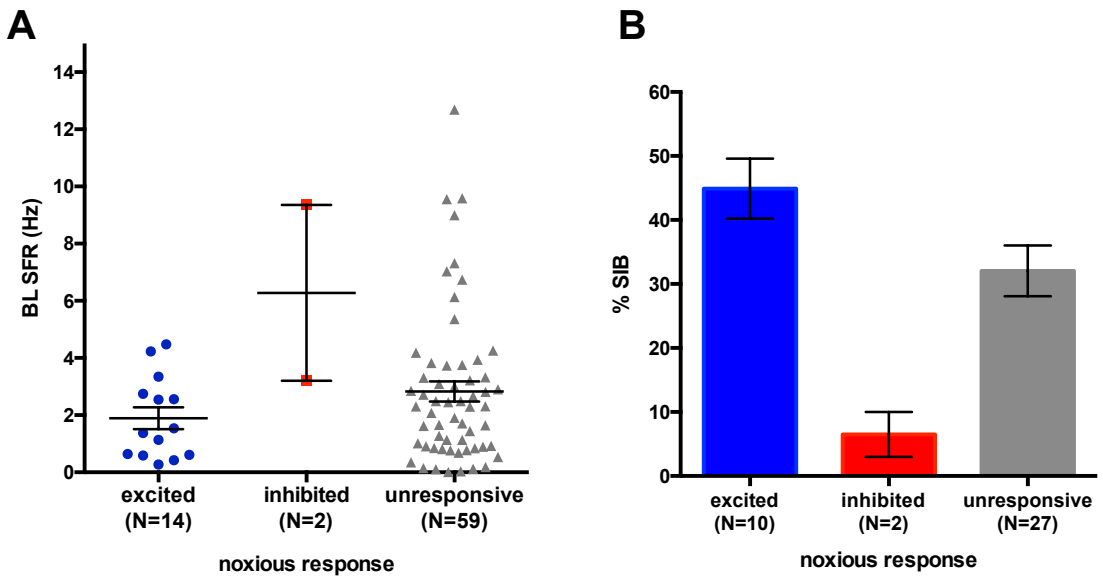

Figure 3.11 Baseline firing characteristics of noxious-excited, -inhibited and –unresponsive neurones. A) The mean baseline spontaneous firing rate (Hz) of each of the recorded neurones falling into the three noxious response-based groupings is plotted. B) Bar graph showing the mean %SIB value for the three noxious response-based neurone groups. Blue data points and bars = noxious-excited neurones, red data points and bars = noxious-inhibited neurones, grey data points and bars = noxious-unresponsive neurones. Error bars represent mean ± SEM.

3.4.6 Morphine response

19 neurones were recorded from morphine injection experiments involving a total of 16 animals. 6 neurones were recorded from saline vehicle control experiments involving a total of 5 animals. A neurone recorded during one of the vehicle control experiments was omitted from analysis due to premature termination of the experiment (criteria 3, section 2.2.5; an unseen blockage in the tracheal tube resulted in an inaccessible occlusion of airflow to the animal).

3.4.6.I Effects on SFR: non-normalized values

Spontaneous firing rate was measured every 10 minutes following the subcutaneous injection of $2mgkg^{-1}$ morphine sulphate. Cluster analysis revealed the existence of one outlier (figure 3.12). For the remainder of the recorded population, baseline spontaneous firing rates were too variable to assess response profile patterns, so further analysis was performed on normalized SFR values.

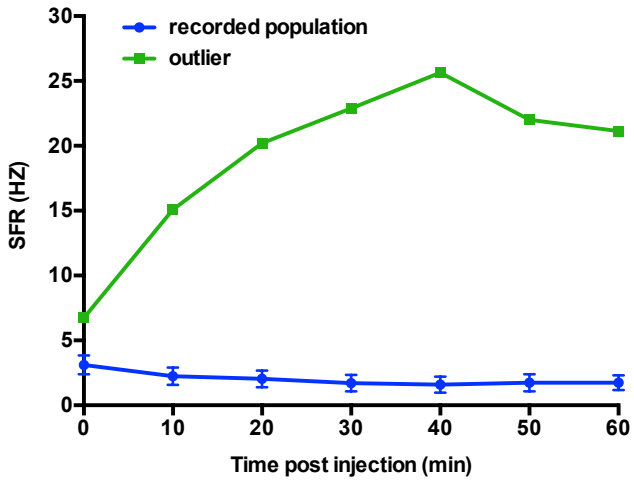

Figure 3.12 Mean spontaneous firing rate of neurones following injection of morphine. Graph shows data points and bars representing the mean spontaneous firing rate (Hz, y-axis) ± SEM of neurones at all time points following the injection of morphine (minutes, x-axis). Cluster analysis revealed the existence of one outlier (green trace) from the rest of the recorded population (blue trace) in terms of mean SFR post-morphine injection.

3.4.6.2 Effects on SFR: normalized values

Mean SFR of each neurone at every time point post-morphine injection was calculated as a percentage of mean baseline SFR (figure 3.13). The outlier previously identified through cluster analysis on post-morphine injection non-normalized SFR values was omitted from this analysis. Two-step and K-means cluster analysis performed using normalized values at all time points revealed the existence of two natural response profile-based clusters within the population: norm mph cluster 1 appeared to show a mean excitatory response to morphine (N=5), while norm mph cluster 2 appeared to show a group mean inhibitory response (N=13). Analysis revealed that norm mph cluster 2 showed a significant % decrease in SFR compared to mean baseline SFR at all time points from 20 minutes post-morphine injection onwards when using a Bonferroni-corrected alpha of 0.008 (Friedman test with post-hoc Wilcoxon signed-rank pairwise comparisons, baseline vs 20min: Z=-2.760, p=0.006; baseline vs 30min: Z=-2.900, p=0.004; baseline vs 40min: Z=-3.180, p=0.001; baseline vs 50min: Z=-3.110, p=0.002; baseline vs 60min: Z=-2.761, p=0.006). Mean normalized SFR of norm mph cluster 2 neurones was significantly different from that of vehicle control neurones at the 40-minute time point (one-way ANOVA using a Bonferroni-adjusted alpha of 0.008, 40min: p=0.002). In contrast, percentage increases in SFR from mean baseline SFR of the norm mph cluster 1 were not significant at any time point post-morphine injection according to a Friedman test with post-hoc Wilcoxon signed-rank pairwise comparisons using a Bonferroni-corrected alpha of 0.008. Similarly, the injection of saline in the vehicle control experiments (N=5) did not result in a significant percentage change in SFR from pre-injection values at any of the measured time points according to a Friedman test followed by post-hoc Wilcoxon signed-rank pairwise comparisons using a Bonferroni-corrected alpha of 0.008.

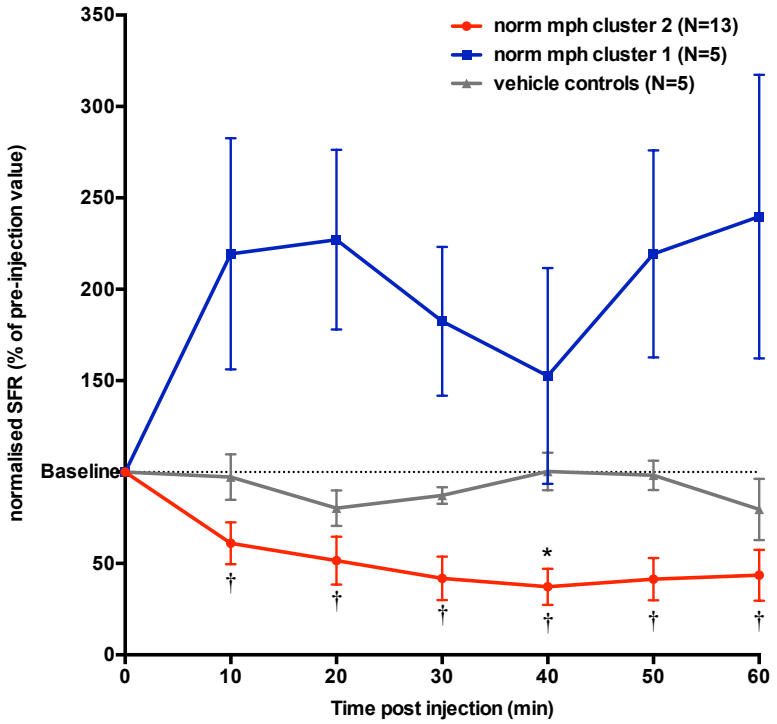

Figure 3.13 Normalized spontaneous firing rate of neurones following injection of morphine or vehicle-only control injection. Data points show mean ± SEM spontaneous firing rate expressed as a percentage of mean pre-injection values of norm mph cluster 2 (N=13; red trace) and norm mph cluster 1 (N=5; blue trace) neurone groups. Response-based groups were determined through cluster analysis involving values at all time points post injection. Mean values for both response-based clusters are shown for all time points post morphine injection. Mean normalized SFR of neurones recorded in experiments involving saline vehicle control injections (grey trace) are shown. The dashed horizontal line at y=100% represents mean pre-injection (baseline in this case) SFR values). Friedman's tests followed by post-hoc Wilcoxon signed-rank pairwise comparisons were conducted to establish whether morphine or vehicle injection caused a significant percentage change in SFR of norm mph cluster 1, cluster 2 and vehicle control neurones, † $P<0.008$ (cluster 2). A one-way ANOVA was conducted to compare normalized SFR values of cluster 2 and vehicle control neurones, * $P<0.008$.

3.4.6.3 Location of neurones within morphine response clusters

The location of neurones in normalized morphine response (norm mph) clusters 1 and 2 were plotted on the Paxinos and Watson (1998) rat brain atlas according to the noted coordinates of the electrode tip during the corresponding recording (figure 3.14). Norm mph cluster 1 neurones – showing no net group response to morphine injection - were recorded in the PN (N=3) and PBP (N=1; on the peripheral boundary) of the VTA, and in the neighbouring RMC (red nucleus magnocellular; N=1), assuming coordinates accurately represented electrode tip location. Norm mph cluster 2 neurones - showing a group mean inhibitory response to morphine injection - were recorded in the PBP (N=2), PIF (N=4), and the caudal VTA (N=6), assuming coordinates accurately represented electrode tip location. In the rostro-caudal axis there appeared to be some separation of the cluster 1 and cluster 2

neurones: 6/13 of cluster 2 neurones were located between 6.8-6.9 mm caudal to bregma, whereas the most caudal location of the cluster 1 neurones was bregma -6.32 mm (figure 3.14D). Neurones recorded in locations between -6.00 mm and -5.80 mm relative to bregma consisted of a mix of those belonging to norm mph clusters 1 and 2.

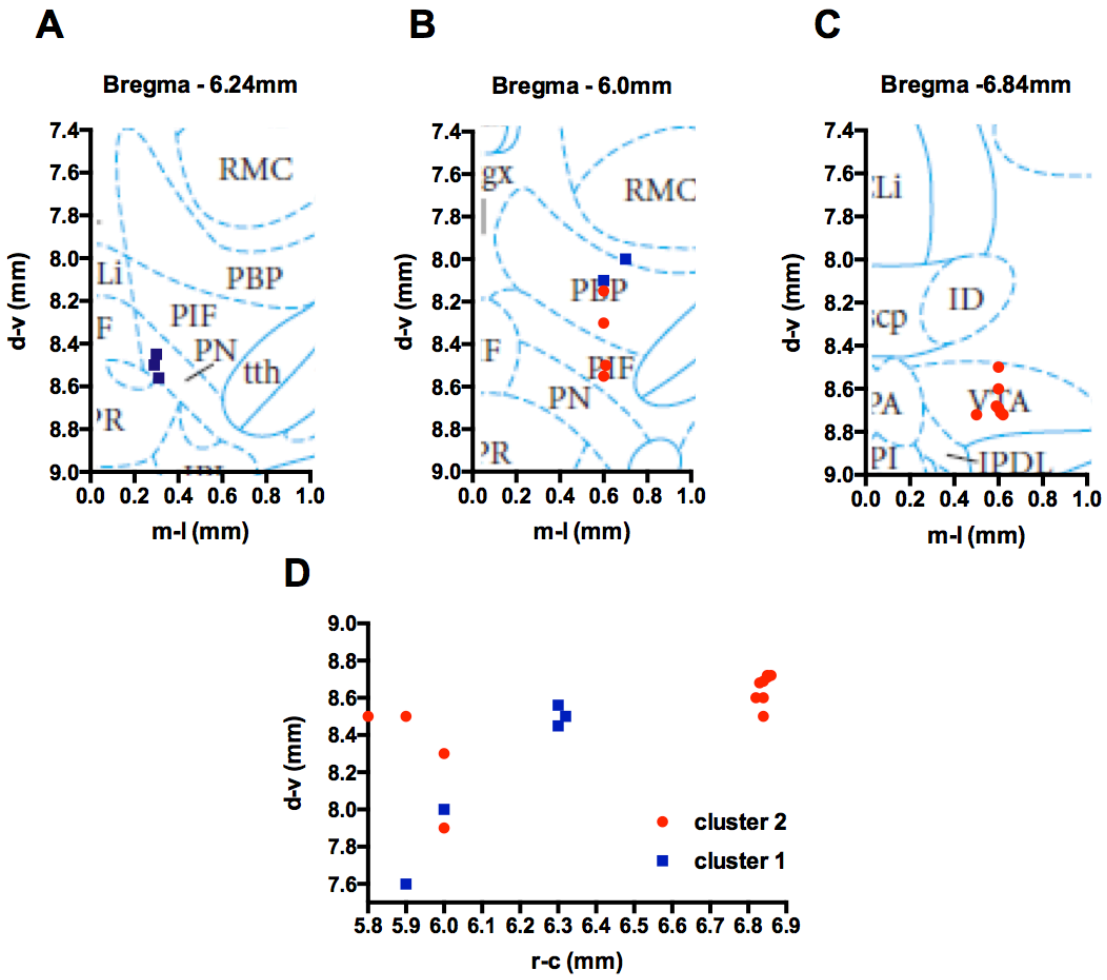

Figure 3.14 Recording location of neurones sorted according to response to systemic morphine injection. A-C) Scatter plots of neurone location are superimposed onto coronal section diagrams taken from the Paxinos and Watson rat brain atlas (1998). Coordinates corresponding to the coordinates of the electrode tip according to readings on the stereotaxic frame are plotted in terms of distances from Bregma (mm) along the dorsovental (d-v, y-axis) and mediolateral (m-l, x-axis) axes. Separate plots are shown for different locations along the rostro-caudal axis. The two morphine response-based clusters are distinguished by colour; norm mph cluster 1 neurones are represented by blue symbols, and norm mph cluster 2 neurones, by red symbols. D) Coordinates corresponding to the coordinates of the electrode tip according to readings on the stereotaxic frame are plotted in terms of distances from Bregma (mm) along the dorsovental (d-v, y-axis) and rostrocaudal (r-c, x-axis) axes.

3.4.6.4 Baseline SFR of neurones within morphine response-based clusters

The baseline SFR values of neurones present in norm mph clusters 1 (N=5) and 2 (N=13) were compared (figure 3.15). Mean ±SEM values were 2.039±1.234Hz for norm mph cluster 1 and 3.805±0.851Hz for cluster 2. Differences in mean BL SFR between the morphine response clusters were not significant (independent samples two-sample *t*-test: t(35)=1.797, p=0.081).

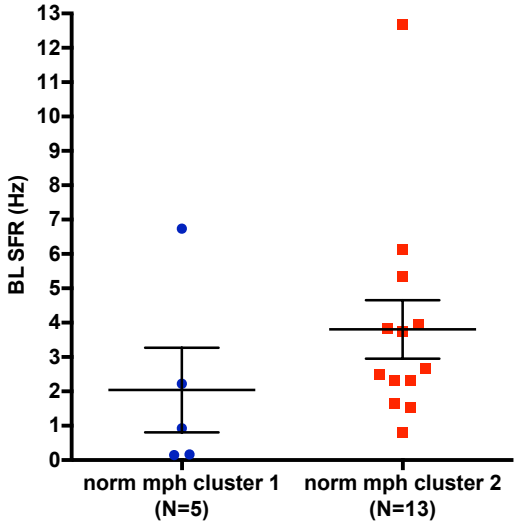

Figure 3.15 Baseline spontaneous firing rate of morphine response-based neurone clusters. Graph shows mean SFR values in the baseline condition of neurones belonging to post-morphine normalized SFR-based clusters: norm mph cluster 1 (blue data points, N=5) and norm mph cluster 2 (red data points, N=13; both referred to as morphine response clusters). Bars represent mean ± SEM.

3.4.6.5 Morphine response of BL SFR-based clusters

In a further analysis, the normalised morphine response of neurones belonging to either the 'high-firing' (BL SFR cluster 1n) or 'low-firing' (BL SFR cluster 2n) baseline SFR clusters established from cluster analysis of the whole recorded population (section 3.4.2) were plotted (figure 3.16). Three of the neurones recorded in the morphine experiments had a cluster identity of BL SFR cluster 1n, whilst 18 neurones belonged to the BL SFR cluster 2n cluster. The BL SFR cluster 2n neurones showed no mean group percentage change in SFR following morphine injection, whereas the BL SFR cluster 1n neurones appeared to show a group mean inhibition at all time points post-injection; however, percentage decreases in SFR from baseline values were not significant at

any time point post-morphine injection (Friedman's test followed by post-hoc Wilcoxon signed-rank pairwise comparisons; figure 3.16).

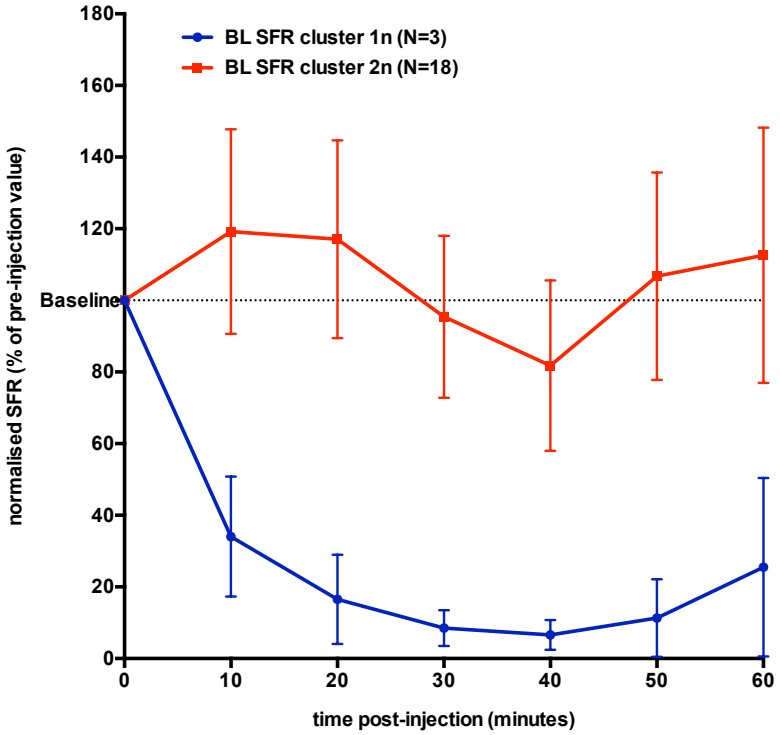

Figure 3.16 Normalized spontaneous firing rate of BL SFR cluster neurones following injection of morphine. Data points show mean ± SEM spontaneous firing rate expressed as a percentage of mean pre-morphine injection values of neurones belonging to BL SFR cluster 2n (N=18; red trace) and BL SFR cluster 1n (N=3; blue trace) neurone groups. Mean values for both response-based clusters are shown for all time points post morphine injection. The dashed horizontal line at y=100% represents mean pre-injection (baseline in this case) SFR values). Friedman's tests followed by post-hoc Wilcoxon signed-rank pairwise comparisons were conducted to establish whether morphine injection caused a significant percentage change in SFR of BL SFR cluster 1n or 2n neurones, but yielded insignificant results.

3.5 Discussion

This study aimed to investigate the separation of VTA neurones according to various electrophysiological and pharmacological characteristics quoted as potential DA neurone markers in the literature. It was hoped that natural groupings would be found within the recorded population with characteristics in-line with those expected for either DA or non-DA neurones. Characteristics investigated included the location, spontaneous firing rate and firing pattern, μ-opioid responsivity and acute noxious responsivity for each neurone. Natural clusters were found within each measure; however, out of all variables, only firing pattern and firing rate values showed a significant coherence. Hence, there was no general separation of neurones into distinct functional groups based on consideration of all of the electrophysiological and pharmacological characteristics tested in this investigation.

3.5.I Time control experiments

The set-up of the current experiments has been designed to minimise any possible uncontrolled source of neuronal firing rate variability (within the apparatus and technical limitations – see limitations sections). However, in an *in vivo* anaesthetised preparation it is difficult to measure and control all possible variables. As experimental time points up to two hours following the injection of any single pharmacological agent contributed to the analysis in this thesis, it was important to check neuronal stability over this time range. Results of these time control experiments showed within-neurone fluctuations in SFR on a ~20-minute time scale, with some neurones showing a much greater degree of variability than others. For three out of the five neurones, mean SFR at the end of the two-hour period showed no significant difference from that measured at the beginning. However, for the remaining two neurons a significant drop in mean SFR was seen when comparing the first and last time points.

There are several conclusions we can draw from these results. Firstly, short-term fluctuations in SFR despite the absence of external pharmacological or physical stimuli suggest that VTA neurones show inherent variability in firing rate over time. Activity of VTA DA neurones in the *in vivo* preparation is driven by diverse synaptic inputs from a wide range of brain regions (5-HT from raphe nuclei, NA from the locus coeruleus, acetylcholine from tegmental nuclei, glutamate from the mPFC and GABA from the nucleus accumbens, ventral pallidum and the pedunculopontine nucleus), synaptic regulation from local sources (GABAergic and glutamatergic interneurones, and somatodendritic dopamine release), and intrinsic pace-maker activity (Adell and Artigas, 2004; Kalivas et al., 1983; Paladini and Roeper, 2014). With all of the above influences in-tact, it is unsurprising that minute-minute variability in neuronal SFR exists.

Secondly, uncontrolled experimental factors do not appear to have a significant and persistent influence on mean SFR. The factors that could foreseeably influence neuronal firing, including level of anaesthesia and blood pressure, would manifest as a gradual and sustained increase or decrease in SFR over the two hours. Although decreases in SFR between 0-120 minutes were seen for two neurones, this was not representative of the pattern of SFR change over the course of the whole two-hour period. In other words, no gradual increases or decreases in SFR over time were seen in these experiments, meaning that any such changes seen post-injection are likely to reflect injection effects (pharmacological or physical). Through comparisons between pharmacological effect on SFR with vehicle control injection effects, it is hoped that the true pharmacological effect will be reliably isolated.

Finally, these results show it is important to take the whole response profile of a neurone into account when assessing pharmacological effect. By including all time points post-injection in the analysis, the impact of time point-time point fluctuations in SFR that do not follow the general pattern of SFR change will be minimised.

3.5.2 Baseline firing characteristics

3.5.2.I Spontaneous firing rate

The mean spontaneous firing rate was measured in the baseline condition – i.e. before the injection of any pharmacological agent. By including values recorded in all experiments involving naïve animals present in this thesis, analysis on a large population of VTA neurones was possible (N=222). The spontaneous firing rate has been adopted as a distinguishing factor between DA and non-DA (predominantly GABA) neurones of the VTA by several separate research groups; it was originally suggested that VTA DA neurones typically displayed SFRs <10Hz, whereas GABAerigc neurones fired at >10Hz (Bunney et al., 1973; Chiodo et al., 1984; Grace and Onn, 1989; Grace and Bunney, 1984a; Guyenet and Aghajanian, 1978; Luo et al., 2008; Steffensen et al., 1998, 2008; Stobbs et al., 2004; White and Wang, 1984).

Ranges of SFR seen for electrophysiologically and pharmacologically-selected DA neurones in anaesthetized or freely-moving rats have been quoted as 2Hz - 9Hz (Grace and Bunney 1984b), 0.5Hz - 10Hz (Marinelli and McCutcheon, 2014b), and 0.8Hz – 8Hz (Hyland et al., 2002). The range of BL SFR seen in the current experiments was 0.1Hz – 14.58Hz, falling beyond the previously reported DA neurone ranges at both ends. It is possible that the sample contained populations of non-dopaminergic neurones with particularly low (<0.5Hz) and particularly

high (>10Hz) firing rates. It is reasonable to suggest that the neurones displaying firing rates >10Hz are GABAergic, based on previous *in vivo* and *in vitro* findings for this neurochemical group (Grace and Onn, 1989; Luo et al., 2008; Steffensen et al., 1998, 2008). Further, a slow-firing non-dopaminergic population has also been reported in previous studies (Chenu et al., 2012; Margolis et al., 2012; Ungless et al., 2004), often possessing firing rates below that typically seen for DA neurones (<1Hz; Ungless et al., 2004; Chenu et al., 2011). Ungless and colleagues (2004) hypothesized that a non-GABAergic, possibly glutamatergic, identity of the low-firing non-DA neurones was more likely given the previous accounts of high SFR within the GABAergic population; however, Margolis and colleagues detected a mean SFR of 3.3±0.6Hz for the GAD+ (i.e. GABAergic) neurone population in their experiments (N=11; Margolis et al., 2012), suggesting that low-firing GABA neurones may have been selectively or unintentionally omitted from some previous studies.

The natural clusters found within the BL SFR data set do not reflect this proposed division of <1Hz firing non-DA neurones, 1-10Hz firing DA neurones, and >10Hz firing GABA neurones; the two clusters established from Two-step and subsequent K-means cluster analyses, BL SFR cluster 1n and 2n, both had group mean SFR values within the typical DA neurone SFR range (BL SFR cluster 1n and 2n means were 8.9Hz and 2.0Hz, respectively). When K-means cluster analysis was performed assuming 3 clusters despite Two-step analysis finding two natural centres, mean SFR value of the middle cluster matched that expected for DA neurones (4.19Hz). However, mean SFR values of the three artificial clusters were all within the previously-reported DA neurone range of 1-10Hz, implying that the three clusters are also likely to represent mixed neurochemical populations. To assess the separation of the two (BL SFR cluster 1n and 2n) or three (BL SFR 1b, 2b and 3b) clusters resulting from the respective K-means analyses, independent-sample *t*-tests were performed on mean BL SFR values of the cluster means. Results showed that both the two cluster- and three cluster-based grouping of neurones was statistically robust, with differences between the cluster means being highly significant in both instances. It was decided that, in response to a lack of statistical clarity, further baseline SFR-based analyses would be performed using the original two–cluster segregation of the recorded population, given that this was the number of clusters recommended by the objective and statistically-validated Two-step cluster analysis process.

It is important to consider the possibility that the spike sorting criteria applied before extraction of baseline SFR values may have over-sorted spikes into templates - that is, sorted spikes emanating from the same neurone into two or more separate templates. This type of error would have a large impact on mean SFR values, reducing them to a half or less of a neurone's actual firing rate. Methods were tailored to minimize this possibility, as differences

in spike amplitude and subtle differences in spike shape were ignored and templates merged if spikes within the separate templates showed parallel firing patterns.

In conclusion, the BL SFR values recorded in the current experiments stretch outside the range of values typically seen for the DA neurone population, suggesting that there are both low-firing and high-firing non-DA neurones present within the recorded population. This theory is supported by the findings of numerous previous studies.

3.5.2.2 Burst firing analysis

A large number of studies assessing the firing patterns of VTA DA neurones have been conducted. These neurones typically show an irregular pattern of firing (although regular firing has also been witnessed in this population *in vivo*), interspersed with clusters of high frequency action potentials, or bursts. Burst firing is thought to be critical for VTA DA neurone function; the resulting high frequency dopamine release at axon terminals transiently increases dopamine concentration to the high levels required to activate certain populations of post-synaptic dopamine receptors (Marinelli and McCutcheon, 2014). In addition, it is thought that these high concentrations may enable dopamine to overwhelm re-uptake mechanisms and 'spillover' to nearby sites (Dreyer et al., 2010). Following the finding that GABA neurones possess a much greater degree of regularity in their spontaneous firing than do DA neurones (Steffensen et al., 1998), assessment of a neurone's burst firing behaviour has repeatedly been adopted as tool to aid VTA neurone identification *in vivo*.

The early experiments of Grace and Bunney (1984b) determined a much-needed universal measure to classify a burst: the start of a burst is described by a maximum interspike interval of 80msec, and its termination occurs when ISI passes a threshold of 160msec. However, in cells displaying fast and irregular firing (~SFR >10Hz), a proportion of spikes would be expected to fall within 80msec of each other, triggering detection of a burst despite the interval simply reflecting variability in an irregular pattern. Further, most subsequent intervals would fail to exceed the 160msec limit for termination of the burst. The net effect would be the false classification of spikes as belonging to bursts, rendering this method of burst quantification as unreliable for neurones with high firing rates (~10Hz and above). Measures were taken to ensure that this issue was not confounding the results obtained in the burst-related analyses performed here (described later).

Quantification of neuronal bursting activity is most-often done by calculating the percentage of all spikes existing within a burst (Marinelli and McCutcheon, 2014), so this measure was adopted for this study. No threshold was

set to separately classify "burst-firing" neurones and "non-burst-firing" neurones, as most accounts report population %SIB values, even within one neurochemical group, falling on a continuum (Mameli-Engvall et al., 2006; Marinelli and McCutcheon, 2014b), thus rendering any division arbitrary.

3.5.2.3 Baseline burst firing values

The population mean %SIB was 39.28±2.56%, which fits in well with mean values found previously for dopamine neurones under similar conditions (30%, Grace and Bunney, 1984b; 45%, Panin et al., 2012). The range of %SIB values (0.43% - 93.97%) was comprised of three natural groups, with SIB clusters 1, 2 and 3 possessing mean values of 79.24%, 43.80% and 14.28%, respectively. The range of %SIB values was large – with values as small as 0.43% and as great as 93.97%. Previous reports have described a similar range of values, with VTA neurones firing from 0% up to 80-90% of spikes within bursts (Grace and Bunney, 1984; Marinelli and McCutcheon, 2014b).

3.5.2.4 Comparisons between burst firing and firing rate measures

Previous studies found that the amount of burst firing of DA neurones (measured in %SIB) does not correlate well with SFR, and noted the recording of low-firing, high-bursting neurones (r=0.38, Grace and Bunney, 1984b; r=0.41, Marinelli and McCutcheon, 2014). It was concluded that the impact of the longer-duration post-burst 'pause' in spike firing on mean firing rate meant that the two variables could remain independent. To contrast these findings, results from the current experiments showed a strong correlation between SFR and BL SFR ($r=0.731$, $p<0.0001$). Possible reasons for the discrepancy in these results include differences in DA neurone population (Grace and Bunney were recording from the substantia nigra), differences in spike detection and recording methods (for example, different spike sorting criteria), differences in experimental set-up (Grace and Bunney used chloral hydrate anaesthesia), and the fact that no pre-selection of neuronal type took place in the current investigation (as opposed to putative neurone selection by Grace and Bunney). The latter factor is likely to have an influence, as one of the criteria for DA neurone identification in the previous study is the firing pattern – imposing a self-selecting influence on the recorded population for high burst firing neurones.

The relationship between %SIB and BL SFR was investigated further by comparing neurone cluster membership for BL SFR and %SIB. Results showed that a neurone's %SIB cluster membership predictive of its BL SFR cluster membership, and that BL SFR values of the three %SIB clusters were significantly different.

The value of %SIB is determined by both the frequency of bursts and the mean number of spikes in each burst. In order to shed light on which of these two factors is responsible to a greater degree for higher %SIB values of faster firing neurones, the relationships between them and SFR were investigated.

As previously mentioned, it is possible for an increase in mean spikes per burst value to occur as a direct result of increased BL SFR. As the mean SFR increases, mean ISI encroaches closer to the value representing the criteria for burst termination; at mean SFR of 6.25Hz mean ISI is 160msec. The result is a greater mean number of spikes per burst as it becomes more likely that subsequent spikes (occurring after the initiation of a burst) will be incorporated into the burst.

It was important to establish whether this was the sole cause of the positive correlation between %SIB with BL SFR, as this would imply that this relationship was inevitable and functionally irrelevant, rather than a functionally-interesting association of independent characteristics. The frequency of burst firing of a given neurone is unlikely to be strongly affected by BL SFR over the range of the recorded population; the ISI criteria for the start of a bust, 80msec, represents the mean ISI of a neurone firing at over 12Hz – only measured for one out of all 222 neurones recorded. Furthermore, the effect of SFR on burst termination criteria and therefore burst length will be much greater than it is on burst initiation criteria and therefore frequency of bursts.

In these investigations, it was found that the frequency of bursts in the baseline condition was more strongly correlated with BL SFR ($r=0.831$) than the number of spikes in a burst ($r=0.649$). This suggests that neurones with a higher BL SFR are more likely to be showing a greater %SIB due to an inherently greater frequency of burst firing than a greater number of spikes in each of their bursts.

Finally, the correlation between %SIB against BL SFR was calculated for neurones with SFR values below 6Hz only. Hylden and colleagues (2002), found that the causal effect of SFR on false burst classification only manifested as a confounding influence at SFR values of ~6Hz and above. It was shown in the current experiments that a highly significant positive correlation existed between %SIB and SFR below 6Hz, again implying that SFR effects on burst classification were not responsible for the positive relationship.

In conclusion, there was a strong relationship between the amount of burst firing and the spontaneous firing rate of a neurone - neurones with greater firing rates tended to show a greater degree of burst firing. This relationship was reflected in a dependency between the BL SFR and %SIB cluster memberships, suggesting that three

populations with low, medium and high mean SFR and %SIB values, respectively, exist within the VTA. While it is possible that direct effects of high SFR values on %SIB contribute to the relationship between the two variables, further analyses ruled out this being the sole cause of the correlation. The neuronal identity of the low, medium and high SFR groups was speculated previously (section 3.5.2.1). The fact that the high SFR group shows the greatest degree of burst firing is potentially problematic for the assumptions of these neurones containing a GABAergic population; previous studies have classified GABA neurones as regular-firing and non-bursting (Steffensen et al., 1998). However, studies conducted since have contradicted these findings. In one study, the range of coefficient of variation of the interspike interval values (ISI CV, a measure of irregularity of firing) of GABA (glutamic acid decarboxylase, an enzyme responsible for GABA production, -positive) neurones was very similar to that of DA (tyrosine hydroxylase, an enzyme responsible for DA production, -positive) neurones (Margolis et al., 2012). In another, neurones with firing rates >10Hz, deemed to be putative GABA neurones, showed a greater ISI CV than putative DA neurones (GABA ISI CV = 207±25%, DA ISI CV = 75±3%; Li *et al*., 2012). These findings suggest that GABA neurone firing pattern isn't that dissimilar to that of DA neurones in the anaesthetized preparation, and that fast-firing, putative GABA neurones may even show less-regularity in firing than slow-firing, putative DA neurones.

3.5.3 Location confirmation of recording sites

The location of the electrode tip, and therefore the location of the recorded neurone(s) was investigated for a subset of the initial experiments. The aim of this investigation was to confirm that the recordings were indeed taking place in the intended location of the VTA; whilst the stereotaxic apparatus together with reference points of the midline skull suture and bregma represent a reliable and accurate method of VTA localisation *in vivo*, electrode tip positioning in this way is susceptible to human error.

In total, 19 brain specimens were electrolytically lesioned to mark the electrode tip recording position, extracted, and stored for frozen sectioning with a microtome. Despite sectioning being attempted with all 19 brains, only 16 were successfully sectioned into 30µm slices of sufficient quality to allow structural identification through comparisons with the Paxinos and Watson rat brain atlas diagrams. Problems experienced with the cryostat apparatus and settings, and slicing technique were thought to be responsible for the insufficient quality of the sections from the remaining 3 specimens. These problems included an inappropriate temperature of the cryostat chamber causing the slices to roll up too fast or to bunch up and tear on the microtome blade, an improperly-

angled specimen causing the slices to be diagonal rather than coronal cross-sections, and a destruction of larger chunks of brain tissue due to OCT thawing.

Lesions were identified in 11 out of the 16 successfully sectioned brain. It is unknown why no lesion scar could be found in 5 of the brains. Possible reasons are that no lesion was made in the first place (due to incorrect setting up of the lesioning apparatus or apparatus malfunction), that the lesion was concealed by distortion of the tissue upon slicing, or that the lesion was made outside of the sectioned portion of the brain (typically, a flat coronally cross-sectioned segment of the whole brain was used for sectioning – created by removing the cerebellum and forebrain). The former two reasons are considered most likely, as electrode entrance holes were seen in each of the sectioned brain segments.

Crucially, results from the electrolytic lesion investigations showed that in 10 brains out of the 11-brain sample, the lesion and therefore recording location resided within the VTA sub-nuclei. 6-7 of the lesions were found in either paranigral or parabrachial pigmented nuclei – the two VTA sub-nuclei previously shown to contain the highest concentration of DA neurones (Nair-Roberts et al., 2008b).

There was one recording location found outside of the VTA, within the neighbouring parvocellular part of the red nucleus (RPC). The RPC is thought to be primarily involved in motor rather than sensory functions, with direct efferent connections to motor neurones in the spinal cord (forming the rubrospinal tract; Herter et al., 2015), and negligible responses of RPC neurones to sensory stimuli (Gibson et al., 1985; Kennedy et al., 1986). These findings imply that there is significant functional separation between VTA and RPC neurones despite the anatomic proximity between the red nucleus and VTA.

The literature on spontaneous firing characteristics of the neurones residing in the RPC and the neighbouring red nucleus region suggest that they exhibit relatively high firing rates in comparison to VTA neurones – in the order of 20-30 spikes per second (or Hz). As baseline SFR values found within the current recorded population ranged from 0.1-14.58Hz, suggesting that either no red nucleus neurones were included in the sample, or that only low firing red nucleus were. Evidence for the existence of the latter was not found within the literature.

In conclusion, these results imply that the majority of recordings described in this thesis are likely to have been made within the VTA as intended. However, some error was shown to have occurred, and therefore it is important to consider the possibility that some of the recordings took place outside the VTA. Extra-VTA recordings, in regions such as the red nucleus or substantia nigra, may explain some of the anomalous results seen amongst data sets. It is also important to note that a sample of 11 recordings is very small, and therefore that there is a chance these results are not representative of the general recorded population analysed in this thesis.

3.5.4 Grouping neurones according to noxious response

Initial *in vivo* electrophysiological studies suggested ventral tegmental DA neurones functioned as a homogeneous population, uniformly excited by rewards and inhibited by aversive events (Mirenowicz and Schultz, 1996; Ungless et al., 2004). Conversely, GABA neurones have been found to be excited by acute noxious stimuli (Tan et al., 2012). Subsequently, Brischoux and colleagues (2009) established that there was in fact a subset of DA neurones excited by aversive stimuli, and that the two populations could be separated anatomically; noxious-inhibited neurones tended to reside within the dorsal VTA, whereas noxious-excited neurones could be found in the ventral VTA. Furthermore, while BL SFR did not differ between the noxious-inhibited and noxious-excited groups, there were significant differences between mean %SIB of the two groups (%SIB: noxious-inhibited = 2.58%, noxious-excited = 28.71%). DA noxious responses of both directions have since been identified in the majority of investigations, with inhibitions occurring in 11-83% and excitations occurring in 0-67% of DA neurones, depending on the study (reviewed in McCutcheon et al., 2012).

As a consequence, neurones recorded in this study were classified and subsequently grouped according to responsivity to both paw von Frey and heat stimuli, and the location and baseline firing characteristics of the response-based groups were compared.

It was initially intended for the responses to both stimuli to be assessed separately to establish any differences in effect of the thermal and mechanical modalities. However, the low numbers of noxious-responsive neurones amongst the recorded population made it necessary to combine neurones inhibited by and excited by the two different stimuli, forming general noxious-inhibited and noxious-excited groups. Given evidence suggesting that the nociceptive modality differentiating property of spinal cord dorsal horn and thalamic neurones is unlikely at

this level of the midbrain (Overton et al., 2014), the combining of responses shouldn't represent an issue for interpretation.

Given the relatively large population of DA neurones in the VTA (~70%) as compared to GABA (~30%) or glutamatergic (2-3%) contingents (Ford et al., 1995; Kalivas, 1993; Nair-Roberts et al., 2008b; Yamaguchi et al., 2007b; Dobi et al., 2010), it is most appropriate to compare the current findings with the literature on DA neurone responsivity. Research on VTA GABA neurone response to noxious stimuli is limited, but there is evidence that the population can be noxious-excited, at least in response to foot shock (Tan et al., 2012). Consequently, it is hypothesised that a proportion of the noxious-excited neurone population is likely to be GABAergic.

Only 2% and 19% of neurones showed an inhibitory and excitatory noxious response, respectively. These values are incredibly low in comparison to those recorded in previous studies, particularly with respect to inhibition; for example, Ungless and colleagues (2004) recorded 85% of DA neurones as foot pinch-inhibited (and 0% noxious-excited), whilst Kiyatkin (1988) found 26% of VTA DA neurones were tail pinch-inhibited. In general, there is a large degree of heterogeneity within studies' reports of nociceptive responsivity (McCutcheon et al., 2012), so some degree of discrepancy is expected. Possible reasons for the differences include the lack of stringent response-classifying criteria in some studies (e.g. Kiaytkin, 1988; Ungless et al., 2004), in contrast to the response classification threshold set here. Further, differences in measured noxious responsivity could come from the differences in intensity and location of noxious stimulation, differences in depth of anaesthesia, and differences in stimulus-evoked firing rate measurement protocols (e.g. Ungless et al., 2004 only used the last 5 seconds of a 10-second stimulus application for their analysis).

5.5.4.I Baseline firing properties of noxious-responsive neurones

The baseline firing properties of noxious-inhibited, noxious-excited and noxious-unresponsive neurones, including firing rate and amount of burst firing (SFR and %SIB), were compared. Unfortunately, the sample of noxious-inhibited neurones (N=2) was too small for any conclusions to be drawn about this population. There was a trend towards noxious-excited neurones displaying reduced BL SFR values yet greater %SIB values than non-responsive neurones; however, these differences were not significant. The latter trend is in-line with the findings of Brischoux and colleagues (2009), suggesting that the criteria imposed on the response classifications in the current experiments may be masking a similar finding. A standardised response criterion is essential to

differentiate general fluctuations in firing from a physiologically-relevant response, however, meaning that broadening of the criteria would only serve to invalidate the analysis. Instead, this relationship would be better explored by increasing the sample number within the noxious-responsive groups.

3.5.4.2 Location of noxious-responsive neurones

Previous reports suggest that there is a dorsoventral separation of noxious response-categorised neurones, with noxious-excited and noxious-inhibited DA neurones found in more ventral and dorsal regions of the VTA, respectively (Brischoux et al., 2009). Specifically, noxious-excited neurones were predominantly found in the PN and PIF, and noxious-inhibited in the PBP and PIF. In agreement with these results, a significant proportion of the noxious-excited neurones found here were located in the PN (N=5), with some also in the PIF (N=2). However, the presence of these neurones in the PBP (N=4) is at odds with the previous findings (N=0; Brischoux et al., 2009). The two noxious-inhibited neurones were recorded in the PBP and PIF – the two locations in which Brischoux and colleagues found these DA neurones. A greater number of this neuronal type would be necessary to test the significance of any alignment or lack thereof between the current and previous results.

It is important to reiterate that these locations are measured from coordinates according to the stereotaxic apparatus, not from actual visualisation of the location of the electrode tip location within the sectioned brain specimen (as described in section 3.3.3.6).

3.5.5 Morphine response of VTA neurones

The original two-neurone canonical model of VTA neurone circuitry proposed by Johnson and North in 1992 has since been challenged by a wide range of evidence. While a tonic inhibitory influence on DA neurones from local GABA interneurones remains an established mechanism (Tan et al., 2012), it is now known that this model is much too simple. This is particularly apparent in mu-opioid receptor (MOR) agonist action on VTA neurones. Heterogeneity in response to MOR activation has been shown in both confirmed GABA and DA neurones (Gysling and Wang, 1983; Matthews and German, 1984; Cameron et al., 1997; Ford et al., 2006; Margolis et al., 2003; Margolis et al., 2012), and it has been shown that many, if not most, of the VTA DA neurones express MORs (Garzón and Pickel, 2001; Margolis et al., 2014), rendering attempts of identifying neurochemical subgroups through MOR pharmacology alone invalid. Nevertheless, given the evidence supporting a role of endogenous opioid action within the VTA in both pain and reward and the lack of studies examining the profile

of MOR agonist response of VTA neurones *in vivo*, the probing of the MOR modulatory system by the injection of the exogenous agonist, morphine, was deemed a necessary investigation.

3.5.5.I Natural clustering according to morphine response

It was found that neurones could be sorted into two groups according to normalized firing rate post-morphine injection: one cluster consisting of the majority of the recorded neurones (cluster 2; N=13, 72.2%) showing a gradual reduction in SFR post injection, and a smaller cluster (cluster 1; N=5, 27.8%) showing an apparently-excitatory response, on average. Cluster 2 neurones showed a significant mean percentage reduction in SFR from baseline at all time points from 20 minutes post-injection-onwards. Normalized values of cluster 2 neurones were only significantly different from those seen following vehicle control injections at the 40-minute time point, implying that inhibitory responses are likely to be at least partially caused by injection effects other than the pharmacological action of morphine on μ-opioid receptors. However, the finding that no significant percentage reduction in SFR from pre-injection values occurred following injection of the vehicle alone suggests that the non-pharmacological injection effects did not have a large impact on the witnessed response to morphine.

The canonical 2-neurone model of opioid action in the VTA proposed by Johnson and North (1992) would predict a most-likely dopaminergic identity of the morphine-excited neurone cluster (1) and a GABAergic identity of the group showing a mean inhibitory response to morphine injection (Gysling and Wang, 1983; Matthews and German, 1984). However, the quoted proportions of VTA neurones belonging to the two most populous neurochemical groups (~60-70% dopaminergic, 30% GABAergic; Ford et al., 1995; Kalivas, 1993; Nair-Roberts et al., 2008b; Yamaguchi et al., 2007b; Dobi et al., 2010), along with the weight of evidence contradicting a simple picture of GABA-mediated DA neurone disinhibition (Ford et al., 2006; Margolis et al., 2012, 2014), suggest that a clear neurochemical split into response-based clusters is unlikely. Instead, it seems more accurate to assume that the morphine injection-inhibited and excited neurone clusters both contain a mixture of neurochemical cell identities.

The size of the morphine-excited neurone cluster was relatively small, comprising of only 27.8% of the recorded population. No reports on the relative proportions of morphine-excited and morphine injection-inhibited neurones amongst the general VTA population were found in the literature, but a few studies have quoted numbers of MOR agonist-responsive neurones within putative or confirmed DA and GABA neurone populations. For example,

Margolis and colleagues reported that 20% and 41% of TH+ neurones were excited and inhibited, respectively, and 15% and 56% of TH- neurones were excited and inhibited, respectively, in response to MOR agonist injection (Margolis et al., 2014). The remaining neurone proportions were unresponsive. Margolis and colleagues also reported that ~1/2 of confirmed GABA neurones recorded were inhibited (2012) by a MOR agonist, and the rest unresponsive. In light of these findings, it is not unexpected that a greater proportion of recorded VTA neurones fell into morphine-inhibited versus unresponsive or excited clusters, and it is proposed that this injection-inhibited group is likely to contain a mix of neurochemical subtypes.

3.5.5.2 VTA location of neurones responding differently to morphine injection

As discussed in relation to the noxious-responsive neurone location analysis, location has previously been found to differentiate functional neuronal groups within neurochemical populations. The location in which the neurones belonging to the morphine-excited and morphine-inhibited neurone clusters were recorded was mapped according to the stereotaxic coordinates. No dorsoventral differentiation of the two morphine response-based clusters was found; however, there was some degree of rostrocaudal separation. Only morphine injection-inhibited neurones (cluster 2) were found in the most caudal recording locations (bregma -6.8-6.9mm). However, due to the low number of the morphine-excited cluster 1 neurones recorded, this finding remains unreliable.

3.5.5.3 Baseline firing rate and morphine response characteristics

Group mean baseline SFR of morphine-excited and injection–inhibited neurone clusters was compared. While a trend towards morphine-inhibited neurones possessing greater baseline firing rates was seen, differences between group mean values were not significant – a finding not unexpected in light of the low numbers of neurones comprising the morphine-excited neurone cluster.

Subsequently, the normalised morphine responses of the high and low firing neurone clusters established from cluster analysis on the baseline SFR values of all neurones recorded in the naïve condition (BL SFR cluster 1n and 2n, respectively) were assessed to see if these neurone populations displayed differing morphine responsivity, No significant effects of morphine were witnessed for either of the BL SFR clusters, suggesting that baseline firing rate characteristics are not predictive of morphine response. However, as the BL SFR cluster 1n high-firing neurones did appear to show a group mean inhibitory response to morphine injection, it is possible that with a

greater number of neurones than the current group size of three this population of VTA neurones would have shown a significant morphine response.

In conclusion, it was not possible to identify coherent populations of VTA neurones when considering the functional characteristics of firing rate, noxious responsivity, MOR agonist response and location. Instead, the natural clustering according to the different characteristics differentially divided the recorded population with no apparent relationship between them. While these findings differ from the early studies suggesting clear-cut neurochemical and functional groupings (Johnson and North, 1992; Ungless et al., 2004, Brischoux et al., 2009), they are in-line with more recent reports of substantial characteristic heterogeneity (e.g. Marinelli and McCutcheon, 2014; Margolis et al., 2014).

An exception to this apparent incongruence between neuronal characteristics was seen in the relationship between the spontaneous firing characteristics of neurones; firing rate was strongly correlated with the amount of burst firing displayed by a neurone. Further analysis of this relationship and that between other burst-firing parameters suggests this was not simply a consequence of a reduced mean interspike interval, but likely represented an interesting association between functionally-relevant firing characteristics.

Another method of characterisation commonly adopted or discussed in the literature is the assessment of dopamine receptor agonist responsivity. In particular, D2 receptor agonists are known to inhibit the firing rate of the VTA DA neurones but leave GABA neurones unaffected, at least for the most part. Further, D2 receptor-mediated inhibition of dopamine neurones forms a significant contribution to the tonic modulation of firing of this population *in vivo*, rendering insights into this receptor system valuable.

4. Pharmacological characterisation with L-DOPA

4.I Introduction

L-DOPA (L-3,4-dihydroxyphenylalanine) is a chemical precursor of catecholamines, which includes DA. When ingested or injected systemically, it crosses the blood-brain barrier and is taken up by neurones of the central nervous system. Within target nerve cells, L-DOPA is converted into DA by the enzyme L-aromatic amino acid decarboxylase, thereby elevating intracellular stores of this neurotransmitter for subsequent release.

The ability of L-DOPA to raise DA levels in existing DA neurones renders it extremely effective in the symptomatic treatment of Parkinsons' Disease, a motor and cognitive disorder resulting from the progressive death of this cell population. Aside from this clinical role and of interest to this investigation, L-DOPA has repeatedly proven to be a useful tool in research in identification of DA neurones, both in labelling *in vitro* and pharmacologically *in vivo*. The latter function stems from L-DOPA's propensity to act as a mixed DA receptor agonist through enhanced physiological DA release.

It is well-established that DA agonists inhibit DA neurone firing (Bunney et al., 1973; Kalivas, 1993; White and Wang, 1984). The D2-type DA autoreceptors, present on the cell bodies and dendrites of most, if not all, of the DA neurones of the VTA, are thought to mediate this effect. Unlike the D1 subtype, D2 receptors are inhibitory, coupling $G_{i/o}$ to inhibit adenylyl cyclase and calcium channels, which in-turn result in activation of G protein-coupled potassium channels (Neve et al., 2004). The opening of these channels permits a potassium conductance that acts to hyperpolarise the DA cell body, thereby reducing action potential firing frequency (Kim et al., 1995; Lacey et al., 1987).

This explains how DA agonists exert their effects, but what is the natural physiological function of the D2 autoreceptors in the awake animal? It appears that, through the vesicular release of DA from their own cell body and dendrites - so-called somatodendritic release, D2-mediated autoinhibition exerts a powerful modulatory

influence on the DA neurons, instating autoreceptor feedback as an important regulator of neuronal activity (Aghajanian and Bunney, 1977; Bunney et al., 1973; Lacey et al., 1987; Mercuri et al., 1997).

L-DOPA, by triggering the synthesis of DA, acts to simply enhance this natural modulatory mechanism. Thus, systemic L-DOPA administration is likely to be more of a physiological and targeted manipulation than the flooding of all regions that results from injection of a DA agonist. Furthermore, co-administration of carbidopa, a powerful inhibitor of the aromatic amino acid decarboxylase enzyme that does not cross the blood-brain barrier, prevents peripheral synthesis of DA from levodopa, thereby limiting effects to central DA systems only. Ultimately, however, in terms of receptor-mediated effects L-DOPA can be said to act as a DA agonist. Indeed, in rodents, the systemic injection of L-DOPA reduces both DA neurone activity (Bunney et al., 1973) and DA release in the NAcc (Abercrombie et al., 1990). As expected from DA's expected role in pain processing, this also translates to an L-DOPA-induced enhancement of pain-related behaviour in rats (Paalzow, 1992). Interestingly, these effects of L-DOPA show strong dose-dependency; injection of a much higher dose – in the realms of ~100mgkg^{-1} (as opposed to the typical dose of ~20mgkg^{-1}) - resulted in the opposite effects of an increase in NAcc DA release and a reduction in pain-related behaviour (Abercrombie et al., 1990; Paalzow, 1992). It is thought that the curiously dichotomous dose-dependency of L-DOPA action reflects the differential expression and affinity of the D2 and D1-type DA receptors, responsible for auto-modulation of VTA DA neurone firing rate and conveying signals to downstream targets, respectively. By probing an in-tact system through L-DOPA administration it is possible to witness the effects of an increase in gain of the endogenous DA system, thereby increasing the understanding of the role of these neurones *in vivo*.

4.2 Aims and predictions

In light of the previously described evidence, separation of neurones according to L-DOPA response is considered to be a promising method of singling out the dopaminergic neurones *in vivo*. Hence, this study aims to establish VTA neurone responses to low doses of L-DOPA, with the prediction that the recorded population will be separable into L-DOPA-inhibited and L-DOPA-excited groups. Subsequently, animals will be injected with a high dose of L-DOPA to test the dose-dependency of any effects soon, thereby testing assumptions of low dose-response group identity. It is predicted that a high dose will have opposite effects on putative DA neurons to the low dose. Finally, the nociceptive properties of all neurones will be examined, both in the pre-drug condition to establish differences between L-DOPA-classified putative DA and non-DA groups, and throughout the experiment to reveal any influence of this neurochemical manipulation on neurone function. Due to the mixed and unclear nociceptive properties of VTA neurones previously recorded in section 3, it will not be surprising if no clear group responses to the painful stimuli are found.

4.3 Materials and Methods

4.3.I Experimental protocol

In vivo electrophysiology was performed as described in section 2. See figure 4.I for the experimental timeline. Stimulation rounds consisted of two noxious modality stimuli and their innocuous controls (all 5 seconds): 4g von Frey filament and 60g von Frey filament, foot submersion in 35°C water and foot submersion in 50°C water. Following establishment of a stable baseline spontaneous firing rate, a low dose of L-DOPA (or vehicle + carbidopa, or vehicle-only control injection) was administered (see section 4.3.2), and spontaneous and evoked firing rates were monitored using two stimulation rounds at each time point of 10, 20, 40, 60, 100 and 120 minutes post-injection. At 120 minutes post-injection of the low dose of L-DOPA (not the control injections), a high dose of L-DOPA was administered and the stimulus round protocol was repeated.

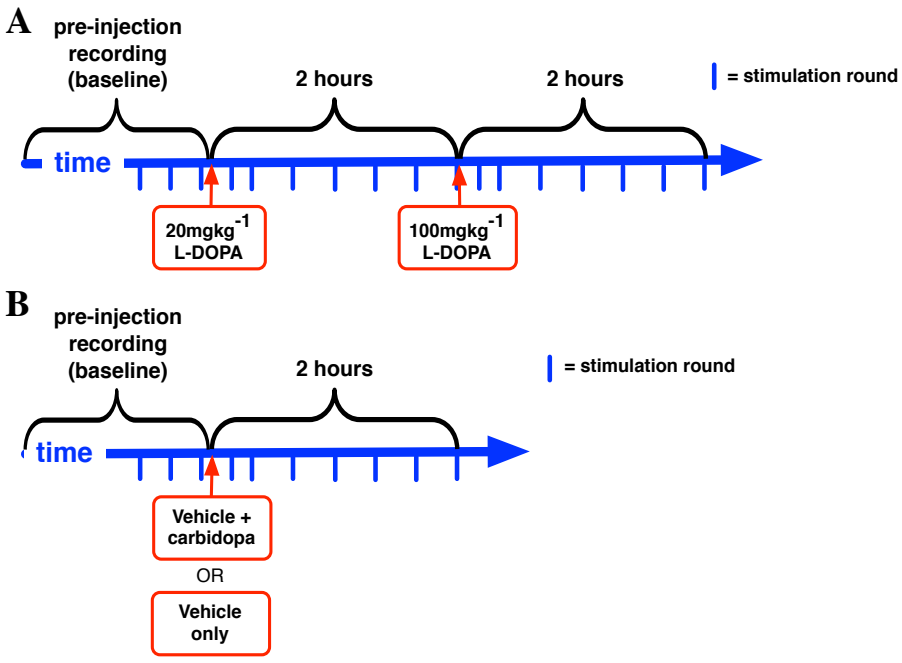

Figure 4.1 Experimental timeline of low and high dose L-DOPA experiments. The thick blue horizontal arrow represents the progression of time during the experiment, while vertical blue dashes indicate the times at which stimulation rounds were performed (stimulation round described in section 4.3.I). A) At least 4 stimulation rounds were performed in the baseline condition (not all rounds are depicted), and then at 10, 20, 40, 60, 80, 100 and 120 minutes following low dose L-DOPA injection, and the subsequent high dose L-DOPA injection. B) Two sets of control experiments were conducted – those in which a vehicle + carbidopa injection replaced the low dose L-DOPA injection, and those in which only the vehicle was injected in replacement of low dose L-DOPA. No high dose was injected in these control experiments.

4.3.2 Drug administration

Carbidopa and L-DOPA (both Sigma-Aldrich, UK) in the dose ratio 1:4 were dissolved in 0.2M HCL and the pH of the solution was adjusted to 6.8 using 7% $NaHCO_3$. Drug solutions, in doses of initially 20mgkg^{-1} ('low dose') and then 100mgkg^{-1} ('high dose'), were made up immediately before injection and administered intraperitoneally in a volume of 20mlkg^{-1}. Two sets of control experiments were performed: carbidopa + vehicle, and vehicle-only, for which injection volumes and pH were matched to that of the L-DOPA injections.

4.3.3 Data analysis

L-DOPA effects on spontaneous firing rate were assessed by first performing a cluster analysis (two-step and K-means) on raw mean SFR values at every time point post-injection, and then by repeating this analysis on the normalized SFR values (calculated as the percentage of mean pre-injection SFR). For the low dose (20mgkg^{-1}) L-DOPA injection, post-injection mean SFR values were normalized relative to mean baseline SFR values; for the high dose (100mgkg^{-1}) L-DOPA injection, values were normalized relative to mean SFR at 120 minutes post low dose injection. Response to low dose L-DOPA injection were compared with responses recorded following injection of both carbidopa + vehicle and vehicle-only controls. Subsequently, baseline spontaneous firing rate, noxious responsivity, and burst firing were calculated for each L-DOPA response-based group as detailed previously in sections 3.3.3.2, 2.2.3.2, and 3.3.3.3, respectively.

4.4 Results

The high and low dose L-DOPA experiments were carried out on 23 animals, plus an additional 5 for carbidopa-only control experiments and 5 for vehicle-only experiments. 32 neurones were characterised from the L-DOPA-injection experiments, 8 from the carbidopa + vehicle controls, and 7 from the vehicle-only controls. 6 neurones from the L-DOPA experiments, 3 from the carbidopa + vehicle control experiments, and 1 from the vehicle control experiments were omitted from further analyses due to highly variable within-time point post-injection firing rates (i.e. substantial minute-to-minute variability in SFR).

4.4.I Effects of low dose L-DOPA (20mgkg^{-1})

4.4.I.I Non-normalized SFR

Cluster analysis (Two-step and K-means) performed using values of mean SFR of all 26 analysed neurones at all time points post-injection of low dose L-DOPA revealed the existence of two natural response-based clusters (figure 4.2). These clusters were named raw L-DOPA cluster 1 and raw L-DOPA cluster 2, to reflect the use of raw data (non-normalised) for this analysis. Raw L-DOPA cluster 1 neurones (N=23) appear to show an inhibitory response to L-DOPA injection, on average, with a gradual reduction in mean SFR occurring over the two hours. However, baseline SFR of this group was too variable to assess response size. Similarly, raw L-DOPA cluster 2 neurones (N=3) showed too much within-cluster variability in baseline SFR to determine injection effects.

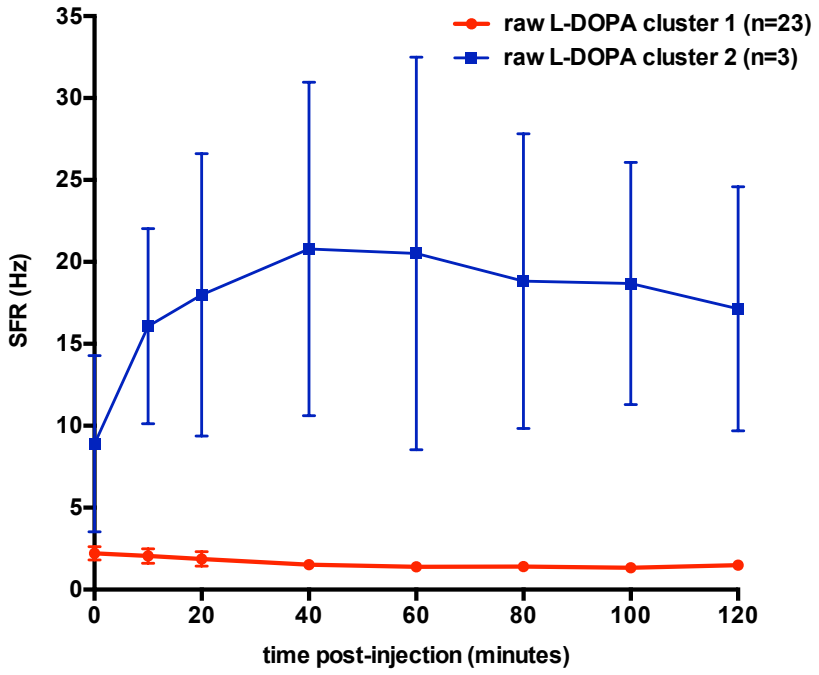

Figure 4.2 Mean spontaneous firing rate of L-DOPA response-based neurone clusters at all time points post-L-DOPA injection. Graph shows data points and bars representing mean SFR ± SEM in Hz of raw L-DOPA cluster 1 (N=23, red trace) and raw L-DOPA cluster 2 (N=3, blue trace) at all time points post injection of 20mgkg^{-1} L-DOPA.

4.4.I.2 Normalized SFR

The two-step and k-means cluster analyses were re-performed using normalized SFR values for each time point (% of pre-injection value). Two clusters were identified: norm L-DOPA cluster 1 showing an apparent inhibition in response to L-DOPA injection (N=22) and norm L-DOPA cluster 2 showing an apparent excitation in response to L-DOPA injection (N=4; figure 4.3). For both norm L-DOPA clusters 1 and 2, there was a rapid onset of L-DOPA effect on SFR, with values reaching 63.96%±9.79% and 328.26%±49.87% of pre-drug values for norm L-DOPA cluster 1 and cluster 2, respectively by the 10 minutes post-injection time point. Thereafter, mean normalized SFR of cluster 1 neurones remained reasonably consistent throughout the 2 hours, whilst cluster 2 neurones showed recovery in SFR from 20 minutes post-injection onwards (figure 4.3). Mean percentage decrease in SFR from mean baseline values of the norm L-DOPA cluster 1 neurones was significant at all time points up to and including 60 minutes post-injection when using a Bonferroni-corrected alpha value of 0.008 (Friedman test with post-hoc Wilcoxon signed-rank pairwise comparisons, baseline vs 10min: Z=-2.873, p=0.004; baseline vs 20min: Z=-3.393, p=0.001; baseline vs 40min: Z=-3.100, p=0.002; baseline vs 60min: Z=-2.646, p=0.008). Mean

percentage increase in SFR from mean baseline (pre-injection) SFR of norm L-DOPA cluster 2 was not found to be significant according to a Friedman test for repeated measures.

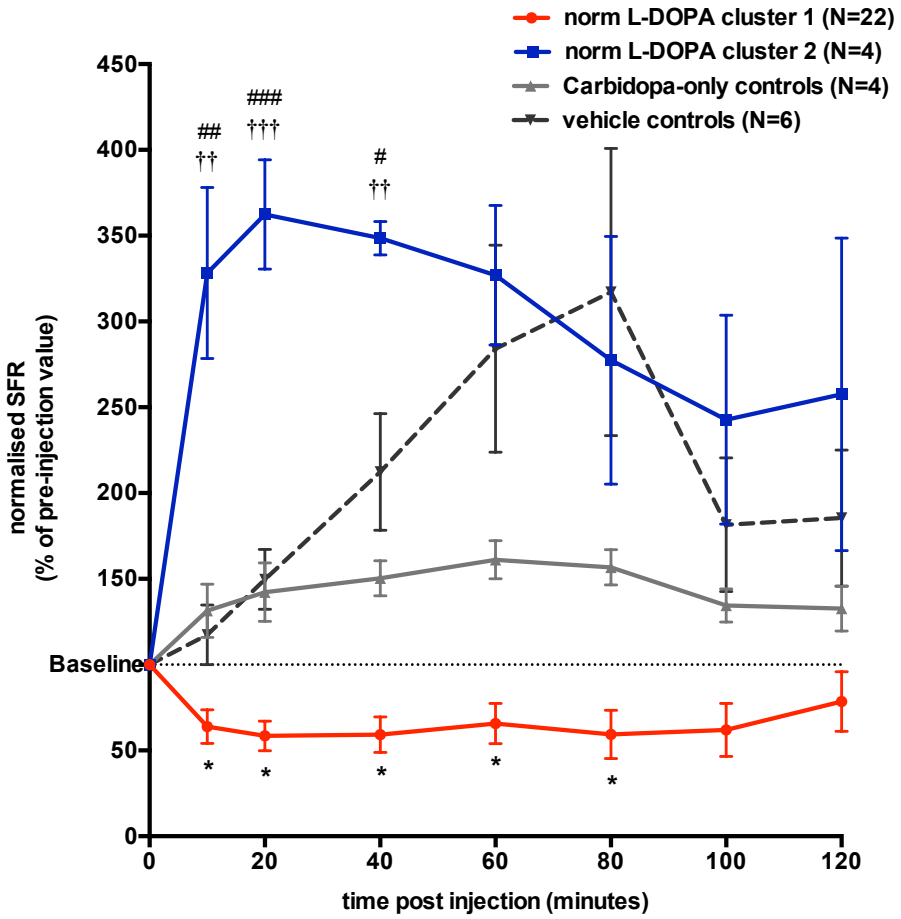

Figure 4.3 Normalized SFR of L-DOPA normalized response-based clusters and control data sets at all time points post L-DOPA or control injection. The graph shows data points and bars representing mean normalized SFR ± SEM (SFR expressed as a percentage of mean baseline SFR) of norm L-DOPA cluster 1 (LDI, N=22, red trace), norm L-DOPA cluster 2 (LDE, N=4, blue trace), carbidopa + vehicle control neurones (N=5, light grey trace) and vehicle-only control neurones (N=6, black dashed trace). Friedman's Tests followed by post-hoc Wilcoxon signed-rank pairwise comparisons using a Bonferroni-corrected alpha of 0.008 were conducted to test for significant percentage changes in SFR from baseline, $p<0.008$ *. One-way ANOVA tests with a post-hoc Bonferroni analysis were carried out to test for differences between norm L-DOPA cluster 2 mean normalized SFR and the two control groups' mean normalized SFR values at all time points post-injection, $p<0.005$ ††, $p<0.0005$ ††† (carbidopa + vehicle controls); $p<0.05$ #, $p<0.005$ ##, $p<0.0005$ ### (vehicle-only controls).

4.4.2 Responses to the two control injections

Friedman's tests followed by post-hoc Wilcoxon signed-rank pairwise comparisons (using a Bonferroni-corrected alpha of 0.008) revealed that neither carbidopa + vehicle nor vehicle-only control groups displayed significant increases in SFR relative to mean baseline values at any of the six time points post-injection (figure 4.3).

The percentage increase in SFR from baseline shown by the norm L-DOPA cluster 2 neurones was significantly greater than that recorded from carbidopa + vehicle control experiments at time points of 10, 20 and 40 minutes post-injection (one-way ANOVA followed by a Bonferroni post-hoc analysis, 10min: $p=0.003$; 20min: $p<0.0005$; 40min: $p=0.002$), and significantly greater than that recorded from vehicle-only experiments at time points of 10, 20 and 40 minutes post-injection (one-way ANOVA followed by a Bonferroni post-hoc analysis, 10min: $p=0.001$; 20min: $p<0.0005$; 40min: $p=0.012$).

4.4.3 Effect of high dose L-DOPA (100mgkg^{-1})

Spontaneous firing rates recorded throughout the two hours following injection of 100mgkg^{-1} (high dose) L-DOPA were normalized by converting SFR values into a percentage of mean pre-injection SFR. Neurones were grouped according to low dose L-DOPA-response cluster (norm L-DOPA cluster 1 and norm L-DOPA cluster 2) and group mean normalized SFR for each time point was calculated for the respective clusters (figure 4.4).

On average, the norm L-DOPA cluster 1 neurons – the group that showed a mean inhibition in response to low dose L-DOPA - displayed a sustained enhancement of SFR relative to pre-injection values, with peak effect at the 100 and 120-minute time points (mean normalized SFR [% of mean baseline SFR]: 100min = 342.7%; 120min = 315.0%). The percentage increase in SFR from mean baseline SFR was significant at all time points from 60 minutes post-injection onwards when using a Bonferroni-corrected alpha of 0.008 (figure 4.4; Friedman test with post-hoc Wilcoxon signed-rank pairwise comparisons, baseline vs 60min: $Z=-2.728$, $p=0.006$; baseline vs 80min: $Z=-3.007$, $p=.003$; baseline vs 100min: $Z=-3.180$, $p=.001$; baseline vs 120min: $Z=-3.215$, $p=0.001$). Conversely, high dose L-DOPA injection had no effect on norm L-DOPA cluster 2 neurones above that seen two hours post-low dose, with mean normalized SFR values remaining near mean pre-injection SFR.

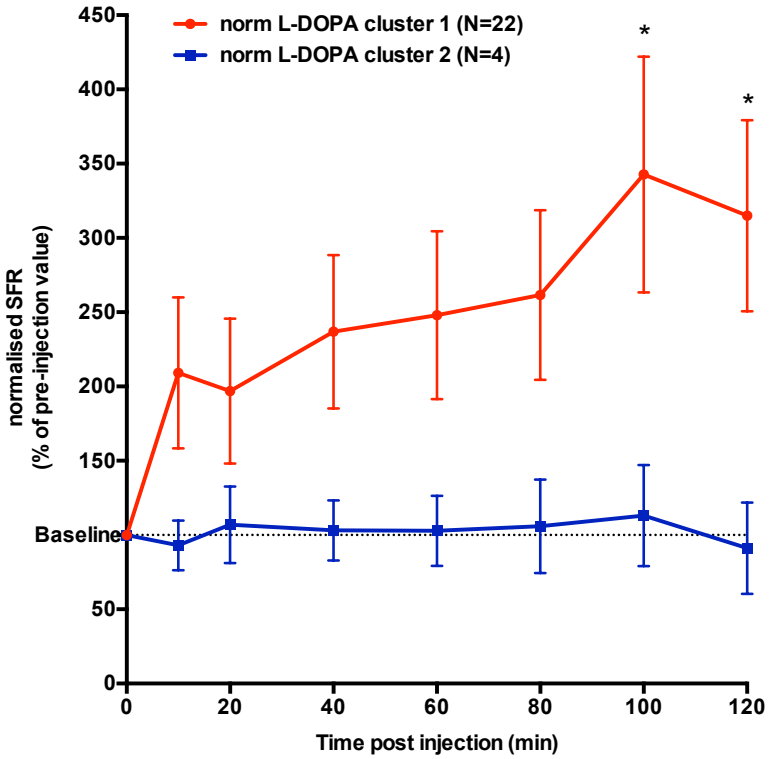

Figure 4.4 High dose L-DOPA effects on the SFR of low dose normalized L-DOPA response-based neurone clusters. Normalized SFR values (% of pre-injection SFR) of low dose (20mgkg^{-1}) norm L-DOPA cluster 1 (N=22, red trace) and norm L-DOPA cluster 2 (N=4, blue trace) were plotted for each time point during the two hours post-injection of 100mgkg^{-1} L-DOPA. Data points and bars represent mean ± SEM values. Friedman tests with post-hoc Wilcoxon signed-rank pairwise comparisons were conducted to establish significant percentage changes in SFR from mean baseline SFR, using a Bonferroni-corrected alpha value of 0.008. * P<0.008.

Thus, by normalising the spontaneous firing rate relative to pre-injection values it was shown that neurones belonging to norm L-DOPA cluster 1 – the cluster showing a group mean inhibitory response to low-dose L-DOPA - were, on average, excited by injection of the high dose. The norm L-DOPA cluster 2 neurones, in contrast, displayed no significant mean change in spontaneous firing rate above that seen two hours post-low dose.

4.4.4 Characterisation of low dose L-DOPA response-sorted neurones

4.4.4.I Baseline spontaneous firing rate

The relationship between baseline SFR and mean normalized SFR across time points of 10, 20 and 40 minutes post-injection was investigated for all recorded neurones (figure 4.5A). An average of these three time points was chosen as it spanned peak normalized L-DOPA effect for both norm L-DOPA cluster 1 and 2. No significant correlation was found between BL SFR and L-DOPA effect size for either norm L-DOPA cluster 1 or 2.

The baseline spontaneous firing rate of norm L-DOPA cluster 1 neurones and norm L-DOPA cluster 2 neurones were compared (figure 4.5B). No significant differences were found between the two groups, and the small group of LDE neurones showed a relatively large degree of variability in BL SFR values (Mean BL SFR: LDI = 2.568±0.608Hz; LDE = 3.188±1.527Hz).

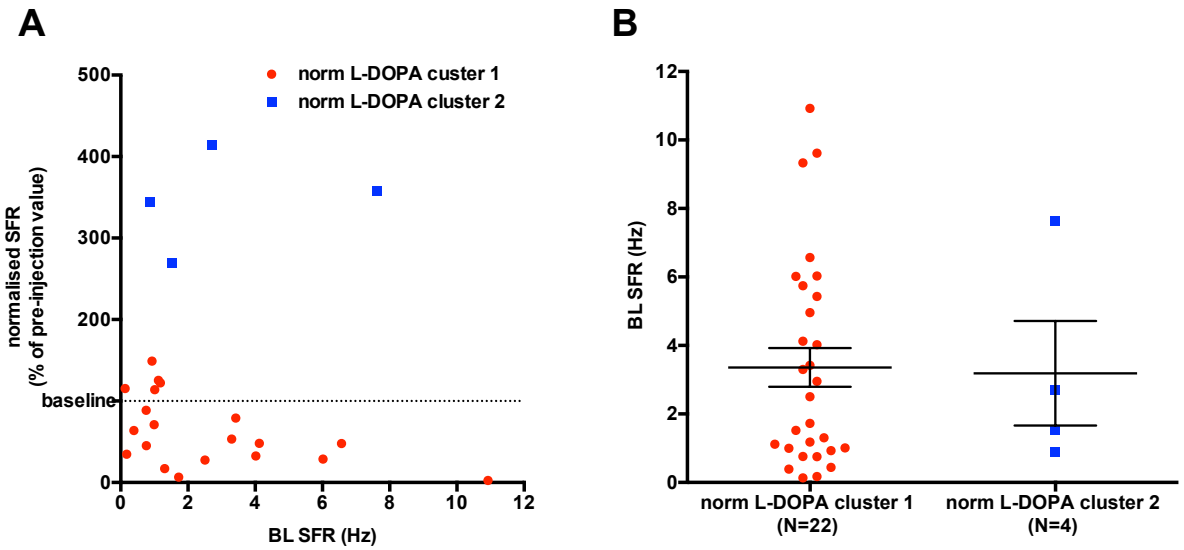

Figure 4.5 The relationship between L-DOPA response and baseline spontaneous firing rate. A) Scatter plot showing the mean normalized SFR (y-axis; expressed as a percentage of mean pre-L-DOPA injection SFR) and BL SFR (x-axis; Hz) of neurones belonging to norm L-DOPA cluster 1 (N=22, red data points) and norm L-DOPA cluster 2 (N=4, blue data points). Horizontal dashed line at y=100% represents mean baseline values. B) Column graph showing BL SFR (y-axis; Hz) of individual neurones in norm L-DOPA cluster 1 (red data points) and cluster 2 (blue data points). Bars represent mean ± SEM.

In a subsequent analysis, the normalised SFR at all time points following low dose L-DOPA injection was plotted for neurones belonging to BL SFR cluster 1n and 2n established in section 3.4.2 (figure 4.6). Four of the neurones recorded in the current L-DOPA experiments had a cluster identity of BL SFR cluster 1n (high firing), whilst 20 neurones belonged to the BL SFR cluster 2n cluster (low firing). Neither BL SFR cluster 1n nor 2n neurones showed a mean group percentage change in SFR following low dose (20mgkg^{-1}) L-DOPA injection according to Friedman's test followed by post-hoc Wilcoxon signed-rank pairwise comparisons; figure 4.6).

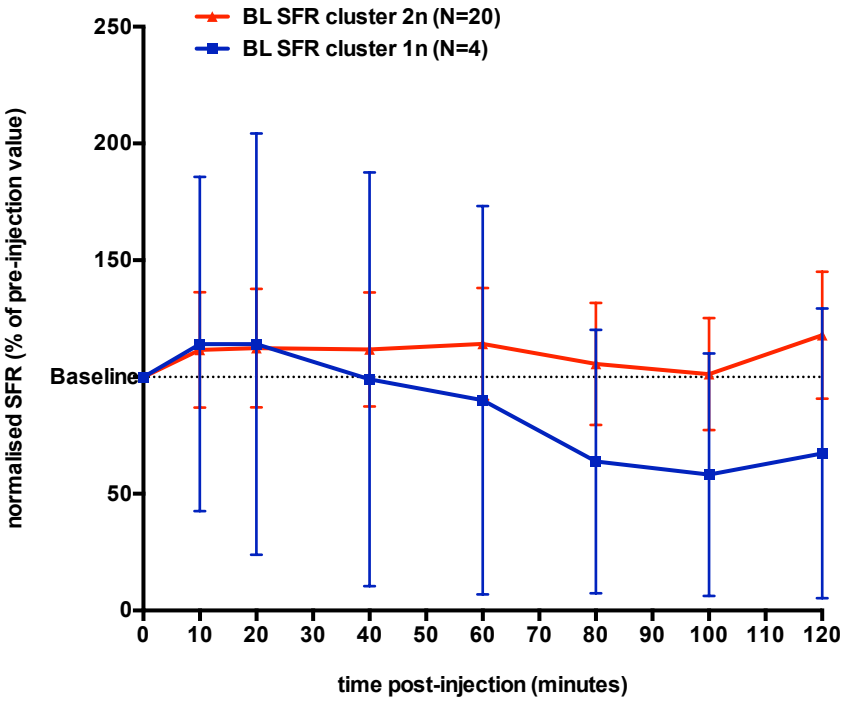

Figure 4.6 Normalized spontaneous firing rate of BL SFR cluster neurones following injection of 20mgkg^{-1} L-DOPA. Data points show mean ± SEM spontaneous firing rate expressed as a percentage of mean pre-L-DOPA injection values of neurones belonging to BL SFR cluster 2n (low firing; N=20; red trace) and BL SFR cluster 1n (high firing; N=4; blue trace) neurone groups. Mean values for both response-based clusters are shown for all time points post L-DOPA injection. The dashed horizontal line at y=100% represents mean pre-injection (baseline in this case) SFR values). Friedman's tests followed by post-hoc Wilcoxon signed-rank pairwise comparisons were conducted to establish whether L-DOPA injection caused a significant percentage change in SFR of BL SFR cluster 1n or 2n neurones, but yielded insignificant results.

4.4.4.2 The percentage of spikes within a burst

The percentage of spikes present within a burst (%SIB) was measured for the baseline condition, the 2 hours following injection of low dose L-DOPA, and the 2 hours following injection of high dose L-DOPA for all neurones recorded in the current experiments. Mean %SIB values of norm L-DOPA 1 cluster (L-DOPA-inhibited) and norm L-DOPA cluster 2 for each condition were compared, and any within-cluster, between-condition changes were assessed (figure 4.7). Neither injection of low dose nor high dose L-DOPA resulted in a significant change in mean %SIB of norm L-DOPA 1 and 2 clusters. Baseline %SFR values of the two L-DOPA response clusters did not differ significantly, possibly due to low number of neurones and high within-cluster variability of norm L-DOPA cluster 2 (mean %SIB: norm L-DOPA cluster 1= 29.31±5.17%; cluster 2 = 38.62±16.26%); however, the group mean %SIB of neurones belonging to norm L-DOPA cluster 2 was significantly greater than that of the norm L-DOPA cluster 2 population during the 2 hours post-low dose L-DOPA injection (mean %SIB: norm L-DOPA cluster 1 = 19.84±3.30%; cluster 2 = 62.19±17.05%; independent samples *t*-test: t(25) = 4.146, p<0.0005).

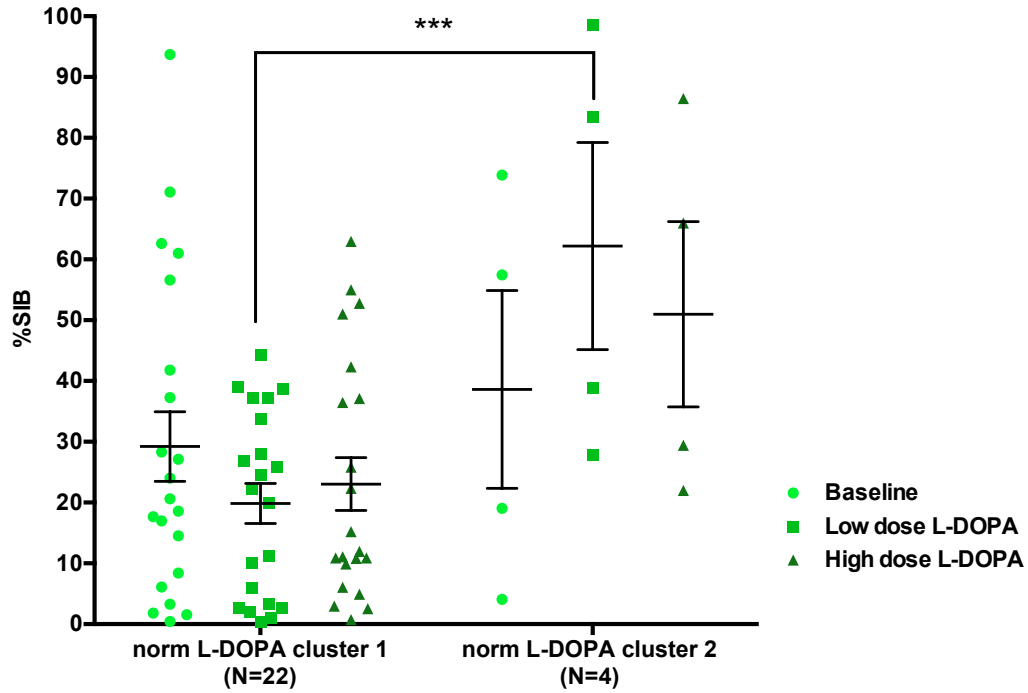

Figure 4.7 Amount of burst firing shown by neurones sorted according to L-DOPA response-based cluster analysis in baseline, low dose L-DOPA-injected and high dose L-DOPA-injected conditions. Graph shows the percentage of all spikes recorded during the baseline condition (light green circles), the 2 hours post-low dose L-DOPA injection (green squares), and the 2 hours post-high dose L-DOPA injection (dark green triangles) present within a burst (%SIB, y-axis) of both norm L-DOPA clusters 1 (N=22) and 2 (N=4). Independent samples *t*-tests were conducted to test for differences between the mean % burst firing of norm L-DOPA clusters 1 and 2 in each experimental condition, *** p<0.0005.

4.4.4.3 Nociceptive responsivity

Mean firing rates during the presentation of a tail pinch or paw heat noxious stimulus for each neurone in the baseline condition were compared with the mean baseline SFR. As described in methods section 2.2.3.2, a neurone was classified as responsive to a given stimulus if the mean stimulus-evoked firing rate was greater or less than the mean BL SFR plus or minus 1.96 times the standard deviation of the BL SFR, respectively.

It was found that none of the recorded neurones met the criteria for noxious responsivity to either paw heat or von Frey stimuli.

4.5 Discussion

4.5.I Response to low dose L-DOPA

DA receptor pharmacology has been widely used in attempts to classify VTA neurones *in vivo*. Because electrophysiological criteria and opioid responsivity painted a confusing and undefined picture, it was deemed necessary to explore the VTA neurone response to L-DOPA injection – known to act as a mixed DA agonist *in vivo*. Previous studies show that systemic injection of L-DOPA inhibits the firing rate of the DA neurone population (Bunney et al., 1973), leading to a reduction in DA release in the nucleus accumbens (Abercrombie et al., 1990). In support, studies have found that D2 receptor agonist application inhibits the firing rate of nearly all antidromically or neurochemically-confirmed DA neurones (Chiodo et al., 1984; Clark and Chiodo, 1988; Gariano et al., 1989; Lammel et al., 2008; Luo et al., 2008; Wang, 1981). A proposed theory to explain the inhibition of DA function by low doses of systemic L-DOPA implicates the high-affinity inhibitory D2 autoreceptors as key (Paalzow, 1992). L-DOPA uptake into target neurones and the subsequent DA synthesis leads to increased intracellular stores, enhancing somatodendritic release of the neurotransmitter. Resultant subtle increases in DA concentration surrounding the soma and dendrites activates the relatively high affinity D2 autoreceptors (Skirboll et al., 1979), modulating DA neurone activity directly via a hyperpolarising potassium conductance (Kim et al., 1995; Lacey et al., 1987). The result is a reduction in spontaneous firing rate of the DA neurones.

In addition to autoinhibitory modulation, the increase in extracellular DA would enhance activation of D1 receptors present on axon terminals of afferent GABAergic projections, thereby increasing GABA-mediated inhibition of DA neurones (Kalivas and Duffy, 1995a). Thus, it seems plausible that firstly, any L-DOPA-inhibited neurones recorded here are dopaminergic, and secondly, that inhibitions in SFR witnessed reflect an augmentation of physiological autoregulation of DA neurones.

The population of neurones recorded in the current investigation could be divided into two groups according to L-DOPA response: one showing a mean inhibitory response to injection and the other, showing a seemingly-excitatory response that failed to represent a significant group response. The majority of recorded neurones (88%) fell into the L-DOPA-inhibited cluster (norm L-DOPA cluster 1), with only 12% in the other seemingly-excited

but statistically unresponsive group (norm L-DOPA cluster 2). This is in agreement with previous reports showing that the VTA neurone population as a whole contains a mixture of inhibitory, excited and insignificant responses to D2 agonist application (li et al., 2012).

4.5.I.I Can we trust these results?

The results from two sets of control experiments – vehicle-only and vehicle + carbidopa - were compared with the L-DOPA injection effects. Both groups of control neurones showed seemingly-excitatory responses post-injection, neither of which represented statistically significant percentage increases from baseline. However, upon visualisation of the results, it appears likely that an excitatory effect of the vehicle injections has not been picked up here due to the low number of neurones within each of the control groups. If a greater number of experiments were to reveal a significant effect of vehicle or vehicle + carbidopa injection, what would be the implications for the current results? It was found that the mean percentage increases in SFR following the control injections were significantly smaller than that seen for the norm L-DOPA cluster 2, implying that pharmacological action is contributing, at least in-part, to the visible yet insignificant response of the latter population; however, it is feasible that some effect of vehicle injection is contributing to the magnitude of any excitatory effects of L-DOPA injection seen. A potentially excitatory effect of vehicle or vehicle + carbidopa injection would serve, if anything, to increase confidence in the inhibitory response of the norm L-DOPA cluster 1 neurone population, suggesting that the real pharmacological effect was even greater than that seen in terms of percentage change from pre-injection SFR.

The mean effect of low dose L-DOPA on spontaneous firing rate was rapid for both L-DOPA response-based clusters, with near maximal changes seen at 10-20 minutes post-injection. This time course of action of systemic L-DOPA is in agreement with previous observations showing that similar doses decrease extracellular DA concentration and significantly facilitate pain behaviour as early as 15-20 minutes post-injection (Abercrombie et al. 1990; Paalzow, 1992), further suggesting that the group responses witnessed here are due to pharmacological action.

4.5.I.2 Neurochemical identity of the L-DOPA response clusters

The previous findings surrounding L-DOPA and D2 receptor agonist action discussed above suggest that the L-DOPA-inhibited cluster (norm L-DOPA cluster 1) most-likely represents a predominantly dopaminergic population. The identity of the other cluster (norm L-DOPA cluster 2) is more uncertain, but the relative proportions of the two non-dopaminergic neurochemical groups within the VTA (GABAergic: 30%, glutamatergic: 2-3%), and previous findings of DA agonist excitation of GABA neurones via excitatory D1 receptors (Matthews and German, 1986), suggest a greater likelihood of a GABAerigc rather than dopaminergic or other identity. However, the findings of some more recent studies imply that neurochemical division by DA pharmacology is not quite so clear-cut; a subset of VTA DA neurones fail to show inhibitory responses to the D2 agonist, quinpirole, whilst a proportion of the non-DA neurones, including confirmed GABA neurones, do (Margolis et al., 2012; Li et al., 2012). Possible explanations for these findings include the discovery of amygdala and PFC-projecting DA neurones lacking D2 autoreceptors, and the witnessing of a direct action of a D2 agonist on a group of GABA neurones (Bannon and Roth, 1983; Chiodo et al., 1984; Kalivas, 1993; Lammel et al., 2008; Margolis et al., 2008; White and Wang, 1984).

Nevertheless, because evidence suggests that the majority of DA neurones tend to show inhibitory responses to D2 receptor agonists (Li et al., 2012; Chiodo et al. 1984; Clark and Chiodo 1988; Gariano et al. 1989; Lammel et al. 2008; Luo et al. 2008; Wang 1981), and because this population represents the largest proportion of neurones within the VTA, it is deemed likely that norm L-DOPA cluster 1 contains mainly dopaminergic neurones. Further investigations into the characteristics of the two L-DOPA-response clusters may help to shed light on their neurochemical composition.

4.5.2 Response to high dose L-DOPA

Both Paalzow (1992) and Abercrombie and colleagues (1990) document an intriguing and pronounced dose-dependency of L-DOPA effect; whereas low doses in the realm of the 20mgkg^{-1} used here cause increases in pain sensitivity (Paalzow, 1992), reductions in DA neurone activity (Bunney et al., 1973), and subsequent DA release in the NAcc (Abercrombie et al., 1990), doses an order of magnitude higher result in opposite effects on both behaviour and DA release. Paalzow (1992) found that doses of L-DOPA between 100-200mgkg^{-1} resulted in a transient increase in pain sensitivity between 10-15 minutes post-injection, followed by a prolonged and

prominent period of analgesia. Similarly, Abercrombie and colleagues observed a long-lasting increase, rather than decrease, in extracellular DA levels after a high dose of L-DOPA, that peaked at 90 minutes post-injection. Current popular theory to explain the disparate dose-related effects of L-DOPA implicates separate mechanisms mediated by DA receptors with different pharmacological properties. As outlined in sections 4.I and 4.5.I, low doses of L-DOPA are thought to suppress spontaneous firing rates of DA neurones through an enhancement of inherent self-modulatory mechanisms (figure 4.8A). The consequence is an overall reduction in axon terminal DA release in projection targets and therefore a dampening of the downstream effects including antinociception. Conversely, it is thought that doses of 100mgkg^{-1} L-DOPA or greater 'overload' the neurones with DA, leading to substantial unphysiological and stimulus-independent release sufficient to activate the higher-affinity post-synaptic D1 receptors on recipient neurones (figure 4.8B; Paalzow, 1992). This would explain the enhanced NAcc DA release and antinociception following a high L-DOPA dose.

In the current experiments, 100mgkg^{-1} L-DOPA was injected two hours after injection of the low dose, and spontaneous firing rates were monitored at subsequent regular time intervals. The low dose-inhibited neurones displayed a significant and long-lasting increase in spontaneous firing rate in response to the high dose, with peak effect at 100 minutes post-injection. If a proportion of the low dose norm L-DOPA cluster 1 neurones recorded here were indeed dopaminergic, the increase in SFR witnessed upon injection of a high dose would tie in with the increase in DA release and reduction in pain behaviour witnessed in the previous studies. In support of a predominantly dopaminergic neurochemical identity of the low dose inhibited, norm L-DOPA cluster 1 group, the time profile of SFR increase closely mirrors that of behaviour and DA release responses (Paalzow, 1992; Abercrombie et al., 1990). It was previously considered that the L-DOPA inhibited cluster 1 may contain a subset of GABA (or other non-DA) neurones, based on findings from the literature on D2 receptor agonist action in the VTA. If so, these GABA neurones would most likely be of the projection rather than interneurone type to be in fitting with the L-DOPA high dose responses witnessed; $GABA_A$ and $GABA_B$ receptor activation is known to lead to a reduction in DA neurone activity and DA release in the NAcc (Lacey, 1993; Westerink et al., 1996, 1998; Xi and Stein, 1999), which is at odds with the upregulation of DA release and with the lack of an inhibitory response reported in previous and current investigations, respectively, in the face of high dose injection. Consequently, it is hypothesised that the low dose-inhibited, high dose-excited neurone group recorded (norm L-DOPA cluster 1) here predominantly contains DA neurones, with a potential addition of GABAergic projection neurones.

This still leaves the question of exactly how high doses of L-DOPA could excite these putative VTA DA neurones. There are several long- and short-range firing rate-modulating loops involving VTA neurones, which could plausibly act to translate enhanced somatodendritic (i.e. local) or axonal DA release following a high L-DOPA dose into changes in DA neurone firing. The endpoint would need to be either an increase in excitatory or decrease in inhibitory modulation to cause the mean percentage increase in SFR seen. Local perfusion of D1 agonists enhances glutamate release from frontal brain regions within the VTA – the principal source of excitatory input to this region (Kalivas and Duffy, 1995b; Lu et al., 1997). This effect was mimicked by increasing DA levels in the VTA through systemic application of cocaine (which acts to block DA re-uptake; Kalivas and Duffy, 1995). Given that L-DOPA ultimately increases interstitial DA within the VTA, albeit through a different mechanism, it appears feasible that a similar D1-mediated enhancement of glutamate excitatory influence on DA neurones occurs upon L-DOPA injection. If accurate, this mechanism would most likely be mediated by AMPA/kainate receptors in order to fit in with the current results; while AMPA/kainate activation causes increases in firing rate without changes in firing pattern (Chergui et al., 1993), NMDA receptor activation robustly promotes burst-firing of VTA neurones – a change that was not seen in the low dose-inhibited neurones upon high dose injection (see %SIB analysis, section 4.4.4.2; Chergui et al., 1993; Johnson et al., 1992; Kretschmer, 1999). Another possible mechanism lies in GABAergic input from the NAcc, shown to synapse specifically onto non-DA neurones in the VTA (Hjelmstad et al., 2013; Xia et al., 2011). It is feasible that enhanced activation of the NAcc medium spiny neurones results in increased GABAergic tone on the VTA GABAergic interneurones, ultimately resulting in a disinhibition of dopaminergic neurones.

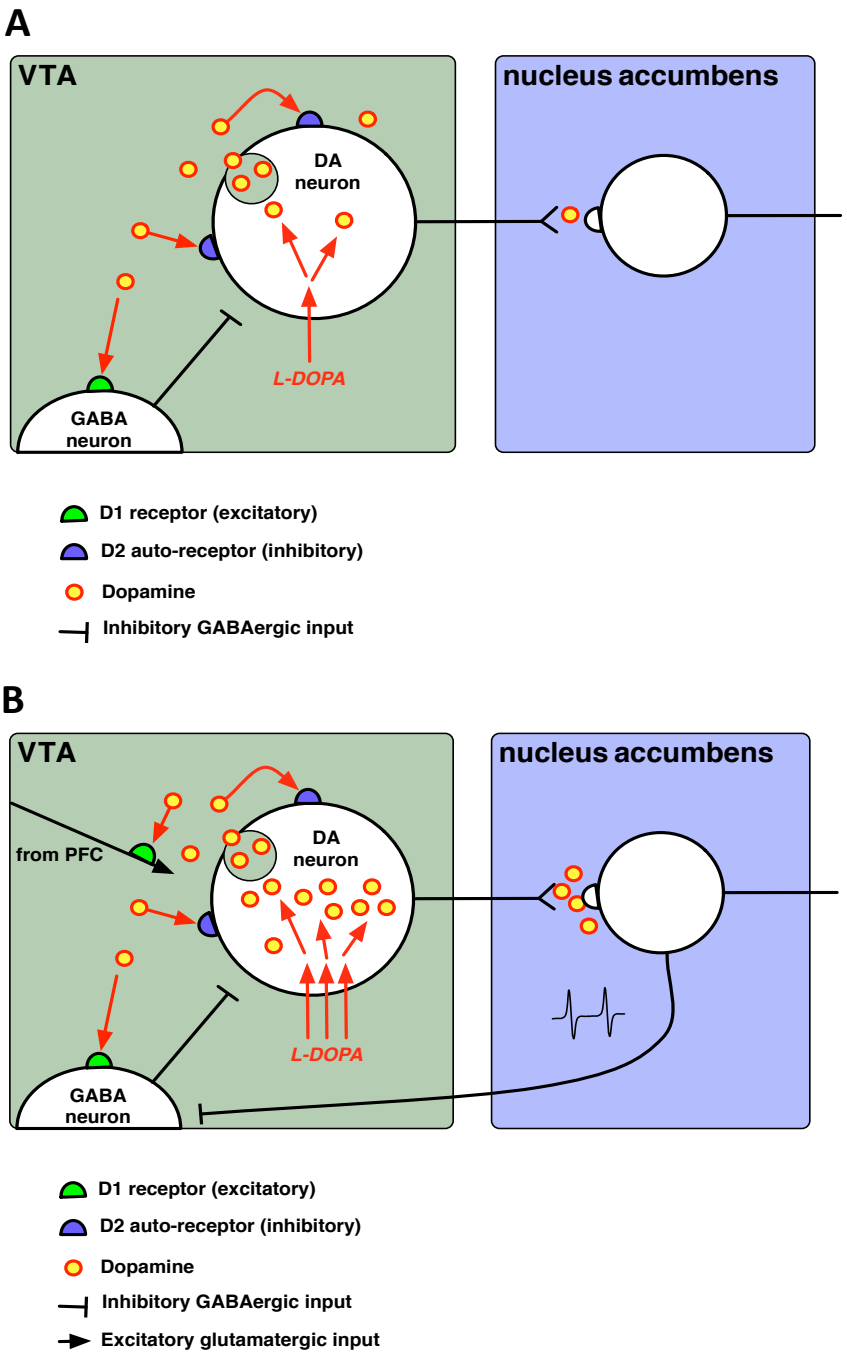

Figure 4.8 Schematic diagram of a proposed model of L-DOPA action on VTA neurones. A) 20mgkg^{-1} L-DOPA causes a moderate increase in DA synthesis within VTA DA neurones (red arrows). Somatodendritic vesicular release causes an increase in DA concentration surrounding the neurones, leading to increased autoinhibition via D2 receptors, as well as enhancement of GABA release via excitatory D1 receptors. **B)** 100mgkg^{-1} L-DOPA causes a large increase in DA synthesis within VTA DA neurones (red arrows). As with the low dose, somatodendritic release and autoinhibition takes place, but more prominently, there is stimulus-independent release at axon terminals on projection target neurones (NAcc in this case). Somatodendritic release of DA within the VTA reaches levels sufficient to activate D1 receptors present on glutamatergic afferents, increasing excitatory tone on VTA DA neurones and therefore firing rate. It is also feasible that disinhibition of DA neurones occurs via GABAergic input from the NAcc onto VTA GABA interneurones. Please note: this diagram is for clarity, and is not an accurate representation of the anatomical structure or neurone-based location of these events.

Interestingly, the high L-DOPA dose had no opposing or even additional effect on the SFR of norm L-DOPA cluster 2 following injection of the low dose. This implies a much simpler one-dimensional mechanism through which L-DOPA-derived DA affects these putative GABAergic cells, one that is already maximally recruited with low concentrations. For example, it is plausible that D1 receptors on GABAergic neurones are fully activated by the increase in extracellular DA seen in the VTA following 20mgkg^{-1} L-DOPA injection.

4.5.3 Spontaneous firing characteristics of L-DOPA-inhibited and –excited neurone clusters

4.5.3.I Baseline spontaneous firing rate

Previous studies report that the firing rate of DA neurones is inversely correlated with the sensitivity to DA agonist-inhibition (White and Wang, 1984). This relationship is thought to be caused by the firing rate-modulating ability of tonic D2 receptor autoinhibition; the more D2 receptors present on the soma and dendrites of a DA neurone, the greater the tonic inhibitory influence and the lower the spontaneous firing rate. However, the current findings revealed no relationship between baseline SFR and magnitude of L-DOPA effect across 10, 20 and 40-minute time points for the neurones showing inhibitory responses to injection. There are many plausible reasons for this discrepancy in findings. Firstly, this study was using L-DOPA rather than a direct D2 receptor agonist, such as quinpirole; L-DOPA uptake into DA neurones, DA synthesis and somatodendritic release are all potential additional sources of neurone-to-neurone variability in DA receptor occupancy for a given dose. The difference between the enhancement of natural modulation mechanisms with L-DOPA and the indiscriminate and homogenous activation of receptors with a direct agonist is the primary reason for using the former in the current experiments. By observing the effects of L-DOPA, neurone differences in DA production and somatodendritic release are taken into account – both functionally important in the natural autoinhibition process. Secondly, White and Wang had filtered neurones according to firing rate, action potential duration and burst-firing characteristics in order to isolate the DA neurones, whereas the current analysis was performed on all recorded neurones. While all neurones in the low dose inhibited norm L-DOPA cluster 1 (with the exception of one) had SFR values <10Hz (White and Wang cut off for DA neurone versus non-DA neurone characterisation), the lack of firing pattern and action potential filtering could be concealing a significant relationship. However, this seems unlikely.

Another explored relationship was the difference between firing rates of norm L-DOPA cluster 1 and 2 neurone groups. Li and colleagues (2012) analysed the effects of quinpirole on VTA neurones sorted according to spontaneous firing rate, with a group separation threshold of 10Hz. They found that the majority of low firing neurones displayed inhibitory responses to quinpirole, with only 30% showing insignificant or excitatory responses, whereas the high firing neurones displayed a normally-distributed response size centred around an un-responsive majority. This would translate into a lower mean SFR of inhibited neurones in comparison to that of excited or unresponsive neurones.

The current analysis showed that the norm L-DOPA cluster 1 and cluster 2 neurone groups showed no significant differences in mean baseline SFR. Similarly, when neurones were sorted according to BL SFR cluster membership (high firing: BL SFR cluster 1n, low firing: BL SFR cluster 2n), no differences in L-DOPA responsivity were seen between neurone groups, further suggesting a lack of relationship between baseline firing rate and L-DOPA effect. While these results appear to disagree with the findings of Li and colleagues, it should be noted that all but one of the recorded neurones here had a SFR <10Hz, and hence would fall into their low firing neurone class. In other words, the current results cannot be reasonably compared with the data provided in the previous study.

4.5.3.2 Burst firing

The amount of burst firing displayed on average by neurones falling into the norm L-DOPA clusters 1 and 2 was compared. Differences between both response-based clusters and between pharmacological conditions (baseline vs low dose L-DOPA vs high dose L-DOPA) were compared. It was found that the amount of burst firing, measured in percentage of spikes within bursts, did not change upon low dose or high dose L-DOPA injection for either norm L-DOPA cluster 1 or 2. This is unexpected in the light of previous studies showing that %SIB changes concurrently with pharmacologically-induced changes in SFR of a given VTA DA neurone (Grace and Bunney, 1984b). However, these previous findings resulted from experiments involving glutamate receptor agonist iontophoresis, which, in principle, could lead to glutamate receptor activation on any VTA neurone in the near vicinity, as opposed to the relatively targeted changes in DA levels (in the immediate vicinity of DA neurones only) resulting from L-DOPA injection. NMDA receptor activation is known to enhance burst firing of dopaminergic neurones both *in vivo* (Chergui et al., 1993) and *in vitro* (Johnson et al., 1992). On the other hand, the mechanisms behind L-DOPA-induced changes in SFR – perhaps mainly D2 receptor activation - may instead only effect single spike firing.

The amount of burst firing shown by the norm L-DOPA cluster 2 neurones was found to be greater, on average, than that of the norm L-DOPA cluster 1 neurones following the injection of L-DOPA only. This condition represents the stage during which the greatest differences between the mean SFR of these two neuronal groups existed. It is possible that the impact of SFR on %SIB values discussed in section 3.5.2.4 pushes previously insignificant between-group differences in burst firing into a statistically-validated result, perhaps unmasking an effect previously invisible due to low neurone numbers.

4.5.3.3 Nociceptive responsivity

It was found that none of the recorded neurones from both norm L-DOPA clusters 1 and 2 met the criteria for nociceptive responsivity. This was not unexpected given the low proportion of neurones found to be responsive in the previous investigation (section 3.4.5), and possible reasons for the relative lack of sensitivity in comparison to that found in the literature have already been discussed (section 3.5.4). In light of these results, it was decided that nociceptive responsivity would not be assessed in subsequent investigations as the recording methodology used to generate all data throughout this thesis appeared to not pick up this VTA neurone trait.

4.5.4 Concluding remarks

This investigation found that the recorded VTA neurones could be divided into two subpopulations according to response to systemic L-DOPA, which on average displayed significant inhibitory and seemingly (but not statistically) excitatory responses to injection of a low dose, respectively. In light of evidence elucidating effects of L-DOPA on the mesolimbic DA system (Abercrombie et al., 1990; Bunney et al., 1973) it was considered plausible that the L-DOPA-inhibited cluster (norm L-DOPA cluster 1) neurones were predominantly dopaminergic. On the other hand, it was hypothesised that the statistically unresponsive cluster (norm L-DOPA cluster 2) most likely contained a majority of GABAergic neurones, albeit with less confidence. A largely dopaminergic identity of the norm L-DOPA cluster 1 population was supported by the high dose response of these neurones; an excitatory response peaking at ~100 minutes post-injection is in-line with the increase in DA release in the NAcc and the reduction in pain-related behaviour witnessed in previous high dose L-DOPA investigations. Further, the proportions of neurones belonging to norm L-DOPA cluster 1 and 2 found within the recorded population fit in well with that of VTA DA and GABA neurone populations quoted in the literature. There was

no agreement between the baseline firing characteristics of the recorded neurones and those reported in previous studies, but in light of key methodological and pharmacological differences including the use of direct D2 receptor agonists rather than L-DOPA, neurone pre-selection criteria, and the use of glutamate rather than L-DOPA to alter SFR (all discussed in sections 4.5.3.I and 4.5.3.2), this was not unexpected. Finally, changes in firing rate upon L-DOPA injection were not matched with concordant changes in burst firing, suggesting that activity modulation involved in generating the observed inhibitory and excitatory responses (presumed to be via D2 and D1 receptors, respectively) were specific to single spike firing properties and not burst-generating mechanisms.

It is important to note that the above theories of interpretation have only incorporated within-VTA mechanisms of action. This is largely because D2 autoreceptor and D1 presynaptic receptor-based mechanisms are discussed in depth in previous literature with respect to L-DOPA actions on midbrain DA neurones. However, systemically injected L-DOPA will inevitably be taken up into DA neurones (or indeed, noradrenergic neurones) elsewhere in the CNS (carbidopa rules out extra-CNS metabolism), making it possible that the changes in firing rate witnessed are in fact due to down-stream effects. Clarifying this may help to unmask neurochemical identity and thereby increase confidence in a number of assumptions tentatively proposed here: firstly, that the L-DOPA-inhibited neurones are likely to be dopaminergic, and secondly, that the quoted mechanistic model is accurate.

5. Investigation of L-DOPA mechanisms with sulpiride-mediated D2 receptor antagonism

5.I Introduction

It is becoming ever-increasingly apparent that the ventral tegmental area is a region complex in terms of both function and neurochemical structure. The originally simple dual-neuron model of the VTA, describing dopaminergic and GABAergic populations only (Johnson and North, 1992), has been expanded through many discoveries of heterogeneity in properties such as pain and reward responsivity and pharmacological modulation. Work from this thesis up until this point reflects this complexity. A high level of intricacy is to be expected when the subtle adjustments in neuronal activity necessary for diverse roles in circumstance-appropriate stimulus-driven behaviour are considered.

One key modulatory influence within the VTA is the tonic autoinhibition of DA neurones via D2 autoreceptors (Ford, 2014; Neve et al., 2004). In the natural state, tonic inhibition via D2 autoreceptors is provided by extracellular DA released somatodendritically from the DA neurones themselves (Kalivas, 1993). Enhancement of this mechanism by administration of D2 receptor agonists has been shown, as expected, to cause a robust inhibition of DA neurone activity, rendering this pharmacological manipulation a valuable in vivo neurochemical identifier in populations found in the substantia nigra and VTA (Kalivas, 1993; Westerink et al., 1996; Georges, 2006; Morzorati & Marunde, 2006; Chiodo et al. 1984; Clark and Chiodo 1988; Mereu et al. 1985; Wang 1981; Li et al., 2014).

In this current investigation of the VTA, the DA precursor L-DOPA, rather than a DA agonist, is used as a classification tool due to the more targeted and physiological nature of its action. Studies using the D2 receptor antagonist sulpiride have provided strong evidence for a large involvement of this receptor in production of

systemic L-DOPA effects; systemic injection of sulpiride reversed the hyperalgesia caused by L-DOPA (Paalzow, 1992), whist injection into the spinal cord completely blocked effects of local L-DOPA application (Shimizu et al., 2004). What remains unclear, however, is the extent to which local D2 receptors are responsible for the previously witnessed L-DOPA effects on firing rate of VTA neurones (section 4); whilst sulpiride application has been shown to block the inhibitory action of L-DOPA on A9 DA neurones in vitro (Mercuri et al., 1990), no such study investigating the local action of L-DOPA within the VTA was found.

The labelling of DA neurone populations as A8-16 reflects the complexity of this neurotransmitter system, with major nigrostriatal and tuberoinfundibular pathways existing alongside the mesocortical and mesolimbic projections from the VTA (Wood, 2008). Furthermore, the distribution of DA receptor expression hints at the extensive brain-wide reach of DA signalling; D2-receptors, for example, are found in high density in the striatum, NAcc, and olfactory tubercle, and some extent in the hippocampus, amygdala, hypothalamus and cortical regions (Beaulieu and Gainetdinov, 2011; De Mei et al., 2009; Missale et al., 1998; Schmitz et al., 2003). It is feasible that, following systemic injection of L-DOPA, uptake and subsequent DA release occurring elsewhere in the central nervous system has a downstream impact on VTA DA neurone activity. The relative contribution of local D2-mediated DA neurone inhibition versus undetermined upstream mechanisms to L-DOPA effects on VTA neurone activity is a question this study aims to clarify.

There are several methods for determining the involvement of a specific brain region in a drug effect pharmacologically. Iontophoresis, reverse microdialysis and microinjection are all techniques adequate at delivering a dose of receptor agonist or antagonist directly to the surrounding area of a neurone of interest (du Hoffmann et al., 2011). In comparison with iontophoresis and microdialysis, localized microinjection allows the delivery of greater volumes that can affect a significantly larger area of interest, whilst avoiding some of the disruption produced by microdialysis (Aksenov et al., 2014). Further, it can be used in concert with in vivo extracellular recordings of multiple units (du Hoffmann et al., 2011), deeming it appropriate for the current study.

5.2 Experimental aims and predictions

This study aims to help elucidate the mechanism and location through which systemic L-DOPA exerts the previously observed excitatory and inhibitory effects on VTA neurones. It is predicted that activation of D2 autoreceptors present on DA, and possibly GABA neurones within the VTA contributes towards the changes in spontaneous firing rate seen following the L-DOPA-induced enhancement of DA levels.

This will be tested through the microinjection of the selective D2 receptor antagonist sulpiride directly into the VTA one hour after systemic L-DOPA injection. The expectation is that sulpiride will go at least some way towards reversing L-DOPA effects on the spontaneous firing rate of recorded neurones. However, the alternative possibility that all L-DOPA effects seen at the level of the VTA are caused by upstream or alternative mechanisms will be considered if no effects of local sulpiride injection are seen.

5.3 Materials and Methods

5.3.I Experimental protocol

In vivo electrophysiology was performed on 12 rats as described in section 2. See figure 5.I for the experimental timeline. Again, stimulation rounds consisted of the two noxious modalities and their two innocuous controls, as listed in section 2.2.2. Four stimulation rounds were performed in the naïve rat before injection of any agent in order to ensure a stable baseline spontaneous firing rate. Subsequently, 20mgkg^{-1} L-DOPA was injected systemically using the technique detailed in section 4.3.2, and spontaneous and evoked firing rates were monitored at 10, 20, 40 and 60 minutes post-injection. Following this, the D2 antagonist sulpiride (or a vehicle-only injection) was microinjected directly into the VTA, and monitoring of SFR and stimulus-evoked firing rate was carried out through repetition of stimulation rounds every 10 minutes up to one hour post-injection. It is important to clarify that, although acute nociceptive and innocuous stimuli were applied throughout the experimental duration, as described in section 2.2.3.2, the stimulus-evoked firing rates at these time points were not included in the current or any future analyses within this thesis. This decision was made because the current methodology appeared to not facilitate sensitivity to acute noxious responsivity when recording a population of neurones that have previously been found to show this trait (see section 4.5.3.3).

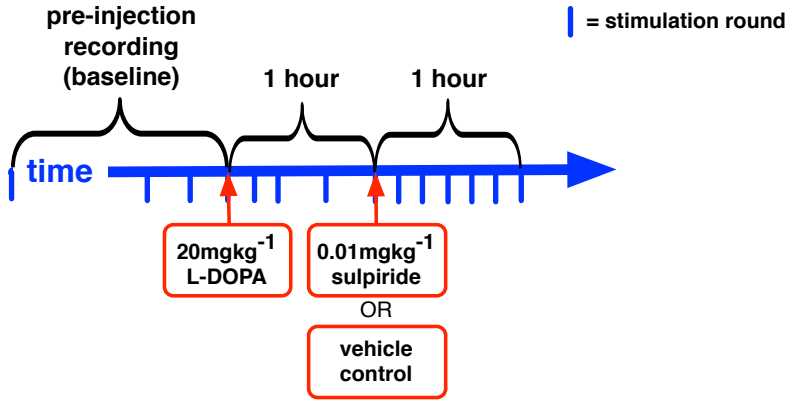

Figure 5.1 Experimental timeline of L-DOPA and sulpiride experiments. The thick blue horizontal arrow represents the progression of time during the experiment, while vertical blue dashes indicate the times at which stimulation rounds were performed (stimulation round described in section 4.3.I). At least 4 stimulation rounds were performed in the baseline condition (not all rounds are depicted), and then at 10, 20, 40, and 60 minutes following low dose L-DOPA injection, and every 10 minutes up to one hour post sulpiride or vehicle injection.

5.3.2 Drug administration

A combined carbidopa-L-DOPA solution in the concentration of 20mgkg^{-1} was made up and administered using identical methods to that of the previous study (detailed in section 4.3.2). (S)-(-)-Sulpiride (Sigma-Aldrich, UK) was dissolved in 1M HCL and pH made up to 6.8 with $NaHCO_3$ solution. Control experiments involving injection of only the vehicle used for sulpiride injections were conducted in 5 animals, with all other variables surrounding drug administration, including the pH, injection volume and injection rate, remaining unchanged.

The sulpiride solution was immediately drawn into a 5.0µl Hamilton syringe (Hamilton, Switzerland), which was subsequently secured to a second headstage positioned laterally to the recording electrode. The correct angle and depth of syringe insertion required to achieve an intra-VTA position 0.4mm lateral from the electrode tip were calculated, and a second bore hole through the skull was drilled appropriately. The syringe was then inserted into the brain such that the tip rested in the desired position before neuronal recording began.

Sulpiride solution was microinjected in a concentration of 40µgµl^{-1} to achieve a 0.01mgkg^{-1} dose. This ensured small injection volumes of around 0.25µl for a 250g rat, for example, which was delivered at a rate of ~0.025µlmin^{-1} manually over 10 minutes. Delivery methods were settled on as a result of other researchers' investigations into optimal volume and injection rate parameters (Aksenov et al., 2014; du Hoffmann et al., 2011) and my own preliminary experimental attempts to minimise volume effects (see section 5.5.4).

5.3.3 Data analysis

Analysis of firing rate of neurones recorded for this study focused on changes in spontaneous firing rate (SFR) following L-DOPA, sulpiride or sulpiride vehicle-only control injection.

5.3.3.I L-DOPA effects

Given that it was necessary to normalise spontaneous firing rate post-injection relative to pre-injection values in order to classify neuronal response for the previous L-DOPA-related investigation (section 4.4.1), the same data processing methods were applied here. This allowed comparison of neuronal responsivity to ensure a comparable sample of the population was collected, and removed confounding effects of different baseline firing rates on quantitative response analysis. Recorded neurones were clustered according to normalized SFR values at all time

points post-injection up until injection of sulpiride or vehicle control (10, 20, 40 and 60 minutes post-injection) through Two-step and K-means cluster analysis.

In a subsequent analysis focusing on the reversal of L-DOPA effects upon sulpiride injection, neurones were re-grouped manually into L-DOPA-inhibited and L-DOPA-excited response-based groups. A neurone was classified as L-DOPA-responsive if the absolute difference between mean SFR across 40 and 60 minutes post-injection time points and the mean BL SFR was greater than 1.96 x standard deviation of the BL SFR measurements. Excited and inhibited classifications were dependent on whether the change in SFR from the BL to the L-DOPA conditions involved an increase or a decrease, respectively. This separate analysis was considered to be necessary because, despite showing a mean inhibitory response to L-DOPA injection, the cluster analysis-identified "L-DOPA-inhibited" group contained some L-DOPA-unresponsive or –excited neurones.

5.3.3.2 Sulpiride or vehicle-only control effects

Mean SFR at each time point post-injection of sulpiride or vehicle was calculated for all neurones recorded in the current study, and mean values for the whole population were plotted to visualise changes in the SFR over time (i.e. response to injection) and differences in vehicle versus sulpiride effect. In order to remove the confounding impact of variability in pre-injection spontaneous firing rate on group response interpretation, mean SFR values at each time point post-injection were normalized relative to mean SFR immediately before injection (that measured at the L-DOPA 60-minute time point) for each neurone. Cluster analysis (two-step and K-means) was performed on all neurones using values normalized relative to pre-sulpiride injection values at all time points post-injection in order to establish natural sulpiride response-based groupings within the recorded population. Sulpiride response in terms of changes in normalized SFR post-injection was compared with the response to vehicle control injection.

Normalized SFR post-sulpiride injection was compared for L-DOPA response-based clusters in order to establish the interaction between sulpiride response and L-DOPA effect. In addition, changes in neuronal SFR following sulpiride injection were normalised relative to baseline SFR (pre-L-DOPA injection). Mean normalised SFR values of the L-DOPA response-based clusters were then plotted for all time points post-sulpiride injection. Subsequently, the degree of reversal of L-DOPA effect upon injection of sulpiride was analysed on neurones grouped according to L-DOPA response manually (see above, section 5.3.3.I). For this analysis, the mean SFR of

L-DOPA-inhibited neurones during the baseline condition, at time points of 40 and 60 minutes post-L-DOPA injection, and 60 minutes post-sulpiride injection were compared. This analysis was repeated for neurones classified as L-DOPA-excited.

5.4 Results

22 neurones were successfully recorded from 12 animals receiving L-DOPA and sulpiride injections, and a further 7 neurones were recorded from 5 animals receiving L-DOPA and vehicle control injections.

5.4.I L-DOPA response

Cluster analysis revealed two natural clusters based on normalized SFR response to a 20mgkg^{-1} systemic dose of L-DOPA; norm L-DOPA cluster 1s ('s' to represent sulpiride experiment recordings) consisted of 19 neurones appearing to show a mean inhibitory response to L-DOPA injection, while norm L-DOPA cluster 2s consisted of 3 neurones appearing to show a mean excitatory response. Friedman tests followed by post-hoc Wilcoxon signed-rank pairwise comparisons using a Bonferroni-corrected alpha of 0.008 showed that the percentage increases and decreases in SFR from pre-injection (baseline) mean SFR values of norm L-DOPA clusters 2s and 1s, respectively, were not significant at any time point post-injection. The relative sizes of the norm L-DOPA clusters 1s and 2s mirrored that found in the previous investigation (norm L-DOPA cluster 1p and 2p – with 'p' representing 'previous' experiment recordings); the seemingly-inhibited cluster (1p, 1s) to seemingly-excited cluster (2p, 2s) neurone ratio recorded in the previous investigation (section 4.4.I) and the current investigation was 22 : 4 neurones and 19 : 3 neurones, respectively. Further the mean normalized SFR values of the L-DOPA response-based clusters at time points up to 60 minutes post injection (limited by the duration of the current experiments) very closely mirrored values recorded in the previous investigation (figure 5.2).

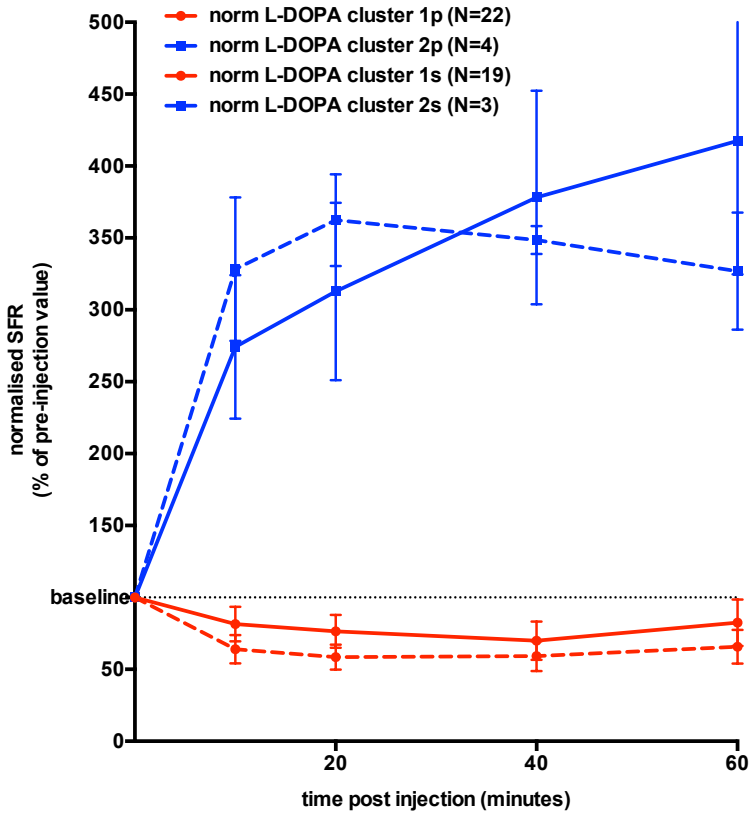

Figure 5.2 Comparison of mean normalized L-DOPA response of neurones recorded in the current sulpiride versus previous L-DOPA experiments. The graph shows mean normalized SFR (y-axis; expressed as a % of mean pre-injection/ baseline SFR) for L-DOPA-based neurone clusters of the previous (norm L-DOPA clusters 1p and 2p) and current (norm L-DOPA clusters 1s and 2s) L-DOPA experiments at all time points (x-axis; minutes) up to 60 minutes post-L-DOPA injection. A cluster of neurones appearing to show a mean inhibitory response to L-DOPA injection was found within both the recorded population of the current (sulpiride) experiments (norm L-DOPA cluster 1s, respectively; solid red trace, N=19) and previous experiments (norm L-DOPA cluster 1p; dashed red trace, N=22). Similarly, a cluster of neurones appearing to show a mean excitatory response to L-DOPA injection were found within both the recorded population of the current (sulpiride) experiments (norm L-DOPA cluster 2s; solid blue trace, N=3) and previous experiments (norm L-DOPA cluster 2p; dashed blue trace, N=4). Data points represent mean ± SEM. The dashed horizontal line at y=100% represents mean baseline SFR.

5.4.2 Sulpiride response

60 minutes after injection of L-DOPA, 0.01mgkg^{-1} sulpiride or the equivalent volume of vehicle control solution was microinjected into the VTA with a Hamilton pipette.

5.4.2.I Injection effects on non-normalized SFR values

In order to establish any general group response patterns and to separate injection effects from pharmacological effects, spontaneous firing rates of all recorded neurones from the sulpiride and control experiments were averaged, and the group sulpiride and control mean values compared at each time point post-injection (figure 5.3).

It was found that spontaneous firing rates of neurones were too variable for a group response profile to be established from the raw data. Mean firing rates of neurones from the sulpiride-injection experiments were within the standard error of the mean of the vehicle control neurones.

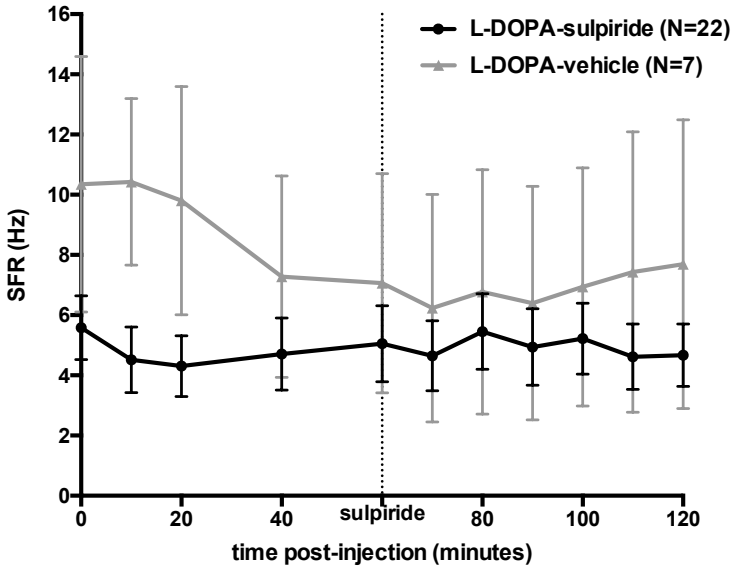

Figure 5.3 Mean spontaneous firing rate of neurones following L-DOPA and sulpiride or vehicle-only injections. The graph shows mean ± SEM values of SFR (Hz, y-axis) of all neurones following the I.P. injection of L-DOPA at all experimental time points (x-axis; 0-60min), and then at all time points (minutes, x-axis) following the intra-VTA injection of sulpiride or vehicle (x-axis; 60-120min). Mean values for neurones recorded in the L-DOPA-sulpiride experiments are shown by the black trace (N=22); mean values for neurones recorded in the L-DOPA-vehicle experiments are shown by the grey trace (N=7). Bars represent mean ± SEM. A vertical dashed line at t=60 minutes represents the time at which sulpiride (or vehicle) was injected.

5.4.2.2 Injection effects on normalized SFR values

To remove the effects of pre-injection SFR variability from subsequent analyses, mean SFR values at every time point post-sulpiride or vehicle control injection of each neurone were normalized relative to mean pre-injection values. One neurone was removed from the analysis and all subsequent analyses on the normalized data set because normalized values for this neurone were an order of magnitude greater than those of the recorded population (e.g. at t=20 minutes post-injection, normalized SFR = 1550%). Cluster analysis performed using normalized SFR at all time points post-injection for the whole recorded population revealed the existence of two natural response-based clusters: 18 of the 22 neurones were classified as norm sulpiride cluster 1, with the remaining 3 forming norm sulpiride cluster 2 (figure 5.4). There was no significant difference found between pre-injection and post-injection mean normalized SFR values at any time point post-injection for both norm sulpiride cluster 1 and 2 neurones (Friedman test with post-hoc Wilcoxon signed-ranks pairwise comparisons using a

Bonferroni-corrected alpha of 0.008). When mean normalized SFR values of norm sulpiride cluster 2 and the vehicle control group were compared, it was found that there was a significant difference between values of norm sulpiride cluster 2 and vehicle controls (one-way ANOVA with post-hoc Bonferroni correction for multiple comparisons, 10min: $p = 0.001$; 20min: $p < 0.0005$; 30min: $p < 0.0005$; 40min: $p < 0.0005$; 50min: $p < 0.0005$; 60min: $p = 0.003$). Conversely, no significant differences were found between norm sulpiride cluster 1 and vehicle control responses.

There was no significant difference found between pre-injection and post-injection mean normalized SFR values at any time point post-injection of the vehicle-only (Friedman test with post-hoc Wilcoxon Signed Ranks Tests, using a Bonferroni-corrected alpha of 0.008), suggesting no significant response to vehicle injection occurred.

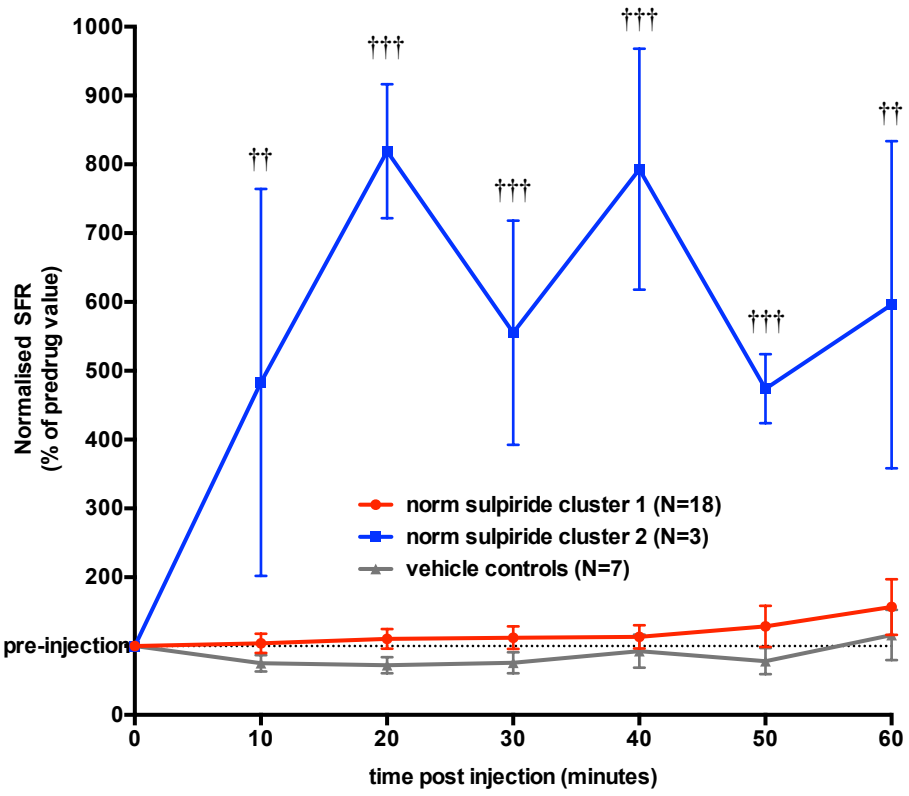

Figure 5.4 Effects of intra-VTA sulpiride microinjection on SFR of VTA neurones. Mean normalized spontaneous firing rate (SFR) of sulpiride response-based neurone cluster norm sulpiride cluster 1(N=18) and norm sulpiride cluster 2 (N=3), and of neurones recorded during vehicle control experiments (N=7) (y-axis; expressed as a percentage of mean pre-injection SFR), shown for all time points post-injection (x-axis; minutes). Data points represent mean ± SEM. Friedman tests with post-hoc Wilcoxon Signed Ranks Tests were performed on normalized SFR values of norm sulpiride cluster 1, norm sulpiride cluster 2, and vehicle control neurones to test for significant percentage changes in firing rate post-injection of sulpiride or vehicle-only. One-way ANOVA with post-hoc Bonferroni tests was carried out to establish differences between mean normalized SFR values of norm sulpiride cluster 2 and cluster 1 or vehicle control neurones at each time point post injection; †† $p<0.005$, ††† $p<0.0005$ (vehicle control vs cluster 2).

5.4.3 Sulpiride response of L-DOPA response-based clusters

5.4.3.I Normalised relative to mean pre-sulpiride SFR

In a subsequent analysis, mean normalized spontaneous firing rate post-sulpiride injection was calculated at each time point for the two L-DOPA response-based neurone clusters (norm L-DOPA clusters 1s and 2s; section 5.4.I). Figure 5.5 depicts these values at all time points throughout the 60 minutes post-sulpiride injection, alongside normalized SFR values of the vehicle control neurones. Norm L-DOPA cluster 1s neurones (N=19) showed a percentage increase in SFR post-injection relative to pre-drug values on average. This was insignificant at all time points, however, presumably due to the large variability in sulpiride effect between neurones of this group. The norm L-DOPA cluster 2s neurones (N=3) appear to show no percentage change in SFR in response to sulpiride injection (figure 5.5).

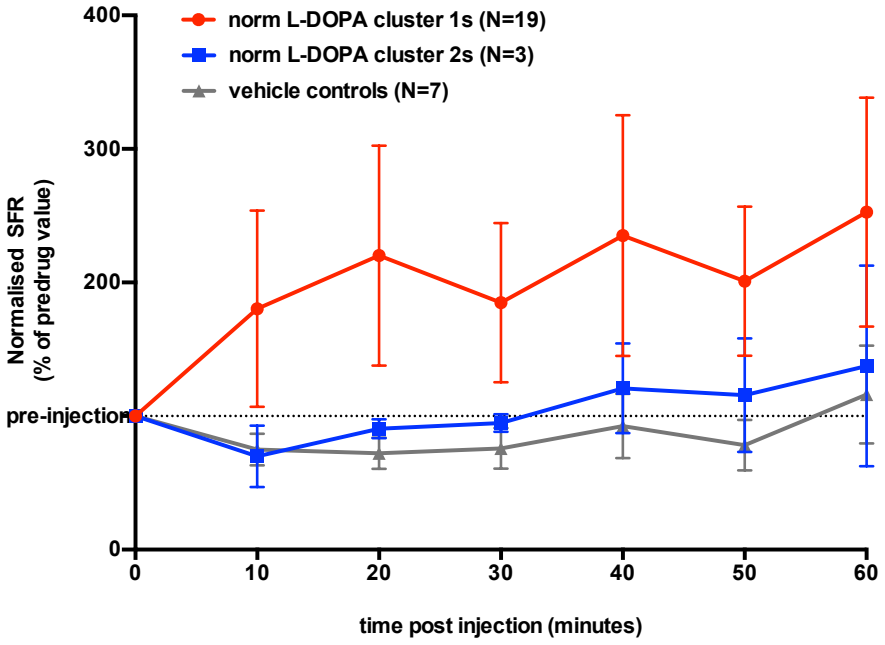

Figure 5.5 Effects of intra-VTA sulpiride microinjection on SFR of L-DOPA response-based neurone clusters. Mean SFR at all time points post-sulpiride injection (x-axis; minutes) expressed as a percentage of mean pre-injection SFR (y-axis; normalized SFR) of neurones clustered according to L-DOPA response (norm L-DOPA cluster 2s: blue trace, N=3; norm L-DOPA cluster 1s: red trace, N=19). Normalized SFR of the vehicle-injected group is also shown for comparison (grey trace, N=7). The horizontal dashed line at y=100% represents mean pre-injection SFR. Data points represent mean ± SEM.

5.4.3.I Normalised relative to mean baseline SFR

Subsequently, mean SFR for each neurone at all time points post-sulpiride injection was normalised relative to mean base SFR (i.e. before L-DOPA injection). Mean baseline-normalised values of all neurones within each of the L-DOPA response-based clusters (norm L-DOPA cluster 1s or 2s) were then calculated and plotted for each time point post-L-DOPA and sulpiride injection (figure 5.6). Results showed that mean baseline-normalised values of the norm L-DOPA cluster 1s and 2s showed high within-cluster variability at all time points post-sulpiride injection. No mean group response in terms of percentage change in SFR relative to base line was seen for either norm L-DOPA cluster 1s or norm L-DOPA cluster 2s.

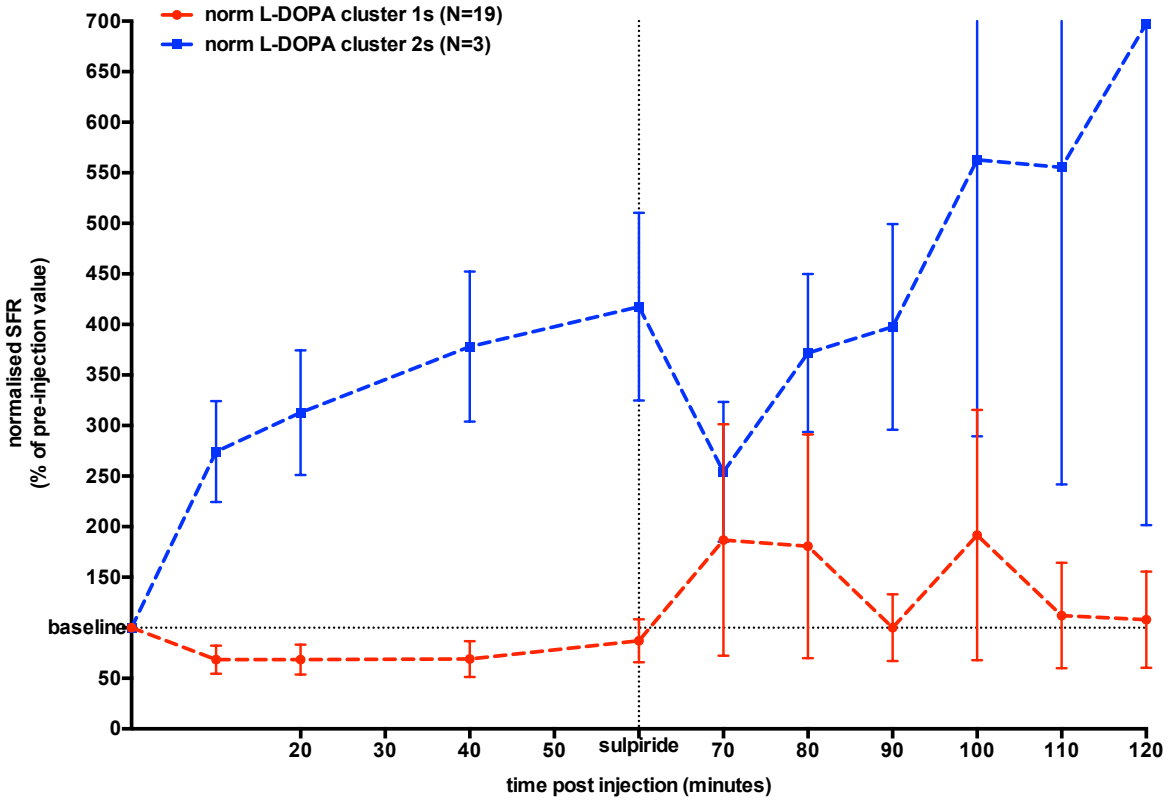

Figure 5.6 Effects of L-DOPA and sulpiride on SFR of L-DOPA response-based neurone clusters, normalised relative to baseline SFR values. Mean SFR at all time points post-L-DOPA injection (0-60 minutes) and a subsequent sulpiride injection (60-120 minutes; x-axis) expressed as a percentage of mean baseline (pre-injection) SFR (y-axis; normalized SFR) of neurones clustered according to L-DOPA response (norm L-DOPA cluster 2s: blue trace, N=3; norm L-DOPA cluster 1s: red trace, N=19). The horizontal dashed line at y=100% represents mean pre-injection SFR. Data points represent mean ± SEM.

5.4.4 Sulpiride reversal of L-DOPA action

In order to establish the reversal of L-DOPA effect through local D2 receptor antagonism upon sulpiride injection, it was necessary to first isolate the neurones displaying significant inhibition and excitation in response to L-DOPA injection. This was achieved by grouping neurones with mean SFR values at 40-60 minutes post-L-DOPA injection greater or less than mean BL SFR ± 1.96 x BL SFR standard deviation. It was found that 9 neurones showed inhibitory responses and 10 neurones showed excitatory responses to L-DOPA, according to these criteria. 7 of the L-DOPA-excited neurones had previously been classified as belonging to cluster 1, the L-DOPA-inhibited cluster, in the whole-population cluster analysis. Only one of the neurones showed an increase or decrease that was smaller than 1.96 x standard deviation of BL SFR.

Mean SFR of the manually-classified L-DOPA-inhibited (LDI) and –excited neurone groups (LDE) in the baseline condition, at 40 minutes and 60 minutes post-L-DOPA injection, and at 60 minutes post-sulpiride injection, were plotted (figure 5.7). This was to visualise the extent to which sulpiride injection reversed the effects of L-DOPA injection. For the LDI neurones, mean SFR at 60 minutes post-sulpiride injection was greater than that seen at 60 minutes post-L-DOPA (figure 5.7A; mean SFR ± SEM: 60min post-L-DOPA = 1.211±0.715Hz; 60min post-sulpiride = 2.049±0.679Hz), implying some degree of reversal of L-DOPA effect; however, this difference was not significant according to a paired-samples *t*-test, and mean SFR at 60min post-sulpiride remained significantly different from baseline values (mean SFR ± SEM: baseline = 6.835±1.990Hz; 60min post-sulpiride = 2.049±0.679Hz). Upon plotting individual neurone values of mean SFR at each of the respective experimental time points, it was observed that a proportion of the LDI neurones showed a greater degree of reversal of L-DOPA effect upon sulpiride injection than others (figure 5.7B).

LDE neurones showed very little difference in mean SFR at 40 and 60min post-L-DOPA and 60min post-sulpiride time points (figure 5.7C; mean SFR ± SEM: 60min post-L-DOPA = 8.215±1.612Hz; 60min post-sulpiride = 7.500±1.305Hz).

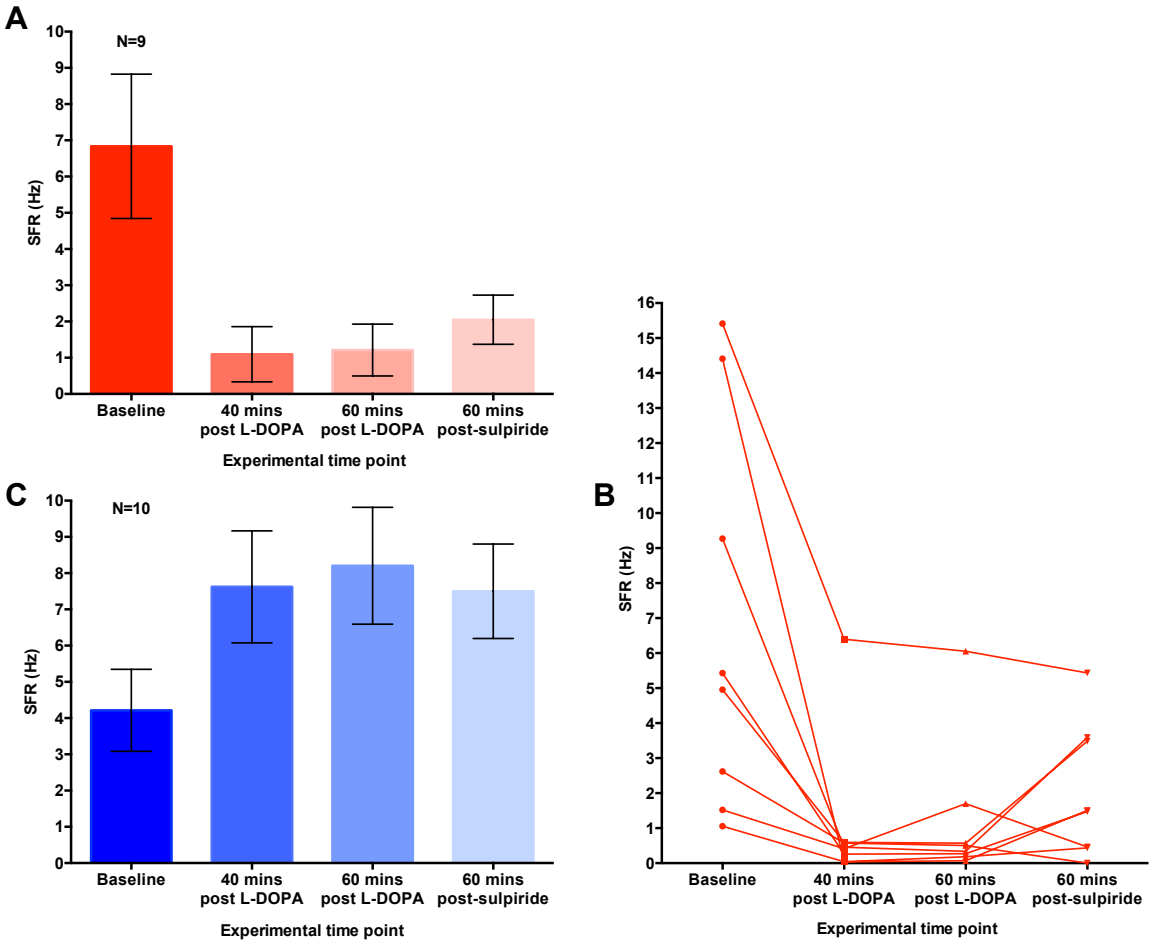

Figure 5.7 Sulpiride effects manually-sorted L-DOPA response-based neurone groups. A) Mean SFR values (y-axis; Hz) of the L-DOPA-inhibited neurone group (N=9) during the baseline condition, at the 40 and 60 minutes post-L-DOPA time points, and at the 60 minutes post-sulpiride time point (x-axis, in order from left to right). B) Mean SFR values of each neurone in the LDI group during the baseline condition, at the 40 and 60 minutes post-L-DOPA time points, and at the 60 minutes post-sulpiride time point. C) Mean SFR values (Hz) of the L-DOPA-excited neurone group (N=10) during the baseline condition, at the 40 and 60 minutes post-L-DOPA time points, and at the 60 minutes post-sulpiride time point. Bars represent mean ± SEM.

The mean SFR values at all time points post-sulpiride injection, normalized relative to mean pre-injection SFR, were calculated for the manually-classified LDI and LDE neurone groups (figure 5.8). In contrast to the sulpiride responses of the cluster analysis-sorted neurone groups (section 5.4.3), there was a greater distinction between the percentage change in SFR of the manually-sorted LDE and LDI groups following injection; the LDI neurones appeared to display a mean excitatory response, while the LDE neurones showed no change in SFR on average from the pre-injection values. However, there was large variability in sulpiride response within the LDI group, and mean normalized SFR was not significantly different from either baseline values (non-parametric Friedman test for repeated measures) or from vehicle control responses (one-way ANOVA) at any time point post-injection.

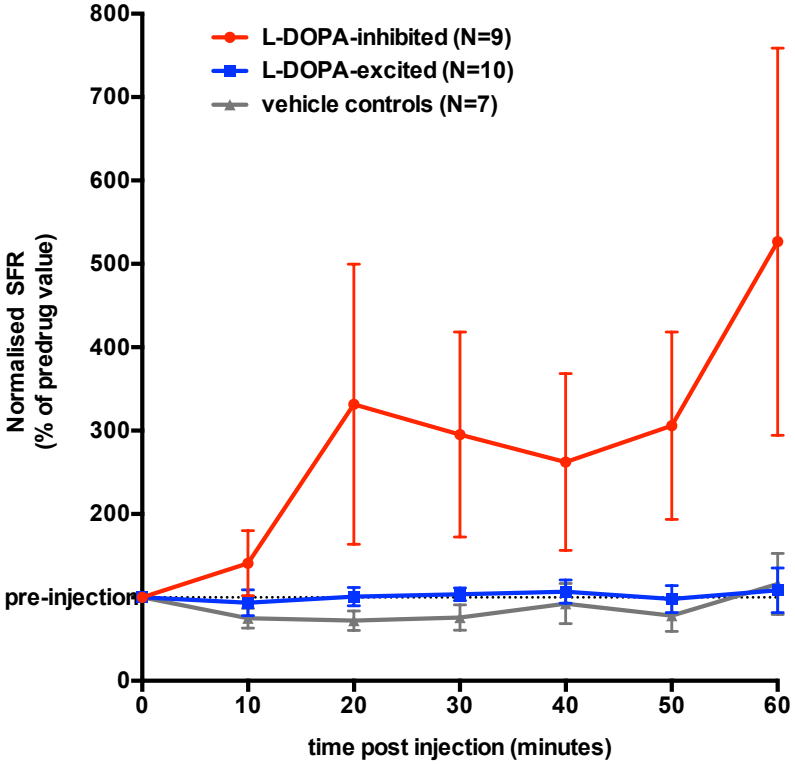

Figure 5.8 Normalized response to sulpiride of the manually sorted L-DOPA-inhibited and –excited neurone groups. Mean normalized SFR values (y-axis; expressed as a percentage of mean pre-injection SFR) are plotted for the L-DOPA-inhibited (red trace, N=9), L-DOPA-excited (blue trace, N=10) and sulpiride vehicle control neurones (N=7) at all time points post-sulpiride injection (x-axis; minutes). The dashed horizontal line at y=100% represents mean pre-sulpiride or vehicle injection SFR. Data points and bars represent mean ± SEM.

5.5 Discussion

The aim of this study was to elucidate the role of local D2 receptor activation in L-DOPA-mediated effects on assorted VTA neurones. This was investigated by microinjecting the D2 receptor antagonist sulpiride directly into the VTA after the systemic injection of a 20mgkg^{-1} L-DOPA. A mixture of sulpiride-excited and –unresponsive neurones were found, in fitting with a mechanistic model in which firing rates of VTA neurones are inhibited by L-DOPA-derived DA action on D2 receptors yet excited by a that on D1 receptors. A low number of sulpiride-excited neurones, as well as large variability in the sulpiride response of L-DOPA-inhibited neurones, implies a substantial degree of D2 receptor density heterogeneity – a quality previously demonstrated within the DArgic population on numerous occasions. Finally, limited and variable reversal of inhibitory L-DOPA action upon sulpiride injection was seen, suggesting that other mechanisms, such as local D1 activation of GABA release and extra-VTA DA synthesis, exert differing yet prominent influence on VTA neurones.

5.5.I L-DOPA response

The method of L-DOPA administration in this current study was identical to that of the previous low dose experiments, hence it was expected that similar responses to L-DOPA injection would be found, provided the recorded population represented a similar sample. In agreement, cluster analysis revealed the existence of two L-DOPA response-based clusters each showing mean normalized SFR values very similar to that of the previously identified norm L-DOPA cluster 1 and 2 (named 1p and 2p for 'previous' in the current results to clarify the separate experimental data). Furthermore, the relative proportions of neurones within these two clusters were reasonably similar for the previous and current investigation. However, in contrast to the previous findings, the seemingly-inhibited L-DOPA response-based cluster of the sulpiride experiments – norm L-DOPA cluster 1s - showed no significant response to L-DOPA injection at all experimental time points. This appeared to be due to a greater degree of variability within the norm L-DOPA cluster 1s versus 1p (i.e. that established in the current experiments relative to that established in the previous experiments), rather than any significant reduction in response magnitude. Nevertheless, the general trend towards inhibition and excitation of the two groups was acknowledged. This was considered appropriate in light of the similarity between the mean post-injection normalized SFR values of the current and previous L-DOPA experiments.

5.5.2 Sulpiride response

The selective D2 receptor antagonist, sulpiride, was microinjected directly into the VTA, and changes in spontaneous firing rate as a result of this injection were assessed.

The VTA is a region found to be rich in D2 receptors, with the majority residing on the dopaminergic neurone cell bodies and dendrites (Bouthenet et al., 1987; Chen et al., 1991; Gurevich and Joyce, 1999; Ardel and Artigas, 2004). Given the weight of evidence supporting intra-VTA autoinhibition of DA neurones via D2 receptors (Kalivas, 1993; Westerink et al., 1996; Georges, 2006; Morzorati & Marunde, 2006; Chiodo et al. 1984; Clark and Chiodo 1988; Mereu et al. 1985; Wang 1981; Li et al., 2014), the blockade of these receptors locally with sulpiride was expected to result in the excitation (increased SFR) of the DA neurones recorded from the VTA. Given the relative proportions of neurochemical types and the presence of neurones displaying an inhibitory response to L-DOPA within the recorded population, it was predicted that at least some of the recorded neurones would be dopaminergic, and therefore excited by sulpiride injection. Research has also identified a subset of non-DA neurones, including those containing GABA, that are directly inhibited via D2 receptors, suggesting that some sulpiride-excited cells may possess this identity. However, with the large majority of D2 receptors being found to reside on dopaminergic neurones (Bouthenet et al., 1987; Chen et al. 1991; Gurevich and Joyce, 1999; Ardel and Artigas, 2004), it is expected that sulpiride-excited cells are most likely to belong to this neurochemical population.

The inhibitory effect of D2 receptors resulting from a coupling of the receptor to G_i and a subsequent downstream activation of a hyperpolarising K^+ conductance is thought to be universal for this receptor class (Beaulieu and Gainetdinov, 2011; Neve et al., 2004); no reports of a direct excitatory effect of D2 receptor activation have been reported in the literature, at least not that referring to findings in the VTA. For this reason, it was expected that no inhibitory effects of sulpiride on VTA neurones would be found. It is important to note, however, that this prediction relies on the assumption that no indirect excitation (perhaps via disinhibition) of VTA neurones occurs within this brain region. While no discussions of such a mechanism were found in the literature, we do not provide evidence to rule out this possibility.

The detection of a population of sulpiride-unresponsive neurones was also predicted. The majority of GABAergic neurones in the VTA have been shown to be unresponsive to D2 receptor agonists and antagonists (Li et al., 2012),

supporting the findings of D2 receptor localisation studies (Bouthenet et al., 1987; Chen et al. 1991; Gurevich and Joyce, 1999; Ardel and Artigas, 2004). In addition, the VTA DA neurone population is thought to possess a degree of heterogeneity in terms of D2 receptor expression (Adell and Artigas, 2004); neurones projecting to cortical regions are relatively deficient in these receptors, resulting in greatly reduced or even absent responses to D2 receptor agonists (Chiodo et al., 1984). Hence, in summary, both sulpiride-excited and unresponsive neurones were expected in light of the existing literature of D2 action within the VTA, with the former population predominantly consisting of dopaminergic neurones with the exception of a small proportion of non-DA neurones, and the latter, of a mixture of dopaminergic and GABAergic neurones.

Cluster analysis performed on the normalized SFR values of the recorded neurones post-sulpiride injection revealed two natural response-based groups: a small group (norm sulpiride cluster 2, N=3) showing mean excitatory responses to sulpiride injection, and a larger, seemingly sulpiride-unresponsive group (norm sulpiride cluster 1, N=18). The observed group mean percentage increase in SFR from mean pre-injection SFR of the cluster 2 neurones was not significant; however, there was a significant difference between the percentage change in firing rate of cluster 2 neurones seen in response sulpiride injection, and that seen in response to vehicle-only injection. This result implies that there was a significant pharmacological effect of sulpiride on a small group of neurones, but that this effect was not consistent or large enough to represent a significant change from baseline. In contrast, there were no significant differences found between normalized SFR values of norm sulpiride cluster 1 and vehicle control neurones across the duration of the experiment, suggesting that there was no pharmacological effect of sulpiride on this population.

The findings of sulpiride-unresponsive (norm sulpiride cluster 1) and generally-excited (norm sulpiride cluster 2) subpopulations are in line with the predictions of response type noted above; however, the relatively low numbers of neurones falling into the cluster showing a mean percentage increase in SFR (albeit insignificant) despite the relatively high proportion of DA neurones in the VTA (~70%; Ford et al., 1995; Kalivas, 1993; Nair-Roberts et al., 2008b; Yamaguchi et al., 2007b), suggesting that most of the DA neurones within the recorded population failed to show excitatory responses sufficient to be grouped with the seemingly excited subpopulation, was unexpected. Clear reports of relative proportions of D2 pharmacological responses among VTA neurones were not found in the literature, but the widespread findings of D2 agonist/antagonist action on DA neurones – to the extent that responsivity is an established DA neurone marker – suggests that three out of 18 neurones is unusually

low. Alternatively, such a low proportion of sulpiride-excited neurones may be due to a disproportionately high sampling of non-DA neurones. Finally, it is important to note that the clustering of neurones according to normalized SFR values post-injection it not the same as separating neurones according to the nature of their response; the spread of neuronal post-injection SFR values may be such that K-means clustering resulted in the concealment of a sulpiride-excited group showing responses of a smaller magnitude – and therefore more similar to that of the unresponsive neurones than to that of the strongly excited neurones.

Hence, it was found that most VTA neurones recorded fell into a generally sulpiride-unresponsive cluster, and only a few were separated out into a cluster showing an insignificant but pharmacologically-induced excitatory response. It is considered likely that the former population includes a mixture of non-DA (possibly GABA) neurones and D2 receptor-lacking (likely prefrontal cortex- or amygdala-projecting) DA neurones. In addition, it is considered most likely that the three members of the seemingly sulpiride-excited cluster possess a dopaminergic identity, but the possibility of a GABAergic identity for a subset of these neurones is not ruled out.

5.5.3 Vehicle control injection response

Many previous studies have mentioned the pitfalls with microinjection of drug solutions directly into the immediate surroundings of the neurones of interest. The so-called 'volume effect' describes the temporary suppression of firing rate and reduction of spike amplitude recorded from a neurone due to physical displacement caused by "flooding" of the local environment (Aksenov et al., 2014; du Hoffmann et al., 2011; Rauch et al., 2008). However, it was found that injection of only the vehicle used for sulpiride administration resulted in no significant percentage change in SFR (figure 5.5). This result suggests that physical or chemical effects of the injection itself were negligible, and that the significant response of the sulpiride-excited cluster neurones represents pharmacological action. Interestingly, the vehicle control response profile very closely mirrored that seen for the sulpiride-unresponsive cluster, implying that, on average, this latter group of neurones was not at all influenced by D2 receptor antagonism.

On a methodological note, the lack of volume effect seen in the current experiments implies that the low rate of injection of ~0.025μlmin^{-1} in combination with a 0.4mm separation between the syringe tip and recording location is sufficient to avoid significant displacement of the neural tissue.

5.5.4 Sulpiride effects on L-DOPA response-based neurone clusters

For the subsequent analysis, the sulpiride responses of the L-DOPA response-based clusters - norm L-DOPA cluster 1s and 2s - were explored separately. This was to try and establish whether changes in the SFR of VTA neurones in response to systemic L-DOPA were due, at least in part, to local VTA D2 receptor activation.

There is much evidence supporting the role of autoinhibitory D2 receptor activation by dopamine as key in the inhibitory effect of systemic L-DOPA on the dopaminergic neurones of the VTA (Bunney et al., 1973; Paalzow, 1992). Hence, it was predicted that local sulpiride application to the VTA would act to reverse any L-DOPA-mediated suppression of spontaneous firing rate, resulting in an excitatory change in SFR post-injection. Conversely, excitatory effects of DA on non-DA neurones have been found to be mediated by D1-type receptors, and therefore SFR values of neurones showing excitatory responses to L-DOPA - the predominant, albeit insignificant, response of norm L-DOPA cluster 2s - were not expected to be influenced by injection of the D2 receptor antagonist.

5.5.4.1 Cluster-sorted L-DOPA response populations

As stated previously (section 4.5.1), it was hypothesised that the most likely identity of L-DOPA-inhibited neurones was predominantly dopaminergic, while that of the insignificantly L-DOPA-excited neurone group was predominantly GABAergic, with a good chance of a small degree of cross-over of these identities between the two groups. Analysis on the effects of sulpiride on the two L-DOPA response-based neurone clusters was carried out despite the lack of significant group mean inhibitory and excitatory responses of norm L-DOPA clusters 1s and 2s, respectively. This was considered appropriate because it remains feasible that natural clustering according to L-DOPA response represents functional VTA neurone divisibility in relation to D2 receptor control, with other physiological factors (e.g. downstream D1 receptor-mediated influences) being responsible for the variability in L-DOPA response. Further, there were observable mean excitatory and inhibitory responses of the two clusters of a similar magnitude to those found to be significant in the previous L-DOPA investigation, suggesting that a low powering (i.e. low numbers within each group) of this data set may be responsible for the lack of a significant effect.

Initial investigation into sulpiride effects on the L-DOPA response-based clusters 1s and 2s was made through analysis of the SFR post-sulpiride injection when expressed as a percentage of pre-sulpiride injection values (i.e. at the last L-DOPA time point). The lack of response to sulpiride of the norm L-DOPA cluster 2s neurones showing a seemingly excitatory response to L-DOPA is in line with expectations based on a proposed D1 receptor-mediated mechanism of L-DOPA-evoked excitation (see section 4.5.I.2). This ties in with a putative GABAergic identity of some members of this cluster, as D1 receptor agonists have been shown to excite the VTA GABAergic population (Matthews and German, 1986). While the norm L-DOPA cluster 1s neurones (i.e. those showing a trend towards an inhibitory response to L-DOPA) appeared to show a mean percentage increase in SFR following sulpiride injection, effects on individual neurones within the cluster were variable and was not found to be significant. Similarly, when the post-sulpiride SFR of neurones of norm L-DOPA clusters 1s and 2s were normalised relative to baseline in a subsequent analysis (as opposed to the pre-sulpiride time point), normalised SFR values of neurones within both norm L-DOPA clusters showed varied responses, resulting in a net lack of significant effect. The inclusion of some L-DOPA-excited neurones in norm L-DOPA cluster 1s (hence the lack of a significant inhibitory response to L-DOPA) may be responsible for a proportion of the variability seen in sulpiride response of this neurone group. To test this, neurones were subsequently sorted manually specifically according to the direction of their response to L-DOPA.

5.5.4.2 Manually-sorted L-DOPA response populations

Combined Two-step and K-means cluster analysis is an unbiased approach to sorting a population of neurones into natural groupings, and therefore represents a valid way to initially classify neurones according to a set of characteristics; neurones within the resultant clusters represent those with statistically-grouped responsivity. However, when trying to assess the reversal of a given pharmacological effect that possesses polarity within the population (i.e. excitation and inhibition), it was considered more appropriate to assess the responses of each neurone recorded and manually sort these into response-based groups before quantifying the degree of reversal. This was done by comparing a neurone's mean SFR at 40 and 60 minutes post-L-DOPA with its mean baseline values, and only categorising it as a responsive neurone if the difference calculated was greater than 1.96 x standard deviation of the BL SFR measurements. The relative proportions of neurones falling into L-DOPA response-based groupings was different following cluster analysis verses manually sorting the recorded population, suggesting that use of this method to re-sort neurones strictly according to response direction before assessing sulpiride reversal of L-DOPA effect was necessary. When the normalized sulpiride response was

replotted according to these manual response-based groupings, the distinction between sulpiride effect on L-DOPA-inhibited (LDI) and –excited neurones (LDE) became much more apparent; the LDE neurones showed no responsivity to sulpiride injection, possessing very little group variability in this respect, whilst the LDI neurones showed a pronounced and sustained excitation, peaking at a mean normalized SFR of ~500% of pre-injection values. However, this response was not significant, again apparently owing to large variability amongst the L-DOPA inhibited population.

This variability in sulpiride effect of L-DOPA-inhibited neurones could be explained by neurone-neurone heterogeneity in the relative contributions of D1 receptor and D2 receptor activation towards the observed L-DOPA effect. Activation of D1 receptors present on GABAergic afferents terminating on DA neurones is thought to result in an enhancement of GABAergic inhibition (Kalivas and Duffy, 1995). Heterogeneity amongst the VTA DA neurone population in terms of D2 receptor expression could be counteracted to some extent by D1 control of GABA release, resulting in a population of L-DOPA-inhibited neurones with within-group differences in the balance between these alternative mechanisms of DA action.

5.5.4.3 Reversal of L-DOPA effect by sulpiride injection

In a subsequent analysis, mean SFR of manually-sorted LDI and LDE neurone groups was compared between the baseline (i.e. pre-injection), post-L-DOPA-injection and post-sulpiride injection conditions. The aim was to visualise and quantify the extent to which sulpiride action within the VTA reversed the inhibitory and excitatory effects of L-DOPA. Given that L-DOPA was administered systemically, it is possible that effects witnessed in VTA neurones were in fact caused by upstream L-DOPA uptake into catecholaminergic neurones, DA (or noradrenaline) synthesis and receptor activation in any of the other seven dopaminergic areas within the CNS. By microinjecting sulpiride locally, the relative contribution of local versus upstream mechanisms can be assessed.

LDI neurones

The manually-sorted LDI neurone group showed a trend towards sulpiride reversal of L-DOPA effect, but this result was not significant. By visualising the individual neurone SFR values, it was possible to see that variability in both the size of L-DOPA-inhibition and sulpiride excitation (or in one case, sulpiride inhibition) was present; even so, none of the recorded neurones appeared to show full reversal of L-DOPA effect upon sulpiride injection. A full reversal of the inhibition was not necessarily expected for the current experiments; various factors including

the relative potencies of L-DOPA and sulpiride, extra-VTA L-DOPA action such as on noradrenergic or other DA neurone populations (Wood, 2008), as well as the inevitable contribution of D1 receptors to the inhibitory response – both within and outside of the VTA - could feasibly exert a downstream effect on VTA neurone activity upon the systemic injection of L-DOPA.

LDE neurones

The LDE neurones showed no reversal of L-DOPA effect upon local sulpiride application. This result is in agreement with theoretical predictions of D1 receptor-based mechanisms of DA action (Adell and Artigas, 2004; Matthews and German, 1984; Seamans et al., 2001) and findings from the previous normalized SFR analysis (section 5.5.4.I), further suggesting that the L-DOPA-excited neurones are likely to be GABAergic, and confirming that D2 receptors to not play a direct role in modulating their activity.

5.5.5 Conclusions

In summary, variable effects of intra-VTA microinjection of sulpiride were found amongst a population of VTA neurones. Responses according to percentage change in SFR from pre-sulpiride injection values naturally fell into two clusters: sulpiride-excited (norm sulpiride cluster 2) and sulpiride-unresponsive (norm sulpiride cluster 1) neurone groups. Analysis of the L-DOPA responsivity of these neurones (both through cluster analysis and a manual sorting process) allowed very tentative suggestions of likely neurochemical identity to be made, with L-DOPA-inhibited neurones thought to be predominantly dopaminergic, and the L-DOPA-excited neurones, most likely largely GABAergic. The lack of group response to sulpiride of the manually sorted L-DOPA-excited neurones fits in with the proposed GABAergic identity, as there is evidence to suggest that this neurochemical group is primarily influenced by D1 rather than D2 receptor sub-types. In contrast, the manually sorted L-DOPA-inhibited (LDI) neurones showed large heterogeneity in response to intra-VTA sulpiride. Responses of this group appeared to be excitatory on average, suggesting that some degree of reversal of L-DOPA effects resulted from antagonism of the local D2 receptors. However, the whole-group effect was not significant, likely due to the large degree of variability witnessed in sulpiride effect of the LDI group. Consequently, it was concluded that, while D2 receptor activation within the VTA is responsible for the witnessed L-DOPA-inhibition of some VTA neurones, other mechanisms – likely D1-mediated GABA release and/or extra-VTA L-DOPA metabolism – are more prominent for a large proportion of the recorded population. These findings of heterogeneity in D2 receptor-

mediated inhibition are in line with several reports of variability in D2 receptor expression within the VTA DA neurone population, and again reinforce the multi-functional nature of this neurochemical group.

6. Investigating the system in tonic pain: the carrageenan model of inflammation

6.I Introduction

One distinction that it is essential to make when investigating the role of DA in pain processing is that between acute and tonic pain. What differentiates the two by definition is the time scale; acute pain lasts for only a few seconds, whereas tonic pain typically has a latency ranging from hours to days. Acute pain tests in animals, such as the tail-flick test that measures withdrawal responses to thermal stimulation, provide good insight into spinal nociception mechanisms. However, this transient, well-localised pain experience bears little resemblance to any clinical situation, limiting the translatability of these studies. Tonic pain, on the other hand, such as that resulting from tissue inflammation or injury, is much more relevant to inescapable persistent pain experienced by humans.

Animal models of tonic pain are generated by intraplantar injection of inflammatory agents. Very similar in effect to formalin injection (Dubuisson and Dennis, 1977), the carrageenan model (Winter et al., 1962) typically results in unilateral inflammation and hyperalgesia peaking 3-4 hours post injection. The carrageenans are a complex group of polysaccharides made up of repeating galactose-related monomers, existing in three main forms: lambda, kappa, and iota. Because it forms a relatively fluid gel in comparison to the other forms at room temperature, λ-carrageenan is most frequently adopted as an injectable inflammatory agent in pain-related investigations.

The short time scale of λ-carrageenan injection-induced inflammation, with maximal effects seen by 3 hours post-injection, make it an optimal model for *in vivo* electrophysiological experiments, in which time is limited by neurone stability and animal welfare (Stanfa et al., 1992). Furthermore, the immune response that results is well researched and highly reproducible, rendering this model an excellent option for research into tonic pain mechanisms. Indeed, this technique has been widely used and several theories around carrageenan-induced CNS modifications have been postulated.

It is important to note that the neural causes of the enhanced pain sensitivity lie partly in alterations in the peripheral primary nociceptive input; both increases and decreases in afferent C and A-delta fibre input to spinal cord dorsal horn neurones have been witnessed (Stanfa et al., 1992), ultimately resulting in altered input to supra-spinal regions generating pain reaction and perception.

This is by no means the whole story, however; as previously discussed (sections I.5 and I.I2), the way in which ascending nociceptive information is processed is also modified by a persistent pain state. Crucially, it appears as if the role of the VTA DA neurones becomes significantly more prominent as the time during which a noxious input exists proceeds (Altier and Stewart, 1999; Cohen et al., 1984; Morgan and Franklin, 1990). For example, DA agonists induce analgesia in tonic but not phasic pain (Altier and Stewart, 1999). Further investigation into changes in the activity of these neurones following the induction of tonic pain could yield interesting results.

One suggested central change associated with carrageenan-induced tonic pain lies in endogenous opioid function. Endogenous opioids are well known for their role in circumstantial pain suppression. Upon both receiving or expecting a reward or placebo, release of endogenous opioids acting primarily on μ-receptors throughout the pain-processing system leads to attenuation of pain sensitivity. It also appears that the presence of tonic pain causes recruitment of this mechanism. The mixed opioid receptor antagonist, naloxone, whilst having no effect in the naïve state, unmasks a large tonic influence of endogenous opioids on behaviour and spinal neurone activity in animals with tonic pain (Le Bars et al., 1981; Kayser and Guilbaud, 1981; Stanfa and Dickenson, 1995). This, at least in part, can be explained by the finding that injection of formalin into the rat paw causes an increase in the levels of beta-endorphin, an endogenous opioid with affinity for the μ-receptor, in the periaqueductal grey, thalamus and ventromedial hypothalamus (Porro et al., 1991). However, studies have also found that exogenous μ-opioids are more potently analgesic following carrageenan injection (Hylden et al., 1991; Kayser and Guilbaud, 1981), suggesting the increase in endogenous opioid influence is also a result of possible μ-receptor up-regulation or amplification of down-stream mechanisms. These changes in MOR function are thought to involve many levels of the pain-processing system; receptor expression patterns suggest sites of action not only include nociceptive primary afferent and dorsal horn neurones, but also several supra-spinal locations such as the hypothalamus, periaqueductal gray (PAG), RVM and, crucially, the VTA (Garzón and Pickel, 2001). In fact, lesions of the VTA

DA neurones block the analgesic effects of morphine in the tonic pain state only, suggesting a heightened importance of this brain region in this state (Morgan and Franklin, 1990).

Through the μ-opioid receptors, endogenous opioids have been suggested to exert a disinhibitory action on VTA dopaminergic neurons by reducing inhibitory GABAergic interneuron activity (Johnson and North, 1992), and many studies have since emphasised their importance as a neural activity modulator in this region (Fields, 2007); however, the role tonic pain-induced changes in endogenous opioids play in the change in DA neurone nociceptive function seen with development of this state remains ambiguous.

6.2 Aims and predictions

These experiments, through use of the λ-carrageenan-induced model of inflammatory pain, aim to investigate the nature of any changes in VTA neurone activity occurring as a tonic pain state develops. Alterations in spontaneous firing rate and firing pattern of recorded VTA neurones will be assessed, and the possibility of subpopulations with distinct carrageenan responsivity will be explored. Predictions surrounding the neurochemical identity of these neurones will be supported through establishment of their response to L-DOPA – a characteristic previously examined and discussed in sections 4.5.I and 4.5.2. The role of endogenous opioid action in causing any changes in neural activity that do occur upon the induction of a tonic inflammatory pain state will be explored using the MOR receptor antagonist, naloxone.

The predicted influence of carrageenan injection on the dopaminergic and non-DA neurones of the VTA is unclear. Origins of the VTA neurone response to tonic nociceptive input are likely to be complex, and no previous studies investigating it were found in the literature. In light of the previously established analgesic role of DA signalling, together with reports of enhanced DA agonist efficacy in tonic pain, it seems plausible that a pathological reduction in DA neurone activity occurs in the face of inflammation; in other words, changes within the VTA contribute to the persistent pain state. This would manifest as an inhibitory response upon carrageenan-injection, and would be expected for a significant proportion of the neurones recorded given the relative proportions of the neurochemical types. Alternatively, the literature hinting at an increase in opioid involvement in the tonic pain state suggests that endogenous analgesic mechanisms may be up-regulated. This would manifest itself in enhancement in SFR following carrageenan injection for most DA neurones (although some would be directly inhibited – see section 3.5.2), and either a reduction or lack of response in SFR of GABA neurones within the VTA following carrageenan injection, according to findings of MOR agonist action on these populations (Margolis et al., 2012).

If this prediction of increased opioid action was accurate one would also expect naloxone injection to reverse changes seen in response to carrageenan, and the size of the naloxone influence to be greater in carrageenan-injected verses naïve state animals.

6.3 Materials and Methods

Male Sprague Dawley rats (250-350g), bred by the Biological Services Unit (UCL, London, UK), were used for electrophysiological experiments

6.3.I Experimental protocol

In vivo electrophysiology on VTA neurones was performed as described in section 2. Following the initial establishment of a stable baseline spontaneous firing rate of the neurone(s) recorded through four stimulation rounds (as detailed in section 2.2.2), protocol in any one experiment followed one of four experimental streams: carrageenan-only, carrageenan followed by L-DOPA, carrageenan followed by naloxone (or vehicle), and naloxone-only (all described below).

6.3.I.I Carrageenan-only experiments

Intraplantar injections of λ-carrageenan were performed in the left hind paw of the rat to induce local inflammation. Spontaneous and evoked firing rates were monitored through two stimulation rounds occurring every 20 minutes up to three hours post-injection (figure 6.1A).

6.3.I.2 Carrageenan-L-DOPA experiments

Carrageenan injection and monitoring of spontaneous and evoked firing rates was carried out as described for the carrageen-only experiments. At the 2-hour post-carrageenan-injection time point, rats were injected with a $20mgkg^{-1}$ dose of L-DOPA. Spontaneous and evoked firing rates were monitored at 10 minutes and 20 minutes post-injection, and then every subsequent 20-minute time interval up to 2 hours post-L-DOPA injection (figure 6.1B).

6.3.I.3 Carrageenan-naloxone experiments

Carrageenan injection and monitoring of spontaneous and evoked firing rates was carried out as described for the carrageen-only experiments. At the 2-hour post-carrageenan-injection time point, rats were injected subcutaneously with a $5mgkg^{-1}$ dose of naloxone. Spontaneous and evoked firing rates were then monitored every 10 minutes up to 1 hour post-injection (figure 6.1C). In a set of 9 experiments, vehicle-only injections replaced naloxone injection in this protocol.

6.3.I.4 Naloxone-only experiments

Animals were injected subcutaneously with a 5mgkg^{-1} dose of naloxone, and spontaneous and evoked firing rates were then monitored every 10 minutes up to 1 hour post-injection. No further pharmacological agents were applied (figure 6.1D).

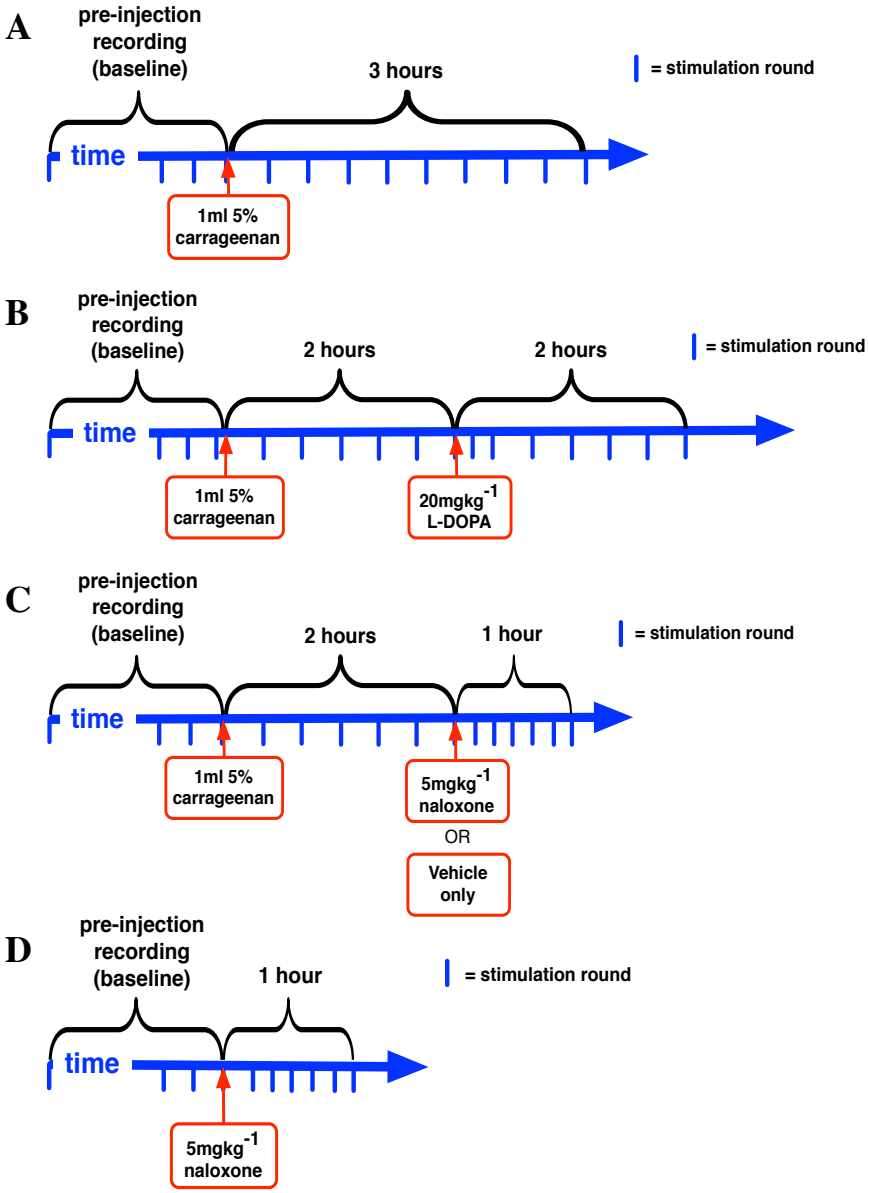

Figure 6.1 Experimental timeline of carrageenan-related experiments. The thick blue horizontal arrow represents the progression of time during the experiment, while vertical blue dashes indicate the times at which stimulation rounds were performed (stimulation round described in section 4.3.I). For all experiments, at least 4 stimulation rounds were performed in the baseline condition (not all rounds are depicted). Following this, one of four different experimental protocols was followed: A) *Carrageenan-only experiments:* rats were injected with carrageenan, and stimulation rounds were performed every 20minute up to three hours post-injection. B) *Carrageenan-L-DOPA experiments:* rats were injected with carrageenan, and stimulation rounds were performed every 20minute up to two hours post-injection. Subsequently, low dose L-DOPA was injected, and stimulation rounds performed at 10, 20, 40, 60, 80, 100 and 120 minutes post injection. C) *Carrageenan-naloxone experiments:* rats were injected with carrageenan, and stimulation rounds were performed every 20 minutes up to two hours post-injection. Subsequently, naloxone (or vehicle) was injected, and stimulation rounds performed every 10 minutes up to one hour post-injection. D) *Naloxone-only experiments*: naloxone was injected, and stimulation rounds performed every 10 minutes up to one hour post-injection.

6.3.2 Drug administration

Carrageenan. 2% λ-Carrageenan (Sigma Chemie, Deisenhofen, Germany) gel was made up in saline, and was administered by intraplantar injection into the left hind paw in a volume of 100µl.

Naloxone. Naloxone HCL (MOR antagonist, Sigma Chemie, Deisenhofen, Germany) solution was made up with double distilled water to a concentration of $5mgml^{-1}$ and injected subcutaneously in a dose of $5mgkg^{-1}$ body weight. Vehicle control injections (i.e. double-distilled water only) of the equivalent volume were completed in a separate set of experiments in place of naloxone. Naloxone was used to unmask the existence of on-going endogenous opioidergic activity in rats both in naïve and carrageenan-injected states.

L-DOPA. A combined carbidopa-levodopa solution (both Sigma-Aldrich, UK) was made immediately previous to injection in the concentration of $20mgml^{-1}$ and administered using the methods detailed in section 4.3.2. The purpose of L-DOPA administration was to pharmacologically characterise neurones recorded by sorting them according to L-DOPA effects on spontaneous firing rate (section 4.4.I).

6.4 Results

6.4.I Neuronal response to carrageenan injection

In total across all three types of carrageenan-based experiment 73 neurones were recorded successfully (i.e. did not disappear mid-way through the experiment) from 42 animals: 24 neurones from 18 animals for the carrageenan-only experiments (figure 6.1A), 28 neurones from 12 animals for the carrageenan-naloxone experiments (figure 6.1C), and 21 neurones from 12 animals for the carrageenan-L-DOPA experiments (figure 6.1B). Two neurones from the carrageenan-naloxone experiments were omitted from further analysis due to unusually high or variable firing rates. SFR values from all of the remaining 71 recorded neurones were included in analyses surrounding carrageenan injection effects.

6.4.I.I Non-normalized SFR

When Two-step followed by K-means cluster analysis was performed using the mean spontaneous firing rates of all 71 recorded neurones at every time point post-carrageenan injection, two natural clusters were found: raw carr cluster 1 consisted of 65 out of the 71 neurones, showed no change in SFR across the whole experimental time period, and had a relatively low mean BL SFR of 2.31±0.35Hz, whilst raw carr cluster 2 consisted of 6 neurones, appearing to show a general and sustained increase in SFR across the time points, with a mean BL SFR of 10.36±1.01Hz (figure 6.2).

A repeated measures ANOVA test was conducted to compare mean SFR values during the baseline condition with those at 80, 100 and 120 minutes post-carrageenan injection to establish whether the increase in mean SFR from baseline values were significant at these time points. Mean SFR values at the 20, 40 and 60-minute time points were not analysed in this way as the literature suggests that both the physical and nociceptive effects of carrageenan increase slowly up until ~3 hours post-injection, and therefore assessment of changes in SFR the latter half of the experiment were most relevant to interpretation of carrageenan-induced tonic pain effects on VTA neurones. It was found that the mean SFR values at the 80, 100 and 120-minute time points of raw carr cluster 2 showed no significant differences from the mean BL SFR value of 10.36Hz, suggesting that there was no significant effect of naloxone injection on the mean firing rate of the "high-firing" neurones.

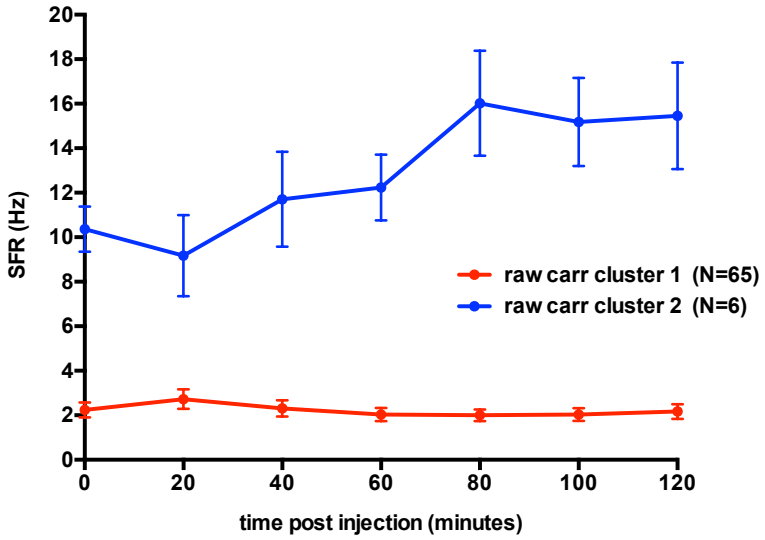

Figure 6.2 Effects of carrageenan injection on VTA neurone SFR. Graph shows the mean SFR values (y-axis, Hz) of post-carrageenan SFR-based neurone clusters: raw carr cluster 2 (N=6, blue trace) and raw carr cluster 1 (N=65, red trace). Mean ± SEM values (data points and bars) of the two clusters are shown at all time points post-carrageenan injection (x-axis, minutes). A repeated measures ANOVA was conducted using SFR values of the raw carr cluster 2 neurones at pre-injection and 80, 100 and 120 minutes post-injection time points.

6.4.I.2 Normalized SFR

In order to examine the BL SFR-independent effects of carrageenan, clustering according to the normalized mean SFR values (expressed as a percentage of mean pre-injection values) for each neurone at 100 and 120-minute time points post-injection was analysed. Three neurones were omitted from the normalized analysis due to normalized post-injection SFR values being extremely high (>1000%). Three natural clusters were identified from the remaining 68 neurones: norm carr cluster 1 containing 42 neurones, norm carr cluster 2 containing 22 neurones, and norm carr cluster 3 containing 4 neurones. On average, norm carr cluster 1 neurones showed no response to carrageenan injection (figure 6.3; Friedmans test with Wilcoxon signed rank pairwise comparisons, using a Bonferroni-corrected alpha of 0.008). Similarly, despite showing an apparent increase in mean normalized SFR following carrageenan injection, the percentage increase in SFR of norm carr cluster 3 neurones was not found to be significant in Wilcoxon signed rank pairwise comparisons when using a Bonferroni-corrected alpha of 0.008. In contrast, norm carr cluster 2 (N=22) showed a significant mean percentage increase in SFR from baseline at 60, 80, 100 and 120 minutes post-injection (Friedmans test with Wilcoxon signed rank pairwise comparisons, using a Bonferroni-corrected alpha of 0.008, 60min: $Z=-3.880$, $p<0.0005$; 80min: $Z=-3.620$, $p<0.0005$; 100min: $Z=-3.685$, $p<0.0005$; 120min: $Z=-4.107$, $p<0.0005$). Norm carr cluster 3 (N=4) neurones showed a greater mean

% increase from baseline on average than cluster 2 at time points from 60 minutes post-injection onwards (mean ± SEM [cluster 2, cluster 3]: 60min = 200±20.60%, 328±32.60; 80min = 186.47±17.73%, 382.78±25.05%; 100min = 191.48±14.59%, 518.57±76.59%; 120min = 278.86±19.82%, 442.50±14.83%).

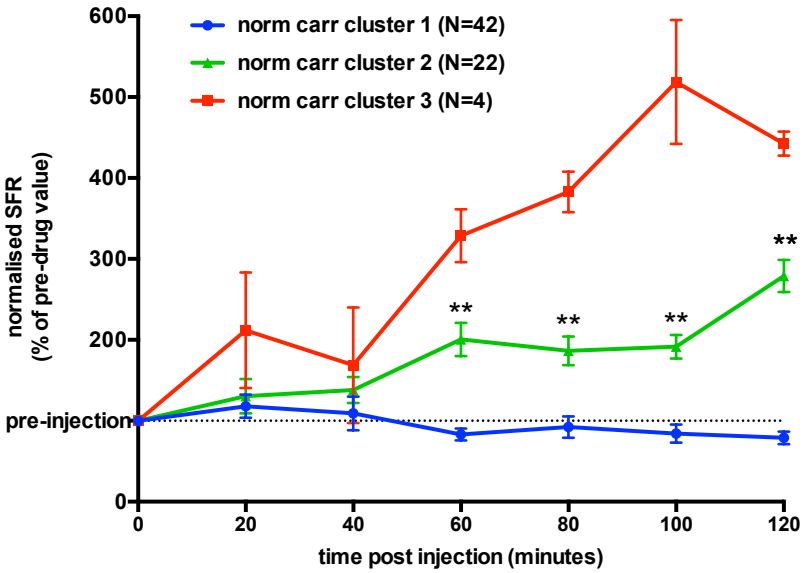

Figure 6.3 Normalized SFR post-carrageenan injection of carrageenan response-based neurone clusters. Data shows mean normalized SFR (expressed as a percentage of pre-carrageenan injection mean SFR, y-axis) of neurones sorted into carrageenan response-based norm carr clusters 1 (blue trace, N=42), 2 (green trace, N=22) and 3 (red trace, N=4) at all time points up to two hours post-carrageenan injection (minutes, y-axis). Dashed horizontal line at y=100% represents mean pre-injection SFR. Friedman tests with post-hoc Wilcoxon signed-rank pairwise comparisons were used to test significance of percentage changes in SFR from pre- to post-carrageenan injection time points, using a Bonferroni-corrected alpha of 0.008, ** $p<0.0008$.

6.4.2 Burst firing characteristics of carrageenan response-based neurone clusters

The effect of carrageenan injection on burst firing characteristics of the carrageenan response-based clusters norm carr cluster 1 (N=42), norm carr cluster 2 (N=22) and norm carr cluster 3 (N=4) was subsequently explored. Burst-firing data was not collected for one of the norm carr cluster 3 neurones, reducing the number of neurones of this cluster to three for this analysis.

Because mean excitatory carrageenan effects on SFR of norm carr cluster 2 neurones were significant from 60 minutes-onwards, the %SIB value for the "post-carrageenan" condition was extracted from each neurone's recording across the time period between 1-2 hours post-carrageenan injection. Subsequently, a paired sample *t*-test was conducted to compare the mean post-carrageenan %SIB with mean baseline %SIB values for the three carrageenan response-based clusters.

6.4.2.I Norm carr cluster 1

It was found that, on average, the %SIB of the norm carr cluster 1 neurones was significantly lower in the 2nd hour following carrageenan injection than it was in the baseline condition (figure 6.4A; %SIB Mean ± SEM: baseline = 46.62±4.83%, carrageenan hr2 = 38.49±4.83%; paired samples *t*-test, t(41)=2.708, p=0.010).

6.4.2.2 Norm carr cluster 2

It was found that, on average, the %SIB of the norm carr cluster 2 neurones was significantly greater in the 2nd hour following carrageenan injection than it was in the baseline condition (figure 6.4B; %SIB Mean ± SEM: baseline = 38.12±6.89%, carrageenan hr2 = 47.17±7.62%; paired samples *t*-test, t(21)=2.365, p=0.031).

6.4.2.3 Norm carr cluster 3

There was no significant difference found between the %SIB of the norm carr cluster 3 neurones in the baseline and the 2nd hour following carrageenan injection (figure 6.4C; %SIB Mean ± SEM: baseline = 34.04±14.45%, carrageenan hr2= 45.05±11.06%).

As an additional observation, it was noted that mean %SIB in the baseline condition for all three carrageenan-response based neurone clusters were similar to the mean value for the entire recorded population, quoted in section 3.4.3.I as being 39.28±2.56%.

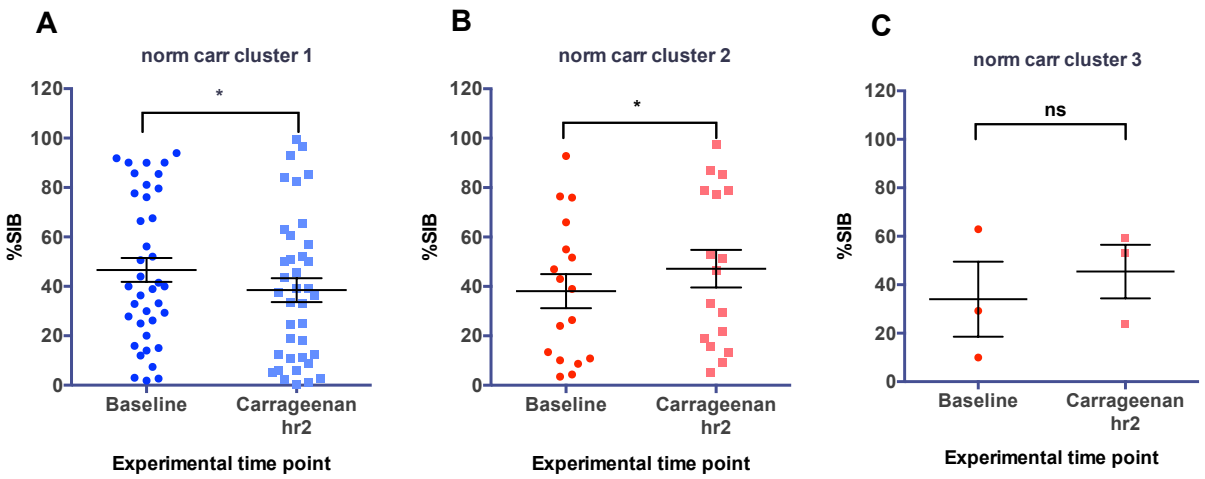

Figure 6.4 Burst firing of neurones of norm carr clusters 1, 2 and 3 in baseline and carrageenan hour two conditions. Graphs show individual neurone values of the percentage of all spikes recorded in either the baseline condition (Baseline) or during the second hour following carrageenan (carrageenan hr2) injection that were present within a burst (%SIB, y-axis). Mean ± SEM values are also shown for each carrageenan response cluster in both the baseline and carrageenan hr2 conditions (black bars). A) Norm carr cluster 1 neurones, N=42. B) Norm carr cluster 2 neurones, N=22. C) Norm carr cluster 3 neurones, N=3. Paired sample *t*-tests were performed to compare mean %SIB values in the baseline and carrageenan hr2 conditions, * $p<0.05$.

6.4.3 Carrageenan response of neurones sorted according to L-DOPA responsivity

6.4.3.I L-DOPA response: cluster analysis

In order to establish L-DOPA-response-based groupings, SFR values at all time points post-injection were normalized relative to mean pre-injection values for each neurone (as in sections 4.4.I & 5.4.I). Cluster analysis on these values revealed two natural clusters based on percentage change in SFR in response to a 20mgkg^{-1} systemic dose of L-DOPA; norm L-DOPA cluster 1c ('c' for carrageenan) consisted of 16 neurones showing a generally inhibitory response to L-DOPA injection, while norm L-DOPA cluster 2c consisted of 5 neurones appearing to show a general excitatory response.

The relative proportions of neurones falling into each of the two natural clusters found when clustering according to normalised post-L-DOPA SFR were similar to that found in previous investigations (norm L-DOPA cluster 1p, norm L-DOPA cluster 2p), with ratios of the seemingly-inhibited: seemingly-excited neurones recorded in the two previous investigations (section 4.4.I & 5.4.I) and the current investigation being 22:4 neurones, 19:3 neurones, and 16:5 neurones respectively. There were no significant differences at any time point between mean normalized SFR values of the seemingly L-DOPA-inhibited cluster (norm L-DOPA cluster 1c) of the current carrageenan experiments and that seen for the L-DOPA-inhibited clusters of the previous investigations (norm L-DOPA cluster 1p; figure 6.5). The mean percentage increase from pre-injection SFR values of the seemingly-excited L-DOPA response-based cluster (norm L-DOPA cluster 2c) was significantly lower than that of the similar cluster of the previous investigations (norm L-DOPA cluster 2p) at time points of 20, 40 and 60 minutes post-injection (figure 6.5; One-way ANOVA with a post-hoc Bonferroni test, 20min: $F(1)=13.472$, $p=0.004$; 40min: $F(1)=22.165$, $p=0.001$; 60min: $F(1)=10.101$, $p=0.010$). The norm L-DOPA cluster 2c neurones showed no significant percentage increase from baseline SFR values at any time point post-injection, on average (Friedman test with post-hoc Wilcoxon signed-rank pairwise comparisons, using a Bonferroni-corrected alpha of 0.0125). On the other hand, the norm L-DOPA cluster 1c neurones showed a significant percentage decrease in SFR at all time points from 20 minutes post-L-DOPA injection onwards (Friedman test with post-hoc Wilcoxon signed-rank pairwise comparisons, using a Bonferroni-corrected alpha of 0.0125, baseline vs 20min: $Z=-2.844$, $p=0.004$; baseline vs 40min: $Z=-3.465$, $p=0.001$; baseline vs 60min: $Z=-2.844$, $p=0.004$).

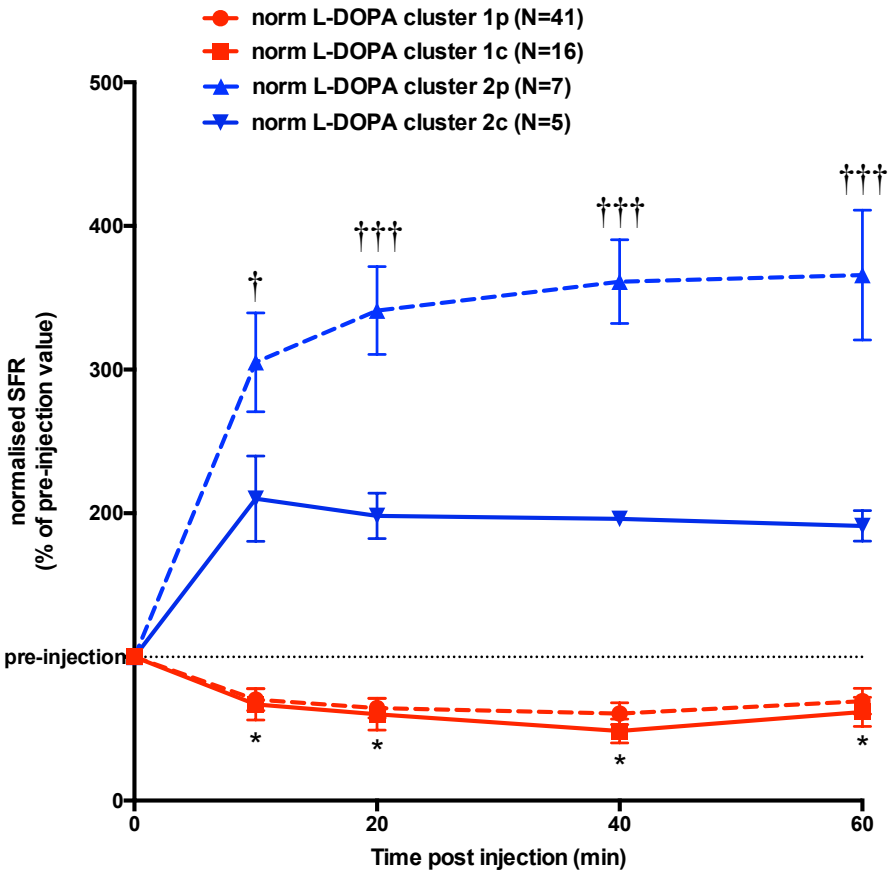

Figure 6.5 Comparison of mean L-DOPA response of neurones recorded in the current vs. previous naïve-state experiments. Normalized SFR of neurones clustered according to normalised SFR at all time points post-L-DOPA injection in the current carrageenan experiments (norm L-DOPA cluster 1c, N=16: solid red trace; norm L-DOPA cluster 2c, N=5: solid blue trace) and all previous L-DOPA experiments (norm L-DOPA cluster 1p, N=41: dashed red trace; norm L-DOPA cluster 2p, N=7: dashed blue trace). Data points represent mean ± SEM. Friedman tests with post-hoc Wilcoxon signed-rank pairwise comparisons were used to test significance of percentage changes in SFR from pre- to post-injection time points, using a Bonferroni-corrected alpha of 0.0125, * P<0.0125, ** P<0.00125. A one-way ANOVA with post-hoc Bonferroni tests was carried out to establish differences in the size of excitatory responses shown by cluster 2 neurones of previous and current L-DOPA experiments, † p<0.0125, ††† p<0.0005.

6.4.3.2 Carrageenan response of L-DOPA response-based neurone clusters: non-normalized SFR values

To begin to investigate the carrageenan response of neurones grouped according to L-DOPA response, the mean SFR values of the two L-DOPA response-based neurone clusters (norm L-DOPA clusters 1c and 2c) were plotted for every time point post-carrageenan injection (figure 6.6). It appeared that norm L-DOPA cluster 2c neurones

displayed no change in SFR following carrageenan injection, on average, whilst norm L-DOPA cluster 1c (mean inhibitory L-DOPA response) neurones showed a slight increase from 60 minutes post-injection onwards; however, no significant group injection effects were not seen in either of the two clusters.

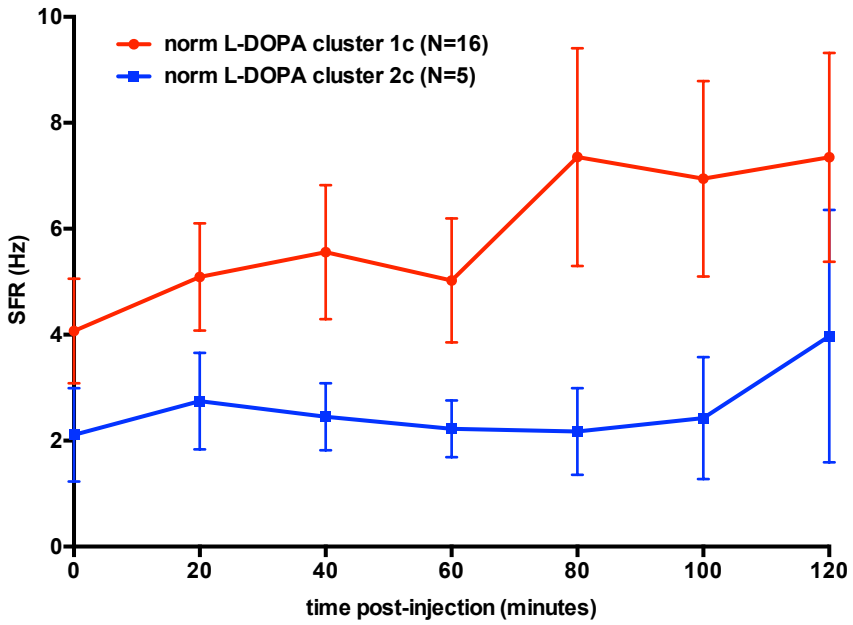

Figure 6.6 Post-carrageenan SFR of L-DOPA response-based neurone clusters. Data shows mean SFR (Hz, y-axis) of norm L-DOPA response cluster 1c (red trace, N=16) and norm L-DOPA cluster 2c (blue trace, N=5) neurones at all time points post-carrageenan injection (minutes, x-axis). Data points and bars represent mean ± SEM.

6.4.3.3 Carrageenan response of L-DOPA-response neurone clusters: normalized SFR values

In order to assess group responses to carrageenan injection, it was necessary to first account for within-group variability in baseline SFR by normalising post-injection values with respect to mean baseline SFR for each neurone (expressing post-injection SFR values as a percentage of BL SFR; figure 6.7).

It was found, as with the non-normalized SFR values, norm L-DOPA cluster 2c neurones displayed no significant % change in SFR across the duration of the two hours post-carrageenan injection. Norm L-DOPA cluster 1c (inhibited) neurones showed a mean excitatory response, which was significant at the 80-minute post-injection time point according to a Friedman test followed by post-hoc Wilcoxon pair-wise comparisons using a Bonferroni-corrected alpha of 0.0125 (mean normalized SFR = 232.4±33.50% of pre-injection SFR; Wilcoxon pair-wise comparison, 80min: Z=-2.746, p=0.006).

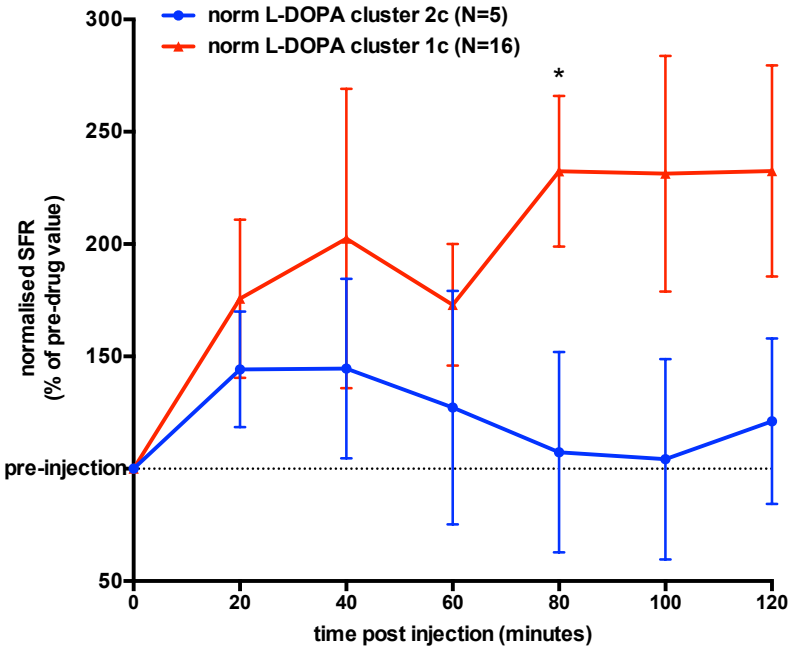

Figure 6.7 Normalized SFR of L-DOPA response-based neurone clusters following carrageenan injection. Mean normalized SFR (expressed as a percentage of mean pre-injection SFR; y-axis) of norm L-DOPA cluster 1c (N=16, red trace) and norm L-DOPA cluster 2c (N=5, blue trace) neurone clusters at all time points post-carrageenan injection (minutes; x-axis). Data points and bars represent mean ± SEM. The horizontal dashed line at y=100% represents mean pre-carrageenan injection SFR. Friedman tests with post-hoc Wilcoxon signed-rank pairwise comparisons were used to establish differences between mean pre-injection SFR and post-carrageenan injection SFR, using a Bonferroni-corrected alpha of 0.0125, * $p<0.0125$.

6.4.4 Carrageenan-naloxone experiments: naloxone effects

In addition to the 26 neurones recorded from animals previously injected with carrageenan, 48 neurones were recorded from 19 animals in experiments involving injection of naloxone only or naloxone followed by L-DOPA (the latter set of experiments were primarily undertaken for analysis in chapter 7).

Antagonism of the μ-opioid receptor (MOR) with systemic naloxone injection was used to unmask the presence of any ongoing endogenous MOR-mediated modulation of VTA neurone activity. For this investigation, the effect of naloxone injected at the 120-minute post-carrageenan time point was assessed, and compared to effects seen when injected in the naïve state (refer to figure 6.1; i.e. no previous pharmacological manipulation).

6.4.4.I Effect of naloxone on all neurones: non-normalized SFR

SFR values of all neurones recorded from naïve animals at all time points post-naloxone injection were sorted into natural groupings via Two-step and K-means cluster analysis. This analysis was repeated for all neurones recorded in carrageenan-injected animals.

Naïve state

Two natural clusters according to SFR values post-naloxone injection were found amongst neurones recoded in naïve animals: a "high firing" cluster – named raw nlx cluster 1n - consisting of 14 neurones with mean BL SFR of 5.607±0.735Hz, and a "low firing" cluster – named raw nlx cluster 2n - consisting of 34 neurones with a mean BL SFR of 1.880±0.363Hz (figure 6.8A). The raw nlx cluster 1n neurones appeared to display a mean excitatory response to naloxone injection. A repeated measures ANOVA with a Bonferroni adjustment for multiple pairwise comparisons was conducted using all pre-injection and post-injection time points for both clusters in order to test for the presence of a significant naloxone effect on SFR. It was found that the excitatory response to naloxone of the raw nlx cluster 1n was significant at 30 minutes post-injection (mean SFR±SEM: BL = 5.607±0.735Hz, 30min = 8.326±0.899Hz; pairwise comparison between BL vs. 30min time points: p=0.003), whereas low firing (raw nlx cluster 2n) neurones showed no SFR response to injection at any time point.

Post-carrageenan injection state

Two natural clusters according to SFR values post-naloxone injection were found amongst neurones recoded in naïve animals: a "high-firing" cluster – raw nlx cluster 1c - consisting of 4 neurones with mean BL SFR of 13.620±1.943Hz, and a "low-firing" cluster – raw nlx cluster 2c - consisting of 22 neurones with a mean BL SFR of 2.073±0.441Hz (figure 6.8B). Neither of the two raw nlx clusters 1c and 2c displayed a significant response to naloxone, with group mean SFR remaining relatively constant across the 60 minutes post-injection.

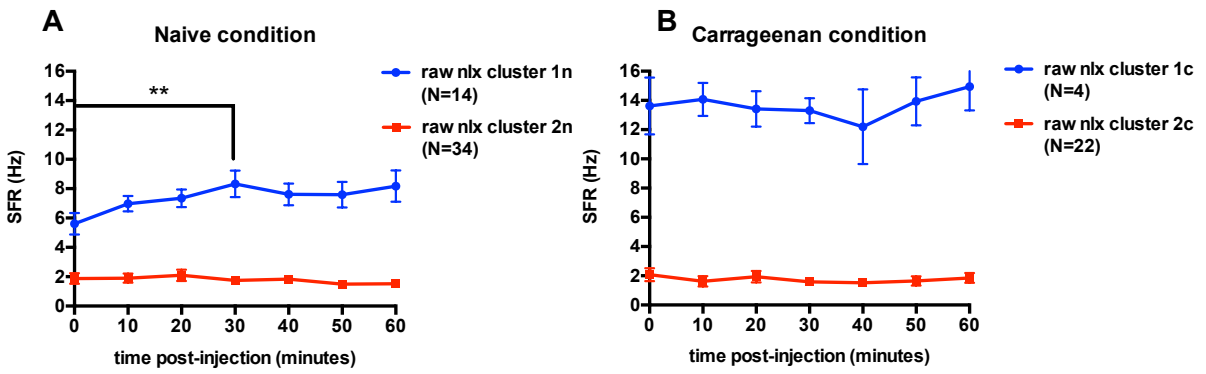

Figure 6.8 Spontaneous firing rate following naloxone injection of neurones recorded in naïve and carrageenan-injected states. Graphs show mean SFR of neurones clustered according to mean SFR values at all time points post-naloxone injection. A) Traces show mean SFR values of raw nlx cluster 1n (N=15, blue trace) and raw nlx cluster 2n (N=34, red trace) neurones recorded in animals in the naïve state at all time points post-naloxone injection. B) Traces show mean SFR values of raw nlx cluster 1c (N=4, blue trace) and raw nlx cluster 2c (N=22, red trace) neurones recorded in animals in the carrageenan-induced tonic inflammatory pain state at all time points post-naloxone injection. Bars represent mean ± SEM. A repeated measures ANOVA with a Bonferroni adjustment for multiple pairwise comparisons was conducted for each cluster to establish injection effects on SFR, **p<0.005

6.4.4.2 Effect of naloxone on all neurones: normalized SFR

In order to facilitate naloxone response-based comparisons within the population of recorded neurones, mean SFR values for each neurone at each time point post-naloxone injection were normalized (expressed as a percentage of pre-injection values). Cluster analysis was then performed on normalized SFR values for the entire population of neurones recorded from animals in the naïve and carrageenan-injected states. Four neurones recorded in naïve animals and one neurone recorded in a carrageenan-injected animal were omitted from the normalized SFR analysis of naloxone response due to them displaying extremely high percentage changes in SFR (>~1000%).

It was found that the naïve neurones could be sorted into two groups based on their response to naloxone injection: a generally naloxone-excited cluster consisting of 3 neurones - named norm nlx cluster 2n, and a generally naloxone-unresponsive cluster consisting of 41 neurones – named norm nlx cluster 1n (figure 6.9A). A Friedman test followed by post-hoc Wilcoxon signed-rank pairwise comparisons using a Bonferroni-corrected alpha of 0.008 revealed that neither of the two naïve neurone clusters (norm nlx clusters 1n and 2n) showed a significant percentage change in SFR from mean pre-injection values at any time point post-injection.

No natural clusters within the population of carrageenan-injected neurones were found in terms of normalized SFR response (figure 6.9B).

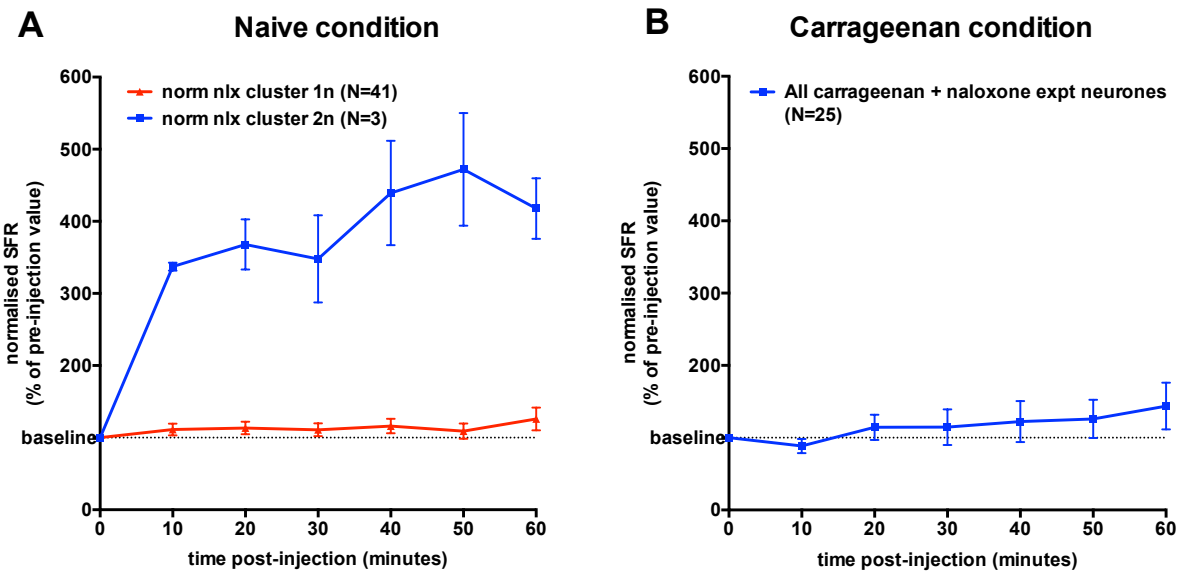

Figure 6.9 Normalized spontaneous firing rate following naloxone injection of neurones recorded in naïve and carrageenan-injected state. A) Traces show mean normalized SFR (y-axis; expressed as a percentage of pre-injection values) of normalized naloxone response-based clusters of neurones recorded in the naïve state: norm nlx cluster 1n (red trace, N=41) and norm nlx cluster 2n (blue trace, N=3) at all time points post-naloxone injection (x-axis; minutes). B) Traces show mean normalized SFR (y-axis; expressed as a percentage of pre-injection values) of neurones recorded in the carrageenan-injected state at all time points post-naloxone injection (N=25). The dashed horizontal line at y=100% represents mean pre-injection SFR. Bars represent mean ± SEM.

6.4.4.3 Normalised naloxone response of BL SFR neurone clusters

In a subsequent analysis, neurones were sorted according to BL SFR cluster membership (i.e. into BL SFR cluster 1n or 2n) and mean normalised naloxone response was calculated for each cluster at all time points post-naloxone injection (figure 6.10). Friedman's tests followed by Wilcoxon signed-rank pairwise comparisons were conducted to establish the significance of any group percentage change in SFR from pre-injection values. There were 39 neurones recorded in naïve-state naloxone experiments classified as BL SFR cluster 2n, and 8 classified as BL SFR cluster 1n.

This analysis revealed that neurones classified as the lower SFR cluster – BL SFR cluster 2n – displayed a significant percentage increase in SFR on average at time points of 20 and 40 minutes post-naloxone injection, when using a Bonferroni-corrected alpha value of 0.008 (20min: p=0.007; 40min: p=0.006). In contrast, the

higher-firing neurones classified as BL SFR cluster 1n displayed no mean percentage change in SFR from baseline following the injection of naloxone.

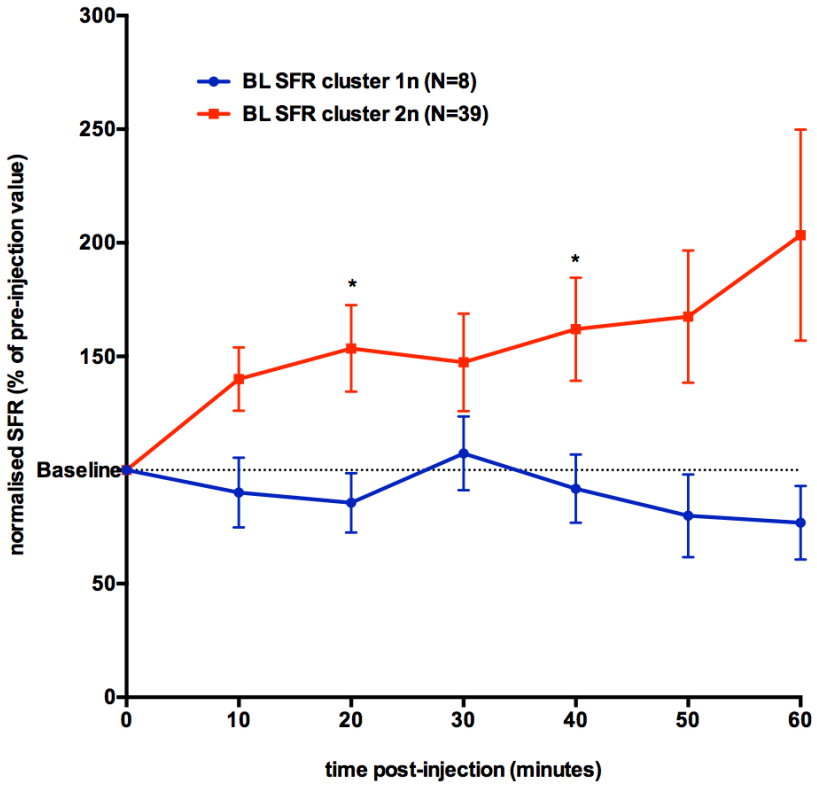

Figure 6.10 Normalized spontaneous firing rate of BL SFR cluster neurones following injection of naloxone. Data points show mean ± SEM spontaneous firing rate expressed as a percentage of mean pre-naloxone injection values of neurones belonging to BL SFR cluster 2n (N=39; red trace) and BL SFR cluster 1n (N=8; blue trace) neurone groups. Mean values for both response-based clusters are shown for all time points post-naloxone injection. The dashed horizontal line at y=100% represents mean pre-injection (baseline in this case) SFR values). Friedman's tests followed by post-hoc Wilcoxon signed-rank pairwise comparisons were conducted to establish whether naloxone injection caused a significant percentage change in SFR of BL SFR cluster 1n or 2n neurones, * $p<0.008$

6.4.4.4 Comparing naloxone effects on neurones recorded in naïve and carrageenan-injected states

Naloxone effects seen in the naïve state were compared with those seen following carrageenan injection by comparing mean normalized SFR of the two populations at all time points post-naloxone injection (figure 6.11). No significant differences between the mean normalized SFR values of neurones recorded in the naïve versus carrageenan-injected states were found at any of the post-naloxone injection time points.

Friedman tests with post-hoc Wilcoxon signed-rank pairwise comparisons were conducted on the normalized values to test for significant differences between the repeated measures of SFR before and after injection of naloxone. It was found that there were no significant percentage changes from pre-injection SFR at any time point post-naloxone injection in both naïve and carrageenan-injected states (when using a Bonferroni-corrected alpha of 0.008; figure 6.11).

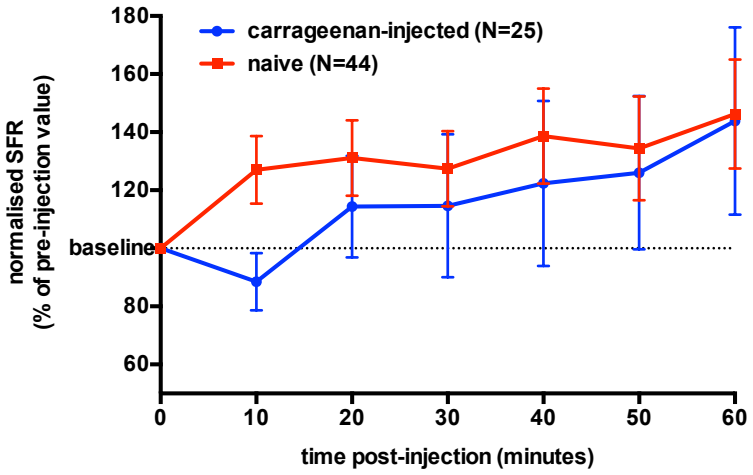

Figure 6.11 Mean normalized SFR following naloxone injection of neurones recorded in naïve and carrageenan-injected conditions. Graph shows the mean normalized spontaneous firing rate (expressed as a percentage of mean pre-naloxone injection SFR) of neurones recorded in the naïve (N=44) and carrageenan-injected (N=25) conditions at all time points post-naloxone injection. The dashed horizontal line at y=100% represents mean pre-naloxone injection SFR. Bars represent mean ± SEM.

6.4.4.5 Comparing naloxone effects in carrageenan-excited and –unresponsive neurones

Neurones recorded in the carrageenan-naloxone experiments were grouped according to their cluster membership established in the whole-population carrageenan response cluster analysis (figure 6.12; section 6.4.I.2), and group mean normalized naloxone responses (in terms of percentage change in SFR from pre-naloxone injection values) were compared at all time points post-naloxone injection (figure 6.13). These group mean values were also compared to the neuronal response to vehicle control injection, similarly expressed as the mean percentage change in SFR from the pre-vehicle injection condition (figure 6.13). No neurones recorded in the carrageenan-naloxone

experiments were found to belong to norm carr cluster 3, and therefore the current analysis involved norm carr clusters 1 and 2 only.

15 neurones recorded as part of the carrageenan-naloxone experiments belonged to the generally-unresponsive norm carr cluster 1, and 11 belonged to the carrageenan excited norm carr cluster 2. It was found that carrageenan-unresponsive norm carr cluster 1 neurones appeared to display a sustained excitatory response to naloxone injection from 20 minutes onwards, on average; however, any group mean changes in SFR were not significant according to a Friedman test for repeated measures. Conversely, norm carr cluster 2 neurones displayed a significant inhibitory response to naloxone injection at 10 minutes post-injection (mean ± SEM, 10min: 58.90±10.87% of pre-injection SFR; Friedman test with post-hoc Wilcoxon signed-rank pairwise comparisons, using a Bonferroni-corrected alpha of 0.008, 10min vs pre-injection: Z=-2.845, p=0.004). This normalized SFR value was significantly different from that seen following vehicle control injection at 10 minutes post-injection (mean ± SEM of vehicle control at 10min [n=9]: 93.22±7.94% of pre-injection SFR; independent-samples *t*-test: t(19)=-2.447, p=0.025).

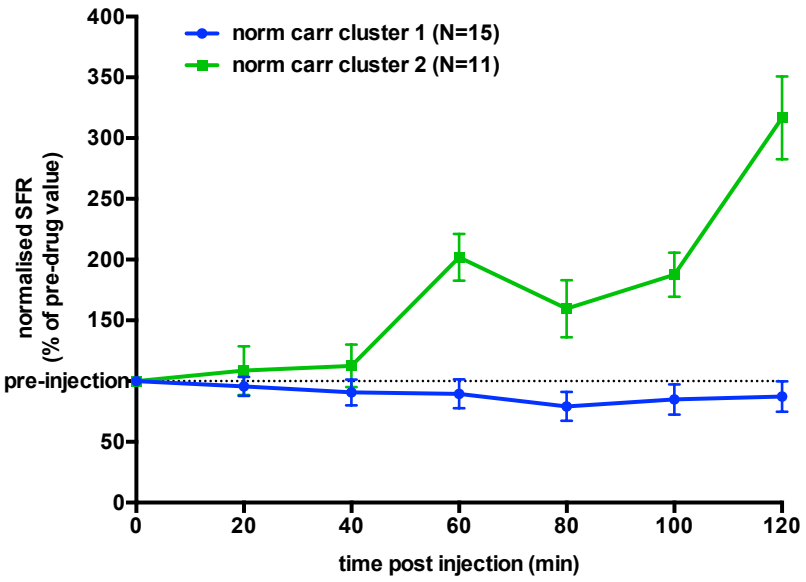

Figure 6.12 Normalized SFR post-carrageenan injection of 100-120-minute-carrageenan response-based neurone clusters: carrageenan-naloxone experiments only. Data shows mean normalized SFR (expressed as a percentage of pre-carrageenan injection mean SFR, y-axis) of neurones recorded in the carrageenan-naloxone experiments sorted into carrageenan response-based clusters at all time points up to two hours post-carrageenan injection (minutes, y-axis): norm carr cluster 1 (carrageenan-unresponsive; blue trace, N=15) and norm carr cluster 2 (carrageenan-excited; red trace, N=11). Dashed horizontal line at y=100% represents mean pre-injection SFR.

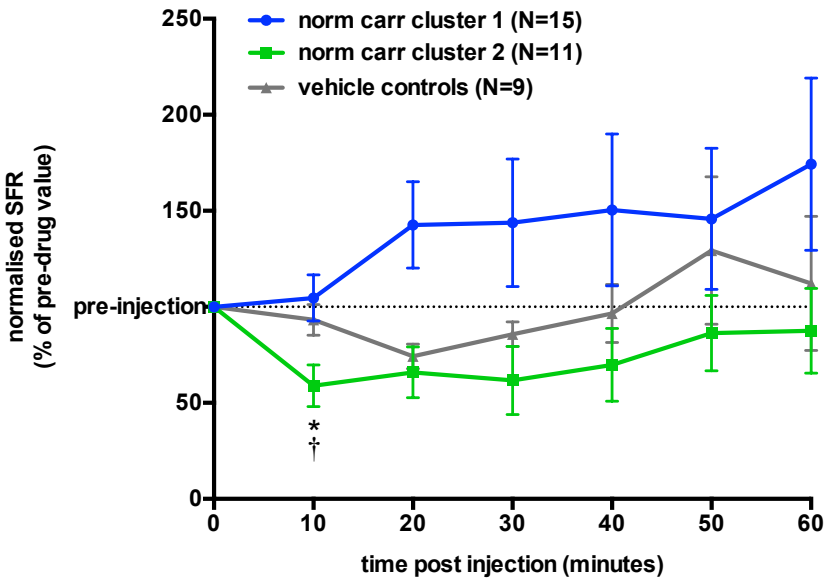

Figure 6.13 Normalized SFR post-naloxone injection of carrageenan response-based neurone clusters. Data shows mean normalized SFR (expressed as a percentage of mean pre-naloxone injection SFR) of carrageenan response-based clusters: norm carr cluster 1 (blue trace, N=15) and norm carr cluster 2 (green trace, N=11) at all time points post-naloxone injection. Mean normalized SFR (expressed as a percentage of mean pre-vehicle injection SFR) of neurones recorded in vehicle control experiments is also shown for all time points post-vehicle injection (grey trace, N=9). The dashed horizontal line at y=100% represents mean pre-naloxone injection SFR. Friedman tests with post-hoc Wilcoxon signed-rank pairwise comparisons, using a Bonferroni-corrected alpha of 0.008 were conducted to test for injection effects on SFR, * $p<0.008$. An Independent-samples *t*-test was conducted using mean normalized SFR values of norm carr cluster 2 and vehicle control neurones at the 10 minutes post-naloxone or vehicle injection time point, † $p<0.05$.

Subsequently, mean SFR for each neurone recorded in the carrageenan-injected state at all time points post-naloxone injection was normalised relative to mean *baseline* SFR (i.e. before carrageenan injection). Mean baseline-normalised values of the neurones belonging to norm carr clusters 1 and 2 were then calculated and plotted for each time point post-carrageenan and naloxone injection (figure 6.14). To investigate the effects on naloxone injection on the normalised SFR of the norm carr cluster 2 neurones, a repeated measures ANOVA with a Bonferroni adjustment for multiple corrections was conducted between 120 minutes post-carrageenan and 10,20 and 30 minutes post-naloxone injection (denoted as 130, 130 and 150 minutes post-injection in figure 6.14). This

analysis revealed a significant reduction in mean normalised SFR of norm carr cluster 2 neurones from the 120-minute post-carrageenan time point to the 10-minutes post-naloxone time point (mean±SEM: 120min post-carrageenan=316.7±34.1%, 10min post-naloxone=158.6±31.3% ; pairwise comparison, $p<0.05$).

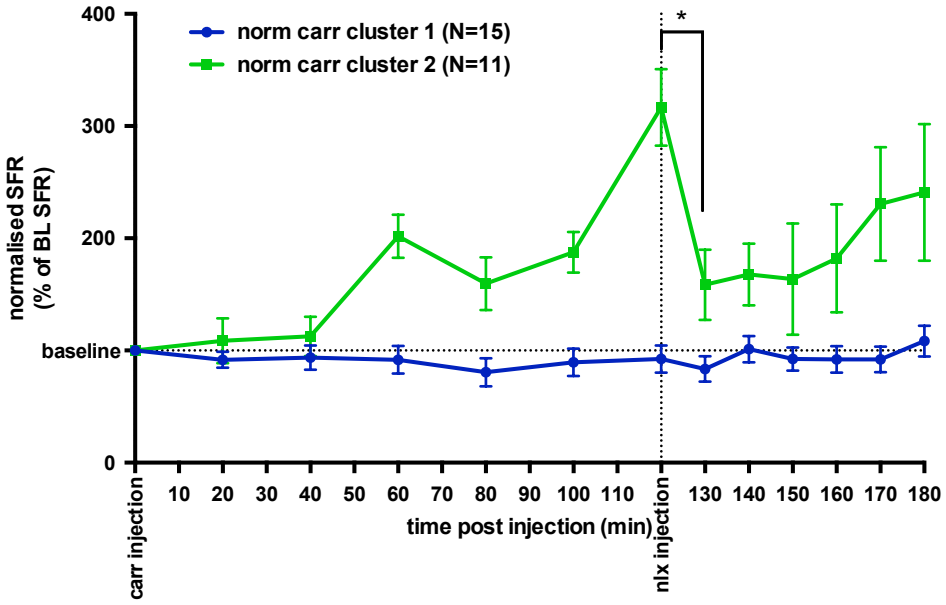

Figure 6.14 Effects of carrageenan and naloxone on SFR of carrageenan response-based neurone clusters, normalised relative to baseline SFR values. Mean SFR at all time points post-carrageenan injection (0-120 minutes) and a subsequent naloxone injection (120-180 minutes, injection represented by vertical dashed line; x-axis) expressed as a percentage of mean baseline (pre-injection) SFR (y-axis; normalized SFR) of neurones clustered according to carrageenan response (norm carr cluster 2: green trace, N=11; norm carr cluster 1: blue trace, N=15). The horizontal dashed line at y=100% represents mean pre-injection SFR. Data points represent mean ± SEM. A repeated measures ANOVA with a Bonferroni adjustment for multiple corrections was conducted between 120 minutes post-carrageenan and 10, 20 and 30 minutes post-naloxone injection to establish injection effects on SFR, *$p<0.05$.

6.4.5 Vehicle control injection effects

No significant percentage change from mean pre-injection SFR was seen at any time point post-injection of the vehicle solution used for the naloxone injections (N=9; Friedman test with post-hoc Wilcoxon signed-rank pairwise comparisons using a Bonferroni-corrected alpha of 0.008).

6.5 Discussion

Intraplantar injection of λ-carrageenan results in an inflammatory reaction known to cause a tonic pain state in the animals subjected to it (Hargreaves et al., 1988; Hylden et al., 1991). Corresponding alterations in activity of spinal cord dorsal horn neurones, the second-order neurones in nociceptive processing pathways, presents a possible explanation for the hypersensitivity (Stanfa et al., 1992). However, evidence suggests that more complicated down-stream changes in brain-based neuronal function are important; for example, the pain system's dependence on dopamine is thought to be enhanced during on-going pain (Altier and Stewart, 1999). For this reason, together with the clinical relevance of elucidating on-going pain mechanisms, this investigation looked into the effect of λ-carrageenan injection on VTA neurone activity.

6.5.I Carrageenan-induced changes in spontaneous firing rate

When investigating the effects of injected lambda-carrageenan on the activity of VTA neurones, it was found that the sampled population could be separated into two populations: a small proportion of relatively high-firing and seemingly carrageenan-excited neurones, and a larger population of relatively low-firing and seemingly carrageenan-unresponsive neurones. The high firing neurone cluster (raw carr cluster 1) displayed an increase in mean SFR across the two hours post-carrageenan injection, tying in with the known time course of carrageenan inflammatory action: a slow onset, reaching peak oedema and pain sensitivity at 3 hours post-injection (Winter et al., 1962; Stanfa et al., 1992). However, this excitatory response did not represent a significant group increase in SFR from pre-injection values. The lack of general responsivity witnessed amongst the recorded population when sorted in this way may be due to the dominant influence of mean SFR value on the cluster analysis process. Consequently, it was considered important to remove the influence of baseline SFR variability on neuronal sorting by normalising neuronal post-injection mean SFR values relative to their mean baseline SFR. By doing this, it is possible to perform further analyses on the response profile only.

Cluster analysis of the normalized SFR values revealed that there were in fact three response-based neurone groups: unresponsive (norm carr cluster 1), excited (norm carr cluster 2), and seemingly, but insignificantly strongly excited (norm carr cluster 3). There are several possible causes of the excitatory effect of carrageenan-induced inflammation. Increased pain-related sensory input from the periphery could feasibly alter the activity of

the VTA neurones, as both dopaminergic and GABAergic populations are known to show changes in firing rate in response to nociceptive stimulation. Alternatively, changes in SFR could be caused by alterations in local or up-stream modulatory mechanisms, including endogenous opioidergic action. The latter suggestion can be investigated by observing changes in the effects of systemic opioid receptor antagonism between the naïve and tonic pain states, thereby unmasking differences in tonic endogenous opioid influence.

If the numbers of the carrageenan-unresponsive, low-firing (raw carr cluster 1) neurone group from the non-normalized data analysis (N=65) are compared with that of the unresponsive cluster established from analysis of the normalized data (norm carr cluster 1, N=42), it is apparent that a proportion of the members of the low-firing neurone cluster were in fact excited in the presence of a tonic inflammatory pain state. Nevertheless, results from both analyses are in agreement when it comes to suggesting that, at least under these experimental circumstances, neurones in the VTA were more likely to be unresponsive to carrageenan injection than excited by it. This relative lack of VTA neuronal responsivity witnessed in the SFR measurements following carrageenan injection suggests that such changes are unlikely to be pivotal in mediating the sensation of tonic pain resulting from inflammation. However, it is possible that changes in other characteristics of these neurones do contribute; firing pattern or stimulus-evoked response both represent changes in functionality that could feasibly generate the alterations in pain-processing – such as hyperalgesia and allodynia - witnessed in tonic pain.

6.5.2 Carrageenan effects on burst firing characteristics

The possibility that changes in firing pattern might occur upon carrageenan administration amongst seemingly-unresponsive neurones was tested by comparing the amount of burst firing of these neurones before (during the whole baseline period, circa 30 minutes) and after (between the 60 to 120-minute time points) injection. Interestingly, neurones belonging to the normalized SFR-based cluster showing no mean change in SFR following carrageenan injection (norm carr cluster 1) did show a reduction in the percentage of spikes existing within a burst. It is known that burst firing of DA neurones acts to transiently and dramatically increase extracellular DA concentration, leading to the activation of lower-affinity receptor populations and the initiation of down-stream signalling mechanisms (Marinelli and McCutcheon, 2014). Although less well studied, a proportion of the GABA neurones within the VTA appear to display equally-irregular firing patterns (Margolis et al., 2012). It seems logical to assume that GABA neurone burst firing would result in a similar boost in downstream signalling. Hence,

in light of the functional impact of burst firing, the enhanced analgesic role of VTA DA neurons in the tonic pain state, and the known modulatory function of GABA release, it seems feasible that the change in firing characteristics witnessed in the carrageenan "unresponsive" group of neurones could lead to functionally important alterations in pain processing, regardless of the neurochemical identity of the constituents. For example, if a proportion of neurones displaying a decrease in burst firing were in fact dopaminergic, a reduction in DA receptor activation in projection targets such as the nucleus accumbens and prefrontal cortex would occur. It is feasible that a pathological reduction in DA signalling – perhaps via a decrease in burst firing as witnessed here - is responsible for the induction of tonic pain sensation. In support, microinjection of the D2 receptor agonist quinpirole in the nucleus accumbens – which would act to counter any reduction in DA neurone activity - has been found to relieve pain in tonic but not phasic pain tests in rodent models (Taylor et al., 2003).

To contrast these findings, the amount of burst firing in the carrageenan-excited norm carr cluster 2 neurone population was enhanced by the induction of tonic inflammatory pain. Again, the identity of neurones residing within this subgroup will affect the precise nature of the functional consequences of this change. The norm carr cluster 3 neurone group, found to show an excitatory but statistically-insignificant response to carrageenan injection, showed no increase or decrease in %SIB values – unsurprising given the low number of neurones in this group (N=3).

If, hypothetically, some of the norm carr cluster 2 carrageenan-excited neurones were dopaminergic, the enhancement of both burst and/or single spike firing could result in antinociception in light of the analgesic effects of DA agonist administration in this pain state (Altier and Stewart, 1999; Wood, 2008). This theory thus speculates that changes in DA signalling may represent an adaptive counteractive mechanism of endogenous analgesia in the face of tonic pain, rather than a pathological contribution.

It is important to consider the possibility that increases in %SIB values of the norm carr cluster 2 neurones are solely due to direct consequences of increased SFR, as discussed in section 3.5.2.4. If so, changes in %SIB would not necessarily represent a functionally-independent response. This possibility does not apply to the %SIB change witnessed for the norm carr cluster 1 carrageenan-unresponsive neurone cluster, however, as this change occur in the absence of parallel changes in group mean SFR values.

Burst firing of VTA DA neurones is modulated in-part by the actions of PFC-derived glutamate on NMDA receptors present on DA neurones; increased activation of PFC glutamateric projection neurones acts to increase the amount of burst firing of VTA DA neurones independently of mean firing rate (Carr and Sesack, 2000; Charlety et al., 1991; Lu et al., 1997; Overton and Clark, 1992; Sesack and Pickel, 1992; Tong et al., 1996). Activity in PFC projection neurones to the VTA is known to result in enhancements in DA release within the NAcc, specifically, which in turn has a modulatory effect on both ascending and descending pain-related signals. Additionally, up to around one third of PFC-VTA projections have been shown to synapse on GABAergic projection neurones (Carr and Seasack, 2000). Given the established role of the PFC in nociceptive signalling, it is possible that the PFC-mediated alterations in VTA neurone firing pattern represents a mechanism through which persistent nociception resulted in the %SIB differences witnessed.

As a final point of interest with respect to burst firing of the VTA neurones, it was noted that the mean %SIB values of all three carrageenan response-based clusters of neurones were very similar during the baseline period (figure 6.4). This result suggests that tonic pain responsivity cannot be predicted by baseline firing characteristics. This could either be due to a neurochemically heterogeneous composition of the carrageenan response-based or %SIB-based neurone clusters, or, most likely, a combination of both.

6.5.2 Carrageenan response of L-DOPA response-based neurone clusters

6.5.2.1 L-DOPA effects

In the current set of experiments, the DA receptor pharmacology of neurones either unresponsive to or excited by carrageenan was investigated through the systemic injection of a low dose of L-DOPA. In the previous studies, L-DOPA injection was found to separate neurones into two response-based groups: one group tending to show a general excitatory response to L-DOPA (norm L-DOPA cluster 2p and 2s), and another tending to show an inhibitory response (norm L-DOPA cluster 1p and 1s).

Given that L-DOPA injections here took place two hours following the administration of carrageenan rather than in the baseline condition, it was considered important to test for the existence of any differences in L-DOPA responsivity of neurones recorded in the previous and the current experiments. For example, it is possible that the induction of a tonic inflammatory pain state results in the reduction in sensitivity of neurones to L-DOPA, which could manifest in a disappearance of population separation into distinct response-based clusters. In agreement

with the results established from the previous L-DOPA experiments, cluster analysis of the normalized SFR following L-DOPA injection in carrageenan-injected animals revealed a separation into two natural neurone groups of similar relative proportions. In addition, the effect size and profile of the cluster showing a generally inhibitory response to L-DOPA (norm L-DOPA cluster 1c) showed no significant differences from that of all L-DOPA-inhibited cluster neurones recorded in the naïve state (norm L-DOPA cluster 1p). However, the seemingly-excited neurone cluster (norm L-DOPA cluster 2c) recorded in the carrageenan-injected state displayed a lower level of excitation in response to L-DOPA injection when expressed in terms of percentage of pre-injection values than those recorded in the naïve state (norm L-DOPA cluster 2p).

These findings could result from a reduction in DA receptor sensitivity of the group of neurones tending to be excited by L-DOPA, or at least a subset of these neurones. As discussed previously (section 4.5.1.2), there is some evidence to indirectly theorise that the population of neurones seemingly excited by L-DOPA injection – norm carr clusters 2p and 2c - are more likely to be GABAergic. It is uncertain how or why a reduction in L-DOPA response would occur in a population of VTA, putative GABAergic neurones. It is plausible that a neurone subpopulation-specific reduction in DA receptor sensitivity occurs. Alternatively, other factors with the ability to selectively influence neuronal firing rate, such as neurone-specific alterations in either excitatory or inhibitory afferent input, could represent a conceivable explanation. For example, increased inhibitory tone on a group of GABAergic, L-DOPA-excited neurones, such as that inflicted by μ-opioid receptors on the majority of GABA neurones, could be responsible for a reduced excitatory response to L-DOPA witnessed in the current experiments. Finally, the witnessed results could simply be the result of sampling a slightly different subset of this functional neurone group; significant variability has been previously witnessed in DA receptor agonist effects, and detection of sets of neurones that are more or less responsive on average could occur across the different L-DOPA experiments. In other words, we cannot assume that the neurones belonging to different response-based clusters recorded in the naïve and carrageenan-injected states represent equivalent subgroups of VTA neurones. What we can say, however, is that the similarity of L-DOPA response profile and magnitude of the inhibited clusters found in naïve and carrageenan-injected states (norm L-DOPA clusters 1p and 1c, respectively) provides evidence in favour of these clusters being equivalent.

In summary, two natural clusters according to L-DOPA response were found within the carrageenan-injected recorded population, which appeared to mirror the inhibited and seemingly-excited neurone clusters found in the

naïve state. As discussed previously in section 4.5.1, evidence hints at a likely DAergic identity of at least a proportion of the neurones of the seemingly L-DOPA-inhibited cluster (norm L-DOPA cluster 1c), and most-likely a GABAergic identity of those of the other seemingly-excited but statistically unresponsive cluster (norm L-DOPA cluster 2c). These neural identities will be tentatively proposed for the subsequent investigation into carrageenan effects, but not without consideration of alternative possibilities.

6.5.2.2 Carrageenan effects on L-DOPA response-based neurone clusters

In order to establish and compare the effects of carrageenan injection on the L-DOPA response-based groups, mean SFR values for norm L-DOPA clusters 1c and 2c were calculated for each time point post-carrageenan injection. However, large within-group variability in baseline SFR values for both clusters 1c and 2c meant that pharmacological effects weren't easy to distinguish. This source of variability was removed by normalising all mean SFR values post-injection with respect to pre-carrageenan injection values, and the analysis was repeated.

It was found that large within-group variability in post-carrageenan normalized SFR remained, suggesting that neurones belonging to a specific L-DOPA-based cluster tended to be heterogeneous in terms of both carrageenan response and baseline spontaneous firing rate. If we assume a predominantly dopaminergic and GABAergic identity of the norm L-DOPA cluster 1c and 2c groups, respectively, these results suggest a substantial degree of variability in tonic pain response within the neurochemical populations. Heterogeneity in acute pain response has been well reported for dopaminergic neurones (reviewed in McCutcheon et al., 2012), hinting at the existence of different functional groups with respect to nociception. This functional division may continue as pain persists, resulting in a large degree of variability in the effects of tonic pain amongst the seemingly-L-DOPA inhibited, putative dopaminergic, cluster 1c. In addition, VTA DA neurones have been found to be differentially affected by MOR agonists – with some indirectly excited and others directly inhibited by local injection of morphine (Cameron et al., 1997; Ford et al., 2006; Gysling and Wang, 1983; Margolis et al., 2012, 2003; Matthews and German, 1984). If opioid modulation of DA release – shown previously to be upregulated in the tonic pain state - underlies the effects of carrageenan injection in the current experiments, it is feasible that variability in responsivity to endogenous opioids also contributed to carrageenan response heterogeneity within the norm L-DOPA cluster 1c group. Interestingly, despite the variability, a significant excitatory effect of carrageenan was witnessed for the norm L-DOPA cluster 1c at 80 minutes post-injection. If opioid action within the VTA is indeed upregulated and this population is predominantly dopaminergic, this result could represent indirect excitation of

DA neurones, as predicted by the two-neurone model of VTA opioid action proposed by Johnson and North (1992).

Heterogeneity in the acute nociceptive responsivity of GABAergic neurones has not been reported, but this may simply reflect the relative lack of research on nociceptive responsivity of this cell group. Subpopulations of GABA neurones have been found to respond differently to MOR agonists – either directly inhibited or unaffected. If opioid action within the VTA is enhanced upon the induction of tonic inflammatory pain, one would expect either lowered or unchanged GABA neurone activity following carrageenan injection. The former could feasibly be responsible for the slightly reduced excitatory response of the putative GABAergic, norm L-DOPA cluster 2c group witnessed here in comparison to that seen with a naïve pre-injection state.

Alternatively, it is possible that the neurochemical groups are in fact relatively consistent in terms of their tonic pain responsivity, and that the variability seen comes from a mix of neurochemical identities within the norm L-DOPA clusters 1c and 2c. As previously discussed (section 6.5.2.I), the suggestions mentioned above of mechanisms underlying within-cluster variability in carrageenan response rely on unsubstantiated assumptions of neurone identity; in other words, we don't know that cluster analysis has separated neurones according to neurochemical profile. It is possible that both heterogeneity in carrageenan response of a given neurochemical group and in neurochemical identity of L-DOPA-response based groups are likely responsible to at least some degree for the within-cluster response variability witnessed.

6.5.3 Naloxone effects in tonic pain

Endogenous opioid action has been strongly implicated in the response to tonic pain (Hylden et al., 1991; Kayser and Guilbaud, 1981; Porro et al., 1991). To test whether alteration in μ-opioid function represents a possible cause for changes in the SFR of VTA neurones, it was necessary to answer two questions: firstly, do endogenous opioids exert a tonic influence over these neurones in the tonic inflammatory pain state, and secondly, if so, do changes in the magnitude of this influence occur in such a way that would result in the recorded responses to carrageenan injection?

These questions were tested by analysing the activity of VTA neurones following injection of the μ-opioid receptor antagonist, naloxone, in the carrageenan-induced tonic inflammatory pain state. Naloxone was also injected in animals not injected with carrageenan (naïve state) to allow comparison of effects between this and the tonic pain states. The naloxone was injected systemically to ensure that all putative body-wide locations of tonic endogenous opioid activity with the potential to ultimately influence VTA neurone activity were targeted.

6.5.3.I Naloxone effects in naïve and carrageenan-injected animals: non-normalized SFR

Cluster analysis performed using SFR values at all time points post-injection (up to 60 minutes) revealed the existence of two separate naloxone response-based groups in both the naïve ('n' clusters) and tonic pain conditions ('c' clusters); one group with a high mean pre-injection firing rate (raw nlx cluster 1n and raw nlx cluster 1c) and one with a low mean pre-injection firing rate (raw nlx cluster 2n and raw nlx cluster 2c).

The mean pre-injection SFR of the high firing cluster in the carrageenan-injected state - raw nlx cluster 1c (~14Hz) - was higher than that of the high firing cluster in the naïve state - raw nlx cluster 1n (~6Hz). This was expected given the excitatory effect of carrageenan witnessed in a proportion of the recorded population. In contrast, low firing neurone clusters found in the naïve and carrageenan-injected states – raw nlx clusters 2n and 2c, respectively - showed equivalent pre-injection mean SFR values of around 2Hz.

Interestingly, the high firing raw nlx cluster 1n neurones in the naïve state displayed a significant excitatory response to naloxone injection at the 30-minute time point, unmasking an inhibitory endogenous μ-opioid action on these neurones. Traditionally, opioid inhibition within the VTA was considered to be a uniquely GABAergic trait (Johnson and North, 1992; Gysling and Wang, 1983), but studies have since revealed the presence of DA neurones directly inhibited by opioid action, suggesting that neurones excited by naloxone could either be GABAergic or dopaminergic (Cameron et al., 1997; Margolis et al., 2003; Ford et al., 2006). However, the high mean firing rate of the raw nlx cluster 1n neurone group – a trait predominantly associated with a GABAergic identity – provides support for a dominant presence of this neurochemical population within this cluster.

In contrast, the high firing neurone cluster in the carrageenan-injected state – raw nlx cluster 1c - showed no significant change in SFR in response to naloxone injection, suggesting a lack of tonic endogenous opioid influence on the high firing subset of VTA neurones in tonic pain. It is possible that downregulation of tonic

opioid influence in either the VTA or in regions affecting the VTA occurs following the injection of carrageenan, resulting in a lack of detectable effects of MOR antagonism. This could tie in with the previously-reported enhancement of analgesic efficacy of exogenous opioids in tonic pain (Hylden et al., 1991; Kayser and Guilbaud, 1983) if the impact of lowered endogenous opioid release is considered; with fewer receptors occupied by endogenous opioids, a higher proportion would remain available for activation by exogenous agonist, thereby increasing the potential effect magnitude. This theory could explain why naloxone was not efficacious in the carrageenan model, as there would be less of an endogenous MOR activity to antagonise. In the naïve condition, on the other hand, a normally-functioning endogenous analgesic opioid system would leave lower capacity for exogenous enhancement, but a significant capacity for antagonist action. This is at odds with reports of enhanced beta-endorphin levels in several supraspinal pain-processing regions of the CNS the tonic pain state (Porro et al., 1991); however, it isn't completely unreasonable to suggest that opioid release in these areas is under dissociable control from that which affects the VTA.

An alternative possibility is raised by the findings of Narita and colleagues (2005). In experiments investigating the effects of formalin injection on opioid action, they found that DA release in the NAcc caused by systemic injection of morphine was reduced in the tonic inflammatory pain state. It was concluded that "the mesolimbic DA system may not be facilitated by μ-opioid agonists under an inflammatory pain-like state". This theory may be responsible for the lack of naloxone effect witnessed in carrageenan-injected animals here. However, findings of a reversal of this effect upon kappa-opioid receptor antagonism in the NAcc suggests that reduction in morphine-induced DA release following formalin injection is down to local, within-NAcc alteration of DA *release* rather than an effect on VTA DA neurone *activity* (Narita et al., 2005). Nevertheless, the idea that opioid efficacy in the VTA is downregulated in the tonic pain state remains an interesting possibility.

Neither of the low firing neurone clusters recorded in naïve (raw nlx cluster 1n) and carrageenan-injected (raw nlx cluster 1c) states showed any group mean response to naloxone injection. The similarity in mean baseline SFR of the neurones recorded in the two conditions points towards these groups representing equivalent populations in the two different experiments. If so, these results suggest that this low firing subpopulation of neurones is unaffected by endogenous opioids (no effect of naloxone), and that they show no change in opioidergic responsivity upon the induction of tonic pain (no change in effect of naloxone with carrageenan injection). This suggestion is based on the assumption that changes in naloxone response of the high firing VTA neurone

subpopulation between naïve and tonic pain states are down to changes in levels of endogenous opioid release, rather than neurone-specific changes in receptor expression. In other words, that a disappearance of naloxone responsivity is due to a reduction in endogenous opioid levels, as discussed above. This assumption is made in light of previous findings of enhanced analgesic efficacy of exogenous opioids in tonic pain (Hylden et al., 1991; Kayser and Guilbaud, 1983), providing evidence against the alternative theory of reduced receptor availability.

6.5.3.2 Naloxone effects in naïve and carrageenan-injected animals: normalized SFR

The large degree of separation in terms of pre-injection spontaneous firing rate of the high-firing and low-firing naloxone response-based clusters - raw nlx clusters 1n, 2n, 1c and 2c - suggests that the cluster analysis performed tended to sort neurones according to SFR value, possibly masking naloxone response profile-based groupings. In order to investigate groupings based solely on changes in SFR induced by naloxone injection (i.e. naloxone effect) in both naïve and carrageenan-injected states, cluster analysis was repeated when time point SFR values had been normalized with respect to mean pre-injection SFR. Neurones recorded in the naïve state were found to be separable into two response-based clusters, of which one – norm nlx cluster 2n - appeared to show mean excitatory responses to naloxone injection; however, the number of neurones within the naloxone "excited" group established using normalized values was only three - much lower than that seen in the non-normalized naloxone-excited cluster (raw nlx cluster 1n; N=14) – and the group mean percentage increase in SFR from pre-injection values was not significant at any time point. This result implies that the high firing raw nlx cluster 1n established in the previous analysis contained only a few more strongly-excited neurones, and that the rest of that sub-population were either unresponsive to, or only weekly excited by, naloxone injection.

Normalized post-naloxone SFR values of neurones recorded in the carrageenan-injected state were not found to be separable into two or more distinct groups. Hence, it can be concluded that within the recorded population in the tonic pain state there are no distinct sub-populations of VTA neurones homogenous and distinct in their responsivity to systemic μ-opioid receptor antagonism, implying that persistent pain somehow 'smooths out' the distribution of naloxone responsivity. This could feasibly be achieved by a lessening of the more extreme responses, such as those of the more strongly-excited neurones recorded in animals in the naïve state, such that normalized SFR values are statistically indistinguishable from that of the unresponsive neurone group.

A subsequent analysis was performed using normalised SFR values following naloxone injection to further clarify whether spontaneous firing rate in the baseline condition bore any relationship with naloxone responsivity (section 6.4.4.3). The results of the non-normalised naloxone response cluster analysis in the naïve state (section 6.5.3.I – clusters raw nlx cluster 1n and 2n) revealed that a cluster of neurones with a group mean baseline SFR value of ~6Hz (as opposed to the ~2Hz mean SFR of the other cluster) displayed an excitatory response to naloxone injection, on average. This result hints at naloxone-excited VTA neurones possessing higher baseline firing rates than naloxone-unresponsive neurones; however, because the cluster analysis on non-normalised SFR values was performed using values from all time points pre- and post-naloxone injection, it is also possible that an excitatory response of a selection low-firing neurones placed them in the 'high-firing' cluster (raw nlx cluster 1n), suggesting that BL SFR didn't bare any relationship to an excitatory naloxone response after all. The current analysis set out to clarify the association between naloxone responsivity and BL SFR.

In order to achieve this, the normalised naloxone responses of the high and low firing neurone clusters established from cluster analysis on the baseline SFR values of all neurones recorded in the naïve condition (BL SFR cluster 1n and 2n, respectively) were assessed. Interestingly, neurones belonging to the low-firing BL SFR cluster (BL SFR cluster 2n) displayed a percentage increase in SFR following naloxone injection that was significant at 20- and 40-minute time points (section 6.4.4.3). In contrast, the high-firing BL SFR cluster 1n neurones showed no group mean response to naloxone injection. Both clusters showed a reasonable degree of within-cluster variability in normalised SFR values post-naloxone. These results suggest that the non-normalised naloxone response cluster analysis performed on neurones recorded in the naïve state was influenced by post-naloxone SFR as well as baseline SFR, which could also explain the lower mean pre-injection SFR of the naïve (raw nlx cluster 1n) versus carrageenan-injected high-firing neurone cluster (raw nlx cluster 1c). Further, results suggest that low-firing neurones are more likely to display excitatory responses to naloxone than high-firing neurones; however, the within-cluster variability of the BL SFR cluster 2n in terms of naloxone response suggests that this is only a general trend and does not apply to all neurones.

6.5.3.3 A possible theory of opioid action on VTA neurones in naïve versus tonic pain states

A possible theory that consolidates findings in the normalized data set with those from the non-normalized data set for neurones recorded in animals in naïve and carrageenan-injected states, as well as effects of carrageenan on SFR, is that of a reduction in tonic inhibitory action of endogenous opioids, as proposed in section 6.5.3.1. In the

naïve condition, tonic opioid influence leads to a suppression of SFR of a subset of the VTA neurones. The literature surrounding MOR agonist action in the VTA suggests that this opioid-inhibited population is likely to include a mixture of GABAergic and dopaminergic neurones (Johnson and North, 1992; Cameron et al., 1997; Margolis et al., 2003; Ford et al., 2006). Upon the injection of naloxone, this inhibition is lifted and an increase in mean SFR of this neurone group is witnessed. Upon the induction of tonic inflammatory pain by carrageenan injection the level of endogenous opioid release decreases, allowing the SFR of this group of neurones to increase, thereby producing the excitatory response profiles in a subset of the recorded neurones. Subsequent injection of naloxone in this state will have no apparent effect, as there is no longer a significant influence of endogenous MOR activation to unmask.

6.5.3.4 Comparing naloxone effects in naïve versus tonic pain states

Because the carrageenan-injected neurones were not separable into distinct response-based groups such as those revealed in the naïve state, comparisons between naloxone effects on neurones recorded in the two states were made using population mean values – grouping together SFR values of neurones in both the naloxone-excited and –unresponsive clusters. While this will inevitably dilute out the strong excitatory effects witnessed for a small population of naïve state-recorded neurones (norm nlx cluster 2n), comparing general naloxone action should provide some insight into changes associated with endogenous opioid levels and therefore endogenous opioid exposure of the VTA neurone population as a whole.

When mean normalized SFR values for neurones recorded in naïve and carrageenan-injected state animals were compared, results revealed that there were no mean significant differences between the naloxone injection responses of the neurones recorded in the two states.

The similarity in the mean response to naloxone in the two states, despite the distinct differences in cluster analysis results, is a potential caveat for the suggested theory involving endogenous opioid release levels rather than opioid receptor expression discussed above (6.5.3.I). If indeed a reduction in the release of endogenous opioids occurred, one would expect the naloxone effects on the VTA population to decrease *in general*. An explanation may lie in the relatively low numbers of neurones in the naloxone-responsive cluster; because there were only three neurones in the naïve state cluster showing strong excitatory responses to naloxone, as opposed to 41 in the cluster showing no response, on average, loss of responsivity would only produce a small impact on the population mean

normalized SFR values. In the face of the relatively large inter-group variability for both carrageenan-injected and naïve state neurone groups, it is feasible that this impact is not enough to result in any significant difference between the conditions.

6.5.3.5 Effects of naloxone in carrageenan response-based clusters

Despite analyses revealing a general lack of mean naloxone responsivity following tonic pain induction across the recorded population as a whole, it was considered important to compare the naloxone responsivity of neurones differentially affected by carrageenan. It is possible that a subset of the carrageenan-excited norm carr cluster 2 neurones did in fact show a response to naloxone, reflecting tonic action of endogenous opioids. This effect could feasibly heave been concealed by the grouping of neurones belonging to this carrageenan-excited cluster with those of the proportionately larger carrageenan-unresponsive cluster (norm carr cluster 1).

In order to investigate this possibility, the normalised naloxone response of neurones belonging to the norm carr clusters 1 and 2 were compared with mean response to control injection. Interestingly, a transient and immediate (10 minutes post-injection) inhibition in response to naloxone, shown in terms of a significant percentage change in SFR from pre-naloxone injection value, was displayed by the carrageenan-excited norm carr cluster 2 neurones. This rapid inhibition of the norm carr cluster 2 neurones upon the injection of naloxone was also witnessed when neurone responses were normalised according to baseline SFR (as opposed to pre-naloxone injection SFR). This inhibitory response was present amongst neurones recorded in vehicle control experiments, implying that it had a pharmacological origin. Hence, this result suggests that the carrageenan-excited neurone cluster, norm carr cluster 2, is under excitatory influence of endogenous μ-opioids, contrasting with the inhibitory influence revealed in a subset of the neurone population recorded in the naïve state (norm nlx cluster 2n). An excitatory opioid influence in this subset of the VTA neurone population suggests that opioids may be responsible, at least partially, for the excitatory response to carrageenan injection. The fact that this inhibitory response to naloxone injection of the carrageenan-excited neurones occurs much more rapidly than the excitatory naloxone effect witnessed in a group of neurones recorded in the naïve-state (10min vs 30min) suggests that these opposite responses reflect different mechanisms of naloxone action with different rates of effect. This is somewhat unexpected, since the pharmacokinetics of systemically-injected naloxone should remain reasonably consistent and certainly shouldn't be affected by pain state. However, it is possible that an upstream action of naloxone (e.g. in the spinal cord or brain) on an opioid mechanism with a tonic excitatory influence on a subset of VTA neurones in the carrageenan-

injected state comes into effect more rapidly than actions on opioid mechanisms exerting a tonic inhibitory influence on VTA neurones.

6.5.4 Methodological considerations

It is important to note that the experimental set up involved procedures likely to be noxiously stimulating for the animal. The maintenance of the skull position with ear bars involves significant and sustained pressure on both sides of the skull, and the tracheotomy and exposure of the skull were both invasive procedures involving substantial tissue damage. Hence, at the time of neuronal recording, the animals could be said to be in a state of persistent pain. This has implications for the interpretation of the witnessed results; comparisons between neuronal responses recorded in animals in "naïve" and carrageenan-injection state are really between a state of persistent mechanical pain and a state of persistent mechanical pain plus tonic inflammatory pain. While studies on spinal neurone activity adopted a similarly-invasive set up (Stanfa et al., 1992), previous investigations into the effects of various pharmacological manipulations (naloxone, DA receptor agonists) on pain-behaviour were performed in freely moving animals (Altier and Stewart, 1999; Hylden et al., 1991; Morgan and Franklin, 1990). Consequently, tonic pain and naïve states of the current and previous studies were not always directly equivalent, and comparisons of the current findings with those reported in the literature should be made with caution.

6.5.5 Conclusions

This study set out to clarify the involvement of the VTA neurones in the development of the tonic pain state. It was found that neurones could be split into distinct subgroups based on changes in SFR in response to carrageenan injection, with two groups of neurones showing a mean excitatory response – only one of which represented a significant change in SFR, and a relatively large group showing no mean changes in firing rate. Interestingly, this latter "unresponsive" group of neurones showed a significant reduction in the amount of burst firing in the tonic versus naïve state, implying that they did show a functionally relevant response after all. The consequences of this reduction in burst firing will depend on the neurochemical identity of the group's constituents. L-DOPA was injected in an attempt to shed light on this, as evidence to support putative neurochemical identity suggestions of neurones residing in certain L-DOPA response-based groups was found in the previous investigations (sections 4.5.1 and 4.5.2). It was found that both L-DOPA response-based neurone clusters displayed variable responses to carrageenan, suggesting perhaps that both dopaminergic and GABAergic neurone populations are heterogeneous

with respect to tonic pain response. This is not unexpected in light of known heterogeneity of opioid responsivity – thought to be altered by persistent pain - of both populations, and of nociceptive responsivity of the dopaminergic contingent, in particular. However, no robust conclusions could be drawn from these results, as the neurochemical identity assumptions remain relatively unsubstantiated, suggesting it is also possible that carrageenan response variability of the L-DOPA response-based clusters is caused by within-cluster neurochemical heterogeneity. Subsequently, the opioid influence on VTA neurones recorded in naïve and tonic pain states was compared in order to investigate the impact of pain state on this key modulatory mechanism. It was found that, while naloxone exerted an excitatory effect on a small group of high-firing neurones recorded in the naïve state, implying the presence of tonic opioid inhibitory action, no such effects were found on the high firing neurones in the carrageenan-injected state. This finding tied in with the greater mean SFR of the high firing neurones in the carrageenan-injected state versus the naïve state, suggesting that tonic pain induction causes excitation of a subgroup of VTA neurones at least in part through the lifting of tonic inhibitory opioid control. It was proposed that these results may be caused by a reduction in the release of endogenous opioids in the VTA upon carrageenan injection to tie in with previous findings of increased exogenous opioid efficacy in the tonic pain state. Finally, when investigating the effects of naloxone in carrageenan-excited and -unresponsive clusters separately, a rapid, transient inhibitory effect was seen in the carrageenan-excited group (norm carr cluster 2). This result implies that the excitatory effects of carrageenan on this subset of VTA neurones may be caused in-part by an excitatory opioidergic influence – an effect presumably masked by the larger number of carrageenan-unresponsive and naloxone-unresponsive neurones when analysing responses of the population as a whole.

Investigating tonic pain in a rodent model will help us to elucidate the key neurochemical processes involved in pathologies of this nature, and ultimately to develop therapies targeting the key neural elements involved in the human condition. Tonic pain presents a very different challenge to phasic pain in terms of optimal behaviour, and this is reflected in the roles of different players in the pain processing system, including the DA neurones of the VTA at the centre of the current investigation. One would expect perhaps even more substantial changes in function of the system as the pain persisted over a length of time significant enough to be labelled as chronic. Given that the longer the pain affects a patient, the greater the impact it has on their lives as a whole, this thesis will next focus on VTA neurone function in a model of chronic neuropathic pain.

7. Investigating the system in chronic pain: the spinal nerve ligation model of chronic neuropathic pain

7.1 Introduction

Chronic pain, defined as any pain lasting more than 12 weeks (McMahon et al., 2013), presents a huge challenge to individuals plagued by it, often presenting with comorbidities such as depression, anxiety and insomnia, resulting in a drastic reduction in quality of life (Nicholson and Verma, 2004). In general, the pain intensity reported by patients experiencing chronic pain appears to be poorly correlated with the extent of tissue damage (Howard, 2009; Szebenyi et al., 2006), shifting the focus of research from peripheral to central processing abnormalities. Despite extensive investigations into the pathology, even the most promising treatments frequently fail to alleviate symptoms. Thus, it is important for us to persist with the pursuit of understanding surrounding these conditions, which the use of the well-established rodent models of neuropathic pain allows us to do effectively.

In contrast to human findings in tonic pain, in which the central antinociceptive beta-endorphin system has been shown to be up-regulated following formalin injection, opioids are generally found to lack potent analgesic efficacy in patients with neuropathic pain (Arnér and Meyerson, 1988). This finding has been replicated in rats with nerve injury, opening up an opportunity to investigate the precise nature of the alterations in the opioid pain modulatory system (Ossipov et al., 1995). One popular theory at the spinal cord level is that the reduction in opioid efficacy is down to a reduced number of postsynaptic opioid receptors, possibly partially as a result of degeneration of primary afferent neurones caused by nerve damage (Ossipov et al., 1995). Alternatively, or

possibly additionally, hyperactivity in the spinal CCK system has been suggested to be responsible for the lower opioid efficacy in neuropathic pain, through CCK modification of opioid receptors (Wang and Han, 1990).

Clinical evidence points towards dopaminergic system dysfunction playing a major role in chronic pain conditions such as fibromyalgia, with sufferers showing alterations in VTA DA neurone firing in relation to aversive stimulation and pain relief (Loggia et al., 2014). Crucially, it appears possible that the changes in VTA neurone function may be initiated by pathological modifications in the opioid modulatory machinery as detailed above; Ozaki and colleagues (2002) found the morphine-induced release of DA in the nucleus accumbens to be reduced in spinal nerve-ligated rats. This was suggested to be down to a reduction in MOR function, following from findings of a down-regulation in G-protein activation in the VTA neurones (Ozaki et al., 2002). Subsequent investigation found evidence pointing towards the uncoupling of MORs from the G-proteins by GPCR kinase 2 in the VTA as the mechanism, ultimately resulting in a suppression of the behavioural effects of morphine in chronic pain (Ozaki et al., 2003).

Further to this reduction in existing receptor function, a decrease in receptor density has been suggested by PET scan study findings of diminished MOR tracer binding in chronic pain (Maarrawi et al., 2007). Conversely, however, this could be down to an increase in endogenous opioid release and therefore agonist receptor binding, which would similarly reduce receptor availability (Jones et al., 1994).

Hence, it appears that the endogenous opioidergic modulation of VTA DA neurones is down-regulated in neuropathic pain conditions, both in patients and rodent models, with a combination of reduced opioid receptor numbers and function likely being responsible. The implications of these findings are that they present a possible explanation of the lack of efficacy of morphine in relieving chronic pain. Furthermore, this diminishing of endogenous opioidergic influence, leading to pathological DA system dysfunction, goes some way towards explaining characteristics of chronic pain conditions: enhanced and maladaptive pain sensitivity could result from the down-regulation of this natural antinociceptive mechanism, and the common comorbidity of depression could foreseeably result from the reduced gain within the VTA, or “pleasure centre”, when it comes to processing everyday rewards. Enhanced understanding of the pathological changes that occur in relation to the opioidergic control of VTA neurones will bring us closer to relieving these most crucial aspects of chronic pain.

7.2 Aims and Predictions

Following on from the previous study, in which the endogenous opioid influence on VTA neurone spontaneous firing rate during tonic pain was investigated, these experiments aim to elucidate the extent of any alterations in baseline firing characteristics and MOR action on these neurones in the chronic pain state. Based on the current literature it is predicted that there will be a reduction in opioid influence on VTA neurones following the development of neuropathic pain. This will be investigated using *in vivo* electrophysiological recordings of the VTA in rats with neuropathic pain (The Spinal Nerve Ligation model, Kim and Chung, 1992), together with the administration of systemic naloxone to unmask any tonic endogenous opioidergic influence on VTA neurone firing rate. L-DOPA will also be administered in an attempt to improve confidence, albeit tentatively, in suggestions surrounding neurochemical identity of different functional groups.

7.3 Materials and Methods

7.3.I Animals

Male Sprague Dawley rats (250-350g), bred by the Biological Services Unit (UCL, London, UK) were used for electrophysiological experiments.

7.3.2 Experimental protocol

In vivo electrophysiology, as described in section 2, was performed in rats in both naïve and 2-week post-spinal nerve ligation (SNL) surgery states. The latter state was assumed to represent a state of neuropathic pain; the spinal nerve ligation model has been previously validated as a model of chronic neuropathic pain, with behavioural experiments showing that mechanical and thermal hyperalgesia and allodynia are well-established by 2 weeks post-surgery (Kim and Chung, 1992). In short, the surgery involves ligation of the L5 and L6 spinal nerves as described by Kim and Chung (1992) – described in more detail in section 7.3.3.

There were two experimental protocols adopted in the current investigation: injection of naloxone alone (31 neurones recorded from 12 animals in the naïve state, and 20 neurones recorded from 9 animals in the SNL state), and injection of naloxone followed by the injection of 20mgkg^{-1} L-DOPA (17 neurones recorded from 7 animals in the naïve state, and 20 neurones recorded from 7 animals in the SNL state). The experimental protocols are depicted in figure 7.I and detailed below.

7.3.2.I Naloxone + L-DOPA experiments

Following establishment of a stable baseline spontaneous firing rate of neurones recorded, each rat was injected systemically with the mixed opioid antagonist naloxone. Spontaneous and evoked firing rates were monitored through stimulation rounds (detailed in section 2.2.2) occurring every 10 minutes up to 60 minutes post injection. Subsequently, each rat was injected with a 20mgkg^{-1} dose of L-DOPA, and spontaneous and evoked firing rates were recorded with stimulation rounds at 10, 20, 40, and 60-minute post-injection time points (figure 7.1A).

7.3.2.2 Naloxone-only experiments

Following establishment of a stable baseline spontaneous firing rate of neurones recorded, each rat was injected systemically with the mixed opioid antagonist naloxone. Spontaneous and evoked firing rates were monitored through stimulation rounds (detailed in section 2.2.2) occurring every 10 minutes up to 60 minutes post injection (figure 7.1B).

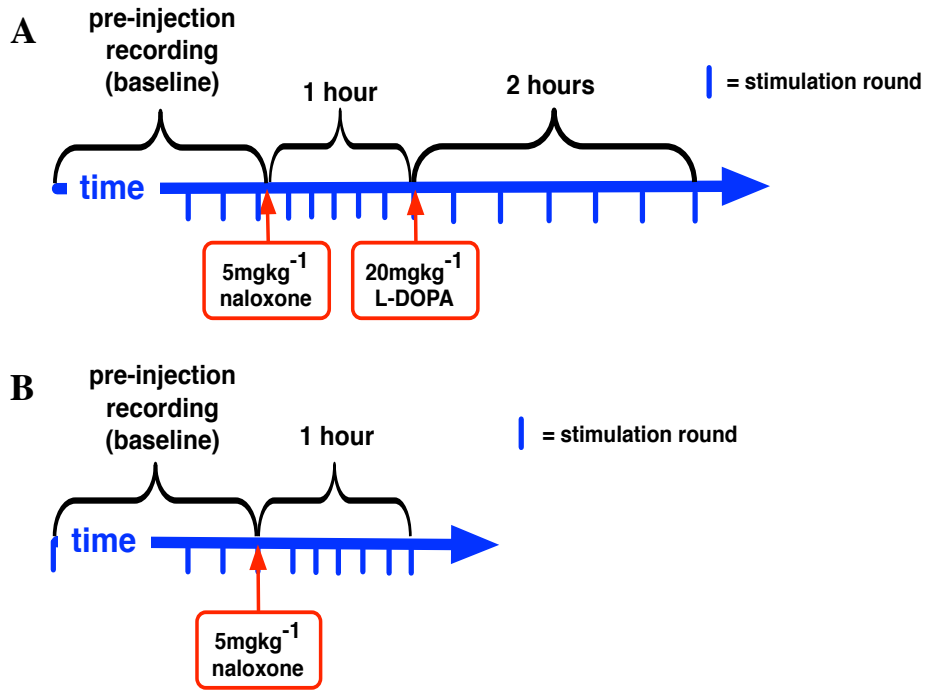

Figure 7.1 Experimental timeline of experiments in spinal nerve-ligated rats. The thick blue horizontal arrow represents the progression of time during the experiment, while vertical blue dashes indicate the times at which stimulation rounds were performed (stimulation round described in section 4.3.I). At least 4 stimulation rounds were performed in the baseline condition (not all rounds are depicted). A) *Naloxone-L-DOPA experiments*: naloxone was injected and stimulation rounds were performed every 10 minutes up to 60 minutes post-injection. At the 60 minute-post naloxone time point (after the stimulation round was performed), 20mgkg^{-1} L-DOPA was injected, and stimulation rounds were performed at 10, 20, 40, 60, 80, 100 and 120 minutes following. B) *Naloxone-only experiments*: naloxone was injected after the baseline stimulation rounds were complete, and stimulation round were performed every 10 minutes up to 60 minutes post-naloxone injection.

7.3.3 Spinal nerve ligation (SNL) surgery

Surgery was performed as described by Kim and Chung, 1992. Rats (125-135 g) were initially anaesthetised until areflexic with 3.5% v/v isoflurane, delivered in a 3:2 ratio of nitrous oxide and oxygen, in an induction box. Following shaving of the hair on the back of the rat and sterilisation of the skin with Betadine, rats were transferred to a nose cone delivering 2% v/v isoflurane to maintain anaesthesia for the remainder of the surgery. If signs of reflexes returning or an increase in breathing rate were detected, the concentration of isoflurane in inhaled air was increased slightly to maintain anaesthesia. Whilst surgery was being performed, rats were positioned on top of a heated mat in order to prevent a substantial decrease in core body temperature. A paraspinal incision into the skin and upper muscle layers was made on the left side just caudal to the ribcage, following which, the left tail muscle was identified and excised. Subsequently, part of the L6 transverse process was removed to expose the underlying nerves. The L5 and L6 spinal nerves were then isolated with a glass nerve hook (Ski-Ry Ltd, London, UK) and ligated with a non-absorbable 6-0 braided silk thread proximal to the formation of the sciatic nerve (figure 7.2). The surrounding muscle was closed with absorbable 3-0 sutures. The skin was sutured with a subcuticular pattern with absorbable 3-0 sutures. Animals recovered from the anaesthesia in a heated recovery chamber before being returned to their cages.

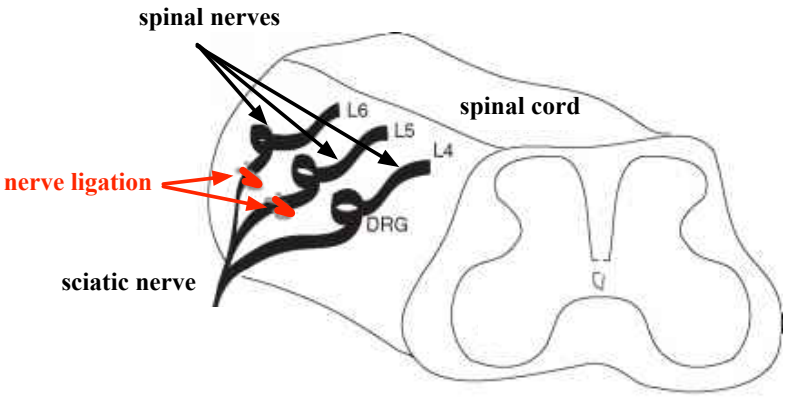

Figure 7.2 Schematic diagram of ligation of the L5 and L6 spinal nerves. A section of the lumbar spinal cord is shown, along with spinal nerves L4, L5 and L6. L5 and L6 are ligated proximal to the formation of the sciatic nerve with non-absorbable 6-0 braided silk thread in order to create the spinal nerve ligation rodent model of neuropathic pain, as described by Kim and Chung (1992). *Adapted from mussenhealth.us/animal-models/models-of-acute-pain.html.*

It is important to note at this point that sham control experiments – that is, experiments on animals who had undergone sham surgery involving an identical method to that of SNL surgery with the key difference of no spinal nerve ligation – were not conducted in the current investigation. The reasoning behind this decision is detailed in section 7.5.4.

7.3.4 Drug administration

Naloxone. Naloxone HCL (MOR antagonist, Sigma Chemie, Deisenhofen, Germany) solution was made up with double distilled water and injected in a dose of 5mgkg^{-1} subcutaneously.

L-DOPA. A combined carbidopa-levodopa solution (both Sigma-Aldrich, UK) in the concentration of 20mgml^{-1} was made up and administered at a dose of 20mgkg^{-1} using methods detailed in section 4.3.2.

7.3.5 Analysis

7.3.5.I Baseline SFR

The mean spontaneous firing rate of all neurones recorded in SNL animals was calculated as described in section 2.2.3.I. The mean BL SFR values of neurones in the SNL condition was compared with mean BL SFR values of all neurones in the naïve condition. Two neurone clusters according to mean BL SFR values of all neurones recorded in the naïve condition (N=222) were previously established in section 3.4.2.

7.3.5.2 Baseline firing pattern

The amount of burst firing in the baseline condition was quantified by calculating the percentage of spikes present within a burst (%SIB), as described in section 3.3.3. Mean %SIB of neurones recorded in the SNL condition was compared with mean %SIB of all neurones recorded in the naïve condition (N=111).

7.3.5.3 L-DOPA-based pharmacological characterisation

L-DOPA response-based characterisation was performed as previously described (section 4.3.3); Two-step and K-means cluster analysis was performed on neuronal mean SFR values normalized with respect to mean pre-injection SFR at each time point post-L-DOPA injection. The mean response to L-DOPA injection, measured as the percentage change in SFR at each time point, of the L-DOPA response-based clusters was compared with that seen in the previous experiments involving naïve animals (sections 4.4.I.2 and 5.4.I) in order to:

A) Test the consistency of L-DOPA action on VTA neurones (e.g. time profile of changes in SFR, relative proportions of neurones falling into L-DOPA-inhibited and -excited clusters)

B) Establish the influence of a chronic neuropathic pain state on DA receptor pharmacology of the VTA neurones

7.3.5.4 Naloxone effects

Neuronal responsivity to naloxone was determined through analysis of changes in spontaneous firing rate post-injection. In an initial analysis, natural groupings amongst all neurones recorded in SNL animals in terms of mean SFR values at all time points post-naloxone injection were established through Two-step and K-means cluster analysis. An equivalent analysis of naloxone effects was undertaken for all neurones recorded in the naïve state in the previous investigation into carrageenan effects (section 6.4.3.I, also described in 7.3.2.2.), and resulted in the establishment of "high firing" (raw nlx clusters 1n and 1c for naïve and carrageenan-injected states, respectively) and "low firing" neurone clusters (raw nlx clusters 2n and 2c for naïve and carrageenan-injected states, respectively). Mean SFR values at all time points of each SNL cluster were compared with that of the two naïve clusters.

In a subsequent analysis, cluster analysis was re-performed on mean SFR values at all time points when they had been normalized with respect to mean baseline SFR of each neurone. The purpose of this analysis was to remove the confounding influence of variability in mean pre-injection SFR when trying to establish natural groupings within the recorded population according to changes in SFR values upon naloxone injection.

In a third naloxone response analysis neurones were re-grouped manually into naloxone-inhibited and naloxone-excited response-based groups. A neurone was classified as naloxone-responsive if the absolute difference between mean SFR across all time points post-injection and the mean BL SFR was greater than 1.96 x standard deviation of the BL SFR measurements. Excited and inhibited classifications were dependent on whether the change in SFR from the BL to the naloxone conditions involved an increase or a decrease, respectively.

In a fourth naloxone response analysis, the absolute naloxone effect size for populations of neurones recorded in the two different states (naïve and SNL) was calculated for each time point post-injection by first converting differences between 100% (representing mean pre-injection SFR) and the mean normalized SFR value – i.e. the percentage change in SFR from pre-injection - for each neurone at each time point into a positive value, and then calculating the mean for all neurones recorded in the same state.

7.4 Results

7.4.I Baseline firing characteristics of VTA neurones in naïve versus SNL conditions

7.4.1.1 Comparing BL SFR of neurones recorded in naïve and SNL animals

Mean baseline firing rate of neurones recorded in the SNL condition (total N=40; figure 7.3B) were compared with that of all neurones recorded in the naïve condition (total N=222; figure 7.3A). The latter population was made up of all neurones recorded in all experimental protocols allowing for the measurement of mean baseline SFR value in the naïve state. Two natural clusters according to BL SFR were previously established within the population of neurones recorded in the naïve state (section 3.4.2). Cluster analysis was similarly performed on BL SFR values of neurones recorded in the SNL state. Two clusters were established: a low firing group (BL SFR cluster 2snl, mean SFR =1.87±0.26Hz) of 33 neurones, and a high firing group (BL SFR cluster 1snl, mean SFR =9.04±1.17Hz) of 7 neurones.

Mean BL SFR values of the high firing and low firing neurone clusters were compared with mean values of the equivalent naïve-condition clusters (raw nlx cluster 1n, N=29; raw nlx cluster 2n, N=193). Independent-samples *t*-tests revealed that there were no differences were between mean neuronal BL SFR in the naïve and SNL states for either low firing or high firing clusters (mean BL SFR ± SEM, raw nlx cluster 2n [naïve low firing]: 1.99±0.12Hz; raw nlx cluster 2snl [SNL low firing]: 1.87±0.26Hz; raw nlx cluster 1n [naïve high firing]: 8.93±0.41Hz; raw nlx cluster 1snl [SNL high firing]: 9.04±1.17Hz).

The relative proportions of neurones present within these low and high firing clusters with equivalent mean BL SFR values recorded in naïve and SNL state animals were investigated. The high firing to low firing cluster size ratios for the naïve and SNL states were 13.0%:87.0% and 17.5%:82.5%, respectively. This result suggests that a slightly larger proportion of the recorded neurones in the SNL state were high-firing in nature than those recorded in the naïve state.

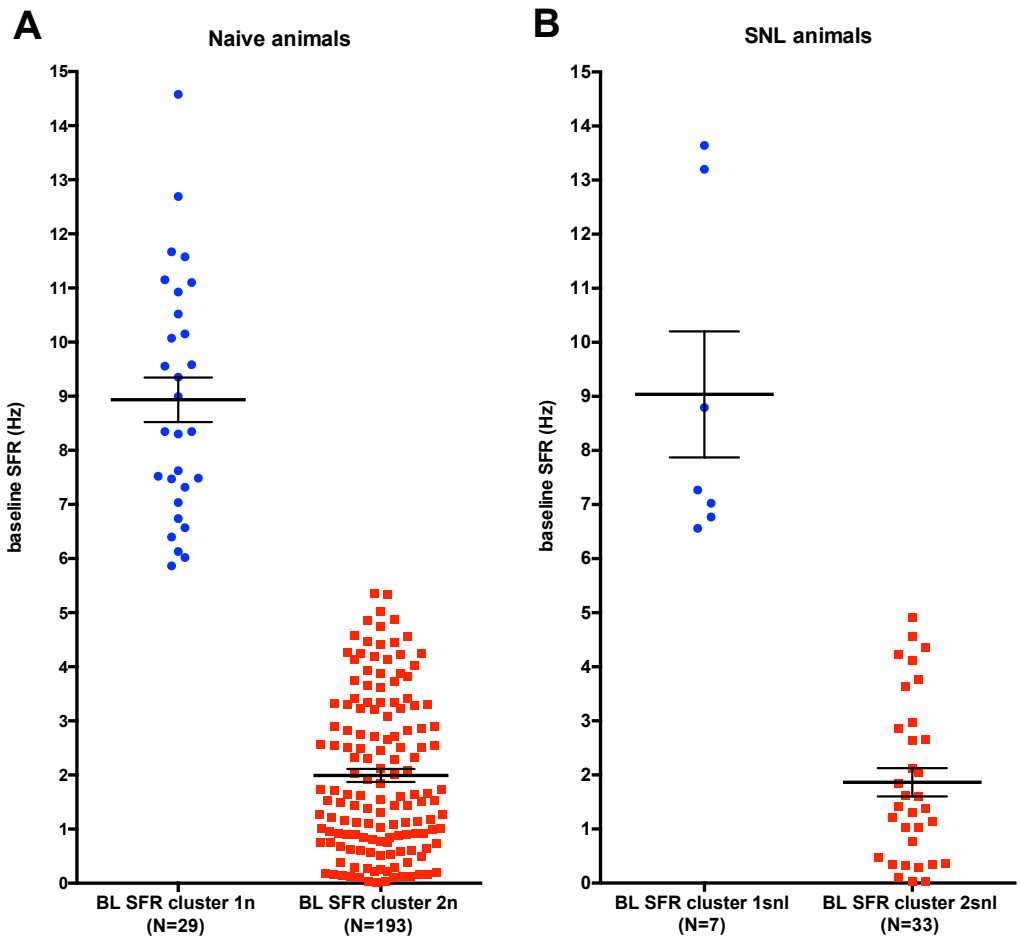

Figure 7.3 Baseline SFR of neurones recorded in animals in naïve and SNL states. A) Data points show mean baseline SFR values (Hz, y-axis) of individual neurones of BL SFR cluster 1n (high firing, N=29, blue data points) and 2n (low firing, N=193, red data points) recorded in the naïve condition. Bars represent mean ± SEM for the two clusters. B) Data points show mean baseline SFR values (Hz, y-axis) of individual neurones of BL SFR cluster 1snl (high firing, N=7, blue data points) and 2snl (low firing, N=33, red data points) recorded in rats in the SNL condition. Bars represent mean ± SEM for the two clusters.

7.4.1.2 Comparing firing pattern of neurones recorded in naïve and SNL animals

The amount of burst firing displayed, measured as the percentage of spikes within a burst (%SIB), by neurones recorded in SNL state animals was compared with that displayed by neurones recorded in naïve state animals. Values of baseline %SIB were obtained for a total of 111 neurones in the naïve state, and 20 neurones in the SNL state. An independent-samples *t*-test revealed that there were no differences between the mean %SIB values of neurones recorded in the naïve and SNL states (figure 7.4; mean %SIB ± SEM, naïve: 39.28±2.56%; SNL: 34.30±5.05%).

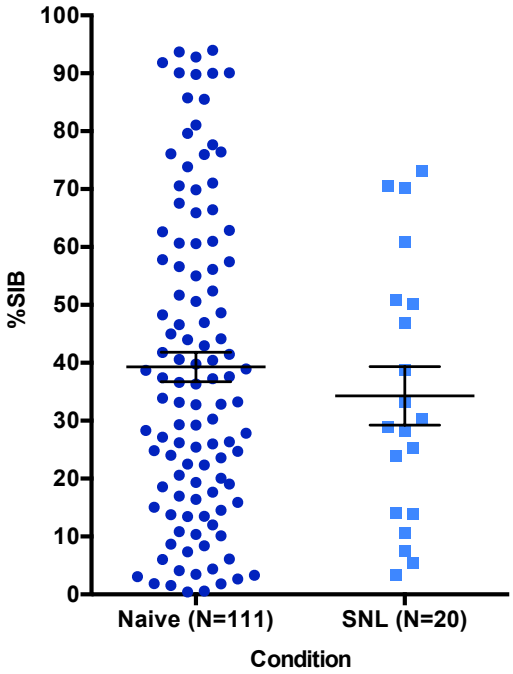

Figure 7.4 Burst firing of neurones recorded in animals in naïve and SNL states. Data points show the percentage of all spikes recorded during the baseline condition that were present within a burst for each individual neurone recorded in naïve (N=111, dark blue circle symbols) and SNL (N=20, light blue square symbols) animals. Bars represent mean ± SEM values for neurones recorded in these two states.

7.4.2 Naloxone effects

7.4.2.I Non-normalized SFR values post-naloxone of neurones recorded in naïve and SNL animals

One neurone was recorded in the naloxone-only SNL experiments was omitted from the analyses on post-naloxone SFR values as SFR dropped to <0.01Hz and never recovered. Two natural clusters according to mean SFR values at all time points pre- and post-naloxone injection were found amongst the remainder of the neurones recorded in SNL animals (N=39); as witnessed in the naïve state (section 6.4.3.1), neurones fell into two clusters: a "high firing" cluster - raw nlx cluster 2snl, and a "low firing" cluster - raw nlx cluster 1snl, in the numbers of 7 and 32 – representing relative proportions of 17.9% to 82.1%, respectively (figure 7.5).

Mean baseline SFR values of the naïve and SNL low firing groups (raw nlx clusters 2n and 2snl, respectively) were very similar (mean ± SEM, raw nlx cluster 2snl: 1.81 ± 0.26Hz, N=32; raw nlx cluster 2n: 1.93 ± 0.37Hz, N=34). The mean BL SFR of the SNL high firing cluster (raw nlx cluster 1snl) was slightly greater than that of the naïve high firing cluster (raw nlx cluster 1n; mean ± SEM, raw nlx cluster 1snl: 7.63 ± 1.09Hz, N=7; raw nlx cluster 1n: 5.61 ± 0.73, N=14); however, this difference was not significant according to the results from an independent-samples *t*-test conducted using mean baseline SFR values of raw nlx cluster 2n and raw nlx cluster 2snl. A slightly lower proportion of the neurones recorded in the SNL condition were classified as high firing as opposed to low firing in comparison to those recorded in the naïve condition: 29.2% of neurones belonged to the high firing cluster in the naïve condition (raw nlx cluster 2n), 17.9% of neurones belonged to the high firing cluster in the SNL condition (raw nlx cluster 2snl).

As previously reported in section 6.4.3.1, the high firing cluster of neurones recorded from animals in the naïve state (raw nlx cluster 2n) showed a significant excitatory response to naloxone at the 30-minute time point. In contrast, results from a non-parametric Friedman test for repeated measures followed by post-hoc Wilcoxon signed-rank pairwise comparisons showed that the high firing neurones recorded in SNL animals (raw nlx cluster 2snl) did not show a significant percentage change in firing rate following naloxone injection.

Both of the low firing neurone clusters recorded in animals in naïve and SNL states showed no change in SFR following naloxone injection (figure 7.5).

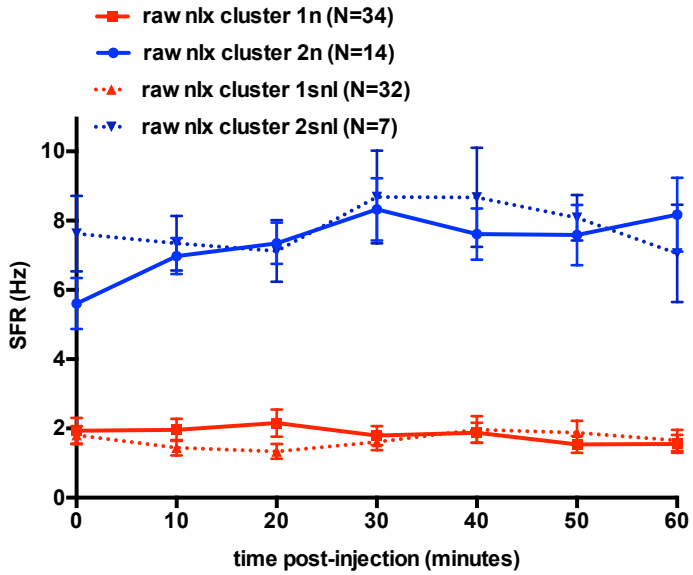

Figure 7.5 Spontaneous firing rate following naloxone injection of neurones recorded from animals in naïve and SNL states. Data points show mean SFR (Hz, y-axis) of neurones clustered according to mean SFR values at all time points post-naloxone injection (minutes, x-axis): naïve - raw nlx cluster 1n (solid red trace, N=34), naïve – raw nlx cluster 2n (solid blue trace, N=14), SNL – raw nlx cluster 1snl (dashed red trace, N=32), SNL – raw nlx cluster 2snl (dashed blue trace, N=7). Bars represent mean ± SEM.

7.4.2.2 Normalized SFR values post-naloxone injection of neurones recorded in naïve and SNL animals

Cluster analysis was re-performed on normalized SFR values (i.e. expressed as a percentage of pre-injection SFR) post-naloxone injection for both naïve and SNL neurone populations. One SNL neurone was removed from the normalized data analysis due to the normalized SFR value being extremely high (>1000%; leaving a remaining 38 neurones in the SNL-state normalized naloxone response analysis). Two natural clusters were established amongst the population of neurones recorded in the SNL condition; one cluster of 30 neurones – norm nlx cluster 1snl - showing an overall inhibitory response (percentage decrease from pre-injection SFR) to naloxone injection that was significant at the 20-minute time point (figure 7.6; mean normalized SFR [percentage of pre-injection SFR]±SEM: 20min= 76.93±7.64%; Friedman test with post-hoc Wilcoxon signed-rank pairwise comparisons, using a Bonferroni-adjusted alpha of 0.008, 20min: Z=-2.724, p=0.006), and another of 8 neurones – norm nlx cluster 2snl - showing a generally excitatory response to naloxone injection that did not represent a significant percentage increase from pre-injection SFR at any time point post-injection (Friedman test with post-hoc Wilcoxon signed-rank pairwise comparisons, using a Bonferroni-adjusted alpha of 0.008).

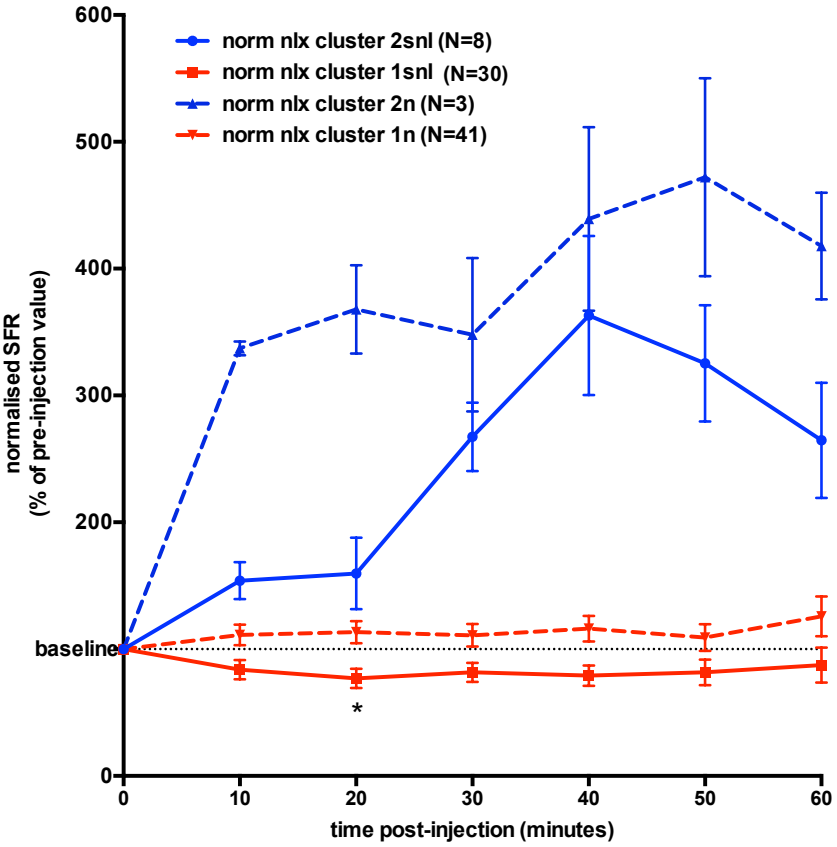

Figure 7.6 Normalized SFR of all recorded neurones following naloxone injection in naïve- and SNL-state animals. Data points show mean normalized SFR values (expressed as a percentage of mean pre-naloxone injection SFR) of neurones falling into either norm nlx cluster 1snl (solid red trace, N=30), norm nlx cluster 2snl (solid blue trace, N=8), norm nlx cluster 1n (dashed red trace, N=41), or norm nlx cluster 2n (dashed blue trace, N=3) at all time points post-injection. Data points and bars represent mean ± SEM. The dashed horizontal line at y=100% represents mean pre-injection SFR. Friedman tests followed by post-hoc Wilcoxon signed-rank pairwise comparisons using a Bonferroni-corrected alpha of 0.008 to account for multiple comparisons were performed to test for significant percentage changes from mean pre-naloxone injection SFR, * $p<0.008$.

7.4.2.3 Comparisons between manually-sorted naloxone response-based neurone groups recorded in naïve and SNL animals

In order to compare the effects of naloxone on VTA neurones in the naïve and SNL conditions, it was considered necessary to manually sort neurones into "naloxone-inhibited" and "naloxone-excited" neurone groups (described in section 7.3.5.4.). Performing this comparison using cluster analysis-sorted neurone groups is not appropriate, as there is a high chance that the neurones residing within the separate clusters are not functionally equivalent across conditions. A change in a neurone's naloxone response magnitude is much more likely than a change in the direction of its response (inhibited to excited, or vice versa), and therefore comparisons of neurones with the same manually-attributed response classification is less likely to involve invalid comparisons.

Neurones were considered to be naloxone-responsive if the difference between mean baseline SFR and mean post-injection SFR (i.e. mean of mean SFR values at all time points post-injection) was greater than 1.96 x standard deviation of the baseline SFR. The "inhibited" and "excited" classification depended on the direction of the change in SFR upon naloxone injection. Numbers of each neurone type found in the naïve and SNL states, as well as the proportion of the total recorded population they represent, are found in table 7.1.

State	Naloxone-excited	Naloxone-unresponsive	Naloxone-inhibited
Naïve (total = 48)	30 (62.5%)	4 (8.3%)	14 (29.2%)
SNL (total = 39)	16 (41.0%)	6 (15.3%)	17 (43.5%)

Table 7.1 Numbers of neurones excited and inhibited by, and unresponsive to, naloxone injection found in naïve and SNL state experiments. Table shows both the actual number of neurones recorded in animals in naïve and SNL states falling into each naloxone response-based category, as well as the proportion of the whole recorded population that number represented (%, in parentheses). Classifications of a naloxone-inhibited, -excited or lack of response were made my comparing the difference between the mean pre-injection SFR (Hz) and mean post-injection SFR (Hz, mean of values at all time points) values with the value of 1.96 times the standard deviation from the mean in the pre-injection condition.

The normalized post-injection SFR values of the naloxone-excited and naloxone-inhibited groups of the SNL and naïve neurone populations were compared (figure 7.7). No differences between the normalized SFR values of neurones recorded in the SNL and naïve conditions were found for either the NI and NE neurone groups. For both

conditions and for both response types, changes in SFR appeared to be immediate (effects seen at 10 min time point), and sustained (effects continued to be seen up to 60 min time point).

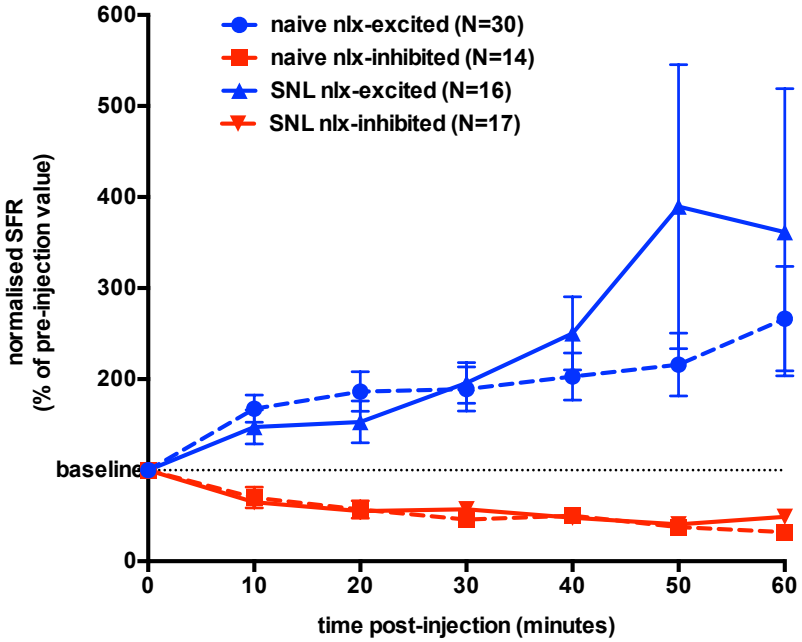

Figure 7.7 Normalized SFR following naloxone injection of manually-established naloxone response-based neurone groups recorded in naïve and SNL states. Data points show mean normalized SFR (y-axis, expressed as a percentage of mean pre-injection SFR) of neurones of the manually classified as naloxone-excited (blue traces; SNL N=16, naïve N=30) and naloxone-inhibited (red traces; SNL N=17, naïve N=14) from both naïve-state (dashed traces) and SNL-state (solid traces) recorded populations at all time points post-injection (minutes, x-axis). Data points and bars represent mean ± SEM. The horizontal dashed line at y=100% represents mean pre-injection SFR.

7.4.2.4 Comparisons between absolute naloxone response of neurones recorded in naïve and SNL animals

General effects of naloxone on the SFR of VTA neurones in the naïve versus SNL conditions were compared by establishing the difference between population mean normalized SFR values at all time points post-injection; in other words, is the neuronal population response in the SNL state greater than, less than, or no different to that seen in neurones recorded in the naïve state? Due to the presence of both naloxone-inhibited and naloxone-excited neurones amongst the population recorded in the SNL and naïve states, it was considered necessary to compare the mean absolute naloxone effect size of the SNL and naïve neurone populations, rather than simply the mean normalized SFR. In this way, the efficacy of naloxone in the two preparations can be compared without inhibitory

and excitatory responses acting to cancel each other out. The absolute naloxone effect size for populations of neurones recorded in the two different states was calculated for each time point post-injection by first converting differences between 100% (representing mean pre-injection SFR) and the mean normalized SFR value – i.e. the percentage change in SFR from pre-injection - for each neurone at each time point into a positive value, and then calculating the mean for all neurones recorded in the same state (i.e. either SNL or naïve; section 7.3.5.4; figure 7.8).

When comparing the absolute normalized naloxone effect size of the SNL (analysis based on 38 neurones) and naïve-state (analysis based on 44 neurones) neurone populations, it was found that there were no significant differences between the populations at all time points post-injection (One-way ANOVA; figure 7.8). For both naïve and SNL recorded neurone populations, mean % change in SFR from baseline increased across the 60-minute recording period, with values rising from 59.07±9.29% and 39.53±4.92% at 10 minutes post-injection to 125.80±35.81% and 82.97±12.86% at 60 minutes post-injection in the naïve and SNL conditions, respectively.

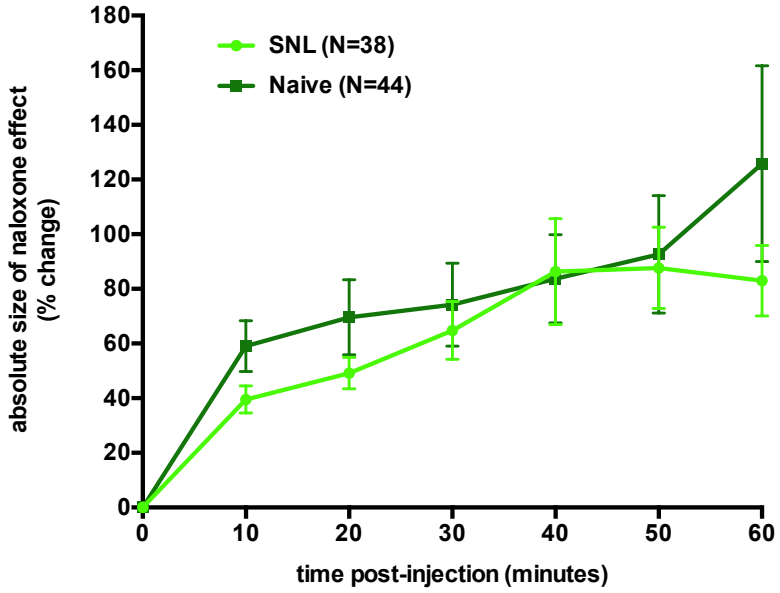

Figure 7.8 Absolute naloxone effect size for neurones recorded in animals in naïve and SNL states. Data points show the mean absolute (i.e. expressed as a positive value) percentage change in SFR of neurones (y-axis, %) recorded in animals in naïve (dark green trace, N=44) and SNL-induced neuropathic pain states (light green trace, N=38) at all time points post-naloxone injection (x-axis, minutes).

7.4.3 Analysis on L-DOPA response-sorted neurone groups

7.4.3.1 L-DOPA responsivity of neurones recorded in naïve versus SNL animals

In order to establish L-DOPA-response-based groupings, SFR values at all time points post-injection were normalized relative to mean pre-injection values for each neurone. Two neurones were omitted from further analysis due to normalized SFR values being anomalous at certain time points (>1000%), leaving a remaining 18 neurones for cluster analysis. Cluster analysis on these values revealed two natural clusters based on percentage change in SFR in response to a 20mgkg^{-1} systemic dose of L-DOPA; norm L-DOPA cluster 1snl consisted of 16 neurones and appeared to show a mean inhibitory response to L-DOPA injection, while norm L-DOPA cluster 2snl consisted of 2 neurones and appeared to show a mean excitatory response (figure 7.9). Friedman tests for non-parametric repeated measures followed by post-hoc Wilcoxon signed-rank pairwise comparisons revealed that norm L-DOPA cluster 1snl showed a significant percentage decrease in SFR from mean pre-injection values at time points of 20 and 40 minutes post-L-DOPA injection when using a Bonferroni-adjusted alpha of 0.0125 (20min: Z=-2.896, p=0.004; 40min: Z=-2.947, p=0.003). The seemingly excitatory response of norm L-DOPA cluster 2snl, however, was not shown to represent a significant change from pre-injection baseline – unexpected in light of the very low numbers in this cluster (N=2).

There were no differences between mean normalized SFR values of the SNL state norm L-DOPA cluster 1snl and that seen for the L-DOPA inhibited cluster of neurones recorded in the previous naïve-state investigations (norm L-DOPA cluster 1p – for 'previous') at all time points post-injection (One-way ANOVA, figure 7.9). Similarly, there were no significant differences found between the mean normalized SFR values of the seemingly-excited clusters of neurones recorded in SNL and naïve states (norm L-DOPA clusters 2snl and 2p, respectively; One-way ANOVA, figure 7.9).

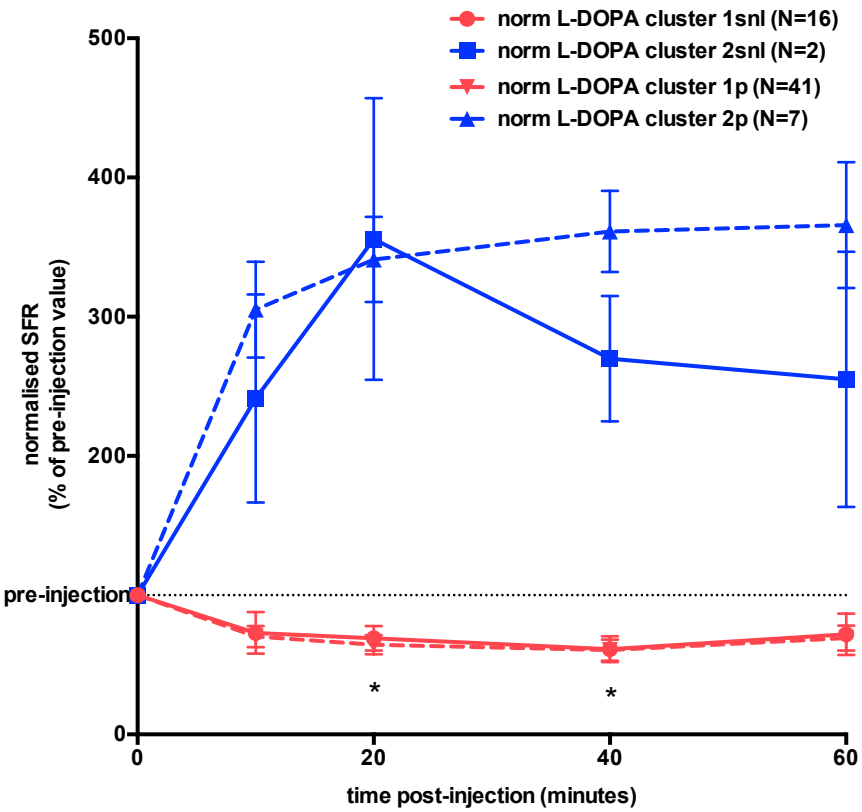

Figure 7.9 Comparison of mean L-DOPA response of neurones recorded in SNL-state animals versus those recorded in the previous L-DOPA experiments conducted in naïve-state animals. Normalized SFR (y-axis; expressed as a percentage of mean pre-injection SFR) of norm L-DOPA cluster 1snl (SNL state experiments, solid red trace, N=16), norm L-DOPA cluster 2snl (SNL state experiments, solid blue trace, N=2), norm L-DOPA cluster 1p (previous naïve state experiments, dashed red trace, N=41) and norm L-DOPA cluster 2p (previous naïve state experiments, dashed blue trace, N=7) are shown separately for all time points up to one hour post 20mgkg^{-1} L-DOPA injection (x-axis; minutes). Data points represent mean ± SEM. The dashed horizontal line at y=100% represents mean pre-L-DOPA injection SFR. Friedman tests with post-hoc Wilcoxon signed-rank pairwise comparisons were used to test significance of percentage changes in SFR from pre- to post-injection time points of the SNL state clusters using a Bonferroni-corrected alpha of 0.0125, * P<0.0125.

7.4.3.2 Baseline spontaneous firing rate of L-DOPA response-based neurone clusters recorded in naïve versus SNL states

The baseline (i.e. pre-injection) spontaneous firing rate of neurones in the normalised L-DOPA response-based clusters established from previous naïve-state (norm L-DOPA cluster 1n and 2n) and current SNL-state (norm L-DOPA cluster 1snl and 2snl) recorded populations were compared. Independent-samples *t*-tests revealed no significant differences between mean BL SFR values of neurones recorded in naïve and SNL states when neurones were split according to the direction of the L-DOPA response for the cluster, whether it be a general excitatory or inhibitory mean change in SFR (figure 7.10; mean BL SFR ±SEM: naïve 'inhibitory', norm L-DOPA cluster 1n = 4.12±0.68Hz, N=41; naïve 'excitatory', norm L-DOPA cluster 2n = 2.64±0.93Hz, N=7; SNL 'inhibitory', norm L-DOPA cluster 1snl = 4.04±1.07Hz, N=16; SNL 'excitatory', norm L-DOPA cluster 2snl = 0.36±0.01Hz, N=2). There were also no differences found between the mean BL SFR values of 'excited' and 'inhibited' neurones recorded in SNL animals - norm L-DOPA clusters 1snl and 2snl, respectively - which was not unexpected in light of low number of neurones in the norm L-DOPA cluster 2snl (N=2).

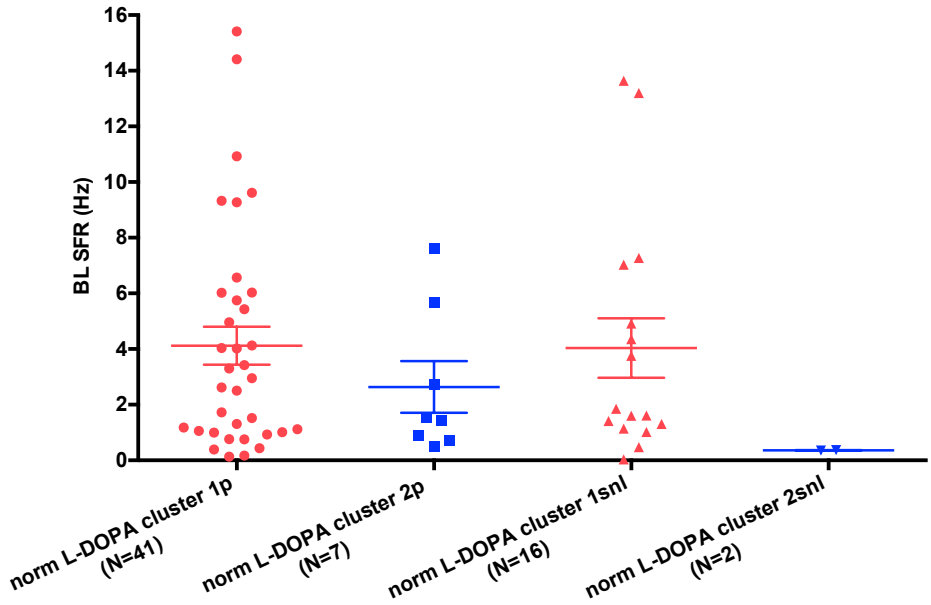

Figure 7.10 Mean baseline spontaneous firing rate of L-DOPA response-based clusters recorded in naïve- and SNL-state animals. Graph shows the mean spontaneous firing rate (Hz, y-axis) recorded in the baseline (pre-injection) condition of all neurones belonging to naïve-state norm L-DOPA cluster 1p (red circular data points and bars, N=41) and norm L-DOPA cluster 2p (blue square data points and bars, N=7) neurone clusters and SNL-state norm L-DOPA cluster 1snl (red triangular data points and bars, N=16) and norm L-DOPA cluster 2snl (blue triangular data points and bars, N=2) neurone clusters. Bars represent mean ± SEM.

7.4.3.3 Naloxone response of LDI and LDE neurone clusters recorded in naïve versus SNL states

In order to establish the existence of neurone population-specific alterations in naloxone responsivity upon the induction of neuropathic pain, the normalized SFR values at all time points post-naloxone injection were compared for L-DOPA response-based clusters of neurones recorded in the naïve and SNL states (figure 7.11).

The 'excited' neurone clusters – norm L-DOPA clusters 2p and 2snl

Neurone clusters showing a seemingly-excitatory response to L-DOPA injection (albeit insignificant) established in recorded populations from both animals in naïve (norm L-DOPA cluster 2p, N=6) and in SNL states (norm L-DOPA cluster 2snl, N=2) showed no significant response to naloxone in terms of changes in SFR values from mean pre-naloxone injection SFR (Friedman test for non-parametric repeated measures followed by post-hoc Wilcoxon signed-rank pairwise comparisons, using a Bonferroni-adjusted alpha value of 0.008; figure 7.11A). Further, there were no significant differences between normalized SFR values of norm L-DOPA cluster 2p and 2snl at all time points post-naloxone injection (One-way ANOVA with post-hoc Bonferroni tests).

The 'inhibited' neurone clusters – norm L-DOPA clusters 1p and 1snl

It was found that seemingly-inhibited neurone clusters established in recorded populations from both animals in naïve (norm L-DOPA cluster 1p, N=11) and in SNL states (norm L-DOPA cluster 1snl, N=16) showed no response to naloxone in terms of changes in SFR values from mean pre-naloxone injection SFR (Friedman test for non-parametric repeated measures followed by post-hoc Wilcoxon signed-rank pairwise comparisons, using a Bonferroni-adjusted alpha value of 0.008; figure 7.11B). Further, there were no significant differences between normalized SFR values of norm L-DOPA clusters 1p and 1snl at all time points post-naloxone injection (One-way ANOVA with post-hoc Bonferroni tests).

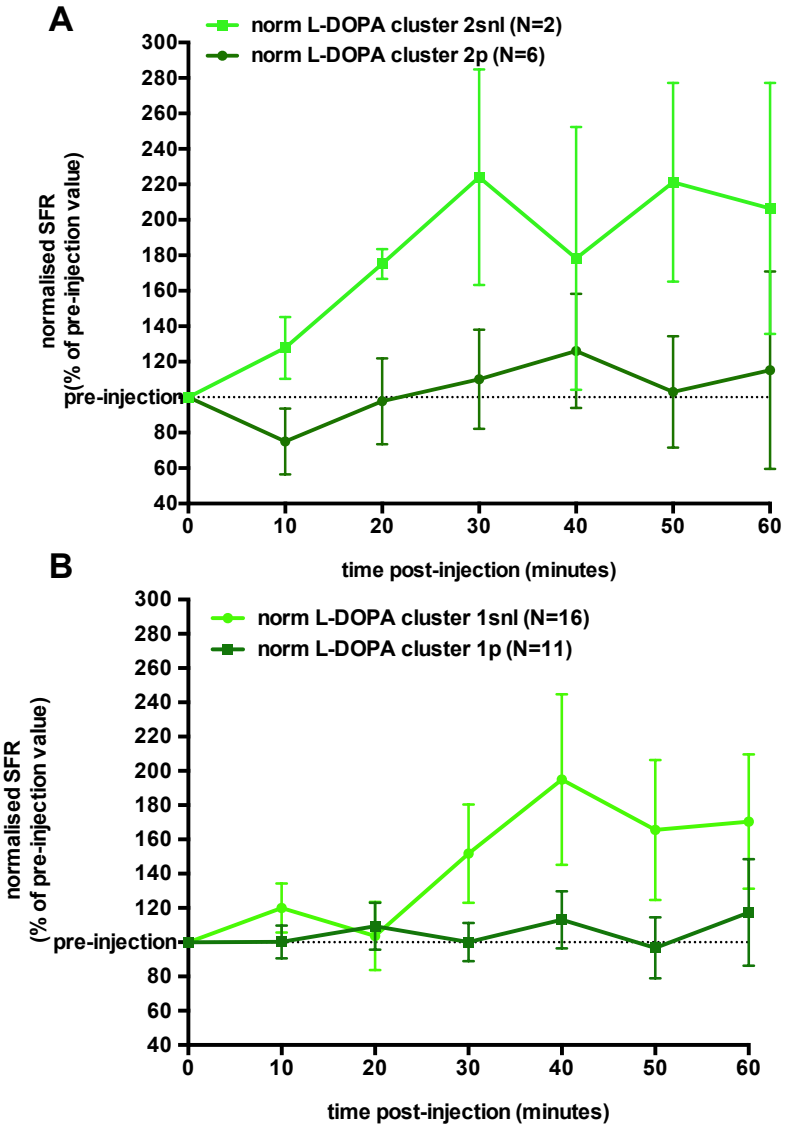

Figure 7.11 Mean normalized SFR following naloxone injection of L-DOPA response-based clusters of neurones recorded in SNL and naïve-state animals. Graph shows data points and bars representing the mean normalized SFR ± SEM (y-axis; expressed as a percentage of mean pre-naloxone injection SFR) of each of the four neurone groups characterised by L-DOPA response cluster membership and pain state at all time points post-naloxone injection (x-axis; minutes). The dashed horizontal line at y=100% represents mean pre-naloxone injection SFR. A) Shows seemingly L-DOPA-excited clusters of neurones recorded in naïve (norm L-DOPA cluster 2p; dark green trace, N=6) and SNL (norm L-DOPA cluster 2snl; light green trace, N=2) state animals. B) Shows seemingly L-DOPA-inhibited clusters of neurones recorded in naïve (norm L-DOPA cluster 1p; dark green trace, N=11) and SNL (norm L-DOPA cluster 1snl; light green trace, N=16) state animals.

7.5 Discussion

The purpose of this investigation was to establish the effects of a spinal nerve ligation-induced neuropathic pain state on the VTA neurone population. Previous findings have hinted at an involvement of these neurones; chronic pain in the form of fibromyalgia is associated with altered dopaminergic function (Loggia et al., 2014), and morphine-induced DA release in the NAcc is reduced in neuropathic pain-state rats due to the uncoupling of μ-opioid receptors on VTA DA neurones from downstream signalling pathways (Ozaki et al., 2002; 2003).

7.5.I Impact of the SNL neuropathic pain state on baseline firing characteristics of VTA neurones

The population of neurones recorded in the SNL animals could be divided into two natural BL SFR-based clusters of high (BL SFR cluster 1snl) and low firing (BL SFR cluster 2snl) neurones, as witnessed in the naïve population (BL SFR clusters 1n and 2n; see section 3.4.2). The mean BL SFR of these two neurone clusters recorded in SNL and naïve states were found to be equivalent. A slightly higher proportion of neurones recorded in the SNL state were high firing in nature than that found within the naïve state population. It is possible that a subset of VTA neurones tend to show an increase in spontaneous activity upon the induction of a neuropathic pain state, resulting in the slight shift in balance of low firing and high firing neurones witnessed here. However, it is very likely that the small changes in relative proportions in the SFR-based clusters seen between naïve and SNL states simply reflect differences in the sampling of VTA neurones in the two independent sets of experiments. The similarity of the high firing and low firing cluster mean values in naïve and SNL states supports a difference in sampling rather than an increase in neuronal firing rates as an explanation for proportion differences by suggesting that the high firing and low firing populations in the two states are equivalent. There was also no difference found between the level of burst firing (measured at the percentage of spikes present within a burst) of neurones recorded in SNL and naïve states.

This discussion highlights a fundamental limitation of the neuropathic pain model; we cannot monitor the activity of any one neurone over the two-week period as this pain state develops as we can with the carrageenan-induced tonic pain model. We can, however, increase our confidence in the assumption of equivalence of recorded subgroups by assessing the alignment of a characteristic of interest – in this case, spontaneous firing rate.

Hence, the results of the current investigations suggest that tonic functional alterations of VTA neurones that lead to changes in activity and therefore DA release at projection targets are not taking place upon the induction of this particular neuropathic pain state. This in-turn suggests that ongoing alterations in the pain processing system inherent to the chronic neuropathic pain state are likely caused by factors independent of spontaneous VTA neurone activity. A study conducted in 2015 by Sagheddu and colleagues similarly investigated the effects of neuropathic pain induction on the spontaneous firing characteristics of VTA DA neurones *in vivo*. Extracellular recordings of histologically confirmed DA neurones revealed that there were no differences between the SFR values of neurones recorded in sham-operated and spinal nerve injured (SNI) rats (Sagheddu et al., 2015), in agreement with the current results. However, Sagheddu and colleagues did shown an enhanced level of burst firing in the SNI versus sham control DA neurone populations – an effect not seen here. Potential reasons for this discrepancy could include differences in sampling; Sagheddu and colleagues pre-selected neurones according to putative DA neurone criteria, notably a firing rate of <10Hz and an action potential duration of 2.5 ms as measured from start to end, whereas no such pre-selection took place in the current experiments.

Chronic neuropathic pain is characterized in part by hyperalgesia, or the perception of a given noxious stimulus as more painful than usual, as well as allodynia, or the eliciting of pain by normally innocuous stimuli (Ozaki et al., 2003). Neither of these phenomena relate to the ongoing perception of pain, as is the case with tonic inflammation, but instead consist of an abnormal response to a given stimulus. In this vain, it is possible that changes involving the VTA neurones do occur – not in terms of their spontaneous, tonic firing properties, but in terms of their phasic responses to environmental perturbations. Unfortunately, phasic activity could not be investigated in the current experiments due to the methodology seemingly resulting in a lack of sensitivity to these VTA neurone responses, as discovered and discussed in section 3.5.5 and 4.5.3.3.

7.5.2 Impact of the SNL neuropathic pain state on opioidergic control of VTA neurone activity

Previous investigations into VTA DA neurone functioning in neuropathic pain highlighted a change in the opioid sensitivity of the DA system (Ozaki et al., 2002, 2003). In light of these findings, it is expected that the influence of tonic endogenous opioid control is also altered in this pain state. A change in this form of tonic modulatory control, discussed in-depth in section 1.11.3, could feasibly result in alterations in nociceptive sensitivity

associated with hyperalgesia and allodynia phenomena. Consequently, the magnitude and nature of any endogenous opioid action on VTA neurones was investigated in the current study by unmasking the ongoing impact on firing rate with the injection of the opioid receptor antagonist, naloxone.

7.5.2.1 Cluster analysis using non-normalized SFR values of all neurones recorded in naïve and SNL states

As found in neurones recorded in the naïve state, neurones recorded from animals having undergone SNL surgery were found to fall into two natural populations when clustered according to their mean SFR values at all time points both before and after injection of naloxone. Both "high firing" (raw nlx cluster 2snl) and "low firing" (raw nlx cluster 1snl) neurone clusters – so-called to reflect the separation in mean pre-injection SFR of the two clusters - displayed no mean changes in SFR across the post-injection time points, in contrast to the significant excitatory response at 30 minutes of the naïve high firing neurone cluster, raw nlx cluster 2n. This result could reflect a general lack of naloxone responsivity amongst all recorded neurones in the SNL state, or, alternatively, could be due to the existence of a mix of naloxone-excited and inhibited neurones in one or both of the two neurone clusters (i.e. both high firing and low firing).

7.5.2.2 Cluster analysis using normalized SFR values of all neurones recorded in naïve and SNL states

In order to further investigate naloxone responsivity, analysis was subsequently performed on normalized mean SFR values, i.e. by transforming all post-naloxone injection mean SFR values into a percentage of the pre-naloxone injection SFR for each neurone. Cluster analysis was performed on the normalized SFR values of the whole recorded population at all time points post-naloxone injection to establish the existence of any naloxone response-based clustering within the VTA neurones.

It was found that neurones fell into two distinct clusters: one appearing to show a mean percentage increase – albeit insignificant - in SFR following naloxone injection (norm nlx cluster 2snl, see figure 7.6), and the other showing a mean inhibitory response that was significant at 20 minutes post-injection (norm nlx cluster 1snl). A natural clustering of neurones showing a mean inhibition in response to naloxone administration was not found amongst the population recorded from naïve animals (section 6.4.4.2). There are two possible explanations for the finding of differing response-based clusters within neurone populations recorded in the two states: either the

induction of an SNL state results in a general diminishing of inhibitory responses to naloxone, or the inhibited responses remained of a similar magnitude but tended to be clustered together with weakly-excited responses of the naïve data set due to there being differences in the pattern of spread of responses (e.g. more separation amongst the magnitude of excitatory responses), causing the naïve state norm nlx cluster 1n to contain more of a mix of responses to naloxone, and therefore possess a generally "unresponsive" group mean identity.

7.5.2.3 Manually sorting neurones into naloxone response-based groups

As these two explanations have significantly different functional implications in terms of the changes associated with SNL surgery, it was considered necessary to manually assess the naloxone responsivity of VTA neurones recorded in the naïve versus SNL conditions. Hence, all neurones recorded were manually classified according to whether or not the change in SFR upon naloxone injection was greater than 1.96 x standard deviation of BL SFR (responsive or unresponsive), as well as the direction of this change in SFR (excited or inhibited). By doing this, we increase the chances that we are comparing "like with like" when looking at the naloxone response-based groups in the two states; a change in the direction of the response to naloxone is much less probable than either a change in the distribution of neurone sampling or in the magnitude of responses (both of which could influence the natural clustering according to naloxone response within the population), meaning that it is reasonable to assume that manually-sorted naloxone-inhibited or –excited neurones found in the SNL state are likely to represent an equivalent functional group to those found in the naïve state.

Naloxone-inhibited –excited and –unresponsive neurones were found in both SNL- and naïve-state recorded populations. When the size and profile of naloxone response in the two states were compared, no differences were found in either the naloxone-inhibited or -excited neurone groups. These results imply that there are no changes in either tonic excitatory or tonic inhibitory endogenous opioidergic influence on VTA neurone activity associated with the induction of the neuropathic pain state. This finding is unexpected in light of the previous discovery of reduced MOR sensitivity within the VTA by Ozaki and colleagues (2002), which would predict that some of the recorded neurones would be less affected by naloxone injection in the SNL versus naïve state.

A possible explanation for the discrepancy in the current and previous findings surrounding opioid influence in naïve versus neuropathic pain states lies in experimental differences with respect to type of pharmacological investigation. Ozaki and colleagues adopted an agonist-based strategy by systemically injecting the MOR agonist,

morphine. A reduction in the efficacy of morphine could be caused by either receptor desensitisation (or reduced receptor density), or increased levels of endogenous opioid agonist release, thereby increasing competition for the receptor binding sites. Conversely, efficacy of an antagonist will be increased by increased levels of endogenous opioids, as there would likely be a greater ongoing agonist effect to block. It is possible that the endogenous opioid release is increased in the neuropathic pain state to the extent that it counteracts the μ-opioid receptor desensitisation discovered by Ozaki and colleagues – in other words, that a balancing out of changes in opioid control occurs, resulting in no net change in naloxone effect (as witnessed in the current results). In support, there is evidence suggesting that endogenous μ-opioid release is increased in mesolimbic regions (amongst others) in the face of persistent pain (Zubieta et al., 2001), and that the increased levels of agonist binding that would result act to increase levels of G-protein coupled receptor kinase 2 – suggested to be responsible for the receptor desensitisation discovered by Ozaki and colleagues (Ozaki et al., 2002, 2003).

Based on the known heterogeneity of opioid responsivity within dopaminergic and GABAergic neurochemical populations in the VTA, it is impossible to confidently assume neurone identity according to naloxone response. It is possible, however, to speculate on neurone composition of the naloxone-inhibited, -excited and –unresponsive groups by taking into account the literature on opioid responsivity of confirmed DA and GABA neurones, reported proportions of these neurones within the VTA, and relative proportions of each response type. In the current investigation, relative proportions of naloxone-excited, naloxone-unresponsive, and naloxone-inhibited neurones found in the naïve state were 62.5%, 8.3% and 29.2%, respectively. Findings of some earlier studies pointed towards a simple theory of opioidergic control within the VTA, with direct inhibitory effects on GABAergic interneurones leading to an indirect disinhibition (i.e. excitation) of VTA DA neurones – the so-called two-neurone model (Johnson and North, 1992; Gysling and Wang, 1983; Matthews and German, 1984). Studies have since found evidence to show there is a significantly greater level of complexity when it comes to opioid action in the VTA, including findings of direct inhibition of a population of DA neurones, as well as a subset of GABAergic neurones lacking opioid sensitivity altogether (Gysling and Wang, 1983; Matthews and German, 1984; Cameron et al., 1997; Ford et al., 2006; Margolis et al., 2003; Margolis et al., 2012); nevertheless, the two-neurone model of opioid action remains an established mechanism with the VTA for at least a subset of the neurone population. Consequently, it is considered reasonable to assume that at least a proportion of the naloxone-inhibited neurones are GABAergic, and, similarly, that a proportion of the naloxone-excited neurones are dopaminergic. In support, the VTA neurone population is thought to consist of ~70% DA neurones and ~30%

GABA neurones (Ford et al., 1995; Kalivas, 1993; Nair-Roberts et al., 2008b; Yamaguchi et al., 2007b) – closely resembling the naloxone response-based group proportions observed here.

7.5.3 SNL-induced changes in characteristics of L-DOPA response-based neurone groups

7.5.3.1 L-DOPA response

In a subset of the experiments, L-DOPA was administered to allow comparisons of the SNL-induced changes in the different response-based groups. As previously discussed in section 4.5.1, the identity of L-DOPA-inhibited neurones was hypothesised to be predominantly dopaminergic, while that of seemingly L-DOPA-excited neurones was thought to be most likely largely GABAergic, with perhaps some degree of cross-over of these identities between the two groups. In order to establish whether the induction of neuropathic pain had an influence on either the L-DOPA responsivity of VTA neurones or the characteristics of the L-DOPA response-based neurone groups, cluster analysis was performed using the normalized post-L-DOPA SFR values (i.e. expressed as a percentage change from pre-injection SFR). After sorting all recorded neurones according to L-DOPA response in this way, comparisons of firing rate and naloxone responsivity were made between any established L-DOPA response-based clusters and between response clusters found in naïve and SNL states. As found for the naïve state neurone population, neurones recorded in the SNL condition fell into two L-DOPA response-based clusters: one showing a generally inhibitory response to injection (norm L-DOPA cluster 1snl), and another showing a generally excitatory response to injection (norm L-DOPA cluster 2snl). Analyses performed on norm L-DOPA cluster 1snl showed that the percentage change in SFR from baseline values represented a significant inhibitory response at both 20 and 40 minutes post injection. In contrast, the seemingly-excitatory response shown by SNL-state norm L-DOPA cluster 2snl was not found to represent a significant group change in SFR from baseline. This was not unexpected given the very low numbers of neurones in this cluster (N=2), suggesting that further experiments may have revealed a significant effect of L-DOPA on this neurone group.

7.5.3.2 Baseline spontaneous firing rate of L-DOPA response-based neurone clusters in naïve versus SNL states

There were no significant differences found between the mean baseline (i.e. pre-injection) spontaneous firing rate values of the two neurone clusters established from neurones recorded in SNL state animals. Further, there were

no differences in mean BL SFR values between the two seemingly-inhibited neurone clusters recorded in naïve and SNL conditions (norm L-DOPA cluster 1p and 1snl, respectively). This result suggests that a subgroup of VTA neurones likely containing a proportion of DA neurones shows no alteration in spontaneous firing rate upon the induction of neuropathic pain. However, this conclusion relies on the assumption that the two neurone clusters appearing to display a similar 'type' of response to L-DOPA on average contain neurones from the same functional subpopulation, which cannot be confirmed when the experiments are performed in separate animals.

The very low numbers of neurones in the SNL-state norm L-DOPA cluster 2snl (N=2) mean that analyses involving this group lack sufficient power to draw any conclusions with confidence. As mentioned previously, it is possible that further experiments may have revealed some interesting results.

7.5.3.3 Naloxone responsivity of L-DOPA response-based neurone clusters in naïve versus SNL states

No significant difference in response to systemic naloxone injection was found between similar response type naïve-state and SNL-state L-DOPA response clusters (i.e. norm L-DOPA cluster 1p vs. cluster 1snl; norm L-DOPA cluster 2p vs. cluster 2snl). Mean percentage post-naloxone change in SFR from pre-injection values of the L-DOPA-inhibited neurones recorded in SNL (norm L-DOPA cluster 1snl) and naïve state (norm L-DOPA cluster 1p) animals were statistically indistinguishable, with both groups showing no significant response across the 60 minutes post-injection. Similarly, there were no significant differences between percentage change from pre-injection SFR of the naïve-state and SNL-state seemingly-excited (albeit insignificantly) clusters at any time point post-naloxone injection, despite mean values of the norm L-DOPA clusters 2p and 2snl appearing to differ across all time points. Further, neither of the SNL-state seemingly-excited clusters showed a significant response to naloxone injection at any time point. These results suggest that subpopulations of VTA neurones as defined by responsivity to L-DOPA injection show no differences in responsivity to naloxone when recorded in naïve versus neuropathic pain states. In turn, this implies that tonic opioidergic control of these neurones does not differ between the pain states. However, the low number of neurones in the norm L-DOPA cluster 2snl means that we cannot confidently extrapolate these findings to the rest of this particular functional VTA neurone population.

All four groups possessed a large degree of variability in normalized SFR at a given time point. This result, together with the findings of a lack of group mean naloxone responsivity in the face of clear inhibitory and excitatory responsivity of the manually-sorted groups, suggests that both L-DOPA response-based neurone

clusters recorded from naïve-state and SNL-state animals contain both naloxone-inhibited and –excited neurones (although perhaps less likely for norm L-DOPA cluster 2snl given N=2).

Hence, results found here reveal that the general lack of difference in naloxone responsivity between naïve-state and neuropathic pain-state recorded populations also applied when the populations were subdivided into L-DOPA response-based functional groups. Further, L-DOPA response-based sub-groups showed no association with naloxone response-based sub-groups, suggesting perhaps that DA and GABA neurochemical populations display varied responsivity to endogenous opioids – a finding not unexpected in light of the literature. However, this suggestion relies on the assumption of L-DOPA response-based groups being relatively neurochemically homogeneous which has not been confirmed in the current investigations.

7.5.4 Control experiments

When conducting any experimental investigation, it is important to also conduct control experiments accounting for as many variables with the potential to influence results as possible, allowing one to to single out the effects of the manipulation/variable of interest alone. For experiments involving SNL surgery, sham surgery involving a procedure identical to that conducted during SNL surgery, with the crucial difference of the spinal nerves not being ligated, represents the most appropriate control. Consequently, the animal experiences all of the resulting effects of surgery – the tissue damage, stress and anaesthesia included – without a neuropathic state being initiated. Comparing neuronal responses of SNL animals with those of sham control animals allows one to single out the effects of the neuropathic state alone. However, the current investigation did not involve the conduction of sham surgery control experiments.

The decision to not conduct sham controls was the outcome of careful consideration of several factors. First and foremost, no significant differences were found between the activity of neurones recorded in the naïve versus SNL-induced neuropathic state, meaning that there was no SNL effect to be validated. In other words, there was no effect that needed to be examined further in terms of origin – surgical/other versus nerve injury-induced. Conducting further animal experiments involving sham controls would have simply served to add animal numbers to the already extensive investigation. Secondly, the spinal nerve ligation surgery is a very well-validated model of neuropathic pain, both within and outside of this lab, in terms of evidence suggesting that the behavioural and neuronal effects witnessed following this manipulation result from neuropathic rather than general tissue damage

mechanisms. For example, a previous study conducted by Patel and colleagues (2014) involving identical surgical methodology have reported that, by 14 days post-SNL surgery, there are no differences between naïve and sham control animals in terms of pain-related behaviour (behavioural hypersensitivity). These results were considered by the authors to be sufficient in validating conclusions drawn from subsequent comparisons between naïve and SNL experiments alone (as opposed to sham versus SNL), such as is done here. Finally, this is not the first investigation to find a lack of effect of neuropathic pain on the activity of VTA DA neurones; as discussed in section 7.5.I, Sagheddu and colleagues showed that DA neurones recorded from spinal nerve injured rats showed statistically-indistinguishable spontaneous firing rates from that of neurones recorded from sham-operated rats (Sagheddu et al., 2015). These results increase confidence in the conclusions of a lack of effect of the neuropathic state on firing rates of VTA DA neurones.

7.5.5 Conclusion

The current investigation aimed to establish the effects of an SNL-induced neuropathic pain state on VTA neurone activity and endogenous opioid influence. A general lack of effect was found in terms of observed changes in baseline spontaneous firing rate, firing pattern and the magnitude of inhibitory and excitatory responses to naloxone. Consequently, it was concluded that any change in function of VTA neurone populations as a result of spinal nerve ligation must involve only the mechanisms governing phasic responsivity to stimuli, if that, and leave mechanisms modulating tonic activity unaffected. This is in line with the stimulation-induced phenomena characteristic of the neuropathic pain state chronic pain – hyperalgesia and allodynia. One potential caveat of this theory was the apparent disagreement with the findings of Ozaki and colleagues, who found that MOR desensitisation occurred within the VTA following SNL surgery. However, this could be reconciled if in fact this down-regulation of function is counteracted *in vivo* by an enhanced release of endogenous opioids in this region, as implied by previous findings in individuals in a persistent pain state (Zubieta et al., 2001). It was noted that a fundamental limitation of these investigations lies in the necessity to record from separate animals when comparing neuronal responses in naïve versus SNL states. Consequently, there is a chance that comparisons of certain characteristics of recorded VTA neurones are being made between neurones belonging to different functional subgroups. This uncertainty was minimised (but not removed) by assessing the alignment of characteristics between the naïve and SNL-state recorded populations.

8. GENERAL DISCUSSION

8.I What were the aims of the thesis and how well have I fulfilled them?

The ultimate aim of this thesis was to increase understanding of the function of ventral tegmental area neurones in a nociceptive context. Core intentions were to gauge potential changes in these systems in different pain models, and to prove the involvement of DA and opioid signalling. Experiments set out to fulfil the individual components of these goals through the analysis of activity of these neurones in an *in vivo* rodent model. Here, I will review the most salient findings of this investigation with respect to the initial aims and predictions.

8.I.I Neuronal classification

Crucially, before drawing conclusions surrounding the pharmacological and neurobiological nature of the proposed key players, the DA-releasing neurons, it was first necessary to attempt to identify these amongst the other, non-dopaminergic contingents. Hence, this investigation initially set out to find a robust electrophysiological and/or pharmacological marker of VTA DA neurones *in vivo,* under guidance of several previous apparently successful attempts by other researchers (Margolis et al., 2006).

Unfortunately, but not unexpectedly, adoption of classification criteria at one point thought to be definitive failed to generate distinct population divisions corresponding to neurochemical identity. Instead, these characteristics, including spontaneous firing rate and pattern, action potential duration, response to noxious stimulation and response to morphine, showed no significant degree of crossover, hinting at the existence of wide range of functional groups.

Doubt and ambiguity in the electrophysiological and pharmacological identification of VTA DA neurones has been previously raised. At first, the reliable distinction of DA neurones in the neighbouring substantia nigra by a given set of electrophysiological markers was used as a guide to single out those in the VTA (Grace and Bunney,

1983; Grace and Onn, 1989; Guyenet and Aghajanian, 1978). Before long, however, the assumption of a similarly straightforward cell differentiation in the VTA was challenged, as cell-labelling techniques revealed discrepancies in the traditional combination of characteristics (Brischoux et al., 2009; Cameron et al., 1997; Ford et al., 2006; Margolis et al., 2003; Matsumoto and Hikosaka, 2009; Zweifel et al., 2011). In a 2012 review of the existing evidence, Ungless and Grace came to the conclusion that VTA DA neurones could indeed be identified with a reasonable degree of confidence, provided the whole range of characteristics was considered. However, even this tentative suggestion may present false hope; a much greater degree of overlap between neurochemical groups in terms of certain characteristics is ever-increasingly reported in the literature (Li et al., 2012; Margolis et al., 2012; Marinelli and McCutcheon, 2014), perhaps owing to the improvement of post-hoc neural identification techniques.

One characteristic that remains a relatively promising neurone identification tool to-date is responsivity to DA receptor activation. Reports have shown that D2 receptor agonists inhibit the firing rates of nearly all neurochemically-confirmed DA neurones (Chiodo et al. 1984; Clark and Chiodo 1988; Gariano et al. 1989; Lammel et al. 2008; Luo et al. 2008; Wang 1981; Yim and Mogenson 1980; Li et al., 2012), and that the great majority of D2 receptors in the VTA are found on DA neurone cell bodies and dentrites (Bouthenet et al., 1987; Chen et al. 1991; Gurevich and Joyce, 1999; Ardel and Artigas, 2004). These findings, together with quoted proportions of dopaminergic versus non-dopaminergic neurones in the VTA, suggest that it is reasonable to assume that most DA-inhibited neurones are dopaminergic. Alternative possibilities must be considered, however, as both a subset of GABAergic neurones directly inhibited by D2 agonists and a proportion of D2 receptor-deficient DA neurones have been found (Bannon and Roth, 1983; Chiodo et al., 1984; Kalivas, 1993; Lammel et al., 2008; Margolis et al., 2012, 2003; White and Wang, 1984).

Hence, a series of investigations were conducted to assess the ability of DA receptor pharmacology to separate VTA neurones into functional sub-populations, and subsequently to establish differences in characteristics of any revealed response-based groups. Exogenous L-DOPA, the DA precursor, was considered to be an appropriate agent for the purposes of this exploratory research. Following administration, L-DOPA is taken up by catecholamine-releasing neurones and subsequently used to synthesise DA (and noradrenaline). This results in enhanced levels of DA release, both presynaptically from axon terminals, and somatodendritically into the area surrounding the DA neurone itself. Through this mechanism, systemic administration of L-DOPA leads to an

increased activation of DA receptors, predominantly D2 and D1 subtypes, within the VTA. Autoinhibitory high-affinity D2 receptors present on the cell bodies of VTA DA neurones exert an autoinhibitory effect when activated; consequently, it was predicted that the injection of L-DOPA would lead to inhibition of SFR of a proportion of the recorded neurones, and that these neurones would most likely possess a dopaminergic identity.

Crucially, the initial L-DOPA investigations did reveal a group of neurones with robust inhibitory responses to injection, of a proportion and over a timescale predicted by previous behavioural and electrophysiological findings (Bunney et al., 1973; Abercrombie, et al., 1990; Paalzow, 1992). This concordance hinted at a likely-dopaminergic identity of a significant proportion of the L-DOPA-inhibited neurones.

The integrity of this L-DOPA response-based classification was tested through the subsequent administration of a much higher dose - in the realm of 100mg per kilogram of body weight. Previous studies found that effects on pain-related behaviour and accumbal DA release were entirely opposite to those seen with a low dose. If the L-DOPA-inhibited neurones were indeed predominantly dopaminergic, one would expect a similar dose-dependency when it came to L-DOPA action on spontaneous firing rate. Crucially, the $100mgkg^{-1}$ dose of L-DOPA did have excitatory effects on the spontaneous firing rate of low dose-inhibited group recorded in these experiments (norm L-DOPA cluster 1).

In contrast, the high dose injection had no apparent effect on the firing rate of the seemingly low dose-excited neurones found in the VTA (norm L-DOPA cluster 2). This result implies that DA effects on this neurone group are much more single-dimensional, likely resulting from the influence of only one DA receptor type that is maximally activated following the injection of $20mgkg^{-1}$ L-DOPA. A possible candidate is the D1 receptor-expressing GABA neurone population; if a low dose of L-DOPA causes the release of DA in concentrations sufficient to activate D1 receptors present on VTA GABA neurones, an excitatory effect on firing rate – as witnessed in this small proportion of recorded neurones – would occur. The maximal activation of these D1 receptors following the injection of low dose L-DOPA would prevent a further increase in firing rate following the subsequent injection of $100mgkg^{-1}$ L-DOPA. In support of a D1-mediated mechanism of excitation upon low dose L-DOPA injection, intra-VTA injection of the D2 receptor antagonist, sulpiride, did not reverse the effects of L-DOPA on this population.

As a final point to note with respect to L-DOPA response-based separation of the VTA population, the size and precise timescale of neurones' responses to low dose L-DOPA injection, along with the relative proportions of the recorded neurones displaying a given response, was remarkably consistent across all studies involving L-DOPA administration conducted in this investigation. These results imply that L-DOPA response is reasonably reliable in separating two distinct neuronal populations in the VTA, whatever the neurochemical identity of these populations may be.

Hence, the evidence collected here suggests that we can use systemic injection of L-DOPA to allow suggestions of neurochemical identity when conducting electrophysiological studies. Consideration of the quoted proportions of DA and non-DA neurone populations in the VTA – ~70% and 30%, respectively – will also help the interpretation of L-DOPA response-based findings. However, while these suggestions serve to provide a useful framework for interpretation of results and for mechanistic speculation, assumptions of neurochemical identity cannot be made with any certainty; populations of both dopaminergic and GABAergic VTA neurones possess a degree of heterogeneity in all characteristics investigated to-date, DA receptor pharmacology included, and therefore alternative interpretations were always considered.

The limitations encountered here represent key issues associated with functional *in vivo* studies. While the true function of any component of the pain-processing system can only be elucidated in the intact, alive animal, studies in these models typically sacrifice some degree of certainty in terms of cell identification. Fortunately, the application of relatively novel techniques to investigations into VTA neurone function has allowed researchers to circumnavigate these limitations. In particular, advances in transgenic technology and the use of optogenetics to activate particular neuronal populations have allowed highly targeted functional investigations. For example, Cohen and colleagues (Cohen et al., 2012) genetically 'tagged' DA and GABA neurones of the VTA with the light-sensitive protein, channelrhodopsin-2, and used this to identify these populations during investigations into reward and punishment processing. However, possible caveats of these methods arise from the potential of a particular genetic manipulation to alter neuronal properties governing excitability, as well as the dependency on mouse models, much less favoured than rats due to several behavioural-testing and anatomical scale limitations.

To summarise, the aim of generating "a robust electrophysiological marker of dopamine neurones in order to reliably identify these amongst interspersed GABAergic and glutamatergic contingents" was not fulfilled. The

diversity and lack of interrelatedness of neuronal characteristics suggests that, on reflection, this aim was perhaps unobtainable in the *in vivo* preparation. These characterisation experiments were intended to provide a platform for the subsequent investigations into the functional role of the VTA neurones. To a certain extent, this has been achieved. Comparisons of neuronal groupings according to L-DOPA response, morphine response, firing pattern and firing rate, among other characteristics, have exposed the presence of differential subdivision of neurones according to individual functional characteristics. This suggests that the importance placed on neurochemical identity is somewhat misplaced, as it is no better at predicting certain functionality than the other response-based characteristics. Consequently, interpretation of subsequent results found in this thesis will not involve the rigid shoe-horning of neurones into distinct functional groups, but will instead remain open to and observant of any heterogeneity displayed in light of the importance of this quality in understanding VTA neurone function.

8.I.2 Unmasking the influence of persistent pain

A subsequent aim of this investigation was to explore alterations in VTA neurone functioning in tonic inflammatory and chronic neuropathic pain models. The drive behind exploration of the effects of these manipulations on the VTA neurones mainly stems from their representation of much more clinically-relevant states in terms of the pain system; the most important insights we can draw from pain research will come from investigations into how pathological and debilitating conditions arise, and therefore how they may be prevented or reversed.

8.I.2.I Investigating the role of the VTA in the persistent pain state

There is much evidence suggesting that the role of the VTA DA neurones is altered in persistent pain states, including findings of DA agonists gaining analgesic function absent in the naïve state, an enhancement of the role of these neurones in opioid-induced analgesia, and the presence of a degree of dopaminergic dysfunction in fibromyalgia patients (Farmer et al., 2012; Navratilova and Porreca, 2014; Wood, 2006; Wood et al., 2007a). However, no previous studies probing changes in activity of individual VTA neurones *in vivo* in the persistent pain state were found. Such investigations are necessary to elucidate both the general population response to prolonged pain (suggestive of changes in regional modulatory influences such as local opioid release) and the within-population heterogeneity in response, implying functional segregation. Hence, it was considered necessary to monitor the firing characteristics of VTA neurones as a state of persistent pain developed, thereby promoting

elucidation of whatever causative or resultant changes occur and allowing extrapolation of the possible functional consequences.

8.I.2.2 An evolutionary perspective

Two persistent pain states were investigated: tonic inflammatory pain and chronic neuropathic pain. With widely differing initiative mechanisms and of very different time scales, these two pain states represent fundamentally different pain-related challenges for the individual. Evolutionarily speaking, tonic inflammatory pain on the time scale of a few hours is a salient stimulus. Enhanced sensitivity of the area is necessary to protect the likely-damaged region from further harm; consequently, a down-regulation of endogenous analgesic mechanisms seems most appropriate. Conversely, chronic neuropathic pain – studied here on the time scale of two weeks – involves nociceptive signalling in the absence of any remaining tissue damage. Adjusting behaviour in consideration of this persistent nociceptive input would not make sense, particularly if other motivational drives were compromised as the Howard Fields model of motivational decision making implies. Hence, it makes most sense to up-regulate endogenous analgesic mechanisms in the chronic neuropathic pain state.

Along this line of reasoning and in light of the weight of evidence implying an antinociceptive effect of VTA DA neurone activation, one would expect DA neurone activity to decrease in the tonic pain state and to increase in the chronic neuropathic pain state. However, there are many other possible scenarios; it may be that no such "evolutionarily beneficial" response occurs – at least not one involving this part of the pain matrix, and instead, that changes in VTA DA neurone function contribute to the pathological processes responsible for generation of the pain state, which would seemingly involve firing rate changes in the opposite direction. Alternatively, VTA DA neurones may lack any sort of involvement in the response to persistent nociceptive input, with the predominant changes that result in the behavioural phenomena witnessed occurring downstream of this region. The latter possibility is less feasible given the integrated network nature of the pain processing "matrix" that ensures individual components, including the VTA, receive input from and deliver output to a large number of the other components.

Hence, in light of the uncertainty deriving from our relative lack of understanding of this complex pain-processing matrix, investigations into VTA neurone responses to tonic and chronic pain were embarked upon with an open mind with respect to expected results.

8.I.2.3 Differential effects of tonic versus chronic pain

The induction of tonic inflammatory pain through carrageenan injection uncovered some interesting persistent pain effects on the VTA neurones. Neurones could be divided into two groups according to changes in firing rate upon carrageenan injection, showing a general excitation and lack of response, respectively. Furthermore, the seemingly "unresponsive" neurones showed a reduction in burst firing as tonic pain developed, and therefore weren't unresponsive on average after all. Conversely, no chances in firing rate or firing pattern were seen when comparing neurones recorded in the neuropathic chronic pain condition with those recorded in naïve animals, in-line with the findings of Sagheddu and colleagues (2015). Hence, it was concluded that the VTA neurones played a role (albeit of an unknown quality) in tonic inflammatory pain, but showed no alteration mirroring the altered nociceptive functioning in the chronic pain state. The latter finding may not necessarily imply a lack of impact of longer-term persistent nociception on the VTA; it is possible that changes occurring in the shorter term are counteracted by the adjustment of modulatory mechanisms. One such mechanism seems plausible upon review of the literature: an increase in endogenous ß-endorphin release within the central nervous system, reported by Porro and colleagues (1991), would lead to increased activation of the mu-opioid receptors, such as those expressed by VTA neurones. Increased stimulation of this receptor group is known to lead to desensitization through mechanisms including the uncoupling of the receptor from G-protein effectors. This desensitization process has been shown to occur within the VTA in the chronic neuropathic pain state (Ozaki et al., 2003), resulting in a reduced indirect inhibition of dopamine neurones (according to the two-neurone model of opioid action in the VTA; Johnson and North, 1992), explaining the reduction of agonist-induced dopamine release in the NAcc (Ozaki et al., 2002). Hence, unchanged spontaneous firing characteristics of the VTA neurones could represent the net effect of a delicate balance between enhanced endogenous opioid release and decrease in receptor efficacy. However, the possibility that neurones recorded in the neuropathic state animals represented a different sample of the whole VTA population than did those recorded in the naïve state animals. While this was considered unlikely for the most part in light of the alignment of characteristics including burst firing and SFR of the two populations, it was important to take this alternative explanation into account.

The functional implications and possible explanation of an increase in firing rate and decrease in burst firing rate of the VTA neurones in response to carrageenan injection remain unclear in the face of neurochemical ambiguity. Following from the findings in the previous two experimental chapters, neuronal response to L-DOPA was

considered to be one method of shedding some light on neurochemical identity; as discussed in section 4.5.1, it was concluded that the most likely identity of a majority of L-DOPA-inhibited and L-DOPA-excited (seemingly – this response was not found to be significant) neurones were dopaminergic and GABAergic, respectively. It was decided that these propositions of neurochemical identity could be made when interpreting the results, provided the likelihood of some degree of cross-over was considered. Hence, carrageenan effects were separately assessed for the two L-DOPA response-based neurone clusters to allow suggestions of putative DA and GABA neurone responsivity. Both neurone groups showed a large degree of variability in the change in SFR seen following carrageenan. Adopting the likelihood-based strategy of neurone identity, these results hint at both dopaminergic and GABAergic populations showing mixed responsivity to the induction of tonic inflammatory pain. This is not unexpected in light of known heterogeneity of opioid responsivity – thought to be altered by persistent pain - of both populations, and of nociceptive responsivity of the dopaminergic contingent, in particular. However, it is possible that a significant proportion of the within-group variability is down to neurochemical heterogeneity within the L-DOPA response-based groups, which limits the specificity and clarity of any conclusions drawn from these experiments.

8.I.2.4 A mechanistic interpretation

The next step after establishing that VTA neurones were indeed responsive to tonic pain was to attempt to identify the possible causative mechanisms. The literature strongly suggests that a plausible candidate for changes in VTA neurone function in persistent pain states is alteration in endogenous opioid modulation; endogenous μ-opioids are known to exert variable control over the firing rates of both DA and GABAergic populations, which have previously been shown to be altered via both changes in endogenous agonist levels and receptor expression or sensitivity in the persistent pain state (Hylden et al., 1991; Kayser and Guilbaud, 1983; Porro et al., 1991; Narita et al., 2005). It was therefore considered possible that carrageenan-induced excitation was due to either the downregulation of direct inhibitory action (MORs are coupled to inhibitory G-protein effectors and therefore MOR activation exerts inhibitory effects on neural activity) or the upregulation of indirect excitatory action on subsets of the VTA neurones (disinhibition). These possibilities were tested by systemically administrating the μ-opioid receptor antagonist, naloxone, in both naïve and tonic pain states. Interestingly, results implied that a tonic inhibitory effect of endogenous opioids was abolished following carrageenan injection. This opioid influence, as revealed by an excitatory effect of naloxone, was present only in a high-firing cluster of neurones and was not displayed by the low-firing neurone cluster that formed the majority of the recorded population. Given than high

firing rates and MOR agonist inhibition (and therefore antagonist excitation) are characteristics typically attributed to GABAergic neurones for the large part (Bunney et al., 1973; Chiodo et al., 1984; Grace and Bunney, 1984a; Guyenet and Aghajanian, 1978; Luo et al., 2008; Steffensen et al., 1998, 2008; Stobbs et al., 2004), it was considered reasonable to suggest a GABAergic identity for most members of this small subset of neurones. Conversely, when assessing the naloxone responsivity of neurones displaying excitatory responses to carrageenan only, a transient inhibitory response at 10 minutes post-naloxone injection was seen. This response suggests that there is a tonic excitatory effect of endogenous opioids on at least a subset of neurones in the tonic pain state – possibly contributing to the tonic pain-induced excitation. However, no evidence to suggest that this endogenous opioid influence was enhanced upon the injection of carrageenan was found, and therefore it was not possible to attribute causality to this mechanism.

The group of neurones displaying alterations in firing pattern but not firing rate in the tonic pain state are likely to be influenced by different mechanisms. One feasible possibility is a reduction in glutamatergic input from the prefrontal cortex, specifically via the NMDA class of receptors, as this specific form of stimulation is known to evoke burst firing of VTA DA neurones. This finding of a dissociation of response type within the population of VTA neurones is a reminder of the variability in inputs integrated by this region. Hence, while it is important to investigate alterations in inputs (local neurotransmitter and neuromodulator release) and outputs (neurotransmitter release at projection targets) of the VTA neurones, it is near-impossible to understand how this connectivity actually relates to function without investigating the nature of associated changes in neurone activity through electrophysiological recording.

8.I.2.5 A proposed model of opioid control of VTA neurones in tonic and chronic pain states

In light of the findings of carrageenan effects on firing rate and naloxone response, a putative model of endogenous opioid action in naïve verses tonic or chronic pain states was proposed (figure 8.I).

In the naïve state, endogenous opioids exert an inhibitory effect on VTA GABAergic neurones (or at least a subset of them – a proportion have been found to be unresponsive; Margolis et al., 2012), and a mixed effect on the dopaminergic population (Margolis et al., 2014). Injection of naloxone in this state consequently results in the excitation of the GABA population (or at least a proportion of-) as the inhibitory influence is blocked, and mixed effects – explaining the net unresponsivity – on the dopaminergic population. The induction of tonic inflammatory pain causes a down-regulation of inhibitory endogenous opioid action, presumably via reductions in levels of ß-endorphin release as this would explain the enhanced efficacy of exogenous MOR agonists previously witnessed in this pain state (Hylden et al., 1991; Kayser and Guilbaud, 1983). GABA neurone activity increases, explaining the excitatory effects of carrageenan on a proportion of the recorded neurones, and naloxone effects diminish as there is a reduced level of ongoing MOR activation to block. Tonic excitatory effects of endogenous opioids on some of the VTA neurones are also at play in the tonic pain state, presumably acting on a different subset of neurones to those under the influence of tonic inhibitory opioidergic control in the naïve state.

The proposed model for the chronic neuropathic pain state is fundamentally different – unsurprising given the differing time scale and nature of the nociceptive insult. Enhanced levels of endogenous opioid release are triggered by the persistent bombardment of nociceptive stimulation from the site of nerve injury, possibly explaining – at least in part - the relative lack of morphine's analgesic efficacy in this state (Arnér and Meyerson, 1988; Ozaki et al., 2002). Over time, the enhanced exposure of VTA MORs to their agonist leads to their reactive desensitization through G-protein uncoupling, thereby reducing the efficacy of endogenous (and exogenous) opioid action (Ozaki et al., 2003). As both an upregulation of opioid release and a downregulation of opioid receptor sensitivity occur concurrently, no net change in endogenous opioid action is witnessed, explaining the near-identical naloxone effects recorded in naïve and SNL states.

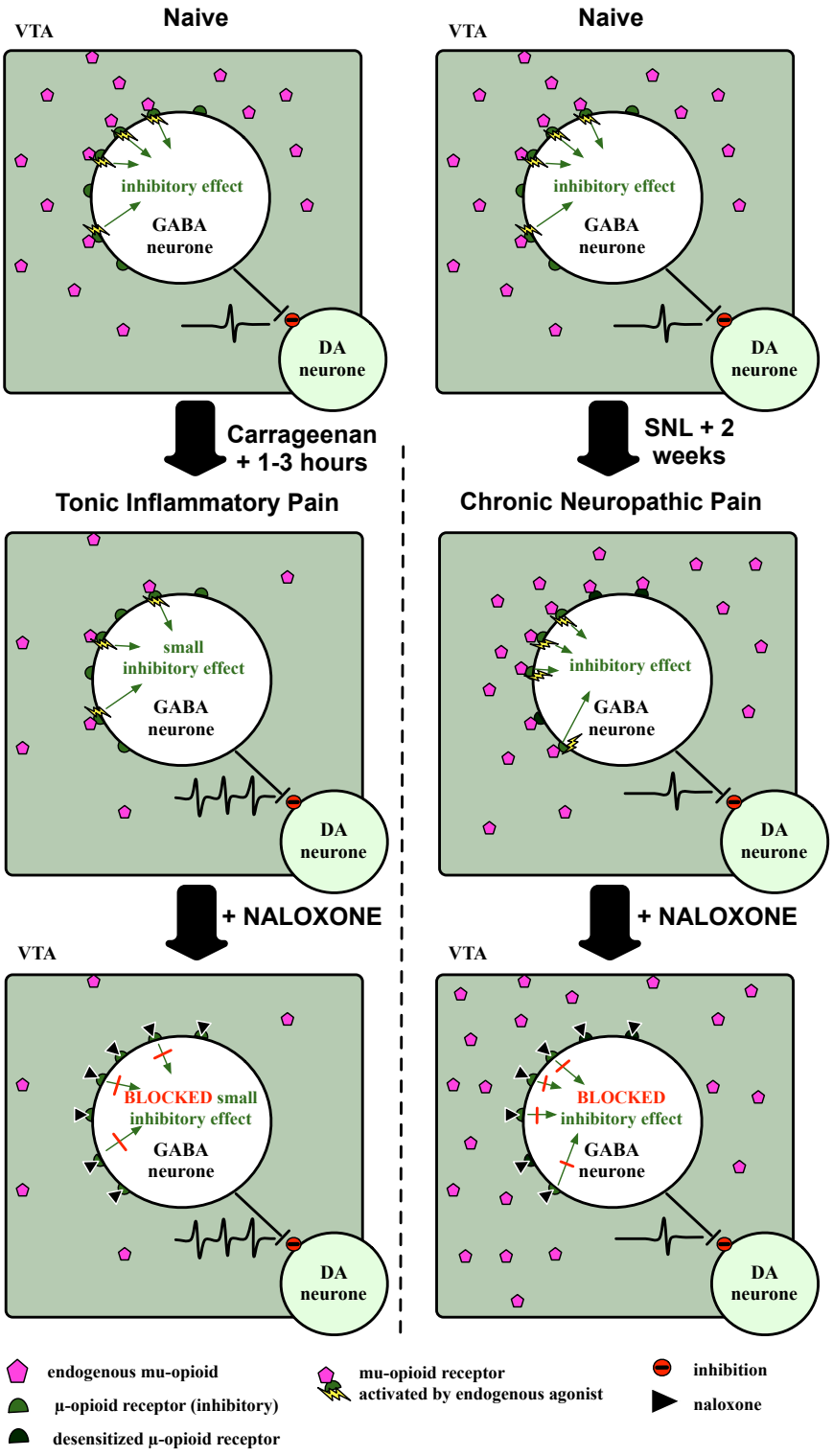

Figure 8.I Schematic diagram of theoretical model of endogenous μ-opioid action in the VTA in different pain states, and the impact of naloxone antagonism. *Tonic inflammatory pain (left hand side)*: *1*-3 hours after carrageenan injection, endogenous opioid levels are reduced in the VTA. This results in a low level of GABA neurone tonic inhibition via MORs. Upon the addition of naloxone, this small inhibitory effect caused by endogenous opioids is blocked, resulting in a small increase in GABA neurone firing rate (small or negligible naloxone effect). *Chronic neuropathic pain (right hand side)*: 2 weeks after SNL surgery, opioid levels are increased in the VTA. However, MORs are also desensitized, resulting in no net change in the level of endogenous opioid influence on VTA neurones. The naloxone effect on GABA neurone firing rate therefore remains the same as seen in the naïve state.

8.I.2.6 A note on agonist versus antagonist-based investigations

One implication of this model is that it highlights the utility of an antagonist agent when attempting to investigate a neurotransmitter system. In some early studies looking into opioid function in persistent pain conditions, Hylden and colleauges (1991) as well as Kayser and Guilbaud (1983) found that injecting the MOR agonist, morphine, had a greater analgesic efficacy in tonic inflammatory pain verses the naïve state. While this allows us to make predictions of the effects of opioid therapeutics in different pain conditions, agonist-based investigations do not allow an understanding of endogenous pathological mechanisms; such an enhancement in agonist efficacy could be caused by either an upregulation of endogenous opioid analgesia via receptor sensitisation or expression, or by a downregulation via reduced endogenous opioid release. By instead administering the MOR antagonist, naloxone, it is possible to reveal the underlying state of endogenous opioid analgesia, and therefore postulate the functional role of this neuromodulatory mechanism in tonic pain.

A similar evaluation of agonist- versus antagonist-based investigations was conducted regarding alpha-2 receptor function in the spinal cord. A collection of studies employing alpha-2-adrenergic agonists to probe the system in rats with neuropathic pain concluded that, if anything, the central action of noradrenergic control was enhanced in this state (Malmberg et al., 2001; Pertovaara and Wei, 2000; Xu et al., 2000, 1992; Yaksh et al., 1995). However, investigations using the alpha-2-antagonist atipamezole found conversely that the tonic descending noradrenergic inhibition of dorsal horn neurones was significantly reduced in neuropathic pain (Rahman et al., 2008). To conclude, as summarised by Rahman and colleagues (2008), thinking logically it appears that "whereas agonists can only reveal the consequences of receptor activation, the use of antagonists sheds light on the physiological roles, and changes induced by pathological processes, of the activity in the transmitter mediated neuronal networks".

What does the interpretation of the current results tell us about the functioning of these VTA neurones in persistent pain? First and foremost, findings here support previous evidence suggesting underlying mechanisms of tonic and chronic pain are different. Upon consideration, this is to be expected; tonic inflammatory pain, lasting in the region of a few hours to days, represents a very different challenge to the individual than does chronic neuropathic pain. Although not as directly useful as a warning sign as acute pain sensation, the sustained hypersensitivity that remains relatively local to the site of inflammation does provide the advantage of protecting this already-damaged region from further harm. In contrast, the location of perceived pain in neuropathic conditions can often lie far

from the actual nerve damage; in the SNL model used here, ligation of the L5 and L6 nerves near the dorsal root produces hypersensitivity at the level of the paw these fibres innervate. Consequently, the unpleasant experience of neuropathic pain serves no obvious purpose. Furthermore, huge differences in the nature of the initial trigger and the time over which pathological changes can develop, will inevitably dictate that precisely how pain-processing components react will be largely condition-specific.

Secondly, we should consider what these changes in endogenous opioid control might represent: a protective measure to protect a potentially damaged part of the body, a counteractive measure to help suppress unnecessary sensitisation, or a pathological mechanism causing it? This is a crucial point to clarify for therapy development, since it dictates precisely which manipulations of a given mechanism will attenuate or, conversely, augment the debilitating pain experience. The apparent reduction in endogenous opioid influence on VTA neurones in tonic pain – as concluded from the reduction in naloxone response - implies that at the 2-hour post-injection time point, endogenous analgesia in this form is suppressed. This may be of value in the acute survival nature of pain by contributing to the sensitisation of the inflamed area necessary to protect it from further insult. The reduction in burst-firing of the neurones showing no overall carrageenan-induced change in mean firing rate would also contribute to increased pain sensitivity, provided a proportion of these neurones were dopaminergic (dopamine release in the NAcc results in analgesia, and burst firing leads to an exponential increase in synaptic dopamine levels). Conversely, in the case of SNL-induced neuropathic pain, any alterations in VTA neurone modulation appear to be either reversed or counter-balanced by the 2-week post-surgery time point. Whatever the underlying mechanisms, it is possible that the return to (or maintenance at) opioid modulatory levels of the naïve state holds some evolutionary value by allowing other motivations to be considered in behavioural decision making.

Finally, results showed significant heterogeneity in VTA neurone responsivity to persistent pain. It was discussed that heterogeneity in the nature and magnitude of carrageenan response likely existed both between and within neurochemical groups. A similar finding occurred with respect to naloxone responsivity in both naïve and neuropathic pain states. Hence, the elucidation of the functional implications of tonic and chronic pain responsivity will require not only robust neurochemical confirmation of the recorded population, but a full characterisation of each individual neurone coupled with an understanding of what certain qualities, including location, nociceptive responsivity, firing pattern and rate, and projection target, mean for a neurone's downstream impact.

8.2 What are the implications of my findings?

Following from the review of the aims of this thesis, it is necessary to speculate as to the implications of the current results for the VTA neurone population's role in pain. As previously discussed in section I.9.I, there is ample evidence to suggest that dopamine neurone activity plays a critical role in antinociception. This can occur in many contexts, but crucially, it is partially through action on the VTA neurones that both endogenous and therapeutically administered opioids exert their effects (Altier and Stewart, 1999; Hnasko et al., 2005). However, studies assessing different aspects of motivation in different contexts suggest that exactly how this antinociceptive role is fulfilled, and to what extent, is highly variable. The findings of this study were not in disagreement.

8.2.I Neuronal heterogeneity

When considering the findings of this thesis as a whole, one can see a general theme running throughout: in contrast to the more clear-cut and binary models of neurochemical identity-centred function proposed by several researchers in the past (Johnson and North, 1992; Tan et al., 2012; Ungless et al., 2004), the overwhelming impression of VTA neuronal neurochemical groups formed here is one of significant heterogeneity. The degree of diversity of characteristics of the putative dopaminergic population, in terms of nociceptive response, and opioid and D2 receptor-related pharmacological intervention, was extensive enough to consider each variable a continuum.

This as a suggestion is by no means novel; there have been many studies and reviews taking the conflicting evidence into consideration and coming to the same conclusion (e.g. Volman et al., 2013). The first widespread acknowledgement of heterogeneity within VTA neurone populations surrounded their aversion and reward encoding properties. Initial theories pinned a reward value encoding label on VTA dopaminergic neurones, such that rewarding stimuli are met with an acute excitation and aversive stimuli, an acute inhibition of firing rate. However, a large number of studies have collectively contradicted this simple model of VTA DA neurone functionality by establishing the existence of subpopulations responding differentially to aversive and rewarding stimuli (Brischoux et al., 2009; Horvitz, 2000; Matsumoto and Hikosaka, 2009; Schultz and Romo, 1987; Zweifel et al., 2011). These findings lead researchers to suggests a functional division of the dopamine neurone population into reward value encoding and salience encoding subpopulations (Matsumoto and Hikosaka, 2009).

This story is not unique to the properties of acute stimulus responsivity; following extensive investigation, DA neurones are now considered to be heterogeneous in a wide range of characteristics relating to both electrophysiological properties and pharmacological sensitivity (Chiodo et al., 1984; Bromberg-Martin et al., 2010; Lammel et al., 2011, 2008; Margolis et al., 2008 Gysling and Wang, 1983; Matthews and German, 1984; Cameron et al., 1997; Ford et al., 2006; Margolis et al., 2003; Margolis et al., 2012; Kiyatkin and Rebec, 2001; Hyland et al., 2002; Pan et al., 2008; Li et al., 2012). For example, a study conducted by Cohen and colleagues (2012), involving recordings of VTA DA neurones in awake, head-fixed mice, found that for any one reward- or punishment-conditioned odour stimulus, burst firing was present in some but never all dopaminergic VTA neurones. This functional diversity within the VTA held true when doubts about identity of DA neurones were ruled out by cell type-specific optogenetic tagging (Cohen et al., 2012). The consideration of such a large number of possible variables leaves us with a complex and confusing picture of functional neuronal subdivision. However, there is a glimmer of hope towards a more comprehensive understanding of the VTA neuronal population; combined electrophysiology and retrograde tracer studies have hinted at sub-populations of neurones being separable in terms of both projection target and anatomical location within the VTA, such that prediction of a dopaminergic identity is more reliable when this quality is known (Brischoux et al., 2009; Margolis et al., 2008b; Lammel et al., 2011).

In order to move towards further clarification, the question surrounding the current findings we now need to ask is how this functional heterogeneity is generated. Fortunately, there have been several lines of evidence that could go some way towards explaining the results witnessed here. Heterogeneity amongst a given population of neurones could feasibly arise through differences in synaptic inputs, differences in physiological properties (i.e. the way a given input affects the firing rate), or a combination of both. Evidence points towards the latter suggestion.

In an optogenetic study, Lammel and colleagues (2012) found inputs from the laterodorsal tegmentum lead to direct activation of VTA dopaminergic neurones, whilst inputs from the lateral habenula contributed the indirect GABA-mediated inhibition of this neurone type in response to aversive events. Crucially, these contrasting aversive stimulus-related inputs appeared to affect different subpopulations of the dopaminergic neurones, thereby providing a plausible explanation for nociceptive functional heterogeneity. Along these lines, several other findings have hinted at the existence of parallel circuits involving VTA neurones that differ in functionality; as

discussed in section I.8.I, glutamatergic inputs from the mPFC only synapse on those VTA DA neurones projecting back to this brain regions (Carr and Sesack, 2000), and GABA inputs from the NAcc and ventral pallidum synapse specifically on non-dopamine and dopamine neurones, respectively (Xia et al., 2011; Hjelmstad et al., 2013).

Whilst extrinsic input variability can conceivably generate disparities in responsivity, differences in how the incoming signals are received and processed by post-synaptic receptors ultimately have the final say in neuronal activity. Consequently, variability in receptor expression and function between dopamine neurones has an enormous capacity to generate subpopulation heterogeneity. For example, nicotinic acetylcholine receptors (nAChRs), known to play a major role in the modulation of DA neurone activity, exist in a huge variety of subunit composition-based subtypes. These subtypes each have subtly different biophysical properties, and crucially are localised differentially throughout the VTA (Faure et al., 2014). Hence, there is the potential for a large degree of heterogeneity in cholinergic fine control, ultimately influencing the physiological neuronal activity recorded. Similarly, variability in another significant source of modulation for DA neurones, D2 autoreceptor-mediated inhibition, has been established (Ford, 2014; White and Wang, 1984). For example, DA neurones that project to the prefrontal cortex exhibit reduced levels of D2 autoreceptors, rendering them less sensitive to autoreceptor-mediated feedback inhibition than the mesolimbic population (Chiodo et al., 1984; Lammel et al., 2008). Further to this, suggestions of heterogeneity among dopamine neurons with respect to expression of the dopamine transporters DAT and VMAT2, responsible for the regulation of extracellular DA levels, may further add to the complexity of somatodendritic signalling by autoreceptors (Li et al., 2013). Findings here were in agreement with this notion, as significant variability was found in VTA neuronal responses to microinjection of the D2 receptor antagonist, sulpiride, following L-DOPA administration.

Further potential for heterogeneity is generated when we consider possible variations in excitability-controlling ion channels. In a comprehensive review, Korotkova and colleagues (2004) discuss the evidence that dopaminergic midbrain neurones can be divided into subpopulations according to firing behaviour as a result of differential expression of membrane ion channels mediating characteristic I_{AHP}, I_h and I_t currents. These factors will have subtle but noticeable effects on the functioning of individual dopamine neurones *in vivo*.

Finally, another potential source of within-population heterogeneity is variability arising from methodological protocol. This is particularly relevant when assessing evidence across studies, but may also contribute to within-study differences. For example, as discussed in a recent review by Ungless and Grace, there is significant ambiguity in the literature surrounding DA neurone identification. This implies that in some cases neurones have been incorrectly attributed a dopaminergic label, and therefore conclusions drawn about their characteristics may be inaccurate. This is perhaps most apparent in the case of dopamine neuron responsivity to noxious stimuli, for which there is a large degree of variability between reported proportions of excited and inhibited neurones (McCutcheon et al., 2012). Possible reasons for the differences include the lack of stringent response-classifying criteria in some studies (e.g. Ungless et al., 2004; Kiyatkin, 1988), in contrast to the response classification threshold set here. Further, differences in measured noxious responsivity could come from the differences in intensity and location of noxious stimulation, differences in depth of anaesthesia, and differences in stimulus-evoked firing rate measurement protocols (e.g. Ungless et al., 2004 only used the last 5 seconds of a 10-second stimulus application for their analysis).

8.2.2 Functional implications of heterogeneity

On reflection of the presented evidence, the findings of heterogeneity amongst recorded populations in the current study are neither anomalous nor counterintuitive. The functional implications of the VTA neurones being divisible into subpopulations on the bases of a plethora of functional characteristics depend on the congruency between these variables and the precise projection targets. To clarify, if, for example, each group of neurones defined by their respective outputs possessed a unique specific combination of electrophysiological, pharmacological and input traits, one could predict the separable groups to function independently in parallel pathways. There is some hint that this may be the case, at least to some extent: distinct VTA dopamine neurone populations receiving inputs from the laterodorsal tegmentum (LDT) and lateral habenula (LHb) have been found to preferentially project to the medial PFC and lateral shell of the NAcc, respectively. It was suggested by Lammel and colleagues (2012) that the former 'circuit' involving the LDT and PFC may act to signal aversive events, whilst the latter may primarily signal reward and perhaps salience. Similarly but on a more general note, evidence suggests that distinct circuits involving VTA DA neurone subpopulations contribute to different behavioural functions; dorsal VTA neurones coding for reward and aversion have been found to project to the NAcc, while ventral VTA neurones represent a saliency signal that projects specifically to mesolimbic regions involved in attention and motor processes (Redgrave et al., 1999).

However, as an alternative to this parallel and independent model of VTA DA neurone subgroup function, it is possible that there is significant overlap of functional characteristics between groups defined in any way. Further, there may be reciprocal connections between separable subsets of DA neurones, such that activity of individual cells is complexly dependent and regulated by the wider "network".

The reality is most likely somewhere in between these two functional models, with distinct circuits existing, but not functioning in isolation. This would be due in part to the anatomical interactions between neurones, as well as the complex nature of real-world events, often possessing both aversive and rewarding aspects. Further to this, it would be naïve to ignore the vast brain-wide contributions to motivational direction of behaviour that inevitably interact with any dopamine-based signalling pathway, and from this, the VTA's position in the pain processing system as a whole.

A review by Wood (2008) provides a helpful framework in which to view the role of any pain system component. It is clarified that nociceptive processes may be broadly characterized into three interrelated mechanisms: firstly, the perception and transfer of information from the peripheral site of occurrence to the CNS, secondly, the supraspinal processing of these signals by parallel circuits, and finally, descending processes that either facilitate or inhibit pain perception at the spinal level (Wood, 2008). In this context, the dopaminergic pathways emanating from the VTA fit in at the supraspinal level. However, the extensive connectivity between brain regions at this level make unpicking independent roles unrealistic; perhaps instead, in the words of Lammel and colleagues (2012) we should 'conceptualize the VTA neurone subpopulations as belonging to a more complex global brain system that assigns motivational valence or value of external and internal stimuli'.

8.2.3 The role of VTA GABA neurones

A key component of the current investigation that is at risk of being overlooked in terms of functional implications is the GABAergic population of the VTA. The precise role of GABAergic VTA neurones in both pain and reward circuitry is not clear, making theoretical suggestions difficult to draw in this case. On the one hand, there is strong evidence that GABA neurones exert tonic inhibitory control over the release of dopamine in the midbrain, including findings that many addictive drugs (e.g. opiates and cannabinoids) increase dopamine levels through

inhibition of GABA neurone activity (Szabo et al., 2002). In this way, the GABA neurones appear to play the more indirect role in motivational control of simply modulating the dopaminergic output. However, local regulation of dopamine neurone activity represents on only one aspect of a seemingly complex combination of roles in pain processing. As discussed in section I.8.3, GABAergic neurones form a large proportion of the projection pathways from the VTA, including around 60% of the mesocortical neurones (Carr and Sesack, 2000). In other words, GABA neurones have distinct long-range actions on other components of the pain and reward systems. One theory, proposed by Steffensen and colleagues (Steffensen et al., 2001), suggests that the role of some of the GABA neurones in the VTA lies in the initial attending to a rewarding or salient stimulus, before dopaminergic influences on behavioural control take hold. Further supporting a separable role of the GABAergic population, some compounds affect GABA and DA neurones in a similar rather than reciprocal manner. For example, nicotine and the neurotransmitter orexin act to increase the firing rate of both GABA and DA neurones in the VTA (Yin and French, 2000), implying that the downstream impact of GABA neurone activation does not rely solely on dopamine neurone modulation.

In support, evidence of possible mechanisms behind separable VTA GABA and DA neurone functionality has previously been found; distinct pathways involving these two neurochemical populations appear to exist, with neurones of the prefrontal cortex sending projections to the mesocortical subpopulation of DAergic neurones, whilst conversely targeting NAcc-projecting GABAergic neurones (Carr and Sesack, 2000). Furthermore, the excitatory synapses on VTA DA and GABA neurones are different, suggesting differential signal processing: synapses on DA neurones exhibit a depression in response to repetitive activation, and exhibit NMDA-dependent LTP, whereas synapses on GABA neurones show facilitation.

Given the uncertainty of neurochemical identity of the neurones recorded in the current investigation, it was not possible to gain reliable insight into the specific function of VTA GABA neurones. However, speculations on neural identity and therefore possible responsivity of GABA neurones could be made by considering both quoted relative populations of neurochemical groups in the VTA and previously reported characteristics of histochemically-confirmed GABA neurones.

It was found that neurones appearing to be excited (albeit insignificantly) by a low dose of L-DOPA (norm L-DOPA cluster 2) showed, on average, no significant change in firing rate in response to injection of a high dose

of L-DOPA. This contrasts the opposite, excitatory effect of the high dose on the L-DOPA-inhibited neurones (norm L-DOPA cluster 1). Based on evidence surrounding dopamine receptor expression and dopamine agonist action on populations of DA and GABA neurones, it was considered most likely that a significant proportion of the norm L-DOPA cluster 2 neurones were GABAergic (with the possible exception of some dopaminergic neurones). Following these assumptions, results suggested that dopaminergic and GABAergic neurones are controlled by distinct mechanisms when it comes to L-DOPA (i.e. DA) action – perhaps the separate inhibitory D2 receptor and excitatory D1 receptor-effector systems. This theory was supported by findings showing that intra-VTA injection of sulpiride, the selective D2 receptor antagonist, did not appear to reverse the excitatory effects of low dose L-DOPA while there was a trend – albeit variable – towards a reversal of L-DOPA inhibition.

Following this line of thought regarding the identity of L-DOPA-inhibited and seeimgly–excited neurones, current findings hinted at the VTA GABA neurone population possessing heterogeneity in terms of response to the induction of tonic inflammatory pain; neurones belonging to a generally L-DOPA-excited cluster (norm L-DOPA cluster 2c) showed wide variety of responses to carrageenan injection, including excitation and inhibition in mean SFR. Heterogeneity of the small seemingly L-DOPA-excited population (norm L-DOPA cluster 2) was also seen in both firing rate and amount of burst firing, such that ranges almost spanned those seen for the much more populous L-DOPA-inhibited group of neurones. Hence, findings suggest – albeit tentatively due to the lack of confidence in neural identity – that the GABAergic neurones of the VTA are just as heterogeneous as the dopaminergic contingent. This is not an original suggestion; as discussed in the various sections, a degree of diversity amongst confirmed GABA neurones has previously been reported with respect to several pharmacological and physiological characteristics (Margolis et al., 2012). It is also not unexpected in light of the above discussions surrounding interneurone and projection neurone function.

Thus, what we can learn from reviewing the current evidence is that it is imperative to consider the action of GABAergic neurones when trying to understand any role of the VTA. The degree of functional independence of these neurones from the DAergic population seems to be highly variable, depending on the precise characteristic and context of interest. This is perhaps unsurprising given the evidence suggesting subpopulation heterogeneity of GABAergic neurones, separable most notably by receptor expression and projection patterns, in the same vain as that found for dopamine.

8.3 Potential methodological limitations

8.3.I Implications of experimenting in the anaesthetised preparation

One potential confounding factor in the current methodology relates to the use of anaesthesia in these studies. There are a couple of key considerations associated with experimenting in this state: firstly, does variability in the depth of anaesthesia between and within experiments represent a source of uncontrolled variability in neurone firing rate, and secondly, how far can findings surrounding neuronal function in the anaesthetized state be translated into conclusions in the natural, freely-moving, state?

8.3.I.I Implications of anaesthesia: translation to the freely-moving state

The end-goal of the pain-processing system is an adjustment of behaviour such as to avoid potential or actual damage to the body of any sort. Individual components of the pain-processing brain "matrix" play differing roles in this unifying goal, which include the automatic relaying of sensory information, reflexive reaction, contextual modulation of the sensory signals, and conscious and subconscious decision-making processes. Ultimately, however, the pain-processing matrix should be thought of as an integrated whole - a network of neurones whose function can only be understood when considering the extensive two-way signalling connecting the entire system. When attempting to study the role of an individual component, such as neurones of the VTA in this case, it is therefore important to maintain the integrity of the pain network's connectivity. This not only involves maintenance of physical connectivity; changes in brain state associated with sleep or anaesthesia can alter the function of certain neurones involved in pain-processing, results in down-stream alterations in the functioning of many other components in the system. Further, certain anaesthetics, such as ketamine, interact with synaptic inputs necessary for activity generation *in vivo*. This leads us to ask the following question: exactly how representative of a neuronal population's natural function in pain processing are the findings established by recording from animals in the anaesthetized state? This question is difficult to answer with confidence, as it is not possible to study behaviour – the integrated outcome of the pain-processing system – in the anaesthetized state. What we can investigate, however, is the equivalence of neuronal behaviour in anaesthetized versus awake states; if neuronal firing characteristics and responsivity to nociceptive and pharmacological manipulations remain relatively unchanged under anaesthesia, we can assume that the function of that population is intact, and therefore can translate findings to the natural state.

Findings elucidating VTA neurone characteristics in the freely moving condition are still relatively limited because most of the available data surrounding VTA neurone function has been obtained from experiments on brain slices, or in paralyzed or anaesthetized states. Nevertheless, the development of recording techniques has enabled some researchers to successfully gather individual neurone data in non-anaesthetised and feely-moving animals. Promisingly, very few differences between mean firing rates and burst-firing of VTA DA neurones recorded in anaesthetized and awake, freely-moving states have been found (Fà et al., 2003; Hyland et al., 2002; Marinelli and McCutcheon, 2014b), strongly suggesting that synaptic inputs remain intact. Most studies have been conducted under chloral hydrate anaesthesia, and therefore direct comparisons have tended to focus on this state (Hyland et al., 2002; Marinelli and McCutcheon, 2014). However, given the comparability of firing rates and bursting intensity of DA neurons recorded in animals anaesthetized by chloral hydrate (4.5 Hz, 30%; Grace and Bunney, 1984b; Marinelli et al., 2006) or isoflurane (5 Hz, 45%; Panin et al., 2012), it is reasonable to assume that isoflurane anaesthesia similarly preserves normal VTA DA neurone function. In contrast, however, VTA GABA neurones have been found to show to display a decrease in firing rate and an alteration in discharge pattern upon chloral hydrate anaesthesia (Lee et al., 2001), meaning that it is likely that characteristics of a proportion of the recorded neurones were not representative of a natural awake state.

Hence, when interpreting the findings surrounding VTA neurone activity in different pain states, it is important to consider that changes in firing rates and firing patterns witnessed may not translate to known outcomes of pain-related behaviour.

8.3.1.2 Implications of anaesthesia: influence on neurone firing rate

Given that anaesthesia has been shown to affect the activity of at least some of the VTA neurones, a further consideration is whether the depth of isoflurane anaesthesia in individual experiments, or at individual time points within experiments, underlies a proportion of the firing rate variability witnessed. Inhaled isoflurane is rapidly taken up by the alveolar blood supply, allowing a steady state of blood isoflurane concentration to be reached on the condition that the concentration in inhaled air, the breathing rate, and the cardiac output remain constant. The concentration in inhaled air is easily controlled, and the breathing rate easily assessed; however, cardiac output was not monitored in the current investigation as non-invasive measuring mechanisms are extremely limited. Echocardiography incorporating pulsed-wave Doppler (PWD), one non-invasive method trialled in previous

studies, requires expensive equipment and specialized technicians and therefore was not considered to be a feasible option in the current investigations (Slama et al., 2003; Sturgess et al., 2008).

Another potential cause of variability in anaesthetic depth is the release of isoflurane by the highly soluble fat tissue. Animals inhale 5% isoflurane for a short period of time during set-up (for initial induction), during which a relatively high concentration of isoflurane may be absorbed by the fat tissue. This store of isoflurane will subsequently be released into the blood as the concentration in arterial blood declines to the steady state necessary for the remainder of the experiment (inhaled isoflurane of 1-1.5% v/v). Animals differing substantially in terms of body fat percentage will thus possess slightly different isoflurane blood concentrations at a given inhaled concentration, breathing rate and cardiac output. However, this is unlikely to have too large an effect on neuronal activity for several reasons: firstly, isoflurane will be released into venous blood which re-equilibrated with inhaled air in the lungs before reaching the brain, and secondly, a greater concentration of isoflurane will act to lower cardiac output and breathing rate, thus reducing the rate of delivery of isoflurane to the brain.

As delivery of isoflurane to the brain tissue was not directly measured, various physiological parameters including breathing rate, skin colour, and reflexive withdrawal were monitored in an attempt to assess anaesthetic depth. Throughout the experiment, isoflurane delivery was adjusted between ~1%-1.5% v/v in inhaled gas such that a breathing rate of one breath per second, a light pink hue visible on the skin of the ears and paws, and areflexia were maintained. It was hoped that by monitoring these physiological signs and adjusting the anaesthetic delivery accordingly, anaesthetic depth would remain relatively constant throughout and across each experiment. In support, time control experiments testing the stability of neuronal firing rate showed that, aside from slight ~20-minute fluctuations, the activity of any one neurone remained relatively stable over the course of 3 hours. This result indicates that no unseen factors were exerting sustained excitatory or inhibitory influences over the timescale used to assess pharmacological action (minimum 1 hour).

8.3.2 The painful nature of experimental set-up

Another issue with the methodology used in this investigation is the painful nature of the experimental set-up. Tracheotomy, necessary to maintain uniform delivery of anaesthetic gas and oxygen to the animals, is an invasive and therefore painful procedure. In addition, securing the skull position with ear bars and a nose clamp requires constant pressure to be applied to these body regions. Whilst essential to allow stable neuronal recordings, this stereotaxic frame is also expected to represent sustained nociceptive stimulation. As a consequence, the naïve

state should be considered to involve a certain degree of persistent pain. The primary implications of persistent nociceptive input in the naïve condition regard the comparisons of neurones recorded in these animals with those recorded from animals in the carrageenan-induced inflammatory tonic pain state. If both states involve a degree of persistent pain, any differences witnessed between the characteristics of recorded neurones, such as firing rate, firing pattern and naloxone sensitivity, cannot be said to reflect changes induced by persistent pain. Instead, changes upon carrageenan injection can be said to reflect the VTA neurone response to an additional, perhaps more intense, nociceptive insult at a different location and of a different nature to that already being inflicted. An alternative explanation for changes in activity lies in the relative salience of the two forms of nociceptive input. A well-established evidence-based theory surrounding VTA dopamine neurone function – or at least that of a proportion of the population – is the encoding of salience (Matsumoto and Hikosaka, 2009). Nociceptive input from the set-up apparatus and procedure may no longer represent a salient stimulus as it remains unchanged from the point of set-up. Conversely, the injection of carrageenan and the inflammation that ensues is a novel form of nociceptive stimulation that continues to grow in intensity as the inflammation develops, thereby maintaining salience across the subsequent two hours of neuronal recording. Hence, if a population of VTA neurones were indeed encoding salience, one would expect carrageenan injection to instigate a sustained change in firing – in fitting with the results obtained here.

The persistently painful nature of the set-up also has implications for the interpretation of baseline neurone characteristics found in naïve animals. It is not possible to confidently extrapolate these findings, including those surrounding population measures of burst firing behaviour, firing rate, and nociception and opioid responsivity, to the natural functioning of the VTA neurones in a pain-free state. Fortunately, most existing data relating to the function of the VTA neurones as part of the pain-processing system was also collected during experiments involving some sort of painful set-up procedure, allowing theoretical models to be constructed from considerations of both current and previous findings. However, any the ability to draw parallels with behavioural findings is limited (e.g. Paalzow et al., 1992), as naïve animals participating in behavioural experiments are typically in a pain-free state to begin with.

8.4 Therapeutic potential of this system

In light of the abundance of evidence suggesting an antinociceptive role for dopamine, this system presents itself as a possible target for therapeutic intervention in chronic pain. Through building our understanding of the unique and intricate role that DA plays in pain processing, we should identify ways to exploit underlying mechanisms to alleviate human suffering.

Prime clinical targets for dopamine-related treatments are the chronic pain conditions partially characterized by dysfunctional dopamine neurone function. For example, fibromyalgia, a disorder characterised by chronic widespread pain and concomitant digit hyperalgesia and allodynia, has been associated with dopaminergic dysfunction; along with evidence suggesting a reduced presynaptic level of dopamine synthesis in widespread brain areas (Wood et al., 2007b), patients also demonstrated a profound disruption of DA release in response to tonic pain (Wood et al., 2007a). Similarly, patients with the chronic orofacial condition, burning mouth syndrome, typically show alterations in striatal dopamine, with reduced presynaptic activity of dopamine neurones and changes in D2 receptor availability (Hagelberg et al., 2003a, 2003b; Jääskeläinen et al., 2001). Finally, a condition well established to be caused solely by the pathological death of dopamine neurones, Parkinson's disease, is also frequently associated with painful symptoms (Lee et al., 2006). The nature of the pain condition experienced by Parkinson's disease patients is highly variable, and often precedes the onset of parkinsonism itself (Ford, 1998). This may be somewhat complicated by the possibility of painful muscle rigidity as a consequence of the dopamine deficit rather than a central role of the transmitter in pain.

Hence, these cases present opportunities to employ dopamine system manipulations as symptomatic relief at the very least. The precise nature of this intervention, however, will depend on which element of dopamine signalling the dysfunction is centred around. For example, reduced dopaminergic synthetic capacity, such as in the case of Parkinson's disease, may be successfully targeted by manoeuvres that either promote dopamine synthesis (L-DOPA) or mimic the activity of DA (DA receptor agonists). Conversely, for conditions in which there is no pathological disruption of DA synthesis, it may make more sense to inhibit synaptic reuptake, effectively amplifying physiological dopamine action.

Unfortunately, application of treatments targeting the dopamine system is not all that straightforward. Alongside negative central side effects of psychosis and vulnerability to addiction (Kapur and Seeman, 2002; Salamone et

al., 2003), a key problem associated with the untargeted systemic administration of these compounds stems from their direct or indirect ability to activate peripheral dopamine-sensitive chemoreceptors, triggering nausea. This holds true for levodopa administration, with conversion to dopamine being abundant in the peripheral as well as the central nervous system. In order to prevent the peripheral synthesis of dopamine from levodopa, we co-administered a. Fortunately, this issue can be overcome by the co-administration of a peripheral DOPA decarboxylase inhibitor, carbidopa, along with L-DOPA, as done here and in the case of Parkinsons' patients. Similarly, a peripheral dopamine receptor antagonist could be administered along with effective dopamine receptor agonists.

Another important detail to consider with dopamine-targeted treatments is dosage. Several studies have encountered biphasic dose-response characteristics of dopamine agonists, characterized by hyperalgesia at low doses, and analgesia at much higher doses (Pelissier et al., 2006). Both the current and previous findings show that this quirk stretches to the effects of L-DOPA at low and high doses in terms of dopamine release (Abercrombie et al., 1990), dopamine neurone activity (the current studies), and behavioural expression of pain (Paalzow, 1992). The mechanisms thought to be behind these results were discussed in section 4.5.5, but crucially, when considering both direct dopamine receptor agonists and L-DOPA-derived dopamine, it is the relatively low affinity of postsynaptic receptors that render high doses necessary.

So, what is the current picture with regards to dopamine-based therapy? As it stands, there is a vast range of candidates, which hitchhike on a wide variety of endogenous control mechanisms. Perhaps most promisingly, dopamine agonists do show hints of being effective analgesics in patients with fibromyalgia (FM). The D2/D3 receptor agonist pramipexole resulted in significant clinical benefits, including reduced pain in both preliminary and subsequent randomised controlled FM trials (Holman, 2003; Holman and Myers, 2005). Of the same ilk, exogenous dopamine reuptake inhibition by the compound bupropion has unsurprisingly lead to significant improvements of pain and quality of life in neuropathic patients (Semenchuk et al., 2001).

At another level, NMDA receptor agonists have also been recognised for their impact on the dopamine system. At low doses, the agonist ketamine produces significant attenuation of both pain intensity and unpleasantness in experimental models of visceral hyperalgesia (Strigo et al., 2005; Willert et al., 2004). This action has been found to occur, at least in part, through the activation of D1 and D2 DA receptors, placing this treatment in the realms

of dopaminergic control (Forman, 1999). Crucially, this intervention currently appears efficacious in subsets of patients with neuropathic pain and fibromyalgia (Henriksson and Sörensen, 2002; Jørum et al., 2003).

Unfortunately, however, there are many cases in which the obvious interventions are entirely unsuccessful. As described, nicotinic acetylcholine receptors exert control over DA neurone activity, and consequently DA release in the NAcc (Champtiaux et al., 2003). Promisingly, exogenous activation of these receptors elicits antinociceptive effects (Jain, 2004); however, the most promising candidate to date, the selective $\alpha 4\beta 2$ receptor agonist ABT-894, failed to produce significant benefits in phase II clinical trials (Rowbotham et al., 2012). Similarly, a D2/D3 agonist ropinirole, very similar in action to pramipexole, failed to produce benefits significantly greater than placebo, despite showing promise at the preliminary stage (Holman, 2003). The latter results are merely a small sample of those highlighting how the dose-dependency and heterogeneity of the system make subtle differences in compounds all-important when it comes to efficacy.

Hence, in conclusion, when it comes to therapeutic success, the multifaceted and heterogeneous nature of the VTA DA system is both a blessing and a curse; whilst opening up opportunity for a many separately targeted approaches, the complexity that ensues leads to a necessity for extremely fine detail in drug design. With further investigation of the VTA and its connectivity, leading to further understanding of the system as a whole, it is possible that a highly effective treatment could emerge.

9. Bibliography

Abercrombie, E.D., Bonatz, A.E., and Zigmond, M.J. (1990). Effects ofl-DOPA on extracellular dopamine in striatum of normal and 6-hydroxydopamine-treated rats. Brain Res. *525*, 36–44.

Adell, A., and Artigas, F. (2004). The somatodendritic release of dopamine in the ventral tegmental area and its regulation by afferent transmitter systems. Neurosci. Biobehav. Rev. *28*, 415–431.

Aghajanian, G.K., and Bunney, B.S. (1977). Dopamine "autoreceptors": pharmacological characterization by microiontophoretic single cell recording studies. Naunyn. Schmiedebergs. Arch. Pharmacol. *297*, 1–7.

Aksenov, D.P., Li, L., Iordanescu, G., Miller, M.J., and Wyrwicz, A.M. (2014). Volume effect of localized injection in functional MRI and electrophysiology. Magn. Reson. Med. *72*, 1170–1175.

Al-Hasani, R., and Bruchas, M.R. (2011). NIH Public Access. Anesthesiology *115*, 1363–1381.

Altier, N., and Stewart, J. (1993). Intra-VTA infusions of the substance P analogue, DiMe-C7, and intra-accumbens infusions of amphetamine induce analgesia in the formalin test for tonic pain. Brain Res. *628*, 279–285.

Altier, N., and Stewart, J. (1999). The role of dopamine in the nucleus accumbens in analgesia. Life Sci. *65*, 2269–2287.

Apkarian, A.V., Bushnell, M.C., Treede, R.-D., and Zubieta, J.-K. (2005). Human brain mechanisms of pain perception and regulation in health and disease. Eur. J. Pain *9*, 463–484.

Arnér, S., and Meyerson, B.A. (1988). Lack of analgesic effect of opioids on neuropathic and idiopathic forms of pain. Pain *33*, 11–23.

Balcita-Pedicino, J.J., Omelchenko, N., Bell, R., and Sesack, S.R. (2011). The inhibitory influence of the lateral habenula on midbrain dopamine cells: ultrastructural evidence for indirect mediation via the rostromedial mesopontine tegmental nucleus. J. Comp. Neurol. *519*, 1143–1164.

Bannon, M.J., and Roth, R.H. (1983). Pharmacology of mesocortical dopamine neurons. Pharmacol. Rev. *35*.

Le Bars, D., Chitour, D., Kraus, E., Dickenson, A.H., and Besson, J.M. (1981). Effect of naloxone upon diffuse noxious inhibitory controls (DNIC) in the rat. Brain Res. *204*, 387–402.

Basbaum, A.I., Bautista, D.M., Scherrer, G., and Julius, D. (2009). Cellular and molecular mechanisms of pain. Cell *139*, 267–284.

Bassareo, V., De Luca, M.A., and Di Chiara, G. (2002). Differential Expression of Motivational Stimulus Properties by Dopamine in Nucleus Accumbens Shell versus Core and Prefrontal Cortex. J. Neurosci. *22*, 4709–4719.

Bayer, V.E., and Pickel, V.M. (1991). GABA-labeled terminals form proportionally more synapses with dopaminergic neurons containing low densities of tyrosine hydroxylase-immunoreactivity in rat ventral tegmental area.

Beart, P.M., and McDonald, D. (1982). 5-Hydroxytryptamine and 5-hydroxytryptaminergic-dopaminergic interactions in the ventral tegmental area of rat brain. J. Pharm. Pharmacol. *34*, 591–593.

Beaulieu, J.-M., and Gainetdinov, R.R. (2011). The Physiology, Signaling, and Pharmacology of Dopamine Receptors. Pharmacol. Rev. *63*, 182–217.

Bernardini, G.L., Gu, X., Viscardi, E., and German, D.C. (1991). Amphetamine-induced and spontaneous release of dopamine from A9 and A10 cell dendrites: an in vitro electrophysiological study in the mouse. J. Neural Transm. *84*, 183–193.

Berridge, K.C. (2003). Pleasures of the brain. Brain Cogn. *52*, 106–128.

Berridge, K.C. (2007). The debate over dopamine's role in reward: the case for incentive salience. Psychopharmacology (Berl). *191*, 391–431.

Berridge, K.C., and Robinson, T.E. (1998). What is the role of dopamine in reward: hedonic impact, reward learning, or incentive salience? Brain Res. Rev. *28*, 309–369.

Bessou, P., and Perl, E.R. (1969). Response of cutaneous sensory units with unmyelinated fibers to noxious stimuli. J Neurophysiol *32*, 1025–1043.

Van Bockstaele, E.J., and Pickel, V.M. (1995). GABA-containing neurons in the ventral tegmental area project to the nucleus accumbens in rat brain. Brain Res. *682*, 215-221.

Bouthenet, M.L., Martres, M.P., Sales, N., and Schwartz, J.C. (1987). A detailed mapping of dopamine D-2 receptors in rat central nervous system by autoradiography with [125I]iodosulpride. Neuroscience *20*, 117–155.

Bradberry, C.W., and Roth, R.H. (1989). Cocaine increases extracellular dopamine in rat nucleus accumbens and ventral tegmental area as shown by in vivo microdialysis. Neurosci. Lett. *103*, 97–102.

Breiter, H.C., Gollub, R.L., Weisskoff, R.M., Kennedy, D.N., Makris, N., Berke, J.D., Goodman, J.M., Kantor, H.L., Gastfriend, D.R., Riorden, J.P., et al. (1997). Acute effects of cocaine on human brain activity and emotion. Neuron *19*, 591–611.

Breivik, H., Collett, B., Ventafridda, V., Cohen, R., and Gallacher, D. (2006). Survey of chronic pain in Europe: prevalence, impact on daily life, and treatment. Eur. J. Pain *10*, 287–333.

Brischoux, F., Chakraborty, S., Brierley, D.I., and Ungless, M.A. (2009). Phasic excitation of dopamine neurons in ventral VTA. PNAS *106,* 4894-4899.

Bromberg-Martin, E.S., Matsumoto, M., and Hikosaka, O. (2010). Dopamine in Motivational Control: Rewarding, Aversive, and Alerting. Neuron *68*, 815–834.

Bronstein, D.M., Schafer, M.K.-H., Watson, S.J., and Akil, H. (1992). Evidence that β-endorphin is synthesized in cells in the nucleus tractus solitarius: detection of POMC mRNA. Brain Res. *587*, 269–275.

Budygin, E.A., Park, J., Bass, C.E., Grinevich, V.P., Bonin, K.D., and Wightman, R.M. (2012). Aversive stimulus differentially triggers subsecond dopamine release in reward regions. Neuroscience *201*, 331–337.

Bunney, B.S., Aghajanian, G.K., and Roth, R.H. (1973). Comparison of Effects of L-Dopa, Amphetamine and Apomorphine on Firing Rate of Rat Dopaminergic Neurones. Nature *245*, 123–125.

Burgess, P.R., and Perl, E.R. (1973). Somatosensory System. A. Iggo, ed. (Berlin, Heidelberg: Springer Berlin Heidelberg), pp. 29–78.

Burkey, A.R., Carstens, E., and Jasmin, L. (1999). Dopamine reuptake inhibition in the rostral agranular insular cortex produces antinociception. J. Neurosci. *19*, 4169–4179.

Cameron, D.L., Wessendorf, M.W., and Williams, J.T. (1997). A subset of ventral tegmental area neurons is inhibited by dopamine, 5-hydroxytryptamine and opioids. Neuroscience *77*, 155–166.

Carey, R.M. (2001). Renal Dopamine System. Hypertension *38*, 297–302.

Carlezon, W.A., Devine, D.P., and Wise, R.A. (1995). Habit-forming actions of nomifensine in nucleus accumbens. Psychopharmacology (Berl). *122*, 194–197.

Carr, D.B., and Sesack, S.R. (2000). Projections from the Rat Prefrontal Cortex to the Ventral Tegmental Area: Target Specificity in the Synaptic Associations with Mesoaccumbens and Mesocortical Neurons. J. Neurosci. *20*, 3864–3873.

Casey, K.L., and Morrow, T.J. (1983). Nocifensive responses to cutaneous thermal stimuli in the cat: stimulus-response profiles, latencies, and afferent activity. J Neurophysiol *50*, 1497–1515.

Champtiaux, N., Gotti, C., Cordero-Erausquin, M., David, D.J., Przybylski, C., Léna, C., Clementi, F., Moretti, M., Rossi, F.M., Le Novère, N., et al. (2003). Subunit composition of functional nicotinic receptors in dopaminergic neurons investigated with knock-out mice. J. Neurosci. *23*, 7820–7829.

Chang, P.-C., Pollema-Mays, S.L., Centeno, M.V., Procissi, D., Contini, M., Baria, A.T., Martina, M., and Apkarian, A.V. (2014). Role of nucleus accumbens in neuropathic pain: linked multi-scale evidence in the rat transitioning to neuropathic pain. Pain *155*, 1128–1139.

Charlety, P.J., Grenhoff, J., Chergui, K., Chapelle, B.D. La, Buda, M., Svensson, T.H., and Chouvet, G. (1991). Burst firing of mesencephalic dopamine neurons is inhibited by somatodendritic application of kynurenate. Acta Physiol. Scand. *142*, 105–112.

Chen, N.-H., and Reith, M.E.A. (2002). Effects of Locally Applied Cocaine, Lidocaine, and Various Uptake Blockers on Monoamine Transmission in the Ventral Tegmental Area of Freely Moving Rats: A Microdialysis Study on Monoamine Interrelationships. J. Neurochem. *63*, 1701–1713.

Chen, J.F., Qin, Z.H., Szele, F., Bai, G., and Weiss, B. (1991). Neuronal localization and modulation of the D2 dopamine receptor mRNA in brain of normal mice and mice lesioned with 6-hydroxydopamine. Neuropharmacology *30*, 927–941.

Chen, Y., Mestek, A., Liu, J., Hurley, J., and Yu, L. (1993). Molecular cloning and functional expression of a mu-opioid receptor from rat brain. Mol. Pharmacol. *44*, 8–12.

Chenu, F., Ghanbari, R., El Mansari, M., and Blier, P. (2012). An enhancement of the firing activity of dopamine neurons as a common denominator of antidepressant treatments? Int. J. Neuropsychopharmacol. *15*, 551-3-7.

Chergui, K., Charléty, P.J., Akaoka, H., Saunier, C.F., Brunet, J.L., Buda, M., Svensson, T.H., and Chouvet, G. (1993). Tonic activation of NMDA receptors causes spontaneous burst discharge of rat midbrain dopamine neurons in vivo. Eur. J. Neurosci. *5*, 137–144.

Chiodo, L.A., Bannon, M.J., Grace, A.A., Roth, R.H., and Bunney, B.S. (1984). Evidence for the absence of impulse-regulating somatodendritic and synthesis-modulating nerve terminal autoreceptors on subpopulations of mesocortical dopamine neurons. Neuroscience *12*, 1–16.

Clark, D., and Chiodo, L.A. (1988). Electrophysiological and pharmacological characterization of identified nigrostriatal and mesoaccumbens dopamine neurons in the rat. Synapse *2*, 474–485.

Clarke, P.B.S., and Franklin, K.B.J. (1992). Infusions of 6-hydroxydopamine into the nucleus accumbens abolish the analgesic effect of amphetamine but not of morphine in the formalin test. Brain Res. *580*, 106–110.

Clements, J.R., and Grant, S. (1990). Glutamate-like immunoreactivity in neurons of the laterodorsal tegmental and pedunculopontine nuclei in the rat. Neurosci. Lett. *120*, 70–73.

Cohen, J.Y., Haesler, S., Vong, L., Lowell, B.B., and Uchida, N. (2012). Neuron-type-specific signals for reward and punishment in the ventral tegmental area. Nature *482*, 85–88.

Cohen, S.R., Abbott, F. V., and Melzack, R. (1984). Unilateral analgesia produced by intraventricular morphine. Brain Res. *303*, 277–287.

Cooper, D.C. (2002). The significance of action potential bursting in the brain reward circuit. Neurochem. Int. *41*, 333–340.

Cox, J.J., Reimann, F., Nicholas, A.K., Thornton, G., Roberts, E., Springell, K., Karbani, G., Jafri, H., Mannan, J., Raashid, Y., et al. (2006). An SCN9A channelopathy causes congenital inability to experience pain. Nature *444*, 894–898.

Cragg, S., Rice, M.E., and Greenfield, S.A. (1997). Heterogeneity of electrically evoked dopamine release and reuptake in substantia nigra, ventral tegmental area, and striatum. J. Neurophysiol. *77*, 863–873.

Dahlstroem, A., and Fuxe, K. (1964). Evidence for the existence of monoamine-containing neurons in the central nervous system. I. Demonstration of monoamines in the cell bodies of brain stem neurons. Acta Physiol. Scand. Suppl. Suppl 232:1-55.

Dobi, A., Margolis, E.B., Wang, H.-L., Harvey, B.K., and Morales, M. (2010). Glutamatergic and nonglutamatergic neurons of the ventral tegmental area establish local synaptic contacts with dopaminergic and nondopaminergic neurons. J. Neurosci. *30*, 218–229.

Drewnowski, A., Krahn, D., Demitrack, M., Nairn, K., and Gosnell, B. (1995). Naloxone, an opiate blocker, reduces the consumption of sweet high-fat foods in obese and lean female binge eaters. Am J Clin Nutr *61*, 1206–1212.

Dreyer, J.K., Herrik, K.F., Berg, R.W., and Hounsgaard, J.D. (2010). Influence of Phasic and Tonic Dopamine Release on Receptor Activation. J. Neurosci. *30*, 14273–14283.

Dubner, R., and Ruda, M.A. (1992). Activity-dependent neuronal plasticity following tissue injury and inflammation. Trends Neurosci. *15*, 96–103.

Dubuisson, D., and Dennis, S.G. (1977). The formalin test: a quantitative study of the analgesic effects of morphine, meperidine, and brain stem stimulation in rats and cats. Pain *4*, 161–174.

Dum, J., and Herz, A. (1984). Endorphinergic Modulation of Neural Reward Systems Indicated by Behavioral Changes. Pharmacol. Biochem. Behav. *21*, 259–266.

Eiden, L.E., Schäfer, M.K.-H., Weihe, E., and Schütz, B. (2004). The vesicular amine transporter family (SLC18): amine/proton antiporters required for vesicular accumulation and regulated exocytotic secretion of monoamines and acetylcholine. Pflügers Arch. Eur. J. Physiol. *447*, 636–640.

Evans, C.J., Keith, D.E., Morrison, H., Magendzo, K., and Edwards, R.H. (1992). Cloning of a delta opioid receptor by functional expression. Science *258*, 1952–1955.

Ewan, E.E., and Martin, T.J. (2011). Opioid facilitation of rewarding electrical brain stimulation is suppressed in rats with neuropathic pain. Anesthesiology *114*, 624–632.

Fà, M., Mereu, G., Ghiglieri, V., Meloni, A., Salis, P., and Gessa, G.L. (2003). Electrophysiological and pharmacological characteristics of nigral dopaminergic neurons in the conscious, head-restrained rat. Synapse *48*, 1–9.

Farmer, M.A., Baliki, M.N., and Apkarian, A.V. (2012). A dynamic network perspective of chronic pain. Neurosci. Lett. *520*, 197–203.

Faure, P., Tolu, S., Valverde, S., and Naudé, J. (2014). Role of nicotinic acetylcholine receptors in regulating dopamine neuron activity. Neuroscience *282C*, 86–100.

Fenu, S., Spina, L., Rivas, E., Longoni, R., and Di Chiara, G. (2006). Morphine-conditioned single-trial place preference: role of nucleus accumbens shell dopamine receptors in acquisition, but not expression. Psychopharmacology (Berl). *187*, 143–153.

Fibiger, H., LePiane, F., Jakubovic, A., and Phillips, A. (1987). The role of dopamine in intracranial self-stimulation of the ventral tegmental area. J. Neurosci. *7*, 3888–3896.

Fields, H.L. (2000). Pain modulation: expectation, opioid analgesia and virtual pain. Prog. Brain Res. *122*, 245–253.

Fields, H.L. (2007). Understanding How Opioids Contribute to Reward and Analgesia. Reg. Anesth. Pain Med. *32*, 242–246.

Fields, H.L., Basbaum, A., and Heinricher, M. (2005). Central Nervous System Mechanisms of Pain Modulation. In Textbook of Pain, (Edinburgh: Churchill Livingstone), pp. 125–142.

Finnerup, N.B., Otto, M., Jensen, T.S., and Sindrup, S.H. (2007). An evidence-based algorithm for the treatment of neuropathic pain. MedGenMed *9*, 36.

Firestone, L.L., Gyulai, F., Mintun, M., Adler, L.J., Urso, K., and Winter, P.M. (1996). Human brain activity response to fentanyl imaged by positron emission tomography. Anesth. Analg. *82*, 1247–1251.

Floresco, S.B., West, A.R., Ash, B., Moore, H., and Grace, A.A. (2003). Afferent modulation of dopamine neuron firing differentially regulates tonic and phasic dopamine transmission. Nat. Neurosci. *6*, 968–973.

Ford, B. (1998). Pain in Parkinson's disease. Clin. Neurosci. *5*, 63–72.

Ford, C.P. (2014). The role of D2-autoreceptors in regulating dopamine neuron activity and transmission. Neuroscience *282*, 13–22.

Ford, B., Holmes, C.J., Mainville, L., and Jones, B.E. (1995). GABAergic neurons in the rat pontomesencephalic tegmentum: codistribution with cholinergic and other tegmental neurons projecting to the posterior lateral hypothalamus. J. Comp. Neurol. *363*, 177–196.

Ford, C.P., Mark, G.P., and Williams, J.T. (2006). Properties and opioid inhibition of mesolimbic dopamine neurons vary according to target location. J. Neurosci. *26*, 2788–2797.

Forman, L.J. (1999). NMDA receptor antagonism produces antinociception which is partially mediated by brain opioids and dopamine. Life Sci. *64*, 1877–1887.

Franklin, K.B.. (1998). Analgesia and Abuse Potential: An Accidental Association or a Common Substrate? Pharmacol. Biochem. Behav. *59*, 993–1002.

Franklin, K.B.J. (1989). Analgesia and the neural substrate of reward. Neurosci. Biobehav. Rev. *13*, 149–154.

Freeman, A.S., Meltzer, L.T., and Bunney, B.S. (1985). Firing properties of substantia nigra dopaminergic neurons in freely moving rats. Life Sci. *36*, 1983–1994.

Fujimura, K., and Matsuda, Y. (1989). Autogenous oscillatory potentials in neurons of the guinea pig substantia nigra pars compacta in vitro. Neurosci. Lett. *104*, 53–57.

Fukuda, K., Kato, S., Mori, K., Nishi, M., and Takeshima, H. (1993). Primary structures and expression from cDNAs of rat opioid receptor delta- and mu-subtypes. FEBS Lett. *327*, 311–314.

Gariano, R.F., Tepper, J.M., Sawyer, S.F., Young, S.J., and Groves, P.M. (1989). Mesocortical dopaminergic neurons. 1. Electrophysiological properties and evidence for soma-dendritic autoreceptors. Brain Res. Bull. *22*, 511–516.

Garzón, M., and Pickel, V.M. (2001). Plasmalemmal mu-opioid receptor distribution mainly in nondopaminergic neurons in the rat ventral tegmental area. Synapse *41*, 311–328.

Gear, R.W., Aley, K.O., and Levine, J.D. (1999). Pain-induced analgesia mediated by mesolimbic reward circuits. J. Neurosci. *19*, 7175–7181.

Geffen, L.B., Jessell, T.M., Cuello, A.C., and Iversen, L.L. (1976). Release of dopamine from dendrites in rat substantia nigra. Nature *260*, 258–260.

Georges, F. (2006). No Effect of Morphine on Ventral Tegmental Dopamine Neurons during Withdrawal. J. Neurosci. *26*, 5720–5726.

Gibson, A.R., Houk, J.C., and Kohlerman, N.J. (1985). Magnocellular red nucleus activity during different types of limb movement in the macaque monkey. J. Physiol. *358*, 527–549.

Gilron, I., Baron, R., and Jensen, T. (2015). Neuropathic Pain: Principles of Diagnosis and Treatment. Mayo Clin. Proc. *90*, 532–545.

Gold, M.S., and Gebhart, G.F. (2010). Nociceptor sensitization in pain pathogenesis. Nat. Med. *16*, 1248–1257.

Gold, C., Henze, D.A., Koch, C., and Buzsáki, G. (2006). On the origin of the extracellular action potential waveform: A modeling study. J. Neurophysiol. *95*, 3113–3128.

Grace, A.A. (1991). Phasic versus tonic dopamine release and the modulation of dopamine system responsivity: A hypothesis for the etiology of schizophrenia. Neuroscience *41*, 1–24.

Grace, A.A., and Bunney, B.S. the Control of Firing Pattern in nigral dopamine Neurons: Burst Firing. J. Neurosci. *4*, 2877–2890.

Grace, A.A., and Bunney, B.S. The control of firing pattern in nigral dopamine neurones: single spike firing. J. Neurosci. *4*, 2866–2876.

Grace, A.A., and Bunney, B.S. (1983). Intracellular and extracellular electrophysiology of nigral dopaminergic neurons-1. Identification and characterisation. *10*, 301–315.

Grace, A.A., and Onn, S.P. (1989). Morphology and electrophysiological properties of immunocytochemically identified rat dopamine neurons recorded in vitro. J. Neurosci. *9*, 3463–3481.

Gresch, P.J., Sved, a F., Zigmond, M.J., and Finlay, J.M. (1995). Local influence of endogenous norepinephrine on extracellular dopamine in rat medial prefrontal cortex. J. Neurochem. *65*, 111–116.

Gurevich, E. V, and Joyce, J.N. (1999). Distribution of dopamine D3 receptor expressing neurons in the human forebrain: comparison with D2 receptor expressing neurons. Neuropsychopharmacology *20*, 60–80.

Guyenet, P.G., and Aghajanian, G.K. (1978). Antidromic identification of dopaminergic and other output neurons of the rat substantia nigra. Brain Res. *150*, 69–84.

Gysling, K., and Wang, R.Y. (1983). Morphine-induced activation of A10 dopamine neurons in the rat. Brain Res. *277*, 119–127.

Hagelberg, N., Martikainen, I.K., Mansikka, H., Hinkka, S., Någren, K., Hietala, J., Scheinin, H., and Pertovaara, A. (2002). Dopamine D2 receptor binding in the human brain is associated with the response to painful stimulation and pain modulatory capacity. Pain *99*, 273–279.

Hagelberg, N., Forssell, H., Aalto, S., Rinne, J.O., Scheinin, H., Taiminen, T., Någren, K., Eskola, O., and Jääskeläinen, S.K. (2003a). Altered dopamine D2 receptor binding in atypical facial pain. Pain *106*, 43–48.

Hagelberg, N., Forssell, H., Rinne, J.O., Scheinin, H., Taiminen, T., Aalto, S., Luutonen, S., Någren, K., and Jääskeläinen, S. (2003b). Striatal dopamine D1 and D2 receptors in burning mouth syndrome. Pain *101*, 149–154.

Hargreaves, K., Dubner, R., Brown, F., Flores, C., and Joris, J. (1988). A new and sensitive method for measuring thermal nociception in cutaneous hyperalgesia. Pain *32*, 77–88.

Harris, Webb, and Greenfield (1989). A possible pacemaker mechanism in pars compacta neurons of the guinea-pig substantia nigra revealed by various ion channel blocking agents. Neuroscience *31*, 355–362.

Harris, K.D., Quiroga, R.Q., Freeman, J., and Smith, S.L. (2016). Improving data quality in neuronal population recordings. Nat. Neurosci. *19*, 1165–1174.

Henriksson, K.G., and Sörensen, J. (2002). The promise of N-methyl-D-aspartate receptor antagonists in fibromyalgia. Rheum. Dis. Clin. North Am. *28*, 343–351.

Herter, T.M., Takei, T., Munoz, D.P., and Scott, S.H. (2015). Neurons in red nucleus and primary motor cortex exhibit similar responses to mechanical perturbations applied to the upper-limb during posture. Front. Integr. Neurosci. *9*, 29.

Hervé, D., Pickel, V.M., Joh, T.H., and Beaudet, A. (1987). Serotonin axon terminals in the ventral tegmental area of the rat: fine structure and synaptic input to dopaminergic neurons. Brain Res. *435*, 71–83.

Hill, K.G., and Kiefer, S.W. (1997). Naltrexone Treatment Increases the Aversiveness of Alcohol for Outbred Rats. Alcohol. Clin. Exp. Res. *21*, 637–641.

Hipólito, L., Wilson-Poe, A., Campos-Jurado, Y., Zhong, E., Gonzalez-Romero, J., Virag, L., Whittington, R., Comer, S.D., Carlton, S.M., Walker, B.M., et al. (2015). Inflammatory Pain Promotes Increased Opioid Self-Administration: Role of Dysregulated Ventral Tegmental Area μ Opioid Receptors. J. Neurosci. *35*, 12217–12231.

Hjelmstad, G.O., Xia, Y., Margolis, E.B., and Fields, H.L. (2013). Opioid modulation of ventral pallidal afferents to ventral tegmental area neurons. J. Neurosci. *33*, 6454–6459.

Hnasko, T.S., Sotak, B.N., and Palmiter, R.D. (2005). Morphine reward in dopamine-deficient mice. Nature *438*, 854–857.

du Hoffmann, J., Kim, J.J., and Nicola, S.M. (2011). An inexpensive drivable cannulated microelectrode array for simultaneous unit recording and drug infusion in the same brain nucleus of behaving rats. J. Neurophysiol. *106*, 1054–1064.

Höllt, V. (1990). Regulation of Opioid Peptide Gene Expression. In Handbook of Experimental Pharmacology, A. Herz, H. Akil, and E.J. Simon, eds. (Berlin, Heidelberg: Springer Berlin Heidelberg), pp. 307–346.

Holman, A.J. (2003). Ropinirole, open preliminary observations of a dopamine agonist for refractory fibromyalgia. J. Clin. Rheumatol. *9*, 277–279.

Holman, A.J., and Myers, R.R. (2005). A randomized, double-blind, placebo-controlled trial of pramipexole, a dopamine agonist, in patients with fibromyalgia receiving concomitant medications. Arthritis Rheum. *52*, 2495–2505.

Horvitz, J.. (2000). Mesolimbocortical and nigrostriatal dopamine responses to salient non-reward events. Neuroscience *96*, 651–656.

Howard, F.M. (2009). Endometriosis and mechanisms of pelvic pain. J. Minim. Invasive Gynecol. *16*, 540–550.

Hur, E.E., and Zaborszky, L. (2005). Vglut2 afferents to the medial prefrontal and primary somatosensory cortices: a combined retrograde tracing in situ hybridization study [corrected]. J. Comp. Neurol. *483*, 351–373.

Hurley, R.W., and Hammond, D.L. (2000). The analgesic effects of supraspinal mu and delta opioid receptor agonists are potentiated during persistent inflammation. J. Neurosci. *20*, 1249–1259.

Hyland, B.I., Reynolds, J.N.J., Hay, J., Perk, C.G., and Miller, R. (2002). Firing Modes of Midbrain Dopamine Cell in the Freely Moving Rat. Neuroscience *114*, 475–492.

Hylden, J.L.K., Thomas, D.A., Iadarola, M.J., Nahin, R.L., and Dubner, R. (1991). Spinal opioid analgesic effects are enhanced in a model of unilateral inflammation/hyperalgesia: possible involvement of noradrenergic mechanisms. Eur. J. Pharmacol. *194*, 135–143.

Ikemoto (2007). Dopamine reward circuitry: two projection systems from the ventral midbrain to the nucleus accumbens-olfactory tubercle coIkemoto. (2007). Dopamine reward circuitry: two projection systems from the ventral midbrain to the nucleus accumbens-olfactory tuber. *56*, 27–78.

Ikemoto, S. (2003). Involvement of the olfactory tubercle in cocaine reward: intracranial self-administration studies. J. Neurosci. *23*, 9305–9311.

Ikemoto, S., Murphy, J.M., and McBride, W.J. (1997). Self-infusion of GABA(A) antagonists directly into the ventral tegmental area and adjacent regions. Behav. Neurosci. *111*, 369–380.

Jääskeläinen, S.K., Rinne, J.O., Forssell, H., Tenovuo, O., Kaasinen, V., Sonninen, P., and Bergman, J. (2001). Role of the dopaminergic system in chronic pain -- a fluorodopa-PET study. Pain *90*, 257–260.

Jain, K.K. (2004). Modulators of nicotinic acetylcholine receptors as analgesics. Curr. Opin. Investig. Drugs *5*, 76–81.

Ji, R.-R., Kohno, T., Moore, K.A., and Woolf, C.J. (2003). Central sensitization and LTP: do pain and memory share similar mechanisms? Trends Neurosci. *26*, 696–705.

Johnson, S., and North, R. (1992a). Opioids excite dopamine neurons by hyperpolarization of local interneurons. J. Neurosci. *12*, 483–488.

Johnson, S.W., and North, R.A. (1992b). Two types of neurone in the rat ventral tegmental area and their synaptic inputs. J. Physiol. *450*, 455–468.

Johnson, S.W., Seutin, V., and North, R.A. (1992). Burst firing in dopamine neurons induced by N-methyl-D-aspartate: role of electrogenic sodium pump. Science *258*, 665–667.

Jones, A.K., Cunningham, V.J., Ha-Kawa, S., Fujiwara, T., Luthra, S.K., Silva, S., Derbyshire, S., and Jones, T. (1994). Changes in central opioid receptor binding in relation to inflammation and pain in patients with rheumatoid arthritis. Br. J. Rheumatol. *33*, 909–916.

Jørum, E., Warncke, T., and Stubhaug, A. (2003). Cold allodynia and hyperalgesia in neuropathic pain: the effect of N-methyl-D-aspartate (NMDA) receptor antagonist ketamine--a double-blind, cross-over comparison with alfentanil and placebo. Pain *101*, 229–235.

Kalivas, P.W. (1993). Neurotransmitter regulation of dopamine neurons in the ventral tegmental area. Brain Res. Brain Res. Rev. *18*, 75–113.

Kalivas, P.W., and Duffy, P. (1995a). D1 receptors modulate glutamate transmission in the ventral tegmental area. J. Neurosci. *15*, 5379–5388.

Kalivas, P.W., and Duffy, P. (1995b). D1 receptors modulate glutamate transmission in the ventral tegmental area. J. Neurosci. *15*, 5379–5388.

Kalivas, P., Widerlov, E., Stanley, D., Breese, G., and Prange, A.J. (1983). Enkephalin action on the mesolimbic system: a dopamine-dependent and a dopamine-independent increase in locomotor activity. J. Pharmacol. Exp. Ther. *227*, 229–237.

Kapur, S., and Seeman, P. (2002). NMDA receptor antagonists ketamine and PCP have direct effects on the dopamine D(2) and serotonin 5-HT(2)receptors-implications for models of schizophrenia. Mol. Psychiatry *7*, 837–844.

Kayser, V., and Guilbaud, G. (1981). Dose-dependent analgesic and hyperalgesic effects of systemic naloxone in arthritic rats. Brain Res. *226*, 344-348.

Kayser, V., and Guilbaud, G. (1983). The analgesic effects of morphine, but not those of the enkephalinase inhibitor thiorphan, are enhanced in arthritic rats. Brain Res. *267*, 131–138.

Kelley, A.E., and Berridge, K.C. (2002). The Neuroscience of Natural Rewards: Relevance to Addictive Drugs. J. Neurosci. *22*, 3306–3311.

Kennedy, P.R., Gibson, A.R., and Houk, J.C. (1986). Functional and anatomic differentiation between parvicellular and magnocellular regions of red nucleus in the monkey. Brain Res. *364*, 124–136.

Kenntner-Mabiala, R., and Pauli, P. (2005). Affective modulation of brain potentials to painful and nonpainful stimuli. Psychophysiology *42*, 559–567.

Khachaturian, H., Lewis, M.E., Schäfer, M.K.-H., and Watson, S.J. (1985). Anatomy of the CNS opioid systems. Trends Neurosci. *8*, 111–119.

Khaliq, Z.M., and Bean, B.P. (2010). Pacemaking in dopaminergic ventral tegmental area neurons: depolarizing drive from background and voltage-dependent sodium conductances. J. Neurosci. *30*, 7401–7413.

Kiaytkin, E.A. (1988). Functional Properties of Presumed Doparmine-Containing and Other Ventral Tegmental Area Neurons in Conscious Rats. Int. J. Neurosci. *42*, 21–43.

Kieffer, B.L., Befort, K., Gaveriaux-Ruff, C., and Hirth, C.G. (1992). The delta-opioid receptor: isolation of a cDNA by expression cloning and pharmacological characterization. Proc. Natl. Acad. Sci. U. S. A. *89*, 12048–12052.

Kim, S.H., and Chung, J.M. (1992). An experimental model for peripheral neuropathy produced by segmental spinal nerve ligation in the rat. Pain *50*, 355–363.

Kim, K.-M., Nakajima, Y., and Nakajima, S. (1995). G protein-coupled inward rectifier modulated by dopamine agonists in cultured substantia nigra neurons. Neuroscience *69*, 1145–1158.

Kita, H., and Kitai, S.T. (1987). Efferent projections of the subthalamic nucleus in the rat: light and electron microscopic analysis with the PHA-L method. J. Comp. Neurol. *260*, 435–452.

Kita, T., Kita, H., and Kitai, S.T. (1986). Electrical membrane properties of rat substantia nigra compacta neurons in an in vitro slice preparation. Brain Res. *372*, 21–30.

Kiyatkin, E.A., and Rebec, G. V (2001). Impulse activity of ventral tegmental area neurons during heroin self-administration in rats. Neuroscience *102*, 565–580.

Koepp, M.J., Gunn, R.N., Lawrence, A.D., Cunningham, V.J., Dagher, A., Jones, T., Brooks, D.J., Bench, C.J., and Grasby, P.M. (1998). Evidence for striatal dopamine release during a video game. Nature *393*, 266–268.

Kornhuber, J., Kim, J.-S., Kornhuber, M.E., and Kornhuber, H.H. (1984). The cortico-nigral projection: reduced glutamate content in the substantia nigra following frontal cortex ablation in the rat. Brain Res. *322*, 124–126.

Korotkova, T.M., Ponomarenko, A.A., Brown, R.E., and Haas, H.L. (2004). Functional Diversity of Ventral Midbrain Dopamine and GABAergic Neurons. Mol. Neurobiol. *29*, 243–259.

Kretschmer, B.D. (1999). Modulation of the mesolimbic dopamine system by glutamate: role of NMDA receptors. J. Neurochem. *73*, 839–848.

Lacey, M.G. (1993). Chapter 17 Neurotransmitter receptors and ionic conductances regulating the activity of neurones in substantia nigra pars compacta and ventral tegmental area. Prog. Brain Res. *99*, 251–276.

Lacey, M.G., Mercuri, N.B., and North, R.A. (1987). Dopamine acts on D2 receptors to increase potassium conductance in neurones of the rat substantia nigra zona compacta. J. Physiol. *392*, 397–416.

LaGraize, S.C., Borzan, J., Peng, Y.B., and Fuchs, P.N. (2006). Selective regulation of pain affect following activation of the opioid anterior cingulate cortex system. Exp. Neurol. *197*, 22–30.

Lammel, S., Hetzel, A., Häckel, O., Jones, I., Liss, B., and Roeper, J. (2008). Unique Properties of Mesoprefrontal Neurons within a Dual Mesocorticolimbic Dopamine System. Neuron *57*, 760–773.

Lammel, S., Ion, D.I., Roeper, J., and Malenka, R.C. (2011). Projection-specific modulation of dopamine neuron synapses by aversive and rewarding stimuli. Neuron *70*, 855–862.

Lammel, S., Lim, B.K., Ran, C., Huang, K.W., Betley, M.J., Tye, K.M., Deisseroth, K., and Malenka, R.C. (2012). Input-specific control of reward and aversion in the ventral tegmental area. Nature *491*, 212–217.

Lee, M.A., Walker, R.W., Hildreth, T.J., and Prentice, W.M. (2006). A survey of pain in idiopathic Parkinson's disease. J. Pain Symptom Manage. *32*, 462–469.

Lee, R.S., Steffensen, S.C., and Henriksen, S.J. (2001). Discharge profiles of ventral tegmental area GABA neurons during movement, anesthesia, and the sleep-wake cycle. J. Neurosci. *21*, 1757–1766.

Leknes, S., and Tracey, I. (2008). A common neurobiology for pain and pleasure. Nat. Rev. Neurosci. *9*, 314–320.

Lever, I., Cunningham, J., Grist, J., Yip, P.K., and Malcangio, M. (2003). Release of BDNF and GABA in the dorsal horn of neuropathic rats. Eur. J. Neurosci. *18*, 1169–1174.

Li, S., Zhu, J., Chen, C., Chen, Y.W., Deriel, J.K., Ashby, B., and Liu-Chen, L.Y. (1993). Molecular cloning and expression of a rat kappa opioid receptor. Biochem. J. *295 (Pt 3*, 629–633.

Li, W., Doyon, W.M., and Dani, J.A. (2012). Quantitative unit classification of ventral tegmental area neurons in vivo. J. Neurophysiol. *107*, 2808–2820.

Li, X., Qi, J., Yamaguchi, T., Wang, H.-L., and Morales, M. (2013). Heterogeneous composition of dopamine neurons of the rat A10 region: molecular evidence for diverse signaling properties. Brain Struct. Funct. *218*, 1159–1176.

Loggia, M.L., Berna, C., Kim, J., Cahalan, C.M., Gollub, R.L., Wasan, A.D., Harris, R.E., Edwards, R.R., and Napadow, V. (2014). Disrupted brain circuitry for pain-related reward/punishment in fibromyalgia. Arthritis Rheumatol. (Hoboken, N.J.) *66*, 203–212.

Lu, Y., Dong, H., Gao, Y., Gong, Y., Ren, Y., Gu, N., Zhou, S., Xia, N., Sun, Y.-Y., Ji, R.-R., et al. (2013). A feed-forward spinal cord glycinergic neural circuit gates mechanical allodynia. J. Clin. Invest. *123*, 4050–4062.

Lu, Y.F., Moriwaki, A., Tomizawa, K., Onuma, H., Cai, X.H., and Matsui, H. (1997). Effects of vasopressin and involvement of receptor subtypes in the rat central amygdaloid nucleus in vitro. Brain Res. *768*, 266–272.

Luo, A.H., Georges, F.E., and Aston-Jones, G.S. (2008). Novel neurons in ventral tegmental area fire selectively during the active phase of the diurnal cycle. Eur. J. Neurosci. *27*, 408–422.

Maarrawi, J., Peyron, R., Mertens, P., Costes, N., Magnin, M., Sindou, M., Laurent, B., and Garcia-Larrea, L. (2007). Differential brain opioid receptor availability in central and peripheral neuropathic pain. Pain *127*, 183–194.

Maley, B.E. (1996). Immunohistochemical localization of neuropeptides and neurotransmitters in the nucleus solitarius. Chem. Senses *21*, 367–376.

Malmberg, A.B., Hedley, L.R., Jasper, J.R., Hunter, J.C., and Basbaum, A.I. (2001). Contribution of alpha(2) receptor subtypes to nerve injury-induced pain and its regulation by dexmedetomidine. Br. J. Pharmacol. *132*, 1827–1836.

Mameli-Engvall, M., Evrard, A., Pons, S., Maskos, U., Svensson, T.H., Changeux, J.-P., and Faure, P. (2006). Hierarchical control of dopamine neuron-firing patterns by nicotinic receptors. Neuron *50*, 911–921.

Marbach, J.J., and Lund, P. (1981). Depression, anhedonia and anxiety in temporomandibular joint and other facial pain syndromes. Pain *11*, 73–84.

Margolis, E., Toy, B., Himmels, P., Morales, M., and Fields, H.L. (2012). Identification of rat ventral tegmental area GABAergic neurons. PLoS One *7*, e42365.

Margolis, E.B., Mitchell, J.M., Ishikawa, J., Hjelmstad, G.O., and Fields, H.L. (2008). Midbrain Dopamine Neurons: Projection Target Determines Action Potential Duration and Dopamine D2 Receptor Inhibition.*36*, 8908-8913.

Margolis, E.B., Hjelmstad, G.O., Bonci, A., and Fields, H.L. (2003). Kappa-opioid agonists directly inhibit midbrain dopaminergic neurons. J. Neurosci. *23*, 9981–9986.

Margolis, E.B., Lock, H., Hjelmstad, G.O., and Fields, H.L. (2006). The ventral tegmental area revisited: is there an electrophysiological marker for dopaminergic neurons? J. Physiol. *577*, 907–924.

Margolis, E.B., Mitchell, J.M., Ishikawa, J., Hjelmstad, G.O., and Fields, H.L. (2008). Midbrain dopamine neurons: projection target determines action potential duration and dopamine D(2) receptor inhibition. J. Neurosci. *28*, 8908–8913.

Margolis, E.B., Hjelmstad, X.G.O., Fujita, X.W., and Fields, X.H.L. (2014). Direct Bidirectional mu-Opioid Control of Midbrain Dopamine Neurons. *34*, 14707–14716.

Marinelli, M., and McCutcheon, J.E. (2014). Heterogeneity of dopamine neuron activity across traits and states.

Neuroscience *282*, 176–197.

Marinelli, M., Rudick, C.N., Hu, X.-T., and White, F.J. (2006). Excitability of dopamine neurons: modulation and physiological consequences. CNS Neurol. Disord. Drug Targets *5*, 79–97.

Marshall, J.F., Richardson, J.S., and Teitelbaum, P. (1974). Nigrostriatal bundle damage and the lateral hypothalamic syndrome. J. Comp. Physiol. Psychol. *87*, 808–830.

Martikainen, I.K., Nuechterlein, E.B., Pecina, M., Love, T.M., Cummiford, C.M., Green, C.R., Stohler, C.S., and Zubieta, J.-K. (2015). Chronic Back Pain Is Associated with Alterations in Dopamine Neurotransmission in the Ventral Striatum. J. Neurosci. *35*, 9957–9965.

Masahiko Funada, Tsutomu Suzuki, Minoru Narita, Miwa Misawa, and Hiroshi Nagase (1993). Blockade of morphine reward through the activation of κ-opioid receptors in mice. Neuropharmacology *32*, 1315–1323.

Matsuda, W., Furuta, T., Nakamura, K.C., Hioki, H., Fujiyama, F., Arai, R., and Kaneko, T. (2009). Single Nigrostriatal Dopaminergic Neurons Form Widely Spread and Highly Dense Axonal Arborizations in the Neostriatum. J. Neurosci. *2*, 444–453.

Matsumoto, M., and Hikosaka, O. (2009). Two types of dopamine neuron distinctly convey positive and negative motivational signals. Nature *459*, 837–841.

Matthews, R.T., and German, D.C. (1984). Electrophysiological evidence for excitation of rat ventral tegmental area dopamine neurons by morphine. Neuroscience *11*, 617–625.

McMahon, S., Koltzenburg, M., Tracey, I., and Turk, D.C. (2013). Wall & Melzack's Textbook of Pain (Elsevier Health Sciences).

De Mei, C., Ramos, M., Iitaka, C., and Borrelli, E. (2009). Getting specialized: presynaptic and postsynaptic dopamine D2 receptors. Curr. Opin. Pharmacol. *9*, 53–58.

Melis, M., Camarini, R., Ungless, M.A., and Bonci, A. (2002). Long-lasting potentiation of GABAergic synapses in dopamine neurons after a single in vivo ethanol exposure. J. Neurosci. *22*, 2074–2082.

Melzack, R., and Casey, K.L. (1968). Sensory, motivational and central control determinants of pain: a new conceptual model. In The Skin Senses, p.

Meng, F., Xie, G.X., Thompson, R.C., Mansour, A., Goldstein, A., Watson, S.J., and Akil, H. (1993). Cloning and pharmacological characterization of a rat kappa opioid receptor. Proc. Natl. Acad. Sci. *90*, 9954–9958.

Mercuri, N.B., Calabresi, P., and Bernardi, G. (1990). Responses of rat substantia nigra compacta neurones to L-DOPA. Br. J. Pharmacol. *100*, 257–260.

Mercuri, N.B., Saiardi, a, and Bonci, a (1997). Loss of Autoreceptor function in dopaminergic neurons from

dopamine D2 receptor deficient mice. Neuroscience *79*, 323–327.

Merskey, H., and Bogduk, N. (1994). Classification of Chronic Pain (Seattle: IASP press).

Millan, M.J. (2002). Descending control of pain. Prog. Neurobiol. *66*, 355–474.

Mirenowicz, J., and Schultz, W. (1996). Preferential activation of midbrain dopamine neurons by appetitive rather than aversive stimuli. Nature *379*, 449–451.

Missale, C., Nash, S.R., Robinson, S.W., Jaber, M., and Caron, M.G. (1998). Dopamine receptors: from structure to function. Physiol. Rev. *78*, 189–225.

Mogenson, G.J., Takigawa, M., Robertson, A., and Wu, M. (1979). Self-stimulation of the nucleus accumbens and ventral tegmental area of tsai attenuated by microinjections of spiroperidol into the nucleus accumbens. Brain Res. *171*, 247–259.

Montague, P.R. (1996). A Framework for Mesencephalic Predictive Hebbian Learning. *76*, 1936–1947.

Moore, K.A., Kohno, T., Karchewski, L.A., Scholz, J., Baba, H., and Woolf, C.J. (2002). Partial peripheral nerve injury promotes a selective loss of GABAergic inhibition in the superficial dorsal horn of the spinal cord. J. Neurosci. *22*, 6724–6731.

Morgan, M.J., and Franklin, K.B.J. (1990). 6-Hydroxydopamine lesions of the ventral tegmentum abolished amphetamine and morphine analgesia in the formalin test but not in the tail flick test. Brain Res. *519*, 144-159.

Morikawa, H., and Paladini, C.A. (2011). Dynamic regulation of midbrain dopamine neuron activity: intrinsic, synaptic, and plasticity mechanisms. Neuroscience *198*, 95–111.

Morzorati, S.L., and Marunde, R.L. (2006). Comparison of VTA dopamine neuron activity in lines of rats selectively bred to prefer or avoid alcohol. Alcohol. Clin. Exp. Res. *30*, 991–997.

Nair-Roberts, R.G., Chatelain-Badie, S.D., Benson, E., White-Cooper, H., Bolam, J.P., and Ungless, M.A. (2008a). Stereological estimates of dopaminergic, GABAergic and glutamatergic neurons in the ventral tegmental area, substantia nigra and retrorubral field in the rat. Neuroscience *152*, 1024–1031.

Nair-Roberts, R.G., Chatelain-Badie, S.D., Benson, E., White-Cooper, H., Bolam, J.P., and Ungless, M.A. (2008b). Stereological estimates of dopaminergic, GABAergic and glutamatergic neurons in the ventral tegmental area, substantia nigra and retrorubral field in the rat. Neuroscience *152*, 1024–1031.

Narita, M., Funada, M., and Suzuki, T. (2001). Regulations of opioid dependence by opioid receptor types. Pharmacol. Ther. *89*, 1–15.

Narita, M., Khotib, J., Suzuki, M., Ozaki, S., Yajima, Y., and Suzuki, T. (2003). Heterologous mu-opioid receptor adaptation by repeated stimulation of kappa-opioid receptor: up-regulation of G-protein activation and antinociception. J. Neurochem. *85*, 1171–1179.

Narita, M., Suzuki, M., Imai, S., Narita, M., Ozaki, S., Kishimoto, Y., Oe, K., Yajima, Y., Yamazaki, M., and Suzuki, T. (2004). Molecular mechanism of changes in the morphine-induced pharmacological actions under chronic pain-like state: suppression of dopaminergic transmission in the brain. Life Sci. *74*, 2655–2673.

Narita, M., Kishimoto, Y., Ise, Y., Yajima, Y., Misawa, K., and Suzuki, T. (2005). Direct Evidence for the Involvement of the Mesolimbic κ-Opioid System in the Morphine-Induced Rewarding Effect Under an Inflammatory Pain-Like State. Neuropsychopharmacology *30*, 111–118.

Nauta, W.J.H. (1958). Hippocampal projections and related neural pathways to the mid-brain in the cat. *81*, 319–341.

Navratilova, E., and Porreca, F. (2014). Reward and motivation in pain and pain relief. Nat. Neurosci. *17*, 1304–1312.

Navratilova, E., Atcherley, C.W., and Porreca, F. (2015). Brain Circuits Encoding Reward from Pain Relief. Trends Neurosci. *38*, 741–750.

Navratilova, E., Morimura, K., Xie, J.Y., Atcherley, C.W., Ossipov, M.H., and Porreca, F. (2016). Positive emotions and brain reward circuits in chronic pain. J. Comp. Neurol.

Neve, K.A., Seamans, J.K., and Trantham-Davidson, H. (2004). Dopamine receptor signaling. J. Recept. Signal Transduct. Res. *24*, 165–205.

Nicholson, B., and Verma, S. (2004). Comorbidities in Chronic Neuropathic Pain. Pain Med. *5*, S9–S27.

Omelchenko, N., and Sesack, S.R. (2010). Periaqueductal gray afferents synapse onto dopamine and GABA neurons in the rat ventral tegmental area. J. Neurosci. Res. *88*, 981-991.

Omelchenko, N., Bell, R., and Sesack, S.R. (2009). Lateral habenula projections to dopamine and GABA neurons in the rat ventral tegmental area. Eur. J. Neurosci. *30*, 1239–1250.

Ossipov, M.H., Lopez, Y., Nichols, M.L., Bian, D., and Porreca, F. (1995). The loss of antinociceptive efficacy of spinal morphine in rats with nerve ligation injury is prevented by reducing spinal afferent drive. Neurosci. Lett. *199*, 87–90.

Overton, P., and Clark, D. (1992). Iontophoretically administered drugs acting at the N-methyl-D-aspartate receptor modulate burst firing in A9 dopamine neurons in the rat. Synapse *10*, 131–140.

Overton, P.G., Vautrelle, N., and Redgrave, P. (2014). Sensory regulation of dopaminergic cell activity: Phenomenology, circuitry and function. Neuroscience *282*, 1–12.

Ozaki, S., Narita, M., Narita, M., Iino, M., Sugita, J., Matsumura, Y., and Suzuki, T. (2002). Suppression of the morphine-induced rewarding effect in the rat with neuropathic pain: implication of the reduction in μ-opioid receptor functions in the ventral tegmental area. J. Neurochem. *82*, 1192–1198.

Ozaki, S., Narita, M., Iino, M., Miyoshi, K., and Suzuki, T. (2003). Suppression of the morphine-induced rewarding effect and G-protein activation in the lower midbrain following nerve injury in the mouse: involvement of G-protein-coupled receptor kinase 2. Neuroscience *116*, 89–97.

Paalzow, H.M. (1992). L-DOPA Induces Opposing Effects on Pain in Intact Rats: SCH 23390 or a-Methyl-DL-p-Tyrosine Methylester Hydrochloride Reveals Profound Hyperalgesia in Large Antinociceptive Doses patients. 470–479.

Paladini, C.A., and Roeper, J. (2014). Generating bursts (and pauses) in the dopamine midbrain neurons. Neuroscience *282*, 109–121.

Pan, W.-X., Schmidt, R., Wickens, J.R., and Hyland, B.I. (2008). Tripartite mechanism of extinction suggested by dopamine neuron activity and temporal difference model. J. Neurosci. *28*, 9619–9631.

Panin, F., Cathala, A., Piazza, P.V., and Spampinato, U. (2012). Coupled intracerebral microdialysis and electrophysiology for the assessment of dopamine neuron function in vivo. J. Pharmacol. Toxicol. Methods *65*, 83–92.

Park, J., Bucher, E.S., Budygin, E.A., and Wightman, R.M. (2015). Norepinephrine and dopamine transmission in 2 limbic regions differentially respond to acute noxious stimulation. Pain *156*, 318–327.

Parker, L.A., and Rennie, M. (1992). Naltrexone-induced aversions: Assessment by place conditioning, taste reactivity, and taste avoidance paradigms. Pharmacol. Biochem. Behav. *41*, 559–565.

Patel, R., Gonçalves, L., Leveridge, M., Mack, S.R., Hendrick, A., Brice, N.L., Dickenson, A.H. (2014). Anti-hyperalgesic effects of a novel TRPM8 agonist in neuropathic rats: a comparison with topical menthol. Pain 155, 2097-107.

Peciña, S., Smith, K.S., and Berridge, K.C. (2006). Hedonic Hot Spots in the Brain. Neurosci. *12*, 500–511.

Pelissier, T., Laurido, C., Hernandez, A., Constandil, L., and Eschalier, A. (2006). Biphasic effect of apomorphine on rat nociception and effect of dopamine D2 receptor antagonists. Eur. J. Pharmacol. *546*, 40–47.

Pertovaara, A., and Wei, H. (2000). Attenuation of ascending nociceptive signals to the rostroventromedial medulla induced by a novel alpha2-adrenoceptor agonist, MPV-2426, following intrathecal application in neuropathic rats. Anesthesiology *92*, 1082–1092.

Phillips, A.G., and LePiane, F.G. (1980). Reinforcing effects of morphine microinjection into the ventral tegmental area. Pharmacol. Biochem. Behav. *12*, 965–968.

Phillipson, O.T. (1979). Afferent projections to the ventral tegmental area of Tsai and interfascicular nucleus: a horseradish peroxidase study in the rat. J. Comp. Neurol. *187*, 117–143.

Porro, C.A., Tassinari, G., Facchinetti, F., Panerai, A.E., and Carli, G. (1991). Central beta-endorphin system involvement in the reaction to acute tonic pain. Exp. Brain Res. *83*, 549–554.

Przewłocki, R., and Przewłocka, B. (2001). Opioids in chronic pain. Eur. J. Pharmacol. *429*, 79–91.

Rahman, W., D'Mello, R., and Dickenson, A.H. (2008). Peripheral nerve injury-induced changes in spinal alpha(2)-adrenoceptor-mediated modulation of mechanically evoked dorsal horn neuronal responses. J. Pain *9*, 350–359.

Rainville, P. (2002). Brain mechanisms of pain affect and pain modulation. Curr. Opin. Neurobiol. *12*, 195–204.

Rauch, A., Rainer, G., Augath, M., Oeltermann, A., and Logothetis, N.K. (2008). Pharmacological MRI combined with electrophysiology in non-human primates: effects of Lidocaine on primary visual cortex. Neuroimage *40*, 590–600.

Rebec, G. V, Christensen, J.R.., Guerra, C., and Bardo, M.T. (1997). Regional and temporal differences in real-time dopamine efflux in the nucleus accumbens during free-choice novelty. Brain Res. *776*, 61–67.

Redgrave, P., Prescott, T.J., and Gurney, K. (1999). The basal ganglia: a vertebrate solution to the selection problem? Neuroscience *89*, 1009–1023.

Reith, M.E.., Xu, C., and Chen, N.-H. (1997). Pharmacology and regulation of the neuronal dopamine transporter. Eur. J. Pharmacol. *324*, 1–10.

Reynolds, J.N., Hyland, B.I., and Wickens, J.R. (2001). A cellular mechanism of reward-related learning. Nature *413*, 67–70.

Rinvik, E., and Ottersen, O.P. Terminals of subthalamonigral fibres are enriched with glutamate-like immunoreactivity: an electron microscopic, immunogold analysis in the cat. J. Chem. Neuroanat. *6*, 19–30.

Rodd-Henricks, Z.A., McKinzie, D.L., Li, T.-K., Murphy, J.M., and McBride, W.J. (2002). Cocaine is self-administered into the shell but not the core of the nucleus accumbens of Wistar rats. J. Pharmacol. Exp. Ther. *303*, 1216–1226.

Roitman, M.F., Wheeler, R.A., Wightman, R.M., and Carelli, R.M. (2008). Real-time chemical responses in the nucleus accumbens differentiate rewarding and aversive stimuli. Nat. Neurosci. *11*, 1376–1377.

Rowbotham, M.C., Arslanian, A., Nothaft, W., Duan, W.R., Best, A.E., Pritchett, Y., Zhou, Q., and Stacey, B.R. (2012). Efficacy and safety of the α4β2 neuronal nicotinic receptor agonist ABT-894 in patients with diabetic peripheral neuropathic pain. Pain *153*, 862–868.

Roy, M., Peretz, I., and Rainville, P. (2008). Emotional valence contributes to music-induced analgesia. Pain *134*, 140–147.

Saadé, N.E., Atweh, S.F., Bahuth, N.B., and Jabbur, S.J. (1997). Augmentation of nociceptive reflexes and chronic deafferentation pain by chemical lesions of either dopaminergic terminals or midbrain dopaminergic neurons. Brain Res. *751*, 1–12.

Sagheddu, Aroni, De Felice, Lecca, Luhicchi, Melis, Muntoni, Romano, Palazzo, Guida, et al. (2015). Enhanced serotonin and mesolimbic dopamine transmissions in a rat model of neuropathic pain. Neuropharmacology *97*, 383–393.

Salamone, J.D., Correa, M., Mingote, S., and Weber, S.M. (2003). Nucleus accumbens dopamine and the regulation of effort in food-seeking behavior: implications for studies of natural motivation, psychiatry, and drug abuse. J. Pharmacol. Exp. Ther. *305*, 1–8.

Sanchez-Catalan, M.J., Kaufling, J., Georges, F., Veinante, P., and Barrot, M. (2014). The antero-posterior heterogeneity of the ventral tegmental area. Neuroscience *282C*, 198–216.

Sanghera, M.K., Trulson, M.E., and German, D.C. (1984). Electrophysiological properties of mouse dopamine neurons: in vivo and in vitro studies. Neuroscience *12*, 793–801.

Schmitz, Y., Benoit-Marand, M., Gonon, F., and Sulzer, D. (2003). Presynaptic regulation of dopaminergic neurotransmission. J. Neurochem. *87*, 273–289.

Schultz, W. (1997). A Neural Substrate of Prediction and Reward. Science. *275*, 1593–1599.

Schultz, W. (1998). Predictive Reward Signal of Dopamine Neurons. J Neurophysiol *80*, 1–27.

Schultz, W., and Romo, R. (1987). Responses of nigrostriatal dopamine neurons to high-intensity somatosensory stimulation in the anesthetized monkey. J. Neurophysiol. *57*, 201–217.

Seamans, J.K., Gorelova, N., Durstewitz, D., and Yang, C.R. (2001). Bidirectional dopamine modulation of GABAergic inhibition in prefrontal cortical pyramidal neurons. J. Neurosci. *21*, 3628–3638.

Semenchuk, M.R., Sherman, S., and Davis, B. (2001). Double-blind, randomized trial of bupropion SR for the treatment of neuropathic pain. Neurology *57*, 1583–1588.

Seminowicz, D. a, Laferriere, A.L., Millecamps, M., Yu, J.S.C., Coderre, T.J., and Bushnell, M.C. (2009). MRI structural brain changes associated with sensory and emotional function in a rat model of long-term neuropathic pain. Neuroimage *47*, 1007–1014.

Sesack, S.R., and Pickel, V.M. (1992). Prefrontal cortical efferents in the rat synapse on unlabeled neuronal targets of catecholamine terminals in the nucleus accumbens septi and on dopamine neurons in the ventral tegmental area. J. Comp. Neurol. *320*, 145–160.

Seymour, B., Daw, N., Dayan, P., Singer, T., and Dolan, R. (2007). Differential encoding of losses and gains in the human striatum. J. Neurosci. *27*, 4826–4831.

Sherrington, C. (1900). Cutaneous sensations. In Textbook of Physiology, pp. 920–1001.

Shimizu, T., Iwata, S., Morioka, H., Masuyama, T., Fukuda, T., and Nomoto, M. (2004). Antinociceptive mechanism of L-DOPA. Pain *110*, 246–249.

Shippenberg, T.S., Bals-Kubik, R., and Herz, a (1993). Examination of the neurochemical substrates mediating the motivational effects of opioids: role of the mesolimbic dopamine system and D-1 vs. D-2 dopamine receptors. J. Pharmacol. Exp. Ther. *265*, 53–59.

Sibley, D.R., Monsma, F.J., and Shen, Y. (1993). Molecular neurobiology of dopaminergic receptors. Int. Rev. Neurobiol. *35*, 391–415.

Sikandar, S., Patel, R., Patel, S., Sikander, S., Bennett, D.L.H., and Dickenson, A.H. (2013). Genes, molecules and patients--emerging topics to guide clinical pain research. Eur. J. Pharmacol. *716*, 188–202.

Silva, Viana, M.A., and Quagliato (2008). Pain in parkinsons disease: Analysis of 50 cases in a clinic of movement disorders. *66*, 26–29.

Skirboll, L.R., Grace, A.A., and Bunney, B.S. (1979). Dopamine auto- and postsynaptic receptors: electrophysiological evidence for differential sensitivity to dopamine agonists. Science *206*, 80–82.

Slama, M., Susic, D., Varagic, J., Ahn, J., and Frohlich, E.D. (2003). Echocardiographic measurement of cardiac output in rats. Am. J. Physiol. Heart Circ. Physiol. *284*, H691-7.

Sotres-Bayón, F., Torres-López, E., López-Ávila, A., del Ángel, R., and Pellicer, F. (2001). Lesion and electrical stimulation of the ventral tegmental area modify persistent nociceptive behavior in the rat. Brain Res. *898*, 342–349.

Spina, L., Fenu, S., Longoni, R., Rivas, E., and Di Chiara, G. (2006). Nicotine-conditioned single-trial place preference: selective role of nucleus accumbens shell dopamine D1 receptors in acquisition. Psychopharmacology (Berl). *184*, 447–455.

Spyraki, C., Fibiger, H.C., and Phillips, A.G. (1983). Attenuation of heroin reward in rats by disruption of the mesolimbic dopamine system. Psychopharmacology (Berl). *79*, 278–283.

Stanfa, L., and Dickenson, A. (1995). Spinal opioid systems in inflammation. Inflamm. Res. *44*, 231–241.

Stanfa, L.C., Sullivan, A.F., and Dickenson, A.H. (1992). Alterations in neuronal excitability and the potency of spinal mu, delta and kappa opioids after carrageenan-induced inflammation. Pain *50*, 345–354.

Steffensen, S.C., Svingos, A.L., Pickel, V.M., and Henriksen, S.J. (1998). Electrophysiological Characterization of GABAergic Neurons in the Ventral Tegmental Area. J. Neurosci. *18*, 8003–8015.

Steffensen, S.C., Lee, R.S., Stobbs, S.H., and Henriksen, S.J. (2001). Responses of ventral tegmental area GABA neurons to brain stimulation reward. Brain Res. *906*, 190–197.

Steffensen, S.C., Taylor, S.R., Horton, M.L., Barber, E.N., Lyle, L.T., Stobbs, S.H., and Allison, D.W. (2008). Cocaine disinhibits dopamine neurons in the ventral tegmental area via use-dependent blockade of GABA neuron voltage-sensitive sodium channels. Eur. J. Neurosci. *28*, 2028–2040.

Stevenson, G.W., Bilsky, E.J., and Negus, S.S. (2006). Targeting pain-suppressed behaviors in preclinical assays of pain and analgesia: effects of morphine on acetic acid-suppressed feeding in C57BL/6J mice. J. Pain *7*, 408–416.

Stobbs, S.H., Ohran, A.J., Lassen, M.B., Allison, D.W., Brown, J.E., and Steffensen, S.C. (2004). Ethanol suppression of ventral tegmental area GABA neuron electrical transmission involves N-methyl-D-aspartate receptors. J. Pharmacol. Exp. Ther. *311*, 282–289.

Strigo, I.A., Duncan, G.H., Bushnell, M.C., Boivin, M., Wainer, I., Rodriguez Rosas, M.E., and Persson, J. (2005). The effects of racemic ketamine on painful stimulation of skin and viscera in human subjects. Pain *113*, 255–264.

Sturgess, D., Haluska, B., Jones, M., and Venkatesh, B. (2008). Noninvasive rodent cardiac output: comparison of a compact clinical monitor with echocardiography and proposal of a simple correction factor. Crit. Care *12*, P84.

Suzuki, R., Rahman, W., Hunt, S.P., and Dickenson, A.H. (2004). Descending facilitatory control of mechanically evoked responses is enhanced in deep dorsal horn neurones following peripheral nerve injury. Brain Res. *1019*, 68–76.

Swanson, L.W. (1982). The projections of the ventral tegmental area and adjacent regions: a combined fluorescent retrograde tracer and immunofluorescence study in the rat. Brain Res. Bull. *9*, 321–353.

Szabo, B., Siemes, S., and Wallmichrath, I. (2002). Inhibition of GABAergic neurotransmission in the ventral tegmental area by cannabinoids. Eur. J. Neurosci. *15*, 2057–2061.

Szebenyi, B., Hollander, A.P., Dieppe, P., Quilty, B., Duddy, J., Clarke, S., and Kirwan, J.R. (2006). Associations between pain, function, and radiographic features in osteoarthritis of the knee. Arthritis Rheum. *54*, 230–235.

Takeda, R., Ikeda, T., Tsuda, F., Abe, H., Hashiguchi, H., Ishida, Y., and Nishimori, T. (2005). Unilateral lesions of mesostriatal dopaminergic pathway alters the withdrawal response of the rat hindpaw to mechanical stimulation. Neurosci. Res. *52*, 31–36.

Tan, A.M., Chang, Y.-W., Zhao, P., Hains, B.C., and Waxman, S.G. (2011). Rac1-regulated dendritic spine remodeling contributes to neuropathic pain after peripheral nerve injury. Exp. Neurol. *232*, 222–233.

Tan, K.R., Yvon, C., Turiault, M., Mirzabekov, J.J., Doehner, J., Labouèbe, G., Deisseroth, K., Tye, K.M., and Lüscher, C. (2012). GABA neurons of the VTA drive conditioned place aversion. Neuron *73*, 1173–1183.

Taylor, A.M.W., Murphy, N.P., Evans, C.J., and Cahill, C.M. (2014). Correlation between ventral striatal catecholamine content and nociceptive thresholds in neuropathic mice. J. Pain *15*, 878–885.

Taylor, A.M.W., Castonguay, A., Taylor, A.J., Murphy, N.P., Ghogha, A., Cook, C., Xue, L., Olmstead, M.C., De Koninck, Y., Evans, C.J., et al. (2015). Microglia disrupt mesolimbic reward circuitry in chronic pain. J. Neurosci. *35*, 8442–8450.

Taylor, A.M.W., Becker, S., Schweinhardt, P., and Cahill, C. (2016). Mesolimbic dopamine signaling in acute and chronic pain: implications for motivation, analgesia, and addiction. Pain *157*, 1194–1198.

Taylor, B.K., Joshi, C., and Uppal, H. (2003). Stimulation of dopamine D2 receptors in the nucleus accumbens inhibits inflammatory pain. Brain Res. *987*, 135–143.

Teitelbaum, P., and Wolgin, D.L. (1975). Neurotransmitters and the regulation of food intake. Prog. Brain Res. *42*, 235–249.

Thompson, R.C., Mansour, A., Akil, H., and Watson, S.J. (1993). Cloning and pharmacological characterization of a rat mu opioid receptor. Neuron *11*, 903–913.

Tong, Z.Y., Overton, P.G., and Clark, D. (1996). Stimulation of the prefrontal cortex in the rat induces patterns of activity in midbrain dopaminergic neurons which resemble natural burst events. Synapse *22*, 195–208.

Tracey, I. (2010). Getting the pain you expect: mechanisms of placebo, nocebo and reappraisal effects in humans. Nat. Med. *16*, 1277–1283.

Tsai, C. (1925). The optic tracts and centers of the opossum. Didelphis virginiana. J. Comp. Neurol. *39*, 173–216.

Tsai, H.-C., Zhang, F., Adamantidis, A., Stuber, G.D., Bonci, A., de Lecea, L., and Deisseroth, K. (2009). Phasic firing in dopaminergic neurons is sufficient for behavioral conditioning. Science *324*, 1080–1084.

Ungless, M., and Grace, A. (2012). Are you or aren't you? Challenges associated with physiologically identifying dopamine neurons. Trends Neurosci. *35*, 422–430.

Ungless, M. a, Magill, P.J., and Bolam, J.P. (2004). Uniform inhibition of dopamine neurons in the ventral tegmental area by aversive stimuli. Science *303*, 2040–2042.

Villemure, C., Slotnick, B.M., and Bushnell, M.C. (2003). Effects of odors on pain perception: deciphering the roles of emotion and attention. Pain *106*, 101–108.

Viveros, O.H., Diliberto, E.J., Hazum, E., and Chang, K.J. (1979). Opiate-like materials in the adrenal medulla: evidence for storage and secretion with catecholamines. Mol. Pharmacol. *16*, 1101–1108.

Volkow, N.D., Wang, G.J., Fowler, J.S., Logan, J., Gatley, S.J., Hitzemann, R., Chen, A.D., Dewey, S.L., and Pappas, N. (1997). Decreased striatal dopaminergic responsiveness in detoxified cocaine-dependent subjects. Nature *386*, 830–833.

Volman, S.F., Lammel, S., Margolis, E.B., Kim, Y., Richard, J.M., Roitman, M.F., and Lobo, M.K. (2013). Mini-Symposium New Insights into the Specificity and Plasticity of Reward and Aversion Encoding in the Mesolimbic System. J. Neurosci. *33*, 17569–17576.

Wang, R. (1981). Dopaminergic neurons in the rat ventral tegmental area. I. Identification and characterization. Brain Res. Rev. *3*, 123–140.

Wang, X.J., and Han, J.S. (1990). Modification by cholecystokinin octapeptide of the binding of mu-, delta-, and kappa-opioid receptors. J. Neurochem. *55*, 1379–1382.

Watson, S.J., Akil, H., Ghazarossian, V.E., and Goldstein, A. (1981). Dynorphin immunocytochemical localization in brain and peripheral nervous system: preliminary studies. Proc. Natl. Acad. Sci. *78*, 1260–1263.

Wenzel, J.M., Rauscher, N.A., Cheer, J.F., and Oleson, E.B. (2015). A Role for Phasic Dopamine Release within the Nucleus Accumbens in Encoding Aversion: A Review of the Neurochemical Literature. ACS Chem. Neurosci. *6*, 16–26.

West, S.J., Bannister, K., Dickenson, A.H., and Bennett, D.L. (2015). Circuitry and plasticity of the dorsal horn - Toward a better understanding of neuropathic pain. Neuroscience *300*, 254–275.

Westerink, B.H., Kwint, H.F., and deVries, J.B. (1996). The pharmacology of mesolimbic dopamine neurons: a dual-probe microdialysis study in the ventral tegmental area and nucleus accumbens of the rat brain. J. Neurosci. *16*, 2605–2611.

Westerink, B.H., Enrico, P., Feimann, J., and De Vries, J.B. (1998). The pharmacology of mesocortical dopamine neurons: a dual-probe microdialysis study in the ventral tegmental area and prefrontal cortex of the rat brain. J. Pharmacol. Exp. Ther. *285*, 143–154.

White, F.J., and Wang, R.Y. (1984). A10 dopamine neurons: Role of autoreceptors in determining firing rate and sensitivity to dopamine agonists. Life Sci. *34*, 1161–1170.

Wightman, R.M., Heien, M.L.A. V, Wassum, K.M., Sombers, L.A., Aragona, B.J., Khan, A.S., Ariansen, J.L., Cheer, J.F., Phillips, P.E.M., and Carelli, R.M. (2007). Dopamine release is heterogeneous within microenvironments of the rat nucleus accumbens. Eur. J. Neurosci. *26*, 2046–2054.

Wilkinson, L.S., Humby, T., Killcross, A.S., Torres, E.M., Everitt, B.J., and Robbins, T.W. (1998). Dissociations in dopamine release in medial prefrontal cortex and ventral striatum during the acquisition and extinction of classical aversive conditioning in the rat. Eur. J. Neurosci. *10*, 1019–1026.

Willert, R.P., Woolf, C.J., Hobson, A.R., Delaney, C., Thompson, D.G., and Aziz, Q. (2004). The development and maintenance of human visceral pain hypersensitivity is dependent on the N-methyl-D-aspartate receptor. Gastroenterology *126*, 683–692.

Willis, W.D., and Coggeshall, R.E. (1991). Sensory Mechanisms of the Spinal Cord. (Boston, MA: Springer US), pp. 79–151.

Winter, C.A., Risley, E.A., and Nuss, G.W. (1962). Carrageenin-Induced Edema in Hind Paw of the Rat as an Assay for Antiinflammatory Drugs. Exp. Biol. Med. *111*, 544–547.

Winyard, P.G., and Willoughby, D. A. (2003). Inflammation Protocols. Methods in Molecular Biology *225,* 239-248

Wood, P.B. (2006). Mesolimbic dopaminergic mechanisms and pain control. Pain *120*, 230–234.

Wood, P.B. (2008). Role of central dopamine in pain and analgesia. Expert Rev. Neurother. *8*, 781–797.

Wood, P.B., Schweinhardt, P., Jaeger, E., Dagher, A., Hakyemez, H., Rabiner, E. a, Bushnell, M.C., and Chizh, B. a (2007a). Fibromyalgia patients show an abnormal dopamine response to pain. Eur. J. Neurosci. *25*, 3576–3582.

Wood, P.B., Patterson, J.C., Sunderland, J.J., Tainter, K.H., Glabus, M.F., and Lilien, D.L. (2007b). Reduced presynaptic dopamine activity in fibromyalgia syndrome demonstrated with positron emission tomography: a pilot study. J. Pain *8*, 51–58.

Woolf, C.J., and Salter, M.W. (2000). Neuronal plasticity: increasing the gain in pain. Science *288*, 1765–1769.

Wu, Y., Na, X., Zang, Y., Cui, Y., Xin, W., Pang, R., Zhou, L., Wei, X., Li, Y., and Liu, X. (2014). Upregulation of tumor necrosis factor-alpha in nucleus accumbens attenuates morphine-induced rewarding in a neuropathic pain model. Biochem. Biophys. Res. Commun. *449*, 502–507.

Xi, Z.X., and Stein, E.A. (1999). Baclofen inhibits heroin self-administration behavior and mesolimbic dopamine release. J. Pharmacol. Exp. Ther. *290*, 1369–1374.

Xia, Y., Driscoll, J.R., Wilbrecht, L., Margolis, E.B., Fields, H.L., and Hjelmstad, G.O. (2011). Nucleus accumbens medium spiny neurons target non-dopaminergic neurons in the ventral tegmental area. J. Neurosci. *31*, 7811–7816.

Xu, M., Kontinen, V.K., and Kalso, E. (2000). Effects of radolmidine, a novel alpha2 -adrenergic agonist compared with dexmedetomidine in different pain models in the rat. Anesthesiology *93*, 473–481.

Xu, X.J., Puke, M.J., and Wiesenfeld-Hallin, Z. (1992). The depressive effect of intrathecal clonidine on the spinal flexor reflex is enhanced after sciatic nerve section in rats. Pain *51*, 145–151.

Yaksh, T.L., Pogrel, J.W., Lee, Y.W., and Chaplan, S.R. (1995). Reversal of nerve ligation-induced allodynia by spinal alpha-2 adrenoceptor agonists. J. Pharmacol. Exp. Ther. *272*, 207–214.

Yamaguchi, T., Sheen, W., and Morales, M. (2007a). Glutamatergic neurons are present in the rat ventral tegmental area. Eur. J. Neurosci. *25*, 106–118.

Yamaguchi, T., Sheen, W., and Morales, M. (2007b). Glutamatergic neurons are present in the rat ventral tegmental area. Eur. J. Neurosci. *25*, 106–118.

Yamaguchi, T., Wang, H.-L., Li, X., Ng, T.H., and Morales, M. (2011). Mesocorticolimbic Glutamatergic Pathway. J. Neurosci. *31*, 8476–8490.

Yeomans, M.R., and Gray, R.W. (1996). Selective effects of naltrexone on food pleasantness and intake. Physiol. Behav. *60*, 439–446.

Yin, R., and French, E.D. (2000). A comparison of the effects of nicotine on dopamine and non-dopamine neurons in the rat ventral tegmental area: an in vitro electrophysiological study. Brain Res. Bull. *51*, 507–514.

Young, A.M.J., Joseph, M.H., and Gray, J.A. (1993). Latent inhibition of conditioned dopamine release in rat nucleus accumbens. Neuroscience *54*, 5–9.

Záborszky, L., Alheid, G.F., Beinfeld, M.C., Eiden, L.E., Heimer, L., and Palkovits, M. (1985). Cholecystokinin innervation of the ventral striatum: A morphological and radioimmunological study. Neuroscience *14*, 427–453.

Zadina, J.E., Martin-Schild, S., Gerall, A.A., Kastin, A.J., Hackler, L., Ge, L.J., and Zhang, X. (1999). Endomorphins: novel endogenous mu-opiate receptor agonists in regions of high mu-opiate receptor density. Ann. N. Y. Acad. Sci. *897*, 136–144.

Zhang, H., Kiyatkin, E.A., and Stein, E.A. (1994). Behavioral and pharmacological modulation of ventral tegmental dendritic dopamine release. *656*, 59–70.

Zhang, M., Liu, Y., Zhao, M., Tang, W., Wang, X., Dong, Z., and Yu, S. (2017). Depression and anxiety behaviour in a rat model of chronic migraine. J. Headache Pain *18*, 27.

Zhang, N., Inan, S., Inan, S., Cowan, A., Sun, R., Wang, J.M., Rogers, T.J., Caterina, M., and Oppenheim, J.J. (2005). A proinflammatory chemokine, CCL3, sensitizes the heat- and capsaicin-gated ion channel TRPV1. Proc. Natl. Acad. Sci. U. S. A. *102*, 4536–4541.

Zigmond, M.J., and Stricker, E.M. (1972). Deficits in feeding behavior after intraventricular injection of 6-hydroxydopamine in rats. Science *177*, 1211–1214.

Zimmermann, M. (1983). Ethical guidelines for investigations of experimental pain in conscious animals. Pain *16*, 109–110.

Zubieta, J.K., Smith, Y.R., Bueller, J.A., Xu, Y., Kilbourn, M.R., Jewett, D.M., Meyer, C.R., Koeppe, R.A., and Stohler, C.S. (2001). Regional mu opioid receptor regulation of sensory and affective dimensions of pain. Science *293*, 311–315.

Zweifel, L.S., Parker, J.G., Lobb, C.J., Rainwater, A., Wall, V.Z., Fadok, J.P., Darvas, M., Kim, M.J., Mizumori, S.J.Y., Paladini, C.A., et al. (2009). Disruption of NMDAR-dependent burst firing by dopamine neurons provides selective assessment of phasic dopamine-dependent behavior. Proc. Natl. Acad. Sci. *106*, 7281–7288.

Zweifel, L.S., Fadok, J.P., Argilli, E., Garelick, M.G., Jones, G.L., Dickerson, T.M.K., Allen, J.M., Mizumori, S.J.Y., Bonci, A., and Palmiter, R.D. (2011). Activation of dopamine neurons is critical for aversive conditioning and prevention of generalized anxiety. Nat. Neurosci. *14*, 620–626.

10. Appendix A

A

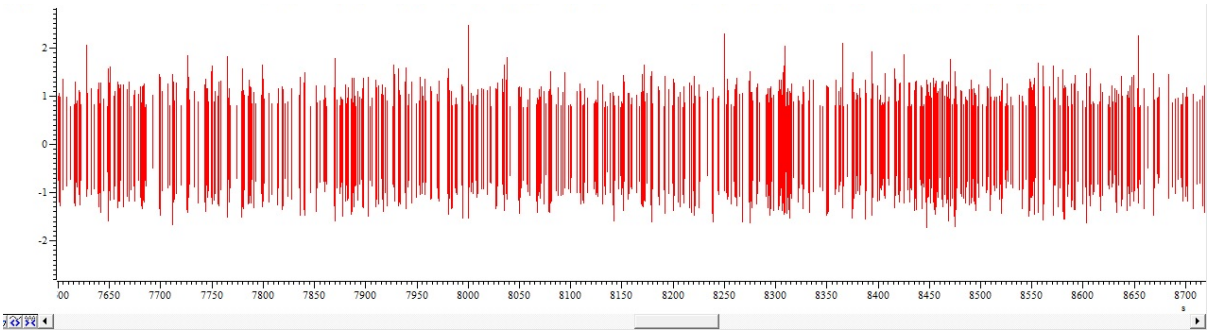

B

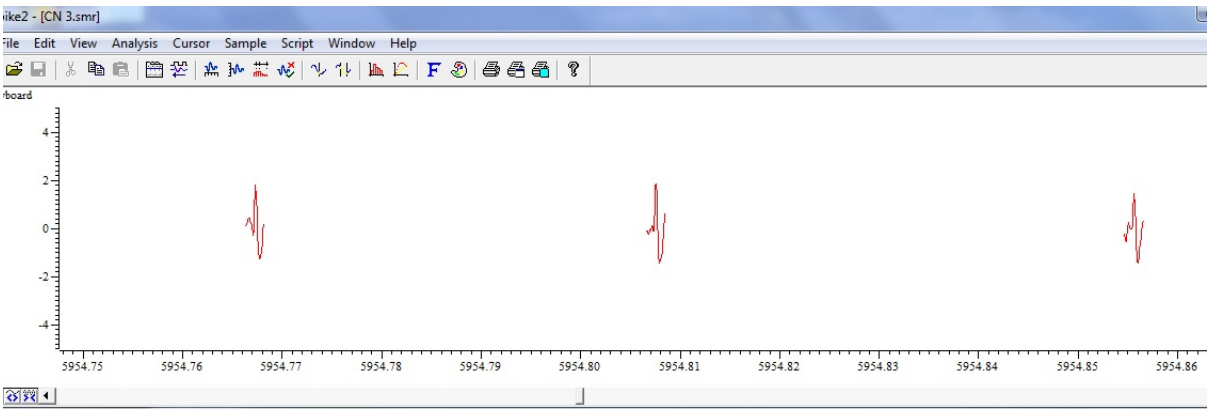

C

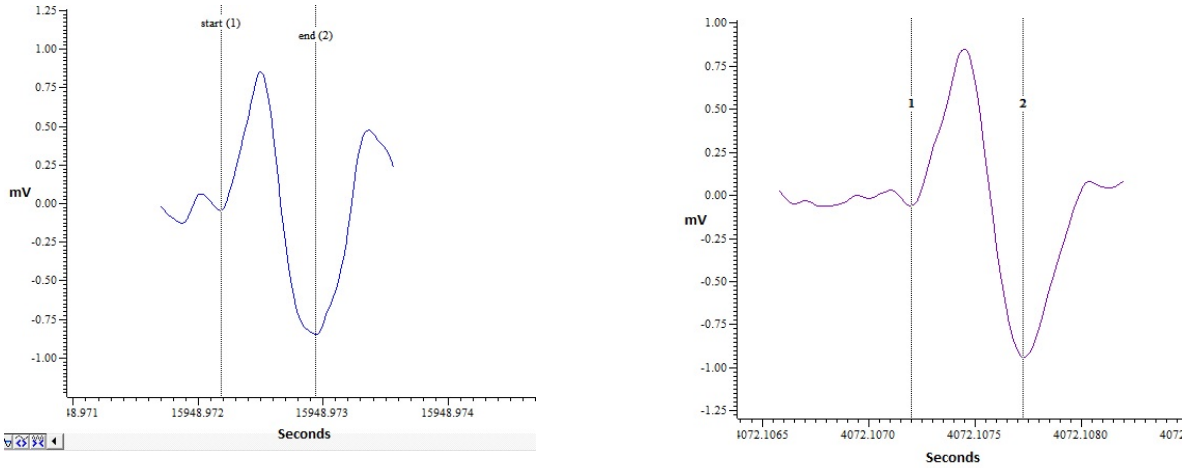

Examples of neuronal recordings shown on different time scales, with amplitude (millivolts) on the y-axis and time (seconds) on the x-axis. A) One wavemark channel showing all spikes classified as belonging to one spike waveform template. Spikes belonging to this template show variability in amplitude, and an irregular, bursting pattern of activity. B) Three individual spikes displayed in one template's Wavemark channel. Slight variability in waveform shape is observed, but stringent template criteria prevent too much discrepancy within the population of included spikes. C) Two action potentials recorded in the current experiments. The typical biphasic waveform is observed, and the biphasic duration – used as a measure of action potential duration – is marked by vertical cursors 1 and 2 (start and end).

11. Appendix B

Table showing numbers of neurones recorded for each experimental protocol, and omitted from and included in analyses throughout this thesis

Experimental protocol *And thesis section for protocol*	**Number of animals**	**Total number of neurones recorded**	**Number of neurones omitted in each analysis type**	**Final number of neurones used for each analysis type**
Time control *Section 3.3.2*	5	9	2 from all	7
Morphine *Section 3.3.2*	16	19	0 omitted from non-normalized data; 1 omitted from normalized response	19 (non-normalized response) 18 (normalized morphine response)
Morphine vehicle control *Section 3.3.2*	5	6	1 from all	5
L-DOPA low and high dose *Section 4.3.I*	23	32	6 from all	26
Carbidopa-only control *Section 4.3.I*	5	8	3 from all	5
L-DOPA vehicle control *Section 4.3.I*	5	7	1 from all	6
L-DOPA-sulpiride *Section 5.3.I*	12	22	0 from normalized L-DOPA response; 0 from non-normalized sulpiride response; 1 from normalized sulpiride response	22 (normalized L-DOPA response) 22 (non-normalized sulpiride response) 21 (normalized sulpiride response)
Sulpiride vehicle control *Section 5.3.I*	5	7	0 from all	7
Carrageenan-only *Section 6.3.I*	18	24	1 from normalized carrageenan response	24 (non-normalized carrageenan response) 23 (normalized carrageenan response)
Carrageenan-naloxone *Section 6.3.I*	12	28	2 from all; 1 from normalized naloxone response	26 (non-normalized naloxone response) 25 (normalized naloxone response)
Carrageenan-naloxone vehicle *Section 6.3.I*	7	9	0 from all	9
Carrageenan-L-DOPA *Section 6.3.I*	12	21	2 from normalized carrageenan response 0 from normalized L-DOPA response	19 (normalized carrageenan response) 21 (normalized L-DOPA response)
Naloxone-L-DOPA naïve state *Section 7.3.2*	7	17	1 from normalized naloxone response	16 (normalized naloxone response)
Naloxone-only naïve state *Section 7.3.2*	12	31	3 from normalized naloxone response	28 (normalized naloxone response)
Naloxone-L-DOPA SNL state *Section 7.3.2*	7	20	0 from non-normalized naloxone response 1 from normalized naloxone response 2 from normalized L-DOPA response	20 (non-normalized naloxone response) 19 (normalized naloxone response) 18 (normalized L-DOPA response)
Naloxone-only SNL state *Section 7.3.2*	9	20	1 from non-normalized naloxone response	19 (non-normalized naloxone response

12. Appendix C

Clusters resulting from all cluster analyses detailed throughout the thesis: cluster ID, thesis section containing cluster results, and description of analysis conducted to establish clusters.

Cluster ID	Section	Derived from (analysis):
BL SFR cluster 1n	3.4.2	Cluster analysis using BL SFR values of all neurones recorded from naïve state animals
BL SFR cluster 2n		
BL SFR cluster 1b	3.4.2	Cluster analysis using BL SFR values of all neurones recorded from naïve state animals, with a pre-determined cluster number of three
BL SFR cluster 2b		
BL SFR cluster 3b		
SIB cluster 1	3.4.3	Cluster analysis using baseline condition %SIB values of all neurones recorded from naïve state animals
SIB cluster 2		
SIB cluster 3		
Norm mph cluster 1	3.4.6.2	Cluster analysis using normalised SFR values at all time points post-morphine injection of all neurones recorded from morphine-injected rats
Norm mph cluster 2		
Raw L-DOPA cluster 1	4.4.I.I	Cluster analysis using mean SFR values for each neurone at all time points following L-DOPA injection in the naïve condition
Raw L-DOPA cluster 2		
Norm L-DOPA cluster 1	4.4.I.2	Cluster analysis using mean normalised SFR values for each neurone at all time points following L-DOPA injection in the naïve condition
Norm L-DOPA cluster 2		
Norm L-DOPA cluster 1p	5.4.I	Cluster analysis using mean normalised SFR values for each neurone at all time points following L-DOPA injection in the naïve state – neurones recorded during L-DOPA-only experiments ('p' for previous)
Norm L-DOPA cluster 2p		
Norm L-DOPA cluster 1s	5.4.I	Cluster analysis using mean normalised SFR values for each neurone at all time points following L-DOPA injection in the naïve state – neurones recorded during L-DOPA-sulpiride experiments ('s' for sulpiride)
Norm L-DOPA cluster 2s		
Norm sulpiride cluster 1	5.4.2.2	Cluster analysis using mean normalised SFR values for each neurone at all time points following sulpiride injection
Norm sulpiride cluster 2		
Raw carr cluster 1	6.4.I.I	Cluster analysis using mean SFR values for each neurone at all time points following carrageenan injection
Raw carr cluster 2		
Norm carr cluster 1	6.4.I.2	Cluster analysis using mean normalised SFR values (expressed as a percentage of mean pre-carrageenan injection values) for each neurone at all time points following carrageenan injection
Norm carr cluster 2		
Norm carr cluster 3		
Norm L-DOPA cluster 1c	6.4.3.I	Cluster analysis using mean normalised SFR values for each neurone at all time points following L-DOPA injection in the carrageenan-injected state ('c' for carrageenan)
Norm L-DOPA cluster 2c		
Raw nlx cluster 1n	6.4.4.I	Cluster analysis using mean SFR values for each neurone at all time points following naloxone injection – neurones recorded in the naïve state ('n' for naïve)
Raw nlx cluster 2n		
Raw nlx cluster 1c	6.4.4.I	Cluster analysis using mean SFR values for each neurone at all time points following naloxone injection – neurones recorded in the carrageenan-injected state ('c' for carrageenan)
Raw nlx cluster 2c		
Norm nlx cluster 1n	6.4.4.2	Cluster analysis using mean normalised SFR values for each neurone at all time points following naloxone injection – neurones recorded in the naïve state ('n' for naïve)
Norm nlx cluster 2n		
BL SFR cluster 1snl	7.4.I.I	Cluster analysis using BL SFR values of all neurones recorded from SNL state animals
BL SFR cluster 2snl		
Raw nlx cluster 1snl	7.4.2.I	Cluster analysis using mean SFR values for each neurone at all time points following naloxone injection – neurones recorded in the SNL state
Raw nlx cluster 2snl		
Norm nlx cluster 1snl	7.4.2.2	Cluster analysis using mean normalised SFR values for each neurone at all time points following naloxone injection – neurones recorded in the SNL state
Norm nlx cluster 2snl		
Norm L-DOPA cluster 1snl	7.4.3.I	Cluster analysis using mean normalised SFR values for each neurone at all time points following L-DOPA injection in the SNL state
Norm L-DOPA cluster 2snl		

13. Appendix D

International Association for the Study of Pain (IASP) 15th World Congress on Pain, Buenos Aires 6th-11th November 2014 - *Poster abstract*

Probing dopaminergic signalling and pain responses in the rat ventral tegmental area

Lauren V Friend[1], Anthony H Dickenson[1]

[1] Department of Neuroscience, Physiology and Pharmacology, University College London, London, UK

Introduction

The detection of potentially harmful stimuli culminating in the perception of pain is crucial for survival; however, when this process becomes dysfunctional as in chronic pain, the result is extreme discomfort serving no apparent purpose and a reduced quality of life due in part to the aversive and unrewarding nature of the pain experience. Efforts to unpick pathological mechanisms require understanding of the affective pain-processing pathway, of which the dopaminergic (DA) neurons of the ventral tegmental area (VTA) are a crucial element. These neurons are well known for their established role in reward, implicating the VTA as a location for pain-reward interactions that frequently contribute to behavioural decisions. This study aims to investigate the DA neurons' precise role in nociceptive signalling, involving manipulation with the DA precursor, L-DOPA, in both normal rats and persistent pain models.

Methods

Extracellular *in vivo* electrophysiology was performed within the VTA of isoflurane anaesthetised naïve rats. Firing rates were monitored and, in order to elucidate identity, neurons were classified electrophysiologically with action potential (AP) duration, functionally with noxious response, and pharmacologically with systemic L-DOPA. This process was repeated in rats with λ-carrageenan-induced tonic pain, and those with spinal nerve ligation-induced chronic pain. Naloxone, the μ-opioid receptor antagonist, was injected systemically to unmask endogenous opioid influence in the various pain conditions.

Results

L-DOPA had a profound and rapid effect on spontaneous firing rate of the VTA neurons. Accordingly, neurons could be effectively divided into those that were inhibited and those that were excited by L-DOPA, segregating the putative DA cells from the non-DA contingents, respectively. The L-DOPA-excited population were significantly excited by peripheral noxious stimulation. Conversely, the L-DOPA-inhibited group consisted of a mixture of noxious-excited and noxious-inhibited neurons, resulting in an insignificant group average response and strongly suggesting functional heterogeneity within this putative DA neuron population. Overall, a complex relationship was observed between the direction of effect of acute and inflammatory noxious stimuli and subsequent actions of L-DOPA and naloxone.

Conclusions

Thus it is concluded that the VTA DA neuron population is unlikely to work in unison to perform any one role in pain processing. Conversely, a division of function as a result of neurons' differing physiological and pharmacological properties, likely reinforced by divergent afferent and efferent projections, is proposed.

It is hoped that ongoing experiments on tonic and chronic pain models will help to reveal and characterise these subdivisions, and provide insight into pathological changes occurring upstream of and within the VTA that contribute to the development of these debilitating human conditions.

The Challenge of Chronic Pain, Wellcome Trust conference, Cambridge
11th-13th March 2015 - *Poster abstract*
AND
NeuroPain meeting, London
16th-17th June 2015 – *Poster-led presentation abstract*

Probing dopaminergic signalling and pain responses in the rat ventral tegmental area

Lauren V Friend[1], Anthony H Dickenson[1]

[1] Department of Neuroscience, Physiology and Pharmacology, University College London, London, UK

Introduction

The detection of potentially harmful stimuli culminating in the perception of pain is crucial for survival; however, when this process becomes dysfunctional as in chronic pain, the result is extreme discomfort serving no apparent purpose and a reduced quality of life due in part to the aversive and unrewarding nature of the pain experience. Efforts to unpick pathological mechanisms require understanding of the affective pain-processing pathway, of which the dopaminergic (DA) neurons of the ventral tegmental area (VTA) are a crucial element. These neurons are well known for their established role in reward, implicating the VTA as a location for pain-reward interactions that frequently contribute to behavioural decisions. This study aims to investigate the DA neurons' precise role in nociceptive processing in both normal rats and persistent pain models, with focus on the specific contribution of endogenous opioid action.

Methods

Extracellular *in vivo* electrophysiology was performed within the VTA of isoflurane anaesthetised naïve rats. Firing rates were monitored and, in order to elucidate identity, neurons were classified pharmacologically according to response to systemic L-DOPA, the DA precursor. This process was repeated in rats with λ-carrageenan-induced tonic pain, and those with spinal nerve ligation-induced chronic pain. Naloxone, the μ-opioid receptor antagonist, was injected systemically to unmask endogenous opioid influence in the various pain conditions.

Results and conclusions

L-DOPA had a profound and rapid effect on spontaneous firing rate of the VTA neurons, effectively dividing them into those that were inhibited and those that were excited by L-DOPA and segregating the putative DA and non-DA contingents, respectively. The L-DOPA-excited population were significantly excited by peripheral noxious stimulation. Conversely, the L-DOPA-inhibited group consisted of a mixture of noxious-excited and noxious-inhibited neurons, strongly suggesting functional heterogeneity within this putative DA neuron population. Naloxone was shown to have a rapid effect on firing rates of the VTA neurons. This effect was altered by the presence of tonic or chronic pain, suggesting changes in the on-going influence of endogenous opioids upstream-to or within this pain-processing region.